

# The suitability of *Mytilus edulis* as proxy archive and its response to ocean acidification

Die Eignung von *Mytilus edulis* als Proxy-Archiv  
und deren Reaktion auf Ozeanversauerung



Dissertation

zur Erlangung des Doktorgrades

der Mathematisch-Naturwissenschaftlichen Fakultät

der Christian-Albrechts-Universität zu Kiel

**vorgelegt von Agnes Heinemann**

**Kiel 2011**

**The suitability of *Mytilus edulis* as proxy archive  
and its response to ocean acidification**

**Die Eignung von *Mytilus edulis* als Proxy-Archiv  
und deren Reaktion auf Ozeanversauerung**

Dissertation

zur Erlangung des Doktorgrades

der Mathematisch-Naturwissenschaftlichen Fakultät

der Christian-Albrechts-Universität zu Kiel

**vorgelegt von Agnes Heinemann**

**Kiel 2011**

Referent: Prof. Anton Eisenhauer

Korreferent/in: Prof. Frank Melzner

Tag der mündlichen Prüfung: 15.04.2011

Zum Druck genehmigt: Kiel,

gez.

## *Für Mama und Paps*

Die **Gelassenheit**, alles das hinzunehmen, was nicht zu ändern ist.

Die **Kraft**, zu ändern, was nicht länger zu ertragen ist.

Die *Weisheit*, das eine vom anderen zu unterscheiden.

*(nach R. Niebuhr)*

# Contents

<b>List of Figures</b>	<b>I</b>
<b>List of Tables</b>	<b>III</b>
<b>Abstract</b>	<b>IV</b>
<b>Zusammenfassung</b>	<b>VI</b>
<b>Introduction</b>	<b>1</b>
I.1 Ocean Acidification and the Baltic Sea	1
I.2 Marine organisms and their responses to Ocean Acidification	4
I.3 Possible pathways and processes of Biomineralization	7
I.4 The blue mussel - <i>Mytilus edulis</i>	11
I.5 Can bivalve shells tell the past and show the future?	13
I.6 Research questions and outline of the thesis	16
I.7 Experimental setup	18
References	20
<b>Chapter 1</b>	<b>32</b>
<b>Disentangling the Biological and Environmental Control of <i>M. edulis</i> Shell Chemistry</b>	
1.1 Abstract	33
1.2 Introduction	34
1.3. Materials and Methods	35
<i>1.3.1 Culturing</i>	35
<i>1.3.2 Sample preparation</i>	36
<i>1.3.3 Analytical methods</i>	36
1.4 Results and Discussion	39
1.5 Conclusions	42
Acknowledgments	43
References	43

<b>Chapter 2</b>	<b>45</b>
<b>The impacts of seawater carbonate chemistry on biomineralization and elemental concentrations of <i>Mytilus edulis</i> body fluids and its potential as a proxy archive</b>	
2.1 Abstract	46
2.2 Introduction	47
2.3 Material and Methods	49
2.3.1 <i>General Setup</i>	49
2.3.2 <i>Experiment 1</i>	50
2.3.3 <i>Experiment 2</i>	51
2.4 Results and Discussions	52
2.4.1 <i>Calcification</i>	53
2.4.1.1 Calcification rates	53
2.4.1.2 Shell length growth	55
2.4.1.3 Internal shell dissolution	58
2.4.2 <i>Elemental composition of body fluids</i>	61
2.4.3 <i>Ca<sup>2+</sup>, Mg<sup>2+</sup> or Sr<sup>2+</sup> concentrations</i>	62
2.5 Conclusions	67
References	68
Supplement	74
<b>Chapter 3</b>	<b>78</b>
<b>Boron isotope ratio determination in carbonates via LA-MC-ICP-MS using soda-lime glass standards as reference material</b>	
3.1 Abstract	79
3.2 Introduction	80
3.3 Experimental	81
3.3.1 <i>Standard and sample preparation</i>	81
3.3.2 <i>Instrumentation, data acquisition and evaluation</i>	82
3.4 Results and discussion	85
3.4.1 <i>Standards</i>	85
3.4.2 <i>Coral samples</i>	87

3.5 Conclusions	89
Acknowledgements	90
References	90
<b>Chapter 4</b>	<b>93</b>
<b>Responses of <i>Mytilus edulis</i> extracellular body fluids and shell composition to decreased pH: acid-base status, trace elements and <math>\delta^{11}\text{B}</math></b>	
4.1 Abstract	94
4.2 Introduction	95
4.3 Material and methods	97
<i>4.3.1 Culture and samples</i>	97
4.3.1.1 General setup	97
4.3.1.2 Experiment 1	98
4.3.1.3 Experiment 2	100
<i>4.3.2 Analytical methods</i>	100
4.4 Results and Discussion	102
<i>4.4.1 Water parameters</i>	102
<i>4.4.2 Acid-base parameters of fluid samples (experiment 1)</i>	102
<i>4.4.3 Elemental ratios of extrapallial fluid and water (experiment 2)</i>	107
<i>4.4.4 Boron isotope (<math>\delta^{11}\text{B}</math>) data of <i>M. edulis</i> shells (experiment 2)</i>	110
4.5 Conclusions	113
Acknowledgments	114
References	114
Supplement	121
<b>Summary and Conclusions</b>	<b>125</b>
<b>Outlook</b>	<b>128</b>
<b>References</b>	<b>129</b>
<b>Danksagung</b>	<b>131</b>
<b>Erklärung</b>	<b>132</b>
<b>Curriculum Vitae</b>	<b>133</b>

## List of Figures

<i>Figure 1.1:</i> Bjerrum Plot and relative distribution of carbon species at today's surface seawater pH	1
<i>Figure 1.2:</i> Concentrations of carbon species, pH and CaCO <sub>3</sub> saturation states of average surface seawater for rising pCO <sub>2</sub> concentrations during different geological times	2
<i>Figure 1.3:</i> Pictures and SEM images of the inner surface (nacre) of shells from low and high pCO <sub>2</sub> treatment	6
<i>Figure 1.4:</i> Modified schematic anatomy of a bivalve	10
<i>Figure 1.5:</i> <i>Mytilus edulis</i> (Linné 1758)	11
<i>Figure 1.6:</i> SEM-picture of shell layer from <i>Mytilus edulis</i>	12
<i>Figure 1.7:</i> Map of Kiel Fjord	18
<i>Figure 1.8:</i> Scheme and picture of the experimental setup	19
<i>Figure 1.1:</i> Growth of mussels since start of experiment	37
<i>Figure 1.2:</i> Scheme of values used for calculations of the relative contribution of individual differences, physiological variability, salinity and temperature to the overall variance of elemental ratios	38
<i>Figure 1.3:</i> a) Mg/Ca and b) Sr/Ca ratios of the different salinity treatments in comparison to temperature	39
<i>Figure 1.4:</i> Temperature effects on Mg/Ca ratios and influence of salinity during constant temperature treatment	40
<i>Figure 1.5:</i> Temperature effects on Sr/Ca ratios and influence of salinity during constant temperature treatment	40
<i>Figure 1.6:</i> Influence of individual differences, physiological state, salinity and temperature on Mg/Ca (a) and Sr/Ca ratios (b) in the prismatic layer of <i>M. edulis</i> shells	42
<i>Figure 2.1:</i> Mean calcification rates in the different treatments	53
<i>Figure 2.2:</i> Calcification rates over time	54
<i>Figure 2.3:</i> Mean increment growth during experiment of all individuals and of eight to ten individually marked specimens per treatment	56
<i>Figure 2.4:</i> Microprobe images of new grown calcite layer from high and low pCO <sub>2</sub> treatment with Mn-markings	57
<i>Figure 2.5:</i> Amount of shells with etched areas at inner shell surface	58
<i>Figure 2.6:</i> Pictures and SEM images of the inner surface (nacre) and the umbo region of shells from high and low pCO <sub>2</sub> treatment	61



<i>Figure 2.7:</i> Changes of Mg <sup>2+</sup> and Sr <sup>2+</sup> concentrations in the body fluids of <i>Mytilus edulis</i> and the ambient water relative to changes in Ca <sup>2+</sup>	63
<i>Figure 2.8:</i> Sr/Ca ratios of body fluids and water from this study and from shell of relative to Mg/Ca	65
<i>Figure 3.1:</i> Spectra around <sup>10</sup> B and <sup>11</sup> B in low and high resolution mode	83
<i>Figure 3.2:</i> One analytical run of 7 ablation periods on NIST610 bracketed by 8 ablation periods on Ce95-1 as bracketing standard	84
<i>Figure 3.3:</i> δ <sup>11</sup> B in corals cultured under different pH conditions	88
<i>Figure 4.1:</i> Position of laser ablation lines on <i>M. edulis</i> shell	100
<i>Figure 4.2:</i> Acid-base status of hemolymph and extrapallial fluid and of the seawater at sampling day compared to treatment pCO <sub>2</sub> at day of sampling	104
<i>Figure 4.3:</i> Elemental ratios vs. calculated internal pH values	107
<i>Figure 4.4:</i> Distribution coefficient of EPF and water elemental ratios compared to shell mass growth of bivalves during experimental time	109
<i>Figure 4.5:</i> δ <sup>11</sup> B measured in <i>M. edulis</i> shells and precipitated under different pCO <sub>2</sub> conditions in relation to data of other carbonates	111

## List of Tables

<i>Table 1.1:</i> Instrument parameters	36
<i>Table 1.2:</i> Means and variances of shell parts grown in nature	37
<i>Table 2.1:</i> Water conditions during experimental trials	52
<i>Table 2.2:</i> Weekly measurements of calcification rates in nmol CaCO <sub>3</sub> /g FW/h	54
<i>Table 2.3:</i> Mean values of increment growth of ten individually marked mussels per treatment at start of the experiment and four different time points until the end of the experiment	58
<i>Table 2.4:</i> Calcification rates before CO <sub>2</sub> gassing and mean calcification rates during the whole experiment, increment of growth from beginning of the experiment to the end and amount of shells with etched areas of the inner surface	60
<i>Table 2.5:</i> Mean elemental ratios of all matrices per aquarium	66
<i>Table 2.S1:</i> Alkalinity measurements of the different treatments with date and incubation time	74
<i>Table 2.S2:</i> Length growth of individually marked specimens at five dates during experiment	75
<i>Table 2.S3:</i> Element concentrations of water, HL and EPF (experiment 1)	76
<i>Table 2.S4:</i> Element concentrations of water and EPF (experiment 2)	77
<i>Table 3.1:</i> Instrumental parameters	82
<i>Table 3.2:</i> $\delta^{11}\text{B}$ results of standards analyzed	86
<i>Table 3.3:</i> $\delta^{11}\text{B}$ results of cultured corals	88
<i>Table 4.1:</i> Water conditions during experimental trials	98
<i>Table 4.2:</i> Instrumental parameters for Laser Ablation	101
<i>Table 4.3:</i> Acid-base status of HL and EPF and of the water at date of sampling	103
<i>Table 4.4:</i> Comparison between the hemolymph acid-base of this study and the studies of Michaelidis et al. (2005) and Thomsen et al. (2010)	105
<i>Table 4.5:</i> pH and Me/Ca ratios of treatment water and EPF	106
<i>Table 4.6:</i> pH and $\delta^{11}\text{B}$ of treatment water and EPF	110
<i>Table 4.S2:</i> Single values of acid-base status of the body fluids	121
<i>Table 4.S3:</i> Results of regressions of body fluid acid-base parameters	123
<i>Table 4.S4:</i> single results of elemental ratios	123
<i>Table 4.S5:</i> single results of $\delta^{11}\text{B}$ and final shell length of the investigated individuals	124

## Abstract

Past climate changes can be used as indicators of future scenarios, however past climatic changes can not be directly observed. Therefore, the reconstruction of past abiotic conditions can be approximated using chemical or isotopic proxies. These proxies can be measured in natural archives (e.g. bivalve shells and coral skeletons). One aspect of current climate change is the acidification of the oceans, a phenomenon caused by the oceanic uptake of anthropogenic CO<sub>2</sub> and a resulting shift in the marine carbonate system. As a result of this, a drop of mean ocean surface pH by ~0.3-0.7 units can be expected until the year 2100. In relation to geological timescales this drop occurs very fast (~0.1-0.2 units per 100 years) and causes species specific reactions which are not fully studied yet. For example, elevated [CO<sub>2</sub>] disturbs the acid-base status of extracellular body fluids and the degree of disturbances depends on animals metabolic rates. Especially marine calcifying organisms are influenced in their ability to form CaCO<sub>3</sub>-shells and skeletons by this decline in pH. The blue mussel (*Mytilus edulis*) is an important calcifier in many marine ecosystems and in aquaculture.

In this Thesis I investigated the impact of ocean acidification on the acid-base status and the calcification of *M. edulis* in experiments conducted under different seawater pCO<sub>2</sub> levels (380-4000 µatm). Furthermore, investigations of *M. edulis* shells as proxy archive have led to contradictory results. Hence, the impact of elevated pCO<sub>2</sub>, as well as temperature and salinity on the inorganic shell composition have been investigated in this study to test the suitability of *M. edulis* shells as a proxy archive in general and for pH construction in particular. Physiological experiments can provide knowledge about acclimation reactions of marine organisms to abiotic stressors but not about their adaptation potential, as the relevant timescales cannot be simulated in laboratory studies. Thus, experiments using already pre-adapted animals from challenging habitats may provide a more accurate picture of potential CO<sub>2</sub> impacts on *M. edulis*. Therefore, in all experiments of this study, *M. edulis* from Kiel Fjord (Western Baltic Sea, Germany) were investigated, as during the summer months, high CO<sub>2</sub>-concentrations have been observed in this habitat.

In **Chapter 1** the suitability of *Mytilus edulis* shells as proxy archive has been proven. For this, the environmental (temperature and salinity) and the biological influence on the elemental ratios (Mg/Ca and Sr/Ca) in the calcite layer have been modeled. The results showed physiological and individual differences having a significant impact on the Mg/Ca distribution in *M. edulis* calcite (~45 and ~34 % respectively). Sr/Ca seemed to be less affected (~24 and ~17 %). A more detailed understanding of the mechanisms of biomineralization is necessary to use biominerals as proxy archives. As shell formation occurs in the extrapallial space, the contained fluid (extrapallial fluid, EPF) should be considered even if the detailed mechanisms of precipitation are still unknown. Thus, in **Chapter 2** the mineralization of the shell and the elemental ratios in the body fluids (hemolymph and EPF) have been observed in long-term experiments conducted under different pCO<sub>2</sub> (380-4000 µatm) values. Elemental concentrations were not influenced by different pCO<sub>2</sub> levels however they were modified during shell

formation. The inorganic composition of the body fluids was very variable between individuals what may explain the results of Chapter 1. Calcification rate measurements indicated net dissolution in the highest  $p\text{CO}_2$  treatment (3352  $\mu\text{atm}$ ) and inner shell surfaces were corroded while length growth did not differ between treatments. This effect could be reduced by high food levels. To better understand past changes related to ocean acidification, B/Ca ratios in the extrapallial fluid and boron isotopes ( $\delta^{11}\text{B}$ ) in the shell of *M. edulis* were investigated in **Chapter 4**. For this purpose a new *in situ* method using LA-MC-ICP-MS for the determination of stable boron isotope ratios ( $\delta^{11}\text{B}$ ) in carbonates was developed and described in **Chapter 3**.  $\delta^{11}\text{B}$  was highly variable between different individuals but also within single shells. This corresponded to a high individual variability in fluid B/Ca ratios. Unless the mean  $\delta^{11}\text{B}$  values showed no trend with pH they appeared to represent internal EPF pH rather than ambient water pH. I also demonstrated that extracellular body fluid  $p\text{CO}_2$  values of *M. edulis* are high due to metabolic  $\text{CO}_2$  and pH was significantly lower than seawater pH. In contrast to Chapter 2, growth rates were much higher due to higher food availability. Elemental ratios (B/Ca, Mg/Ca and Sr/Ca) in EPF increased slightly with pH which was in accordance with increasing growth and calcification rates at higher seawater pH values.

In summary, the results of this study showed a very large biological impact on the elemental and isotopic composition of *M. edulis* shell. To use *M. edulis* shells as proxy archive, several abiotic as well as biological factors have to be considered and the whole animal has to be investigated. Thus, it is questionable if a sufficient calibration for the proper use of *M. edulis* as proxy archive is feasible at all.

## Zusammenfassung

Die Klimageschichte kann einen Blick in die Zukunft ermöglichen, aber selbst nicht mehr direkt untersucht werden. Daher sind chemische oder isotopische Stellvertreter (sogenannte Proxies), welche in natürlichen Archiven (z. B. Muschelschalen und Korallenskelette) gemessen werden, für die Rekonstruktion des Klimas notwendig. Ein wichtiger Aspekt des Klimawandels ist die Ozeanversauerung, die durch die Aufnahme des anthropogen emittierten Kohlenstoffdioxids ( $\text{CO}_2$ ) durch die Ozeane verursacht wird. Dies hat eine Veränderung im Kohlensäuregleichgewicht zur Folge. Daraus resultiert eine Senkung des pH-Wertes im Meerwasser um  $\sim 0.3\text{-}0.7$  Einheiten bis zum Jahre 2100. Relativ zu geologischen Zeitskalen verläuft die Versauerung der Ozeane mit  $\sim 0.1\text{-}0.2$  pH Einheiten pro einhundert Jahre sehr schnell und löst in verschiedenen marinen Tierarten unterschiedliche Reaktionen aus, die noch nicht ausreichend verstanden sind. Die Auswirkungen der erhöhten  $\text{CO}_2$ -Konzentrationen auf den Säure-Base-Haushalt hängen z. B. vom Metabolismus der Tiere ab. Besonders kalzifizierende Organismen sind in ihrer Fähigkeit, Schalen und Skelette aus Kalziumkarbonat zu bilden, durch den sinkenden Wasser-pH gefährdet. Die Miesmuschel (*Mytilus edulis*) spielt in vielen marinen Ökosystemen, sowie in der Aquakultur eine wichtige Rolle. Um die individuelle Gefährdung dieser wichtigen Art besser erfassen zu können, habe ich im Rahmen meiner Dissertation in verschiedenen Experimenten mit unterschiedlichen  $\text{CO}_2$ -Konzentrationen () die Auswirkungen der Ozeanversauerung auf den Säure-Base-Haushalt, als auch die Kalzifizierung von *M. edulis* näher untersucht. Weiterhin wird *M. edulis* als Proxy-Archiv genutzt, was aber in zahlreichen Studien zu kontroversen Ergebnissen führt. In dieser Arbeit wurden deshalb die Auswirkungen der Ozeanversauerung, sowie von Temperatur und Salinität auf die Zusammensetzung der Schale näher betrachtet, um so ein Fazit über die Eignung der Schale von *M. edulis* als Proxy-Archiv, insbesondere im Hinblick auf pH-Rekonstruktionen, ziehen zu können. Im Allgemeinen erlauben physiologische Experimente nur einen Einblick in die Kurzzeitreaktionen auf Veränderungen bestimmter Umweltparameter und liefern keine Aussage über mögliche Adaptionen. Tieren aus Lebensräumen, die bereits heute Bedingungen ausweisen wie sie für die Zukunft vorausgesagt sind, weisen daher bereits eine zielgerichtete Anpassung auf. Somit können Experimente mit diesen voradaptierten Individuen genauere Abschätzungen liefern. Diesem Ansatz folgend stammten die Miesmuscheln dieser Arbeit alle aus der Kieler Förde (westliche Ostsee, Deutschland), da in diesem Habitat in den Sommermonaten hohe  $p\text{CO}_2$ -Werte gemessen wurden.

In **Kapitel 1** wurde die Eignung der Schale von *M. edulis* als Proxy-Archiv anhand von Elementverhältnissen (Mg/Ca und Sr/Ca) in der Kalzitlage getestet. Dafür wurden das Ausmaß des Einflusses der Umweltparameter (Temperatur und Salinität) und der Biologie modelliert. Die physiologischen, sowie individuellen Unterschiede zeigten mit  $\sim 45$  bzw.  $\sim 34$  % einen signifikanten Einfluss auf die Verteilung von Mg/Ca in der Schale, während Sr/Ca weniger beeinflusst ( $\sim 24$  bzw.  $\sim 17$  %) waren. Um die Schalen der Miesmuscheln als Proxy-Archiv nutzen zu können, müssen die

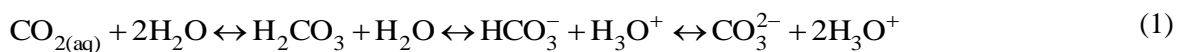
Mechanismen der Schalenbildung erst besser verstanden werden. Auch, wenn die genauen Mechanismen noch ungeklärt sind, muss hierbei das extrapalliale Fluid (EPF) berücksichtigt werden, da es den Raum füllt, in dem die Schalenbildung stattfindet. Aus diesem Grund wurden in einem Langzeitexperiment (3 Monate) sowohl die Kalzifizierung, als auch die Elementzusammensetzung der Hämolymphe und des EPF unter Einfluss verschiedener  $p\text{CO}_2$ -Level untersucht (380-4000  $\mu\text{atm}$ , **Kapitel 2**). Die Elementkonzentrationen wurden nicht durch die  $p\text{CO}_2$ -Level beeinflusst, aber durch die Schalenbildung und waren sehr variabel zwischen verschiedenen Individuen. Dies könnte eine Erklärung für die Ergebnisse aus Kapitel 1 sein. Obwohl im höchsten  $p\text{CO}_2$ -Level (3352  $\mu\text{atm}$ ) Längenwachstum der Schale beobachtet wurde, deuteten die Messungen der Kalzifizierungsraten eine Auflösung der Schalen an und die Innenseite der Schalen wies aufgelöste Flächen auf. Unter optimalen Futterbedingungen wurde dieser Effekt vermindert. In **Kapitel 4** sind die B/Ca Verhältnisse im EPF, sowie die Borisotopie ( $\delta^{11}\text{B}$ ) der Schale untersucht worden, um zu testen, ob sich so vergangene pH-Bedingungen rekonstruieren lassen. Hierfür wurde zuerst eine *in situ* Messmethode für  $\delta^{11}\text{B}$  in den Schalen entwickelt (**Kapitel 3**). Sowohl  $\delta^{11}\text{B}$ , als auch B/Ca waren sehr variabel zwischen verschiedenen Individuen und  $\delta^{11}\text{B}$  auch innerhalb einer Schale. Die mittleren  $\delta^{11}\text{B}$ -Werte zeigten keine Abhängigkeit vom pH Wert des Umgebungswassers, sondern scheinen den internen pH (extrapalliale Flüssigkeit, EPF) wiederzuspiegeln. In Kapitel 4 wurde ebenfalls gezeigt, dass der pH-Wert der Körperfluide (HL und EPF) signifikant niedriger ist, als der des Wassers. Dies ist ein Effekt des durch Atmung produzierten Kohlenstoffdioxids. Im Gegensatz zum 2. Kapitel waren die Wachstumsraten in den Experimenten aus diesem Kapitel aufgrund von optimierten Futterbedingungen deutlich höher. Die Elementverhältnisse (B/Ca, Mg/Ca, Sr/Ca) wurden mit steigendem pH leicht erhöht. Dies scheint eher ein Effekt der steigenden Wachstumsraten unter hohem pH zu sein, als der direkte Einfluss des pH.

Zusammenfassend lässt sich sagen, dass eine große biologische Kontrolle die Zusammensetzung der Schale beeinflusst. Um die Schale von *M. edulis* als Proxy-Archiv nutzen zu können, müssen viele abiotische, als auch biotische Faktoren berücksichtigt werden und es sind Untersuchungen am ganzen Tier notwendig. Daher ist es fragwürdig, ob eine ausreichende Kalibration für die einwandfreie Nutzung von *M. edulis* als Proxy-Archiv möglich ist.

## Introduction

### I.1 Ocean Acidification and the Baltic Sea

The consequences of anthropogenic carbon dioxide (CO<sub>2</sub>) release to the atmosphere are major topics in current research across disciplines such as biology and geochemistry. This CO<sub>2</sub> release is a result of fossil fuel combustion (coal, oil, and natural gases), deforestation and production of cement (IPCC 2007). One specific effect is the so-called ocean acidification due to the lowering of ocean pH as a result of CO<sub>2</sub> absorption. The oceans will become less alkaline because CO<sub>2</sub> not only dissolves but also reacts with H<sub>2</sub>O (Dickson et al. 2007) following the equation:



Therefore, the carbonate system will be shifted towards higher CO<sub>2</sub> and lower carbonate (CO<sub>3</sub><sup>2-</sup>) concentrations whereby proton (H<sup>+</sup>) concentration in the water increases and in consequence pH declines (Figure I.1).

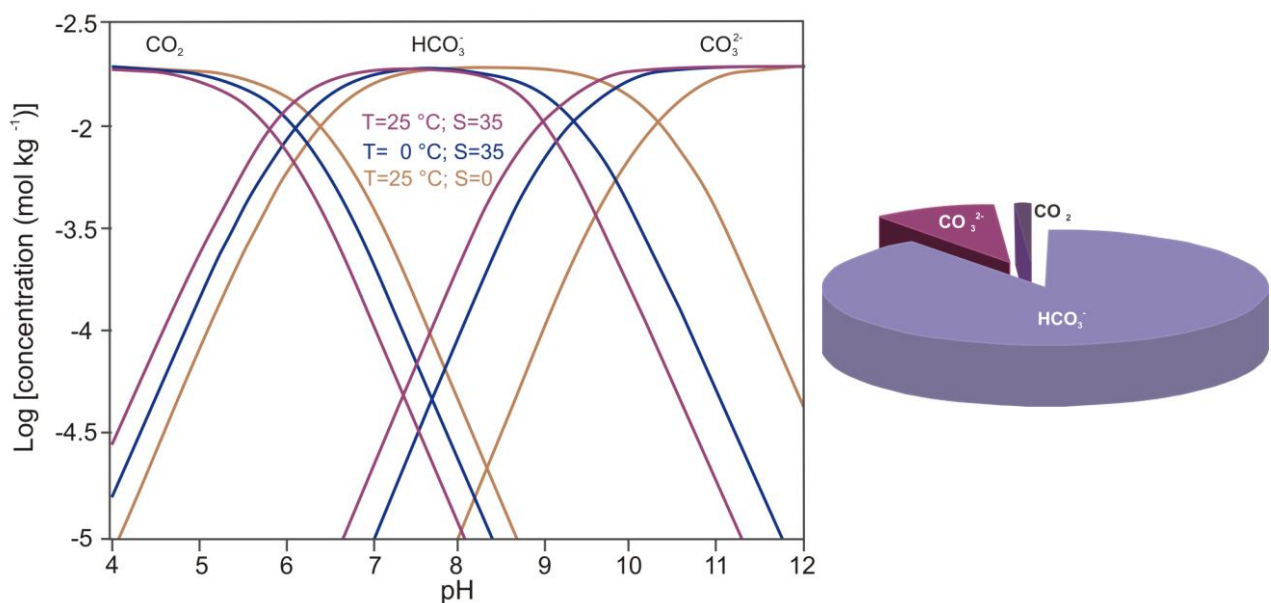


Figure I.1: Bjerrum-plot and relative distribution of carbon species at today's surface seawater pH. Distribution of the different carbon species related to pH at different temperature and salinity combinations. Bjerrum Plot modified after Zeebe and Wolf-Gladrow (2001).

The relative speciation of the total dissolved inorganic carbon ( $C_T$ ) in today's surface seawater is dominated by bicarbonate (HCO<sub>3</sub><sup>-</sup>, 90 %), while CO<sub>3</sub><sup>2-</sup> (~9 %) and CO<sub>2</sub> (1 %) exist in much smaller concentrations.

The absorption of  $\text{CO}_2$  by the ocean is a result of its equilibrium with the atmosphere and follows Henry's law, which declares that the concentration of a gas in a solution is dependent on the partial pressure of the gas in the atmosphere, and on its solubility coefficient. Thus, around half of the anthropogenic  $\text{CO}_2$  released to the atmosphere is expected to be absorbed by the global oceans (Sabine et al. 2004). Atmospheric  $p\text{CO}_2$  has increased from 280-390  $\mu\text{atm}$  (<http://www.esrl.noaa.gov/gmd/ccgg/trends/>) since pre-industrial time and average ocean surface pH already decreased by 0.1 units and is  $\sim 8.1$  today (Orr et al. 2009). So the oceans provide an important sink for  $\text{CO}_2$ , preventing higher  $p\text{CO}_2$  values in the atmosphere and hence decreasing the rate of global warming. However, they are consequently predicted to acidify to a pH of 7.8 by the end of the century and to  $\sim 7.3$  within the next 300 years (Caldeira and Wickett 2003).

	Glacial	Pre industrial	Present	2*present	3*present	change from industrial to 3*present
atmosphere $\text{CO}_{2(g)}$	180	280	380	560	840	200 %
gas exchange $\text{CO}_{2(aq)} + \text{H}_2\text{O} \rightleftharpoons \text{H}_2\text{CO}_3$ carbonic acid	7	9	13	18	25	178 %
$\text{H}_2\text{CO}_3 \rightleftharpoons \text{H}^+ + \text{HCO}_3^-$ bicarbonate	1666	1739	1827	1925	2004	15 %
$\text{HCO}_3^- \rightleftharpoons \text{H}^+ + \text{CO}_3^{2-}$ carbonate	279	222	186	146	115	-48 %
DIC	1952	1970	2026	2090	2144	8.8 %
$\text{pH}_{(\text{SWS})}$	8.32	8.16	8.05	7.91	7.76	-0.4 %
$\Omega_{\text{calcite}}$	6.63	5.32	4.46	3.52	2.77	-48 %
$\Omega_{\text{aragonite}}$	4.26	3.44	2.90	2.29	1.81	-47 %
ocean						

Figure 1.2: Concentrations of carbon species (in  $\mu\text{mol/kg}$ ), pH and  $\text{CaCO}_3$  saturation states of average surface seawater for rising  $p\text{CO}_2$  concentrations (in  $\mu\text{atm}$ ) during different geological times. Modified after Fabry et al. (2008).

Such a pH value has not been experienced in the oceans for several million years (Pearson and Palmer 2000, Caldeira and Wickett 2003) and pH is decreasing extremely fast. Caldeira and Wickett (2003) estimated an atmospheric  $p\text{CO}_2$  of 1900  $\mu\text{atm}$  which results in a similar increase of seawater  $p\text{CO}_2$  and a maximum drop in surface pH of 0.77 at around the year 2300 based on the IPCC business as usual scenario IS92a of  $\text{CO}_2$  emissions (Houghton et al. 2001). Data from ice-cores indicate that the increase in  $p\text{CO}_2$  is highest in the last 420,000 years (Petit et al. 1999). A pH drop of 0.5 units is drastic as the scale of pH is logarithmic and the concentration of  $\text{H}^+$  increases threefold.



Today's open oceans are super saturated with respect to calcium carbonate ( $\text{CaCO}_3$ ), which is expressed by a saturation state ( $\Omega$ ) of greater than one. The calcium carbonate saturation state ( $\Omega$ ):

$$\Omega = \frac{[\text{CO}_3^{2-}][\text{Ca}^{2+}]}{K'_{\text{sp}}} \quad (2)$$

where  $K'_{\text{sp}}$  is the stoichiometric solubility product, depends mostly on the concentration of  $\text{CO}_3^{2-}$  as the calcium ( $\text{Ca}^{2+}$ ) concentration is quite constant in the ocean at constant salinity.

As a result of rising  $p\text{CO}_2$  and the consequent shift in the carbonate system towards lower  $[\text{CO}_3^{2-}]$  the oceans will become under saturated by the year 2050 (Orr et al. 2009, Cao and Caldeira 2008). The main two polymorphs of  $\text{CaCO}_3$  are aragonite and calcite. As aragonite is 50 % more soluble than calcite (Mucci 1983) oceans first will become under saturated with respect to this polymorph.

The total alkalinity ( $A_T$ ) is the amount of weak bases in the water and describes the ability of a solution to neutralize acids by accepting protons. Thus, it is the natural buffer of the oceans and is defined as:

$$A_T = [\text{HCO}_3^-] + 2[\text{CO}_3^{2-}] + [\text{B}(\text{OH})_4^-] + [\text{OH}^-] + [\text{HPO}_4^{2-}] + 2[\text{PO}_4^{3-}] + [\text{SiO}(\text{OH})_3^-] + [\text{NH}_3] + [\text{HS}^-] + \dots - [\text{H}^+] - [\text{HSO}_4^-] - [\text{HF}] - [\text{H}_3\text{PO}_4] - \dots \quad (3)$$

It is primarily influenced by its main components,  $\text{HCO}_3^-$  and  $\text{CO}_3^{2-}$  (described as carbonate alkalinity). As a result of reduced ion concentrations  $A_T$  is lower at low salinity and therefore this water is less buffered. One such example is the brackish Baltic Sea. Due to excess river runoff and the influence of marine waters in the western parts a salinity gradient in the west-east direction with mean values of 20 in the west and down to 0 in the east and a corresponding gradient in alkalinity can be observed.  $A_T$  decreases with decreasing salinity and results in a strong  $C_T$  gradient in the surface water between the Kattegat and the northern regions of the Baltic Sea (Beldowski et al. 2010). This gradient depends on the seawater inflow, the magnitude and  $A_T$  concentration of the river discharge (Hjalmarsson et al. 2008). Rivers which enter the southern part of the Baltic Sea have higher  $A_T$  concentrations (due to limestone rich areas) than rivers entering the northern part of the Baltic Sea (bedrocks here are dominated by granite) (Hjalmarsson et al. 2008).

Kiel Fjord in particular (Western Baltic Sea, Germany,  $54^\circ 19.8'$  N;  $10^\circ 9.0'$  E) is characterized by challenging abiotic conditions and high fluctuations in  $p\text{CO}_2$ . Low salinity (10-20) and alkalinity (1900-2150  $\mu\text{mol/kg}$ ) produce a reduced buffering capacity of the water. Therefore, high  $p\text{CO}_2$  values (with maximum values of  $>2300 \mu\text{atm}$  in summer months) result in a considerable drop in pH with minimum values of 7.5. These high  $p\text{CO}_2$  values are caused by strong stratification during summer because of heated surface water. Sinking organic matter then leads to hypoxic conditions in the bottom water and therefore to an increase in  $[\text{CO}_2]$ . Upwelling of this water induces strong fluctuations in shallow waters. These conditions cause a low  $\text{CaCO}_3$  saturation state with minimum values of  $\Omega_{\text{arag}} = 0.34$  and  $\Omega_{\text{calc}} = 0.58$  (Thomsen et al. 2010). Further regions with such challenging conditions are

areas with volcanic activity where shallow water can be acidified (e.g. Hall-Spencer et al. 2008), coastal salt marshes (Cochran and Burnett 1996) or submarine volcanoes (Tunnicliffe et al. 2009). Furthermore, upwelling zones (Feely et al. 2004) and estuaries (e.g. Frankignoulle et al. 1996) were reported to reach extremely high  $p\text{CO}_2$  levels. In such habitats ocean acidification may be more serious than in the open ocean and organisms must have adapted already today to resist such challenging conditions.

Most ocean acidification perturbation experiments are not able to properly account for the genetic adaptation potential of marine species, as time limitations usually prevent multi generation experiments. Thus, experiments with already adapted animals from habitats like Kiel Fjord may better improve models of future responses (Kuffner et al. 2008, Hall-Spencer et al. 2008).

## **I.2 Marine organisms and their responses to Ocean Acidification**

The intensive study of biological responses to ocean acidification is a young field of research. First studies investigating the impact of elevated  $\text{CO}_2$  and accordingly decreased  $\text{CO}_3^{2-}$  concentration were conducted about a decade ago (e.g. Gattuso et al. 1998, Kleypas 1999, Langdon et al. 2000, 2003) and reveal strong effects on corals and coccolithophores (Riebesell et al. 2000). Several organisms (Ries et al. 2009, for review see Doney et al. 2009) and therefore ecosystems may be influenced drastically by ocean acidification and may not have enough time to adapt to these currently fast changes.

Elevated  $[\text{CO}_2]$  disturbs the acid-base status of extracellular body fluids and the degree of disturbances depends on the way animals deal with them (see Pörtner et al. 2004 for review). High extracellular  $p\text{CO}_2$  values (1000-4000  $\mu\text{atm}$ ) can be found in all aquatic ectothermic metazoans (see Melzner et al. 2009 for review). This is a result of a relatively steep gradient of  $\text{CO}_2$  partial pressure from the body fluids to the ambient water which is necessary for diffusive excretion of metabolic  $\text{CO}_2$ . In order to maintain metabolic  $\text{CO}_2$  flux extracellular  $p\text{CO}_2$  increases under hypercapnia (Pörtner et al. 2004, Michaelidis et al. 2005, Melzner et al. 2009, Thomsen et al. 2010). This may not only lead to reductions in growth and calcification but also reproduction and fitness. Thomsen et al. (2010) found the buffer value of *M. edulis* hemolymph from Kiel Fjord to be low (0.49  $\text{mmol HCO}_3^-/\text{pH}$ ). This is in accordance with findings from other studies (Booth et al. 1984, Lindinger et al. 1984) on *M. edulis* from different habitats. Increased  $\text{HCO}_3^-$  concentrations in *M. edulis* and *M. galloprovincialis* have been reported to buffer extracellular pH in closed/recirculating systems (Lindinger et al. 1984, Michaelidis et al. 2005). It is likely that this increase in extracellular  $[\text{HCO}_3^-]$  was a result of increases in ambient water  $[\text{HCO}_3^-]$  caused by external/internal shell dissolution (Thomsen et al. 2010). In contrast to both these studies, Thomsen et al. (2010) demonstrated no  $[\text{HCO}_3^-]$  accumulation in *M. edulis* in a long-term flow-through experiment. Therefore, *M. edulis*, and also other bivalves and animals with low metabolic rates, do not perform extracellular pH compensation and the carbonate

system of the body fluids shifts to lower carbonate concentrations. In more active animals accumulation of extracellular  $[\text{HCO}_3^-]$  is an efficient mechanism of extracellular pH stabilization after an initial drop to conserve pH sensitive respiratory pigments (see Melzner et al. 2009 for a review). The magnitude of this  $\text{HCO}_3^-$  accumulation response varies between taxa, but the highest degrees of  $[\text{HCO}_3^-]$  related pH compensation are found in fish (Larsen et al. 1997, Michaelidis et al. 2007), crustaceans (Pane and Barry 2007, Spicer et al. 2007) and cephalopod mollusks (Gutowska et al. 2010). These active marine species naturally experience strong extracellular pH variability as a result of high metabolic rate and respiratory acidosis. However, some studies reported increasing metabolism under hypercapnia. Thomsen and Melzner (2010) observed increasing respiration rate and  $\text{NH}_4^+$  excretion as well as enhanced protein metabolism indicated by decreased N:O ratios in Baltic *M. edulis* under elevated  $p\text{CO}_2$ . A temperature dependent increase in oxygen consumption was found in *Crassostrea gigas* by Lannig et al. (2010).

Marine calcifiers are especially threatened by decreasing  $\text{CaCO}_3$  saturation state and declining pH in their habitat, as they form their shells or skeletons out of polymorphs of  $\text{CaCO}_3$  (Figure I.3) following the simplified reaction:



Additionally, it can be assumed that limited energy under low food and therefore to negligence of maintaining the shell structure (Chapter 2 of this thesis, Melzner et al. submitted). The calcification of different species like foraminifera (e.g. Bijma et al. 1999), coccolithophores (e.g. Riebesell et al. 2000), bivalves (e.g. Gazeau et al. 2007, Thomsen et al. 2010, Waldbusser et al. 2010), echinoderms (e.g. Dupont et al. 2008), corals (e.g. Langdon et al. 2000, Hoegh-Guldberg et al. 2007) and coralline red algae (Martin and Gattuso 2009) is assumed to be negatively influenced by rising  $[\text{CO}_2]$  as the equilibrium of inorganic carbon moves and causes a lower  $\text{CaCO}_3$  saturation state. Only a few marine calcifying organisms such as decapods crustaceans (Ries et al. 2009) and cephalopods (Gutowska et al. 2008), have been reported to actually benefit from high  $p\text{CO}_2$  conditions and show increased calcification. Hall-Spencer et al. (2008) found a shift in typical rocky shore communities towards an absence of scleractinian corals and significant reductions in sea urchin abundance. However, in an area with pH values of 7.6 (1800  $\mu\text{atm}$ ) they observed sea-grass production to be highest, as plants are often  $\text{CO}_2$  limited and therefore hypercapnia may have beneficial effects on them. Palacios and Zimmerman (2007) observed an increase in biomass and reproductive output under high- $\text{CO}_2$  conditions, suggesting potentially higher productivity of sea grasses. However, in the same area mentioned above Hall-Spencer et al. (2008) also found significantly reduced coralline red algal biomass and dissolving gastropod shells due to periods of carbonate sub saturation.

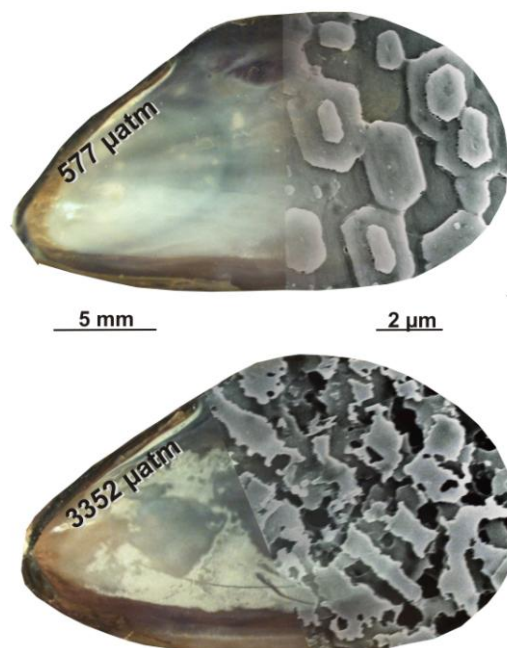


Figure 1.3: Pictures and SEM images of the inner surface (nacre) of shells from low and high  $p\text{CO}_2$  treatment (modified after Chapter 2 of this thesis). SEM images display enlargements of the pictures.

Several studies showed a more or less distinct decline in growth rates with increasing  $p\text{CO}_2$ , at least in the highest  $p\text{CO}_2$  treatment, for adult (Michaelidis et al. 2005, Berge et al. 2006, Thomsen et al. 2010, Thomsen and Melzner 2010) as well as early development stages/larval bivalves (Kurihara et al. 2007 and 2008, Gazeau et al. 2010). Kurihara et al. (2007, 2008) showed a significant decrease in hatching rates and shell growth during early (up to 6 days) development of *Mytilus galloprovincialis* and *Crassostrea gigas* when pH decreased 0.7 units to 7.4. Gazeau et al. (2007) showed negative calcification rates of *Mytilus edulis* with a threshold of 1800  $\mu\text{atm}$  in a short-term experiment. After long-term acclimation, mussel calcification response was less sensitive to elevated  $p\text{CO}_2$  when food supply was sufficient (Thomsen and Melzner 2010). Thomsen and Melzner (2010) observed a linear decreased growth of shell length and shell mass with increasing  $p\text{CO}_2$  by 6-20 and 10-34 % relative to the control treatment in individuals from Kiel Fjord but net growth and calcification was still very high even under 4000  $\mu\text{atm}$  (6.3 mm; ~130 mg). In a summer experiment, Thomsen et al. (2010) found calcification rates similar to control rates under 1400  $\mu\text{atm}$   $p\text{CO}_2$  ( $\Omega_{\text{arag}} < 0.5$ ) and still high growth under 4000  $\mu\text{atm}$  ( $\Omega_{\text{arag}} < 0.2$ ). Nevertheless, bivalves are also reported to live successfully in extreme habitats. An example is discussed by Tunnicliffe et al. (2009) who investigated the vent mussel *Bathymodiolus brevior* living at a submarine volcano where natural pH values of 5.36 to 7.29 are dominant. Mussels showed clearly thinner shells at this location compared to a location with higher pH values but can survive because of the absence of crabs at vents. Furthermore, Tunnicliffe et al. (2009) found a dead mussel with only a small disc of  $\text{CaCO}_3$  left and embedded in a husk of periostracum. Therefore, the periostracum might be the most important protection against hypercapnia. Another aspect of disturbances by rising  $p\text{CO}_2$  is the possible future food limitation. Zoo- as well as phytoplankton is reported to be affected negatively by changes in water  $p\text{CO}_2/\text{pH}$  (Riebesell et al.

2000, Yamada and Ikeda 2000, Hinga 2002) and changes in  $[\text{CO}_2]$  could alter the phytoplankton species composition (e.g. Kim et al. 2006, Hare et al. 2007). Thus, ocean acidification may indirectly impact plankton feeding organisms already at lower hypercapnia.

However, effects on the whole ecosystem can be estimated if marine biodiversity decreases, due to reduced fitness or actual loss of individual groups or increasing populations of single groups (e.g. sea grass) which benefit from increased  $[\text{CO}_2]$  (e.g. Hall-Spencer et al. 2008). Further research with different model species is necessary, as each reacts to ocean acidification in its own way.

### **I.3 Possible pathways and processes of Biomineralization**

Biomineralization is the process by which organisms form minerals (e.g. skeletons, shells) and can be divided in two groups, the “biologically induced” and the “organic matrix-mediated” or “biologically controlled” biomineralization (Lowenstam 1981). The first describes the process of secondary precipitation as a result of the interactions between biological activity and the environment. In the latter process cellular activity locates and controls the formation of the biominerals. Due to the control exerted by many organisms biominerals show characteristics (like shape, size, crystallinity and elemental composition) which distinguish them from inorganic minerals (Weiner and Dove 2003). They are composite materials comprising mineral as well as organic components (Weiner and Dove 2003). Half of the known biominerals contain calcium ( $\text{Ca}^{2+}$ ) and the calcium carbonates ( $\text{CaCO}_3$ ) are the most abundant biogenic minerals in terms of quantities produced and their widespread distribution among many different taxa (Lowenstam and Weiner 1989). Three of the eight known polymorphs are pure  $\text{CaCO}_3$ : calcite, aragonite and vaterite (Addadi et al. 2003). Several groups (e.g. Porifera, Cnidaria, Mollusca, Brachiopoda, Echinodermata) started to evolve their shells during the Cambrian explosion and a radiation of heavily calcified skeletons took place in the Ordovician (Knoll 2003). The driving factor for formation of robust shells and skeletons was probably the overall increase in biological diversity and predation pressure. In the highly over saturated ocean of the Proterozoic spontaneous calcification of cell and tissue surface could have been a problem (Knoll et al. 1993). Therefore, anti-calcifying molecules were necessary and it is reasoned that these inhibitors were recruited for the physiological control of skeleton growth (Marin et al. 1996). As  $\text{Ca}^{2+}$  is toxic for cells above a certain level a large number of cells deposit  $\text{Ca}^{2+}$ -rich minerals to eliminate these ions. The minerals can either be precipitated within the cell, leave it as crystals or precipitated extracellularly (Krampitz and Graser 1988). Many species like foraminifera, corals, coccolithophores or brachiopods build  $\text{CaCO}_3$  exoskeletons and shells. Bivalvia also form  $\text{CaCO}_3$ -shells (two valves) as aragonitic, calcitic or bimineralic. Which polymorph is used seems to be at least dependent on the marine chemistry during evolution of these shells/skeletons. But not all shells respond to seawater chemistry as in several species a strong physiological control appropriates the formation process (Stanley and

Hardie 1998). In a recent study (Jacob et al. 2010), amorphous calcium carbonate (ACC) was found as a precursor phase in shells of adult Unionoida. The authors observed ACC in a narrow zone at the interface between periostracum and the prism layer. Mollusk shells are composed of 95-99.9 % CaCO<sub>3</sub> by weight and a residual mass of biological macromolecules (Wilbur 1984). Carbonate shells are of broad interest in different fields. Nacre in particular has attractive material properties (tough and strong but light), for example for bionic research (Jackson et al. 1990, Barthelat et al. 2006). Furthermore, bivalve shells can have the potential to serve as proxy archives like foraminifera and corals already do. But the fact that biominerals are formed by organisms means that they are produced under biological control (so-called “vital effect”). Hence, biominerals are not passive recorders of their environment and it is required to disentangle biological and environmental influences to enable accurate interpretation of elemental ratios as proxies of the environment (e.g. Cusack and Freer 2008, Heinemann et al. 2008, Chapter 1 of this thesis). This requires a more detailed understanding of the still not fully known mechanisms controlling biomineralization. A series of different calcification models in bivalves has been suggested and steadily advanced.

Bivalve shell formation occurs in the fluid filled space which is separated from the external solution by the shell, the mantle and the periostracum. This extrapallial fluid was already described in a study of de Waele (1930, cited by Kobayashi 1964) as the fluid from which crystals and shell organics are formed from. It is proposed to be divided into an inner (where nacre is formed) and an outer (where calcite is formed) section (Wilbur and Saleuddin 1983, Wheeler 1992, Vander Putten et al. 2000) (Figure I.4) and secreted from the outer mantle cells. Due to the small amount of the outer extrapallial fluid (EPF), which therefore is difficult to sample, most studies investigated the inner EPF while the bulk of geochemical studies concentrated on the outer calcite shell layer. It is believed that shell material is precipitated from the EPF (Wilbur 1972) and the regulation of aragonite-calcite polymorphism depends on the concentrations of ions in the EPF (Kitano et al. 1979, Lorens and Bender 1980, Wilbur and Bernhardt 1984, Niedermayr et al. 2010). Magnesium (Mg<sup>2+</sup>) in particular, which inhibits calcite formation and favors the formation of aragonite, has been subject of these studies. As early as in 1855 Frémy reported insoluble shell organic matrices which he named Conchiolin. Further studies observed different organic molecules (also in the EPF) and interlamellar sheets which were found to influence crystal formation at the mineralizing front (e.g. Mutvei 1969, Kitano et al. 1969, Crenshaw 1972, Misogianes and Chasteen 1979, Wheeler and Sikes 1984, Wheeler 1992). They have been suggested to form complexes with calcium (Misogianes and Chasteen 1979). Furthermore, the enzyme carbonic anhydrase (CA) which catalyses the conversion of carbon dioxide and water into carbonic acid, protons and bicarbonate has been found to catalyze shell formation (Wilbur and Saleuddin 1983). Kobayashi (1964) showed that the EPF of calcite-shell producers has a different composition with respect to proteins, from the EPF of bivalves which have pure aragonite or bimineralic shells. Falini et al. (1996) showed for the first time that organic macromolecules ( $\beta$ -chitin,

silk fibroin and aspartate-rich soluble macromolecules) are the determining molecules for the precipitation of either aragonite or calcite. Multiple studies reported several organic compounds such as different proteins, glycoproteins, chitin, silk and amino acids as being involved in mollusk shell formation (see Samata 2004 for a review). In 2001, Hattan et al. investigated the EPF (probably the inner type) of *Mytilus edulis* and found the major acidic glycoprotein component of the EPF to be a 56,000 molecular weight glycoprotein that is a homodimer composed of 14.3 % carbohydrate. It reversely binds to calcium and appears to be a building block of the soluble organic shell matrix. Miyamoto et al. (2005) suggested that Nacrein is a negative regulator in calcification of *Pinctada fucata*. Nacrein, an organic matrix protein that accumulates in shells, is composed of an anhydrase domain and a Gly-X-Asn repeat domain. Recent studies increasingly demonstrate how complex the biological mechanisms are and propose different calcification models. Some of them are summarized here.

Levi-Kalishman et al. (2001) presented a scheme of dematerialized *Atrina serrata* nacreous layer organic matrix composed of  $\beta$ -chitin, silk-like proteins, and acidic glycoproteins rich in aspartic acid. Addadi et al. (2006) suggested a microenvironment formed by 2  $\beta$ -chitin layers where nacre formation occurs. It is proposed to be filled with a gel of silk-like protein which may inhibit non-specific crystallization and already be loaded with colloidal mineral particles (Addadi et al. 2006). When a mineral grows (induced by acidic proteins) water and silk are displaced. In comparison to the study of Addadi et al. (2006), who investigated nacre, Nudelman et al. (2007) investigated the prismatic calcite layer of *Atrina rigida*. They proposed that prism growth starts by deposition of a dense chitin fibers, meshwork on top of an already formed mineral layer. Afterwards, amorphous calcium carbonate (ACC) crystallizes by epitaxial nucleation on the chitin fibers, forming a new calcite layer. It occludes the chitin within the crystals. Suzuki et al. (2009) identified acidic matrix proteins (Pif 80 and Pif 97) in the pearl oyster *Pinctada fucata*. Their results strongly indicate that Pif regulates nacre formation. They suggest that the protein complex is formed in the mantle epithelial cells and secreted into the EPF. While Pif 97 might bind to chitin microfibrils Pif 80 might concentrate calcium carbonate and induce aragonite crystal formation. An extension of the model suggested by Suzuki et al. (2009) was presented by Weiss (2010). Weiss (2010) proposes among others a model combining the results from Falini et al. (1996), Levi-Kalishman et al. (2001) and Suzuki et al. (2009), where nacre formation occurs by means of Pif complex in a microenvironment separated by two chitin layers.

Adjacent to calcification models focused on the organic components involved, McConnaughey and Gillikin (2008) investigated and reviewed already existing data with respect to carbon isotopes ( $\delta^{13}\text{C}$ ) in mollusk shell carbonates, to better understand the calcification mechanisms. They concluded that the shell carbon in aquatic mollusks is mainly derived from ambient  $C_T$ .

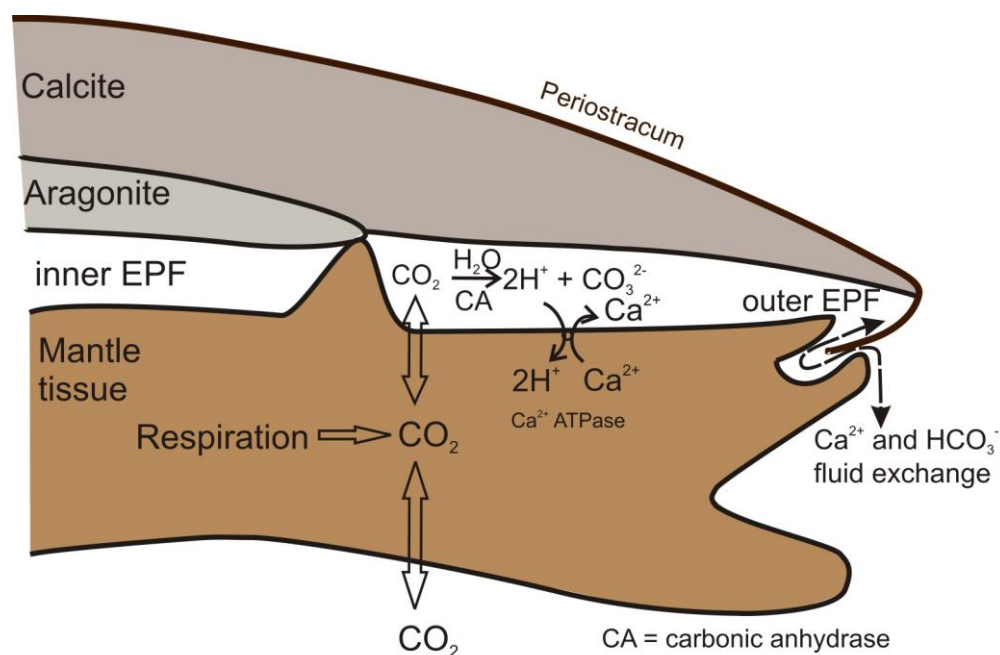


Figure 1.4: Modified schematic anatomy of a bivalve (redrawn after McConnaughey and Gillikin 2008).

They proposed a model (Figure 4) with likely transport routes of Ca<sup>2+</sup> and the inorganic carbon. According to this model, HCO<sub>3</sub><sup>-</sup> may enter the EPF by fluid exchange around the periostracum and by transport through the mantle. It will then be deprotonated in the EPF to yield CO<sub>3</sub><sup>2-</sup>. CO<sub>2</sub> diffuses from the mantle tissues into the EPF, and reacts with H<sub>2</sub>O and OH<sup>-</sup> to produce CO<sub>3</sub><sup>2-</sup>. Based on studies of pH regulation in the EPF of bivalves (Crenshaw and Neff 1969, Ip et al. 2006) their model assumes that EPF pH is raised under calcifying conditions (by ca 0.5 units) which would then elevate the CO<sub>3</sub><sup>2-</sup> concentration. They suggested the Ca<sup>2+</sup>-ATPase could be responsible for the alkaline EPF as it exchanges Ca<sup>2+</sup> and H<sup>+</sup>. Following the authors the consequence of an increasing EPF pH would be a conversion of CO<sub>2</sub> into HCO<sub>3</sub><sup>-</sup> catalyzed by carbonic anhydrase (CA). This modification of the carbonate system causes a diffusive CO<sub>2</sub> influx, CO<sub>3</sub><sup>2-</sup> accumulation and therefore a CaCO<sub>3</sub> super saturation (Cohen and McConnaughey 2003). However, elevated pH values in the EPF could not be observed in *M. edulis* from Kiel Fjord (Thomsen et al. 2010, Chapter 4).

The whole mechanism of biomineralization in bivalves is still insufficiently understood and research in different fields focusing on several perspectives has to be done and to be combined with each other.



#### I.4 The blue mussel - *Mytilus edulis*

One of the most important and abundant calcifying organisms in several shallow marine ecosystems is the common blue mussel, *Mytilus edulis* (Linné 1758) (Figure I.5) belonging to the phylum Mollusca and the family Mytilidae. The reproductive cycle depends on food supply and the time varies in different areas. In Kiel Bight the spawning period starts in June (Boje 1965).

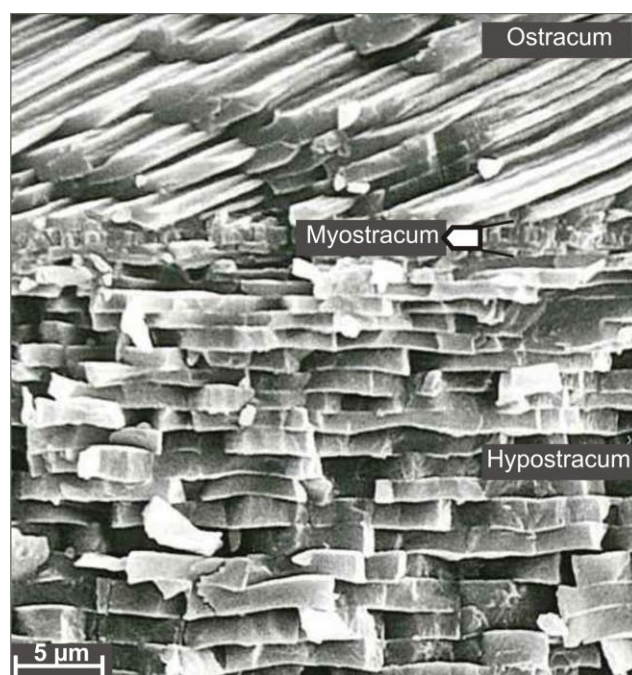


Figure I.5: *Mytilus edulis* (Linné 1758)

The first development stage is the ciliated embryo which differentiates to the non-feeding trochophore within 24 h. The following veliger stage is characterized by, amongst others, the secretion of a thin shell layer (prodissoconch I) by the shell gland and then initial production of the prodissoconch II. The prodissoconch II is characterized by the development of a pronounced umbo. Afterwards the pediveliger develops and makes contact with the substrate. Then the larva metamorphoses into the juvenile form (plantigrade) and attaches with byssus threads (primary settlement). After growing to about 1.5 mm shell length the plantigrades release themselves from the filamentous substrate and produce new byssus threads to attach themselves when they contact adult mussels (reference for whole live history: Newell 1989). Settled adult *M. edulis* live semi-sessile. Therefore, it is exposed to several different abiotic stressors such as e.g. hypoxia. *M. edulis* lives attached to rocks and other solid substrates (Seed and Suchanek 1992) or as loose beds on sandy substrata (Lozan et al. 1996). *M. edulis* is highly tolerant to a wide range of environmental conditions such as salinity (~5-33) and temperature (5-29 °C) and is an important engineer in several ecosystems as it provides a habitat for other animals. For example Markert et al. (2010) found *Crassostrea gigas* settling predominantly on intertidal *M. edulis* beds. In some areas of the Baltic Sea this species makes up to 80 % of the macro benthic biomass forming huge mussel beds (Jansson and Kautsky 1977, Suchanek 1985, Enderlein and Wahl 2004). The major protection of bivalves against predators is their shell. The shell of *M. edulis* is composed by an inner aragonitic nacre layer (Hypostracum) and an outer calcitic prism layer (Ostracum) which is covered by an organic layer (Periostracum) (Wilbur 1972). The two carbonate layers are separated by a thin band (~4 µm, Myostracum) of irregular aragonite prisms (Bourgoin 1988) (Figure I.6). The inner aragonitic layer consists of tablet-like crystals deposited in regular layers parallel to the shell interior while the outer calcitic layer consists of columnar polygonal prisms arranged in sheet-like rows (Bourgoin 1988). *M. edulis* grows posteriorily from the umbo region where the first stages of shell mineralization are recorded (Lutz and Kennish 1992). The shell is precipitated in a space which is restricted by the old shell, the periostracum, and the outer mantle

margin (Wilbur and Saleuddin 1983). The majority (up to 83 %) of *M. edulis* shells is made of aragonite (e.g. Hubbard et al. 1981) which is 50 % more soluble than calcite (Berner 1975).

Baltic blue mussels form thinner shells smaller in length than North Sea mussels probably as a result of lower salinity (Seed 1968, Kautsky et al. 1990). *M. edulis* also is a highly efficient filter feeder and thus provides a main trophic link between phytoplankton and benthos and significantly reduces water turbidity (Kautsky 1981; Kautsky and Evans 1987; Lozan et al. 1996). Furthermore, it plays a major role in aquaculture as global production of *M. edulis* was 391,210 tons in 2005, of which 93 % were produced in Europe (FAO 2008) where it is the primary bivalve species cultured.



*Figure 1.6:* SEM-image of a shell cross section from *Mytilus edulis*. The top of the images shows the calcite needles of the outer shell layer (the organic periostracum is not shown). The arrow indicates the irregular prisms of the Myostracum and below the nacre layer (Hypostracum) can be seen.

Due to its importance in aquaculture (Gosling 1992), usefulness as a monitor of water quality (Gordon et al. 1980), and presence in archaeological middens (Killingley 1981) *M. edulis* has been extensively studied and is the subject of different research fields. In geochemistry, bivalves including *M. edulis* are often studied to reconstruct paleo-climate. Its longevity (50–100 years in undisturbed patches (Suchanek 1981)) gives *M. edulis* the potential of being a good archive of past environmental changes. They are widely distributed (Gosling 1992) and geological old (Seed 1976). The family Mytilidae is believed to have its origin in the Devonian era (Soot-Ryen 1969). However, several studies on different bivalve species show contradictory results regarding the use of bivalve shells as a proxy archive (e.g. Klein et al. 1996b, Vander Putten et al. 2000, Gillikin et al. 2005, Carré et al. 2006, Heinemann et al. 2008).

## I.5 Can bivalve shells tell the past and show the future?

Understanding the climate conditions and changes of the past is the basis to improve climate models and allow predictions of the future. But as it is not possible to observe these environmental parameters directly, a tool for reconstruction is needed. Variables such as temperature, salinity and pH influence sediments and biominerals in a measurable way and therefore the past can possibly be mirrored by proxies. But the application of most proxies is challenging, as the underlying processes are still poorly understood. Furthermore, biology controls the mechanism of mineralization in many species (so-called “vital effect”) and thus conceals a possible record. Several elemental and isotope ratios have been proven valuable in different species for their suitability as proxies for e.g. paleo-temperature. The stable fractionation of oxygen isotopes ( $\delta^{18}\text{O}$ ) was found to reflect changes in temperature as well as ice volume already in the middle of the last century (Emiliani 1955). The carbon isotope ratio ( $\delta^{13}\text{C}$ ) of shell material is primarily a function of dissolved inorganic carbon ( $C_T$ ) in the habitat (e.g. Graham et al. 1981) and serves as tool for the reconstruction of changes in carbon sources and sinks. These traditional, well-established proxies have been complemented by a series of new proxies (e.g. Mg/Ca, Sr/Ca, B/Ca,  $\delta^{44}\text{Ca}$ ,  $\delta^{11}\text{B}$ ,  $\delta^{26}\text{Mg}$ ,  $^{87}\text{Sr}/^{86}\text{Sr}$ ). Calcium isotope ratios derived from foraminifera and bivalve shells have been shown to possibly provide paleo-temperatures (e.g. Nägler et al. 2000 Immenhauser et al. 2005). Strontium isotope ratios provide an important correlation tool in stratigraphic studies of marine sediments (e.g. DePaolo 1985) while magnesium isotope fractionation is dominated by weathering and dolomite formation (Pogge von Strandmann 2008). Minor and trace elements can displace  $\text{Ca}^{2+}$  or the carbonate ion ( $\text{CO}_3^{2-}$ ) during the calcification process. While  $\text{Mg}^{2+}$  and  $\text{Sr}^{2+}$  substitute  $\text{Ca}^{2+}$  in minor amounts, boron is believed to be incorporated into carbonates as  $\text{B}(\text{OH})_4^-$  (borate), replacing the carbonate ion in the lattice (Vengosch et al. 1991, Hemming and Hanson 1992, Hemming et al. 1995, Pagani et al. 2005, Klochko et al. 2009). The uptake of these elements is often a function of environmental conditions like temperature, salinity or pH. Mg/Ca ratios were shown to provide a temperature proxy in foraminifera (e.g. Nürnberg et al. 1996, Lea et al. 1999, Elderfield and Ganssen 2000, Kısakürek et al., 2008) and in corals (e.g. Mitsuguchi et al. 1996). A temperature relationship has also been found for Sr/Ca ratios, although no uniform calibration exists (Corrège 2006) and biological effects, rather than temperature, have been suggested to influence the coralline Sr/Ca. Analyzing B/Ca ratios is a very new approach and it has been shown that B/Ca is related to pH in different carbonates (Hemming and Hanson 1992, Hobbs and Reardon 1999, Sanyal et al. 2000, Foster et al. 2008). Ni et al. (2007) found a systematic increase of B/Ca in *G. ruber* and *G. sacculifer* with increasing test size and suggested growth rate variations influencing the incorporation of boron. Boron isotope ratios ( $\delta^{11}\text{B}$ ) have been measured in skeletons of different organisms such as corals (Reynaud et al. 2004, Hönisch et al. 2004) and foraminifera (Hönisch et al. 2003, Foster et al. 2008, Rollion-Bard and Erez 2010) as a pH proxy.

However, first of all an appropriate archive like ice cores, sediments or carbonates has to be available to reconstruct environmental conditions. Quite a few species like corals, foraminifera, coccolithophores and fish, build carbonate shells, skeletons or oolith which have been frequently used as proxy archives (see some examples given above). Bivalves could also fulfill this role as they are mostly sessile and therefore record changes in the environmental conditions at a particular site over many years. As several bivalve species are long living (Suchanek 1981, Schöne et al. 2005, Abele et al. 2008) changes over long time may be recorded in one individual. The high tolerance to a broad range of conditions and wide distribution (Gosling 1992) offers the possibility to investigate and compare individuals belonging to the same species but originating from extremely different areas. But still the mechanism of biomineralization in bivalves is poorly understood. As a result several studies on elemental ratios in the shells of different bivalve species showed contradictory results (e.g. Klein et al. 1996b, Vander Putten et al. 2000, Gillikin et al. 2005, Carré et al. 2006, Heinemann et al. 2008). Direct relationship between skeletal Mg/Ca and temperature was shown by Klein et al. (1996a) for *Mytilus trossulus* but could not be found for *Pecten maximus* (Lorrain et al. 2005). Freitas et al. (2005) observed Mg/Ca in *Pinna nobilis* shells to be sensitive to specimen age and no temperature dependency of Mg/Ca between different bivalve species was observed by Freitas et al. (2006). A salinity effect for Mg/Ca ratios in *M. edulis* calcite was reported (Dodd 1965). Sr/Ca seems to be influenced by both temperature and salinity (Dodd 1965, Wanamaker et al. 2008) but also by precipitation rates (Lorens 1981, Lorrain et al. 2005, Freitas et al. 2006). Klein et al. (1996b) found significantly higher Sr/Ca ratios in a young, rapidly grown *M. trossulus* than in a slowly grown adult individual, and concluded shell precipitation along lateral margins to be dominantly controlled by mantle metabolic activity at the site of carbonate formation. Carré et al. (2006) observed increasing Me/Ca ratios (for Mg, Ba, Mn and especially Sr) in aragonitic bivalve shells (*Mesodesma donacium*, *Chione subrugosa*) with increasing crystal growth rates and predicted a decreasing Ca<sup>2+</sup>-channel selectivity. Carré et al. (2006) suggested the Sr/Ca measurements from different sections of *M. trossulus* shells (measured by Klein et al. 1996b) can also be explained by differences in crystal growth. Takesue et al. (2008) found growth rate dependent alterations in Sr/Ca, B/Ca and Ba/Ca ratios in valves from *Corbula amurensis* and Ford et al. (2010) also showed Mg/Ca ratios in shells of *Mytilus californianus* to be a function of growth rate rather than of temperature. Recently, Schöne et al. (2010) found a strong influence of organic matrix on the determination of Mg<sup>2+</sup>, Sr<sup>2+</sup> and Ca<sup>2+</sup> in *Artica islandica*. Their results indicate that the insoluble organic matrix is strongly enriched in Mg<sup>2+</sup> and depleted in Sr<sup>2+</sup> and Ca<sup>2+</sup> when compared to the whole biomineral. To my knowledge no further studies of boron in bivalve shells have been published so far. On a poster presentation McCoy et al. (2009) showed that there is no distinct year-to-year correlation of boron concentrations in *M. californianus* shell and found organic-rich winter growth bands containing elevated B/Ca ratios. The authors concluded that biological control of pH and/or boron concentrations in the EPF are the reasons

for these observations. In general, a strong biological control seems to influence the calcification process (e.g. 2000, Gillikin et al. 2005, Carré et al. 2006, Heinemann et al. 2008, Heinemann et al. in press) and much more research is needed on the details of the biomineralization mechanisms and the elemental as well as isotope incorporation and transport in bivalves.

## I.6 Research questions and outline of the thesis

The main aim of this study was to better understand the sensitivity of *Mytilus edulis* to elevated  $p\text{CO}_2$ . A second goal was to test the suitability of the mytilid shell as a proxy archive in general and in particular for pH reconstruction. Physiological experiments can provide knowledge about acclimation reactions of marine organisms to abiotic stressors but not about their adaptation potential, as the relevant timescales cannot be simulated in laboratory studies. Therefore, experiments with already adapted animals from naturally  $\text{CO}_2$  enriched habitats are needed. Whole animal performance (e.g. growth rate and metabolism), acid-base status and calcification rates must be considered. For the use of *M. edulis* shells as a reliable proxy archive, a more detailed understanding of mechanisms controlling the elemental and isotopic composition of the shell is needed, including the examination of extracellular body fluids. Hence, this study is aimed at answering the following research questions:

- Are elemental ratios in *M. edulis* calcite controlled mainly by abiotic or biotic factors?
- How do shell growth and calcification respond to prolonged exposure to elevated seawater  $p\text{CO}_2$ ?
- Do elemental concentrations in the extracellular body fluids differ from those in seawater and shell?
- To which extent does the acid-base status of extracellular body fluids change under high  $p\text{CO}_2$  conditions and how does this influence the shell chemistry?
- Can B/Ca ratios and  $\delta^{11}\text{B}$  in *M. edulis* shell help to reconstruct paleo-pH?

This thesis is divided into four main chapters. Each of these chapters is divided into an abstract, introduction, material and method, results and discussion and a conclusion. In the **first Chapter** the biological and the environmental influence on elemental ratios (Mg/Ca and Sr/Ca) in the calcite of *M. edulis* were modeled. Shells of specimens, which were cultured under different salinities and temperature in a previous study, were analyzed via LA-MC-ICP-MS. In **Chapter 2**, the influence of elevated  $p\text{CO}_2$  on shell growth using different techniques (alkalinity anomaly technique, caliper measurements and  $\text{MnCl}_2$ -marking, optically and SEM) in a three month experiment was investigated. Trace metal concentrations ( $\text{Ca}^{2+}$ ,  $\text{Mg}^{2+}$  and  $\text{Sr}^{2+}$ ) of hemolymph (HL) and extrapallial fluid (EPF) samples from two experiments were measured via ICP-OES. In **Chapter 3**, an important new *in situ* method for the determination of stable boron isotope ratios ( $\delta^{11}\text{B}$ ) in carbonates using LA-MC-ICP-MS was described which was necessary for the investigations presented in Chapter 4. In **Chapter 4**  $\delta^{11}\text{B}$  was measured in the shell of *M. edulis* held under hypercapnia conditions. In this chapter also B/Ca and the acid-base status in the extracellular body fluids were determined.

**My contributions to the Chapters were as followed:**

Chapter 1: Agnes Heinemann, Claas Hiebenthal, Jan Fietzke, Anton Eisenhauer, Martin Wahl; Disentangling the Biological and Environmental Control of *M. edulis* Shell Chemistry. *Geochemistry Geophysics Geosystems*. doi:10.1029/2010GC003340, in press.

The experiment was planned by myself and by JF, AE and MW. The sample selection and preparation was done by myself. The experiment and data analysis was performed by myself and JF. CH, MW and myself did statistical modeling. The manuscript was written by myself and partly by CH. JF, MW and AE assisted the manuscript preparation and did proofreading.

Chapter 2: Agnes Heinemann, Jörn Thomsen, Jan Fietzke, Magdalena A. Gutowska, Florian Böhm, Anton Eisenhauer, Dieter Garbe-Schönberg, Frank Melzner; The impacts of seawater carbonate chemistry on biomineralization and elemental concentrations of *Mytilus edulis* body fluids and its potential as a proxy archive. To be submitted.

The experiment and analysis were planned by myself and by JT, JF, MAG and FM. Setting up and supervising culture experiment was performed by myself and JT. The sample collection and preparation was done by myself, JT, and MAG. Alkalinity anomaly technique, caliper measurements and MnCl<sub>2</sub>-marking, optical observations and SEM investigations were performed by myself. I assisted and participated in ICP-OES and EMP analysis. The manuscript was written by myself. All co-authors helped improving the quality of the manuscript by discussion of the data and their interpretation and proofreading.

Chapter 3: Jan Fietzke, Agnes Heinemann, Isabelle Taubner, Florian Böhm, Jonathan Erez and Anton Eisenhauer; Boron isotope ratio determination in carbonates via LA-MC-ICP-MS using soda-lime glass standards as reference material. Published in *Journal of Analytical Atomic Spectrometry*.

I prepared samples and standard material, participated in LA-ICP-MS analysis and assisted the manuscript preparation.

Chapter 4: Agnes Heinemann, Jan Fietzke, Frank Melzner, Florian Böhm, Jörn Thomsen, Dieter Garbe-Schönberg, Anton Eisenhauer; Responses of *Mytilus edulis* extracellular body fluids and shell composition to decreased pH: acid-base status, trace elements and  $\delta^{11}\text{B}$ . Under review at *Chemical Geology*.

The experiment was planned by myself and by JT, JF, and FM. Setting up and supervising culture experiment was performed by myself and JT. The sample collection and preparation was done by myself and JT. I participated and assisted in ICP-OES and LA-ICP-MS analysis. LA-ICP-MS analysis was done by JF. The manuscript was written by myself. All co-authors helped improving the quality of the manuscript by discussion of the data and their interpretation and proofreading.

## I.7 Experimental setup

All *Mytilus edulis* investigated in this thesis originated from a subtidal population (approximately 1-2 m depth) in Kiel Fjord (Western Baltic Sea; 54° 19.8' N; 10° 9.0' E, Figure I.7).

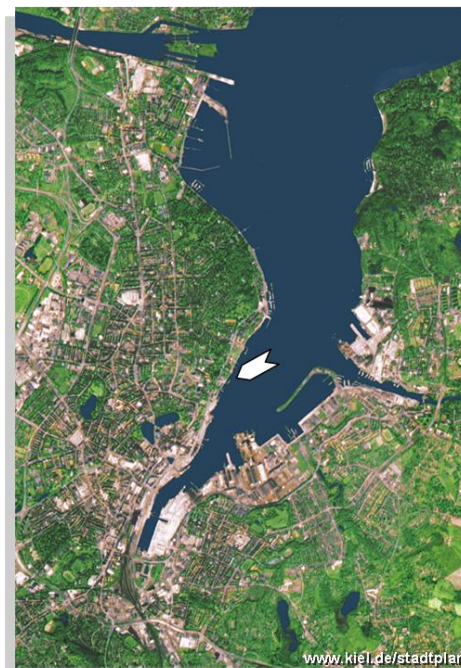


Figure I.7: Map of Kiel Fjord. Arrow marks the sampling site.

Shells were cleaned from epibionts and immediately transferred to aquaria with seawater flow-through (Figure I.8). The water originated from ~6 m depth nearby the sampling site. It was filtered through a series of 50, 20, and 5 m water filters, UV-sterilized and subsequently pumped at a rate of 5 l/min into a storage tank of 300 l volume. To keep the water air saturated it was aerated and mixed by a pump (universal pump 1260, Eheim, Deizisau, Germany) in the storage tank. The temperature of the water was kept constant by a flow-through cooler (TITAN 1500, Aqua Medic, Bissendorf, Germany). From the storage tank it was pumped to a header tank which provided the aquaria (16 l each) by gravity feed adjusted to 100 ml/min. The water level was kept constant in all tanks by overflow drain pipes. The experimental aquaria were continuously aerated with air-CO<sub>2</sub>-mixtures using aquarium diffuser stones (Dohse, Grafschaft-Gelsdorf, Germany). Gas mixtures containing different partial pressures of CO<sub>2</sub> were provided by a central air-CO<sub>2</sub>-mixing device at the IFM-GEOMAR. This CO<sub>2</sub> manipulation facility (Linde Gas & HTK Hamburg, Germany) measures ambient *p*CO<sub>2</sub> and adds the required amount of CO<sub>2</sub> to reach the pre-adjusted value into the air which is piped to the culturing rooms. The CO<sub>2</sub>-air mixtures were continuously added to the aquaria. Ambient water was used as control (390 μatm). *A<sub>T</sub>* values were measured by potentiometric open cell titration with hydrochloric acid (Mintrop et al. 2000, Dickson et al. 2007) with a VINDTA (Versatile Instrument for the Determination of Titration Alkalinity, MARIANDA, Kiel, Germany) autoanalyzer.



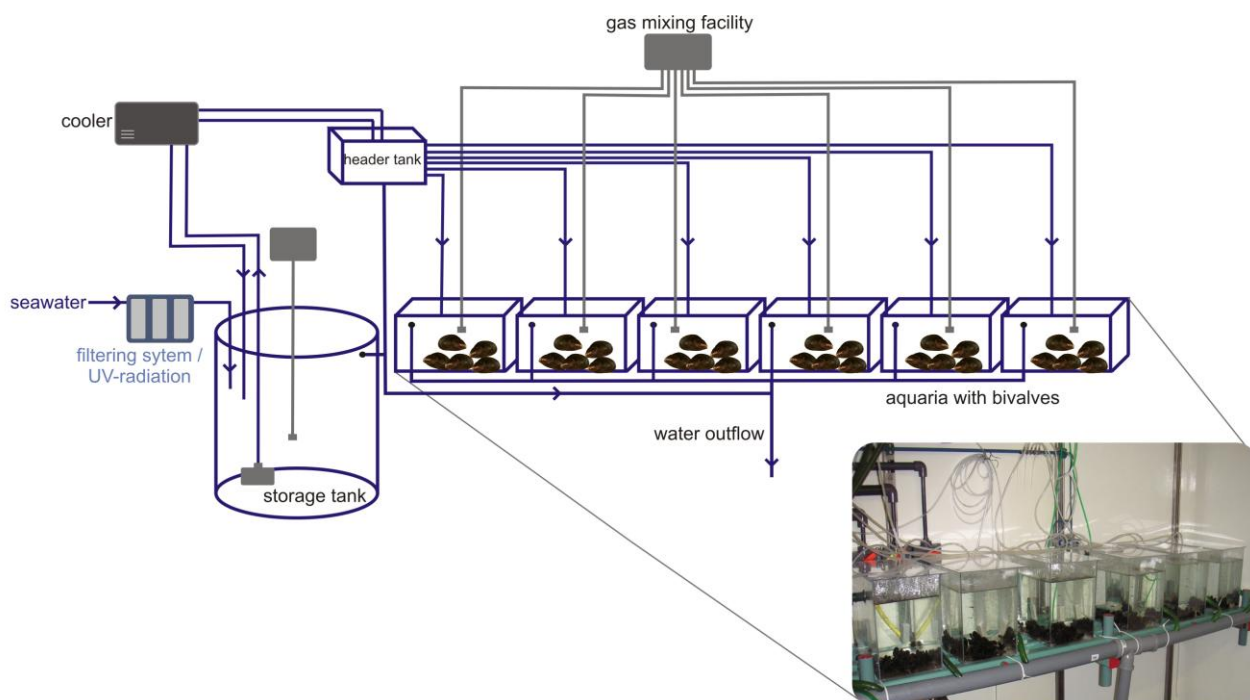


Figure 1.8: Scheme (modified after a scheme of J. Thomsen) and picture of the experimental setup.

$C_T$  values of treatment water were coulometrically measured after Dickson et al. (2007) with a SOMMA (Single-Operator Multi-Metabolic Analyzer, University of Rhode Island, Kingston, RI) autoanalyzer. Certified reference material provided by Andrew Dickson (Scripps Institution of Oceanography) was used for  $A_T$  and  $C_T$  measurements. Water  $p\text{CO}_2$  was calculated via CO2sys program (Dickson et al. 2003, Lewis and Wallace 1998) using the following parameters: Dissociation constants  $K_1$  and  $K_2$  (Mehrbach et al. 1973, Dickson and Millero 1987),  $\text{KHSO}_4$  dissociation constant (Dickson 1990) and  $\text{pH}_{\text{NBS}}$  scale.

Material and methods for the single experiments are described in each chapter. A detailed description of the method of boron isotope measurements (Chapter 4) is given in Chapter 3.

## References

- Abele, D., Strahl, J., Brey, T., Philipp, E., 2008. Imperceptible senescence: Ageing in the ocean quahog *Arctica islandica*. *Free Radical Res.* 42(5), 474-480.
- Addadi, L., Raz, S., Weiner, S., 2003. Taking advantage of disorder: amorphous calcium carbonate and its role in biomineralization. *Adv. Mater.* 15, 959-970.
- Addadi, L., Joester, D., Nudelman, F., Weiner, S., 2006. Mollusk shell formation: a source of new concepts for understanding biomineralization processes. *Chem. Eur. J.* 12, 980-987.
- Barthelat, F., Li, C.M., Comi, C., Espinosa, H.D., 2006. Mechanical properties of nacre constituents and their impact on mechanical performance. *J. Mater. Res.* 21, 1977-1986.
- Beldowski, J., Löffler, A., Schneider, B., Joensuu, L., 2010. Distribution and biogeochemical control of total CO<sub>2</sub> and total alkalinity in the Baltic Sea. *J. Marine Syst.* 81, 252-259. doi:10.1016/j.jmarsys.2009.12.020
- Berge, J., Bjerkgang, B., Pettersen, O., Schaanning, M., and Øxnevad, S. 2006. Effects of increased sea water concentrations of CO<sub>2</sub> on growth of the bivalve *Mytilus edulis* L. *Chemosphere*, 62(4), 681-687.
- Berner, R. A., 1975. The role of magnesium in the crystal growth of calcite and aragonite from sea water, *Geochim. Cosmochim. Acta* 39, 489-504.
- Bijma, J., Spero, H. J., and Lea, D. W.: Reassessing Foraminiferal Stable Isotope Geochemistry: Impact of the Oceanic Carbonate System (Experimental Results), in: *Use of Proxies in Paleooceanography: Examples from the South Atlantic.*, edited by: Fischer, G. and Wefer, G., 489-512, Springer-Verlag, Heidelberg, 1999.
- Boje, R., 1965. Die Bedeutung von Nahrungsfaktoren für das Wachstum von *Mytilus edulis* in der Kieler Förde und im Nord-Ostsee-Kanal. *Kieler Meeresforschung* 21, 81-100.
- Booth, C. E., McDonald, D. G., and Walsh, P. J., 1984. Acid-base-balance in the sea mussel, *Mytilus-edulis*, 1. Effects of hypoxia and airexposure on hemolymph acid-base status, *Mar. Biol. Lett.* 5, 347-358.
- Bourgoin, B. P., 1988. A Rapid and Inexpensive Technique to Separate the Calcite and Nacreous Layers in *Mytilus edulis* Shells. *Marine Environmental Research* 25, 125-129
- Caldeira, K. and Wickett, M.E., 2003. Anthropogenic carbon and ocean pH. *Nature.* 25(6956), 365-365.
- Cao, L. and Caldeira, K., 2008. Atmospheric CO<sub>2</sub> stabilization and ocean acidification. *Geophys. Res. Lett.* 35(19).
- Carré, M., Bentaleb, I., Bruguier, O., Ordinola, E., Barrett, N.T., Fontugne, M., 2006. Calcification rate influence on trace elements concentrations in aragonitic bivalve shells: Evidences and mechanisms. *Geochim. Cosmochim. Ac.* 70 (19), 4906-4920.
- Cochran, R. E. and Burnett L. E., 1996. Respiratory responses of the salt marsh animals, *Fundulus heteroclitus*, *Leiostomus xanthurus*, and *Palaemonetes pugio* to environmental hypoxia and hypercapnia and to the organophosphate pesticide, azinphosmethyl. *J. Exp. Mar. Biol. Ecol.* 195(1), 125-144.

- Cohen, A. L. and McConnaughey, T., 2003. Geochemical perspectives on coral mineralization. In: Dove, P. M., De Yoreo, J. J. and Weiner, S. (eds) *Biom mineralization. Reviews in Mineralogy and Geochemistry* 54, 151–187.
- Corrège, T., 2006. Sea surface temperature and salinity reconstruction from coral geochemical tracers. *Palaeogeogr. Palaeoclimatol.* 232, 408–428.
- Crenshaw, M. A. and Neff, J. M., 1969. Decalcification at the mantle-shell interface in molluscs. *Am. Zool.* 9, 881–889.
- Crenshaw, M. A., 1972. Inorganic composition of molluscan extrapallial fluid. *Biol. Bull.* 143, 506–512.
- Cusack, M. and Freer, A., 2008. Biom mineralization: Elemental and Organic Influence in Carbonate Systems. *Chem. Rev.* 108, 4433–4454
- DePaolo, D. J., and Ingram, B. L., 1985. High-resolution stratigraphy with strontium isotopes. *Science* 227, 938–940.
- De Waele, A., 1930. Le sang d'*Anodonta cygnea* et la formation de la coquille. *Mém. Acad. Roy. Belg., Cl. Sci.*, 10: 1-52
- Dickson, A. G., and Millero, F. J., 1987. A comparison of the equilibrium-constants for the dissociation of carbonic-acid in seawater media, *Deep-Sea.* 34, 1733-1743.
- Dickson, A. G., 1990. Standard potential of the reaction  $-AgCl_s + 1/2 H_2 = Ag_s + HCl_{aq}$  and the standard acidity constant of the ion  $HSO_4^-$  in synthetic sea-water from 273.15-K to 318.15-K. *J. Chem. Thermodyn.* 22, 113-127.
- Dickson, A. G., Afghan J. D., Anderson, G. C., 2003. Reference materials for oceanic CO<sub>2</sub> analysis: a method for the certification of total alkalinity. *Mar. Chem.* 80(2-3), 185-197.
- Dickson, A. G., Sabine, C. L., Christian, J. R., 2007. Guide to best practices for ocean CO<sub>2</sub> measurements. *PICES Special Publication 3, IOCCP Report No. 8.* 191 pp.
- Dodd, J. R., 1965. Environmental control of strontium and magnesium in *Mytilus edulis*. *Geochim. Cosmochim. Ac.* 29 (5), 385-398.
- Doney, S. C., Fabry, V. J., R., Feely, R. A., Kleypas, J. A., 2009. Ocean Acidification: The Other CO<sub>2</sub> Problem. *Annu. Rev. Mar. Sci.* 1, 169–92.
- Dupont, S., Havenhand, J., Thorndyke, W., Peck, L., Thorndyke, M., 2008. Near-future level of CO<sub>2</sub>-driven ocean acidification radically affects larval survival and development in the brittlestar *Ophiothrix fragilis*, *Mar. Ecol.-Prog. Ser.*, 373, 285– 294.
- Elderfield, H. and Ganssen, G., 2000. Past temperature and delta O-18 of surface ocean waters inferred from foraminiferal Mg/Ca ratios. *Nature* 405(6785), 442-445.
- Emiliani, C., 1955. Pleistocene temperatures. *J. Geol.* 63, 538–578.
- Enderlein, P. and M. Wahl, 2004. Dominance of blue mussels versus consumer-mediated enhancement of benthic diversity. *J. Sea Res.* 51(2), 145-155.

- Fabry, V. J., Seibel, B. A., Feely, R. A., and Orr, J. C., 2008. Impacts of ocean acidification on marine fauna and ecosystem processes. *ICES J. Mar. Sci.* 65, 414–432.
- Falini, G., Albeck, S., Weiner, S., Addadi, L., 1996. Control of aragonite or calcite polymorphism by mollusk shell macromolecules. *Science* 271, 67–69.
- FAO (2008) Global aquaculture production 1950–2005. FIGIS, fisheries global information system.
- Feely, R. A., Sabine, C. L., Lee, K., Berelson, W., Kleypas, J., Fabry, V. J., Millero, F. J., 2004. Impact of anthropogenic CO<sub>2</sub> on the CaCO<sub>3</sub> system in the oceans. *Science* 305(5682), 362–366.
- Ford, H., Schellenberg, S. A., Becker, B. J., Deutschman, D. L., Dyck, K. A., Koch P. L., 2010. Evaluating the skeletal chemistry of *Mytilus californianus* as a temperature proxy: Effects of microenvironment and ontogeny *Paleoceanography* 25, PA1203, doi:10.1029/2008PA001677
- Foster, G. L., 2008. Seawater pH, pCO<sub>2</sub> and [CO<sub>3</sub><sup>2-</sup>] variations in the Caribbean Sea over the last 130 kyr: A boron isotope and B/Ca study of planktic foraminifera. *Earth Planet. Sci. Lett.* 271, 254–266, doi:10.1016/j.epsl.2008.04.015.
- Frankignoulle, M., Bourge, I., Wollast, R., 1996. Atmospheric CO<sub>2</sub> fluxes in a highly polluted estuary (the Scheldt). *Limnol. Oceanogr.* 41(2), 365–369.
- Freitas, P., Clarke L. J., Kennedy, H., Richardson, C., Abrantes, F., 2005. Mg/Ca, Sr/Ca, and stable-isotope (delta O-18 and delta C-13) ratio profiles from the fan mussel *Pinna nobilis*: Seasonal records and temperature relationships. *Geochem. Geophys. Geosys.* 6, Q04D14, doi:10.1029/2004GC000872, 2005.
- Freitas, P., Clarke L. J., Kennedy, H., Richardson, C., Abrantes, F., 2006. Environmental and biological controls on elemental (Mg/Ca, Sr/Ca and Mn/Ca) ratios in shells of the king scallop *Pecten maximus*, *Geochim. Cosmochim. Ac.*, 70, 5119–5133.
- Frémy, M.E., 1855. *Ann. Chim. Phys.* 43, 45–107.
- Furuhashi, T., Schwarzinger, C., Miksik, I., Smrz, M., Beran, A., 2009. Molluscan shell evolution with review of shell calcification hypothesis. *J. Comp. Biochem. Physiol. B* 154, 351–371
- Gattuso J.-P., Frankignoulle M., Bourge I., Romaine S., Buddemeier R. W., 1998. Effect of calcium carbonate saturation of seawater on coral calcification. *Global and Planetary Change* 18(1-2), 37-46.
- Gazeau, F., Quiblier, C., Jansen, J. M., Gattuso, J.-P., Middelburg, J. J., Heip, C. H. R., 2007. Impact of elevated CO<sub>2</sub> on shellfish calcification, *Geophys. Res. Lett.* 34, 5.
- Gazeau, F., Gattuso, J.-P., Dawber, C., Pronker, A. E., Peene, F., Peene, J., Heip, C. H. R., Middelburg, J. J. 2010. Effect of ocean acidification on the early life stages of the blue mussel (*Mytilus edulis*). *Biogeosciences Discuss.* 7, 2927–2947. doi:10.5194/bgd-7-2927-2010.
- Gillikin D. P., Lorrain A., Navez J., Taylor J. W., Keppens E., Baeyens W., Dehairs F., 2005. Strong biological controls on Sr/Ca ratios in aragonitic marine bivalve shells. *Geochem. Geophys. Geosyst.* 6, Q05009 doi:10.1029/2004GC000874.
- Gordon, M., Knauer, G. A., Martin, J. H., 1980. *Mytilus californianus* as a bioindicator of trace metal pollution: Variability and statistical considerations. *Mar. Pollut. Bull.* 11, 195–198, doi:10.1016/0025-326X(80)90492-0.

- Gosling, E. 1992. Systematics and Geographic Distribution of *Mytilus*, in Gosling, E. (Ed.) The Mussel *Mytilus*: Ecology, Physiology, Genetics and Culture. Amsterdam, Elsevier Science Publishers B.V. pp. 1-19.
- Graham, D. W., Corliss, B. H., Bender, M. L., Keigwin, L. D. Jr., 1981. Carbon and oxygen isotopic disequilibria of recent deep-sea benthic foraminifera. *Mar. Micropaleont.* 6(5-6), 483-497.
- Gutowska, M. A., Pörtner, H.-O., Melzner F., 2008. Growth and calcification in the cephalopod *Sepia officinalis* under elevated seawater  $p\text{CO}_2$ . *Mar. Ecol.-Prog. Ser.* 373, 303-309.
- Gutowska, M. A., Melzner, F., Langenbuch, M., Bock, C., Claireaux, G., Pörtner, H. O., 2010. Acid-base regulatory ability of the cephalopod (*Sepia officinalis*) in response to environmental hypercapnia. *J. Comp. Physiol. B.* 180, 323-335.
- Hall-Spencer, J. M., Rodolfo-Metalpa, R., Martin, S., Ransome, E., Fine, M., Turner, S. M., Rowley, S. J., Tedesco, D., Buia, M. C., 2008. Volcanic carbon dioxide vents show ecosystem effects of ocean acidification. *Nature* 454, 96–99.
- Hare, C. E., Leblanc, K., DiTullio, G. R., Kudela, R. M., Zhang, Y., Lee, P. A., Riseman, S., Hutchins, D. A., 2007. Consequences of increased temperature and  $\text{CO}_2$  for phytoplankton community structure in the Bering Sea, *Mar. Ecol.-Prog. Ser.* 352, 9–16.
- Hattan, S. J., Laue, T. M., Chasteen, N. D., 2001. Purification and characterization of a novel calcium-binding protein from the extrapallial fluid of the mollusc, *Mytilus edulis*. *J. Biol. Chem.* 276, 4461-4468
- Heinemann, A., Fietzke, J., Eisenhauer, A., Zumholz, K., 2008. Modification of Ca isotope and trace metal composition of the major matrices involved in shell formation of *Mytilus edulis*. *Geochem. Geophys. Geosyst.* 9 (1), Q01006, doi:10.1029/2007GC001777.
- Heinemann, A., Hiebenthal, C., Fietzke, J., Eisenhauer, A., Wahl, M. Disentangling the Biological and Environmental Control of *M. edulis* Shell Chemistry. *Geochem. Geophys. Geosyst.* doi:10.1029/2010GC003340, in press.
- Heinemann, A., Fietzke, J., Melzner, F., Böhm, F., Thomsen, J., Garbe-Schönberg, D., Eisenhauer, A., Responses of *Mytilus edulis* extracellular body fluids and shell composition to decreased pH: acid-base status, trace elements and  $\delta^{11}\text{B}$ . Submitted to *Chemical Geology*.
- Hemming, N. G., Hanson, G. N., 1992. Boron isotopic composition and concentration in modern marine carbonates. *Geochim. Cosmochim. Ac.* 56, 537–543.
- Hemming N. G., Reeder R. J., Hart S. R., 1995. Mineral-fluid partitioning and isotopic fractionation of boron in synthetic calcium carbonate. *Geochim. Cosmochim. Ac.* 59, 371–379.
- Hinga K. R., 2002. Effects of pH on coastal marine phytoplankton. *Mar. Ecol. Prog. Ser.* 238:281–300.
- Hjalmarsson, S., Wesslander, K., Anderson, L. G., Omstedt, A., Perttila, M., Mintrop, L., 2008. Distribution, long-term development and mass balance calculation of total alkalinity in the Baltic Sea. *Cont. Shelf Res.* 28, 593–601.
- Hobbs, M. Y., Reardon, E. J., 1999. Effect of pH on boron coprecipitation by calcite: Further evidence for nonequilibrium partitioning of trace elements. *Geochim. Cosmochim. Ac.* 63, 1013-1021.

Hoegh-Guldberg, O., Mumby, P. J., Hooten, A. J., Steneck, R. S., Greenfield, P., Gomez, E., Harvell, C. D., Sale, P. F., Edwards, A. J., Caldeira, K., Knowlton, N., Eakin, C. M., Iglesias-Prieto, R., Muthiga, N., Bradbury, R. H., Dubi, A., Hatziolos, M. A., 2007. Coral Reefs Under Rapid Climate Change and Ocean Acidification. *Science* 318, 1737. DOI: 10.1126/science.1152509

Hönisch B., Bijma J., Russell A. D., Spero H. J., Palmer M. R., Zeebe R. E., Eisenhauer A., 2003. The influence of photosynthesis on the boron isotopic composition of foraminifera shells. *Mar. Micropaleontol.* 49, 87–96.

Hönisch, B., Hemming, N. G., Grottoli, A. G., Amat, A., Hanson, G. N., Bijma, J., 2004. Assessing scleractinian corals as recorders for paleo-pH: empirical calibration and vital effects. *Geochim. Cosmochim. Ac.* 68, 3675–3685.

Houghton, J., Ding, Y., Griggs, D., Noguer, M., van der Linden, P., Xiaosu, D., 2001. *Climate Change 2001: The Scientific Basis (Contribution of Working Group I to the Third Assessment Report of the IPCC)*. Cambridge University Press, Cambridge.

Hubbard F., McManus J., Al-Dabbas M., 1981. Environmental influences on the shell mineralogy of *Mytilus edulis*. *Geo.-Mar. Lett.* 1, 267–269.

Immenhauser, A., Nägler, T. F., Steuber, T., Hippler, D., 2005. A critical assessment of mollusk  $^{18}\text{O}/^{16}\text{O}$ , Mg/Ca, and  $^{44}\text{Ca}/^{40}\text{Ca}$  ratios as proxies for Cretaceous seawater temperature seasonality. *Palaeogeogr. Palaeoclimatol.* 215(3-4), 221-237.

Ip, Y. K., Loong, A. M., Hiong, K. C., Wong, W. P., Chew, S. F., Reddy, K., Sivaloganathan, B., Ballantyne, J. S., 2006. Light induces an increase in the pH of and a decrease in the ammonia concentration in the extrapallial fluid of the giant clam *Tridacna squamosa*. *Physiol Biochem Zool.* 79(3), 656-64.

IPCC: *Climate Change 2007: The Physical Science Basis. Contribution of Working Group I to the Fourth Assessment Report of the Intergovernmental Panel on Climate Change*, Cambridge University Press, Cambridge, United Kingdom and New York, NY, USA, 2007.

Jacob, D. E., Wirth, R., Soldati, A. L., Wehrmeister, U., Schreiber, A., (2010). Amorphous calcium carbonate in the shells of adult Unionoida. *J. Struct. Biol.* 10.1016/j.jsb.2010.09.011.

Jackson, A. P., Vincent, J. F. V., Turner, R. M., 1990. Comparison of nacre with other ceramic composites. *J. Mater. Sci.* 25, 3173.

Jansson, A.-M. and Kautsky, N. 1977. Quantitative survey of hard bottom communities in a Baltic archipelago. *Biology of benthic organisms. 11th Europ. Symp. Mar. Biol.*, Galway, Oct. 1976 B. F. Keegan, P. O'Ceidigh and P. J. S. Boaden. Oxford, Perg. Press: 359-366.

Kautsky, N., 1981. On the trophic role of the blue mussel (*Mytilus edulis* L.) in a Baltic coastal ecosystem and the fate of the organic matter produced by the mussels. *Kieler Meeresforschung, Sonderheft* 5, 454-461.

Kautsky, N., Johannesson, K., Tedengren, M., 1990. Genotypic and phenotypic differences between Baltic and North Sea populations of *Mytilus edulis* evaluated through reciprocal transplantations: I. Growth and morphology. *Mar. Ecol. Prog. Ser.* 59, 203-210.

Kautsky, N. and Evans, S. 1987. Role of Biodeposition by *Mytilus edulis* in the Circulation of Matter and Nutrients in a Baltic Coastal Ecosystem. *Mar. Ecol.-Prog. Ser.* 38(3), 201-212.

- Killingley, J. S., 1981. Seasonality of mollusk collecting determined from O-18 profiles of midden shells, *Am. Antiq.* 46, 152 – 158. doi:10.2307/279994.
- Kim, J.-M., Lee, K., Shin, K., Kang, J.-H., Lee, H.-W., Kim, M., Jang, P.-G., Jang, M.-C., 2006. The effect of seawater CO<sub>2</sub> concentration on growth of a natural phytoplankton assemblage in a controlled mesocosm experiment, *Limnol. Oceanogr.* 51, 1629–1636.
- Kısakürek, B., Eisenhauer, A., Böhm, F., Garbe-Schönberg, D., Erez, J., 2008. Controls on shell Mg/Ca and Sr/Ca in cultured planktonic foraminiferan, *Globigerinoides ruber* (white). *Earth Planet. Sc. Lett.* 273 (3-4), 260-269. ISSN 0012-821X.
- Kitano, Y., Kanamori, N., Tokuyama, A., 1969. Effects of Organic Matter on Solubilities and Crystal Form of Carbonates. *Am. Zool.* 9, 681.
- Kitano, Y., Akira, T., Arakaki, T., 1979. Magnesium calcite synthesis from calcium bicarbonate solution containing magnesium and barium ions. *Geochem. J.* 13, 181–185.
- Klein, R. T., Lohmann, K. C., Thayer, C. W., 1996a. Bivalve skeletons record sea-surface temperature and δ<sup>18</sup>O via Mg/Ca and <sup>18</sup>O/<sup>16</sup>O ratios. *Geology* 24 (5), 415-418.
- Klein, R. T., Lohmann, K. C., Thayer, C. W., 1996b. Sr/Ca and <sup>13</sup>C/<sup>12</sup>C ratios in skeletal calcite of *Mytilus trossolus*: covariation with metabolic rate, salinity and carbon isotopic composition of sea water. *Geochim. Cosmochim. Ac.*, 60, 4207-4221.
- Kleypas, J. A., Buddemeier, R. W., Archer, D., Gattuso, J.-P., Langdon, C., Opdyke, B. N., 1999. Geochemical consequences of increased atmospheric CO<sub>2</sub> on coral reefs. *Science* 284, 118-120.
- Klochko K., Cody G. D., Tossell J. A., Dera P., Kaufman A. J., 2009. Re-evaluating boron speciation in biogenic calcite and aragonite using <sup>11</sup>B MAS NMR. *Geochim. Cosmochim. Ac.* 73, 1890–1900.
- Knoll A. H., Fairchild I. J. , Swett K., 1993. Calcified microbes in Neoproterozoic carbonates: implications for our understanding of the Proterozoic-Cambrian transition. *Palaios* 8 ,512–525.
- Knoll A. H., 2003. Biomineralization and evolutionary history. In: Dove, P. M., De Yoreo, J. J., Weiner, S. (eds). *Biomineralization. Reviews in Mineralogy and Geochemistry* 54, 329–356.
- Kobayashi, S., 1964. Calcification in fish and shellfish. II. A paper electrophoretic study on the acid mucopolysaccharides and PAS positive materials of the extrapallial fluid in some molluscan species. *Bull. Jap. Soc. Sci. Fish.* 30, 893–907.
- Krampitz, G. and Graser, G., 1988. Molecular Mechanisms of Biomineralization in the Formation of Calcified Shells. *Anqew Chem Inr Ed Engl* 27, 1145-1156.
- Kuffner, I. B., Andersson, A. J., Jokiel, P. L., Rodgers, K. S., Mackenzie, F. T., 2008. Decreased abundance of crustose coralline algae due to ocean acidification. *Nature Geosci.* 1, 114-117.
- Kurihara, H., Ishimatsu, A., 2008. Effects of high CO<sub>2</sub> seawater on the copepod (*Acartia tsuensis*) through all life stages and subsequent generations. *Mar. Pollut. Bull.*, 56(6):1086-1090.
- Kurihara, H., Kato, S., Ishimatsu, A., 2007. Effects of increased seawater pCO<sub>2</sub> on early development of the oyster *Crassostrea gigas*. *Aquatic Biology* 1, 91-98.

- Langdon, C., Takahashi, T., Sweeney, C., Chipman, D., Goddard, J., Marubini, F., Aceves, H., Barnett, H., Atkinson, M. J., 2000. Effect of calcium carbonate saturation state on the calcification rate of an experimental coral reef. *Global Biogeochemical Cycles* 14, 639-654.
- Langdon, C., Broecker, W. S., Hammond, D. E., Glenn, E., Fitzsimmons, K., Nelson, S. G., Peng, T.-H., Hajdas, I., Bonani, G., 2003. Effect of elevated CO<sub>2</sub> on the community metabolism of an experimental coral reef. *Global Biogeochem. Cy.* 17(1), 1011, doi: 10.1029/2002GB001941.
- Lannig, G., Eilers, S., Pörtner, H. O., Sokolova, I. M., Bock, C., 2010. Impact of Ocean Acidification on Energy Metabolism of Oyster, *Crassostrea gigas*-Changes in Metabolic Pathways and Thermal Response. *Mar. Drugs* 8, 2318-2339. doi:10.3390/md8082318.
- Larsen, B., Pörtner, H., Jensen, F., 1997. Extra- and intracellular acid-base balance and ionic regulation in cod (*Gadus morhua*) during combined and isolated exposures to hypercapnia and copper. *Mar. Biol.*, 128(2), 337-346.
- Lea, D. W., Mashiotto, T. A., Spero, H. J., 1999. Controls on magnesium and strontium uptake in planktonic foraminifera determined by live culturing. *Geochim. Cosmochim. Ac.* 63, 2369-2379.
- Levi-Kalisman, Y., Falini G., Addadi, L., Weiner, S., 2001. Structure of the Nacreous Organic Matrix of a Bivalve Mollusk Shell Examined in the Hydrated State Using Cryo-TEM. *J. Struct. Biol.* 135, 8-17. doi:10.1006/jsbi.2001.4372
- Lewis, E. and Wallace, D., 1998. Program Developed for CO<sub>2</sub> System Calculations. ORNL/CDIAC-105. Carbon Dioxide Information Analysis Center, Oak Ridge National Laboratory, U.S. Department of Energy. Oak Ridge, Tennessee.
- Lindinger, M. I., Lauren, D. J., McDonald, D.G., 1984. Acid-base-balance in the sea mussel, *Mytilus edulis*. 3. Effects of environmental hypercapnia on intracellular and extracellular acid-base-balance, *Mar. Biol. Lett.* 5, 371-381.
- Lorens, R. B. and Bender, M. L., 1980. The impact of solution chemistry on *Mytilus edulis* calcite and aragonite. *Geochim. Cosmochim. Ac.* 44, 1265-1278.
- Lorens, R., 1981. Sr, Cd, Mn and Co distribution coefficients in calcite as a function of calcite precipitation rate. *Geochim. Cosmochim. Ac.* 45, 553-561.
- Lorrain, A., Gillikin, D., Paulet, Y.M., Chavaud, L., Lemercier, A., Navez, J., Andre, L., 2005. Strong kinetic effects on Sr/Ca ratios in the calcitic bivalve *Pecten maximus*. *Geology* 33, 965-968.
- Lowenstam, H. A. 1981. Minerals formed by organisms. *Science* 211, 1126-1131.
- Lowenstam, H. A. and Weiner, S., 1989. *On Biomineralization*. Oxford University Press, New York, 7-24,
- Lozan, J., Lampe, R., Matthäus, W., Rachor, E., Rumohr, H., v. Westernhagen, H., 1996. Warnsignale aus der Ostsee J. Lozan, R. Lampe, W. Matthäus et al. Berlin, Parey: 385.
- Lutz, R. A. and Kennish, M. J., 1992. Developments in Aquaculture and Fisheries Science, in *The Mussel Mytilus: Ecology, Physiology, Genetics and Culture*, ed. E. Gosling, Elsevier, Amsterdam, vol. 25, 53-85.
- Marin F. and Luquet, G., 2004. Molluscan shell proteins. *Comptes Rendus Palevol* 3, 469-492.



- Markert, A., Wehrmann, A., Kröncke, I., 2010. Recently established *Crassostrea*-reefs versus native *Mytilus*-beds: differences in ecosystem engineering affects the macrofaunal communities (Wadden Sea of Lower Saxony, southern German Bight). *Biol. Invasions* 12, 15–32. DOI 10.1007/s10530-009-9425-4.
- Martin, S. and Gattuso, J.-P., 2009. Response of Mediterranean coralline algae to ocean acidification and elevated temperature. 2009 Blackwell Publishing Ltd. *Issue Global Change Biology* 15(8), 2089–2100. DOI: 10.1111/j.1365-2486.2009.01874.x.
- McConnaughey, T. A. and Gillikin D. P., 2008. Carbon isotopes in mollusk shell carbonates. *Geo-Mar. Lett.* 28(5-6), 287-299.
- McCoy, S.J., Robinson, L.F., Pfister, C.A., Wootton, J., Shimizu, N., Glover, D.M., 2009. High-resolution B concentration analyses by SIMS in *M. californianus* as a potential record of ocean acidification American Geophysical Union, Fall Meeting 2009, abstract #V51E-1787.
- Mehrbach, C., Culberso, C.H., Hawley, J.E., Pytkowic, R.M., 1973. Measurement of apparent dissociation-constants of carbonic-acid in seawater at atmospheric-pressure. *Limnol. Oceanogr.* 18, 897-907.
- Melzner, F., Gutowska, M. A., Langenbuch, M., Dupont, S., Lucassen, M., Thorndyke, M. C., Bleich, M., Pörtner, H.-O., 2009. Physiological basis for high CO<sub>2</sub> tolerance in marine ectothermic animals: pre-adaptation through lifestyle and ontogeny?. *Biogeosciences* 6, 2313–2331. doi:10.5194/bg-6-2313-2009.
- Melzner, F., Stange, P., Trübenbach, K., Thomsen, J., Casties, I., Panknin, U., Gutowska, M. A., 2010. Interactive effects of food supply and seawater pCO<sub>2</sub> on calcification and internal shell dissolution in the blue mussel *Mytilus edulis*. submitted to PLoS ONE.
- Michaelidis, B., Ouzounis, C., Palaras, A., Pörtner, H.-O., 2005. Effects of long-term moderate hypercapnia on acid-base balance and growth rate in marine mussels *Mytilus galloprovincialis*. *Mar. Ecol.-Prog. Ser.* 293, 109-118.
- Michaelidis B., Spring A., Pörtner H.-O, 2007. Effects of long-term acclimation to environmental hypercapnia on extracellular acid-base status and metabolic capacity in Mediterranean fish *Sparus aurata*. *Mar. Biol.* 150, 1417-1429.
- Mintrop, L., Perez, F. F., Gonzalez-Davila, M., Santana-Casiano, M. J., Körtzinger, A., 2000. Alkalinity determination by potentiometry: Intercalibration using three different methods. *Cienc. Mar.* 26, 23-37.
- Misogianes, M. J., and Chasteen, N. D., 1979. Extrapallial fluid: a chemical and spectral characterization of the extrapallial fluid of *Mytilus edulis*. *Anal. Biochem.* 100, 324-334.
- Mitsuguchi, T., Matsumoto, E., Abe, O., Uchida, T., Isdale, P.J., 1996. Mg/Ca thermometry in coral skeletons. *Science* 274, 961–963.
- Miyamoto, H, Miyoshi F, Kohno J., 2005. The carbonic anhydrase domain protein nacrein is expressed in the epithelial cells of the mantle and acts as a negative regulator in calcification in the mollusc *Pinctada fucata*. *Zoolog Sci. Mar.* 22(3), 311-5.
- Mucci, A., 1983. The solubility of calcite and aragonite in seawater at various salinities, temperatures, and 1 atmosphere total pressure. *Am. J. Sci.* 238, 780–799.

Mutvei, H., 1969. On the micro and ultrastructure of conchiolin in the nacreous layer of some recent and fossil molluscs. *Stockholm Contr. Geol.* 20, 1–17.

Nägler, T. F., Eisenhauer, A., Müller, A., Hemleben, C., Kramers, J., 2000. The  $\delta^{44}\text{Ca}$ -temperature calibration on fossil and cultured *Globigerinoides sacculifer*: New tool for reconstruction of past sea surface temperatures. *Geochem. Geophys. Geosys.* 1(9), 2000GC000091.

Newell, R. I. E., 1959. Species profiles: Life histories and environmental requirements of coastal fishes and invertebrates (North and Mid-Atlantic): Blue mussel. *Biol. Report* 82: 11.102

Ni, Y., Foster, G. L., Bailey, B., Elliott, T., Schmidt, D. N., Pearson, P., Haley, B., Coath, C., 2007. A core top assessment of proxies for the ocean carbonate system in surface-dwelling foraminifers. *Paleoceanography* 22, PA3212. doi:10.1029/2006PA001337.

Niedermayr, A., Dietzel, M., Köhler, S.J., Petautschnig, S., 2010. Magnesium and Strontium Incorporation into Calcium Carbonate Polymorphs and ACC – Experimental Study. *Geophysical Research Abstracts* Vol. 12, EGU2010-12633.

Nudelman, F., Chen, H. H., Goldberg, H. A., Weiner, S., Addadi, L., 2007. Lessons from biomineralization: comparing the growth strategies of mollusc shell prismatic and nacreous layers in *Atrina rigida*. *Faraday Discuss.* 136, 9–25.

Nürnberg, D., Bijma, J., Hemleben, C., 1996. Assessing the reliability of magnesium in foraminiferal calcite as a proxy for water mass temperatures. *Geochim. Cosmochim. Ac.* 60(5), 803–814.

Orr, J. C., Caldeira, K., Fabry, V., Gattuso, J.-P., Haugan, P., Lehodey, P., Pantoja, S., Pörtner, H.-O., Riebesell, U., Trull, T., Urban, E., Hood, M., Broadgate, W., 2009. Research priorities for understanding ocean acidification: Summary from the Second Symposium on the Ocean in a High- $\text{CO}_2$  World. *Oceanography* 22(4), 182–189.

Pagani, M., Lemarchand, D., Spivack, A., Gaillardet, J., 2005. A critical evaluation of the boron isotope-pH proxy: the accuracy of ancient pH estimates. *Geochim. Cosmochim. Ac.* 69, 953–961.

Palacios, S., Zimmerman, R. C., 2007. Response of eelgrass *Zostera marina* to  $\text{CO}_2$  enrichment: possible impacts of climate change and potential for remediation of coastal habitats. *Mar. Ecol. Prog. Ser.* 344, 1–13.

Pane, E. F., Barry, J. P., 2007. Extracellular acid–base regulation during short-term hypercapnia is effective in a shallow-water crab but ineffective in a deep-sea crab. *Mar. Ecol. Prog. Ser.* 334, 1–9.

Pearson, P. N. and Palmer, J. D., 2000. Atmospheric carbon dioxide concentrations over the past 60 million years. *Nature* 406, 695–699.

Petit, J. R., Jouzel, J., Raynaud, D., Barkov, N. I., Barnola, J.-M., Basile, I., Bender, M., Chappellaz, J., Davis, M., Delaygue, G., Delmotte, M., Kotlyakov, V. M., Legrand, M., Lipenkov, V. Y., Lorius, C., Pépin, L., Ritz, C., Saltzman, E., Stievenard, M., 1999. Climate and atmospheric history of the past 420,000 years from the Vostok ice core, Antarctica. *Nature* 399, 429–436.

Pogge von Strandmann, P. A. E., 2008. Precise magnesium isotope measurements in core top planktic and benthic foraminifera. *Geochem. Geophys. Geosys.* 9, Q12015, doi:10.1029/2008GC002209.

Pörtner H.-O., Langenbuch, M., Reipschläger, A., 2004. Biological Impact of Elevated Ocean  $\text{CO}_2$  Concentrations: Lessons from Animal Physiology and Earth History. *J. Oceanogr.* 60, 705–718.

- Reynaud, S., Hemming, N. G., Leclerc, A. J., Gattuso, J.-P., 2004. Effect of  $p\text{CO}_2$  and temperature on the boron isotopic composition of the zooxanthellate coral *Acropora sp.*. *Coral Reefs* 23, 539–546. DOI 10.1007/s00338-004-0399-5.
- Riebesell, U., Zondervan, I., Rost, B., Tortell, P. D., Zeebe, R. E., Morel, F. M. M.: Reduced calcification of marine plankton in response to increased atmospheric  $\text{CO}_2$ . *Nature* 407, 364–367.
- Ries, J. B., Cohen, A. L., McCorkle, D. C., 2009. Marine calcifiers exhibit mixed responses to  $\text{CO}_2$ -induced ocean acidification. *Geology* 37, 1131–1134.
- Rollion-Bard, C. and Erez, J., 2010. Intra-shell boron isotope ratios in the symbiont-bearing benthic foraminiferan *Amphistegina lobifera*: Implications for  $\delta^{11}\text{B}$  vital effects and paleo-pH reconstructions. *Geochim. Cosmochim. Ac.* 74, 1530–1536.
- Sabine, C. L., Feely, R. A., Gruber, N., Key, R. M., Lee, K., Bullister, J. L., Wanninkhof, R., Wong, C. S., Wallace, D. W. R., Tilbrook, B., Millero, F. J., Peng, T. H., Kozyr, A., Ono, T., Rios, A. F., 2004. The oceanic sink for anthropogenic  $\text{CO}_2$ . *Science* 305(5682), 367–371.
- Samata, T., 2004. Recent advances in studies on nacreous layer biomineralization. *Molecular and cellular aspects. Thalassas* 20 (1), 25–44.
- Sanyal, A., Nugent, M., Reeder, R. J., Bijma, J., 2000. Seawater pH control on the boron isotopic composition of calcite: evidence from inorganic calcite precipitation experiments. *Geochim. Cosmochim. Ac.* 64, 1551–1555.
- Schöne, B. R., Fiebig, J., Pfeiffer, M., Gless, R., Hickson, J., Johnson, A. L. A., Dreyer, W., Oschmann, W., 2005. Climate records from a bivalved Methuselah (*Arctica islandica*, Mollusca; Iceland). *Palaeogeogr. Palaeoclimatol.* 228(1-2), 130–148.
- Schöne, B. R., Zhang, Z., Jacob, J., Gillikin, D. G., Tütken, T., Garbe-Schönberg, D., MacConnaughey, T., Soldati, A., 2010. Effect of organic matrices on the determination of the trace element chemistry (Mg, Sr, Mg/Ca, Sr/Ca) of aragonitic bivalve shells (*Arctica islandica*)-Comparison of ICP-OES and LA-ICP-MS data. *Geochem. J.* 44, 23–37.
- Seed, R., 1968. Factors influencing shell shape in the mussel *Mytilus edulis*. *J. Mar. Biol. Assoc. UK* 48, 561–584.
- Seed, R., 1969. The ecology of *Mytilus edulis* L. on exposed rocky shores. 1. Breeding and settlement. *Oecologia (Berlin)* 3, pp. 277–316.
- Seed, R. 1976. Ecology. In: Bayne, B. L. (Ed.), *Marine Mussels*. Cambridge Univ. Press, Cambridge, 13–66.
- Seed, R. and Suchanek, T., 1992. Population and community ecology of *Mytilus*. *The mussel Mytilus: ecology, physiology, genetics and culture*. E. Gosling. Amsterdam, Elsevier Science Publishers: 87–170.
- Soot-Ryen, T., 1969. Family Mytilidae Rafinesque 1815. In R. C. Moore (Ed.), *Treatise on Invertebrate Paleontology. Part N, Vol. 1, Mollusca 6, Bivalvia*. Geological Society of America and University of Kansas Press, Lawrence, N271–N280.
- Spicer, J. I., Raffo, A., Widdicombe, S., 2007. Influence of  $\text{CO}_2$ -related seawater acidification on extracellular acid–base balance in the velvet swimming crab *Necora puber*. *Mar. Biol.* 151, 1117–1125.

Stanley, S. M., and Hardie, L. A.. 1998. Secular oscillations in the carbonate mineralogy of reef-building and sediment-producing organisms driven by tectonically forced shifts in seawater chemistry. *Paleogr., Paleocl.* 144, 3-19.

Suchanek, T. H., 1981. The role of disturbance in the evolution of life history strategies in the intertidal mussels *Mytilus edulis* and *Mytilus californianus*. *Oecologia*, 50, 143 – 152. doi:10.1007/BF00348028.

Suchanek, T. H., 1985. Mussels and their role in structuring rocky shore communities. *The Ecology of Rocky Coasts*. P. G. Moore and R. Seed. London, Hodder and Stoughton: 70-96.

Suzuki, M., Saruwatari, K., Kogure, T., Yamamoto, Y., Nishimura, T., Kato, T., Nagasawa, H., 2009. An Acidic Matrix Protein, Pif, Is a Key Macromolecule for Nacre Formation. *Science* 325, 1388. DOI: 10.1126/science.1173793

Takesue, R. K., Bacon, C. R., Thompson, J. K., 2008. Influences of organic matter and calcification rate on trace elements in aragonitic estuarine bivalve shells. *Geochim. Cosmochim. Ac.* 72, 22, 5431-5445. doi:10.1016/j.gca.2008.09.003

Thomsen, J., Gutowska, M.A., Saphörster, J., Heinemann, A., Trübenbach, K., Fietzke, J., Hiebenthal, C., Eisenhauer, A., Körtzinger, A., Wahl, M., Melzner, F., 2010. Calcifying invertebrates succeed in a naturally CO<sub>2</sub> enriched coastal habitat but are threatened by high levels of future acidification. *Biogeosciences*, 7, 3879–3891. doi:10.5194/bg-7-3879-2010

Thomsen, J. and Melzner, F., 2010. Moderate seawater acidification does not elicit long-term metabolic depression in the blue mussel *Mytilus edulis*. *Mar. Biol.* 157(12), 2667-2676. DOI: 10.1007/s00227-010-1527-0

Tunnicliffe V., Davies, K. T. A., Butterfield, D. A., Embley, R. W., Rose, J. M., Chadwick Jr., W. W., 2009. Survival of mussels in extremely acidic waters on a submarine volcano. *Nature Geoscience*. DOI: 10.1038/NGEO500 .

Vander Putten, E., Dehairs, F., Keppens, E., Baeyens, W., 2000. High distribution of trace elements in the calcite shell layer of modern *Mytilus edulis*: Environmental and biological controls. *Geochim. Cosmochim. Ac.* 64(6), 997–1011.

Vengosh, A., Kolodny Y., Starinsky A., Chivas A. R., McCulloch, M.T., 1991. Coprecipitation and isotopic fractionation of boron in modern biogenic carbonates. *Geochim. Cosmochim. Ac.* 55, 2901–2910. doi:10.1016/0016-7037 (91)90455-E.

Waldbusser, G. G., Voigt, E. B., Bergschneider, H., Green, M. A., Newell, R. I. E., 2010. Biocalcification in the Eastern Oyster (*Crassostrea virginica*) in Relation to Long-term Trends in Chesapeake Bay pH. *Estuaries and Coasts*. DOI 10.1007/s12237-010-9307-0.

Wanamaker, A. D., Kreutz, K. J., Wilson, T., Borns, H. W., Introne, D. S., Feindel S., 2008. Experimentally determined Mg/Ca and Sr/Ca ratios in juvenile bivalve calcite for *Mytilus edulis*: implications for paleotemperature reconstructions. *Geo-Mar. Lett.* 28(5-6), 359-368.

Weiner, S., and Dove, P. M., 2003. An overview of biomineralization processes and the problem of vital effect, In *Biomineralization. Reviews in Mineralogy and Geochemistry* 54, edited by Dove, P. M., De Yoreo, J. J., Weiner, S., 1-29, Mineralogical Society of America, Geochemical Society.

Weiss, I. M., 2010. Jewels in the Pearl. *Chem. Bio. Chem.* 11, 297-300. DOI: 10.1002/cbic.200900677

Wheeler, A.P., 1992. Mechanisms of molluscan shell formation. In: Bonucci, E. (Ed.), *Calcification in Biological Systems*. CRC press, Boca Raton, FL, 179–216.

Wheeler, A. P. and Sikes, C. S., 1984. Regulation of Carbonate Calcification by Organic Matrix. *Amer. Zool.* 24, 933-944.

Wilbur K. M., 1972. Shell formation in molluscs. In: *Chemical Zoology Vol. 7* (eds M. Florkin and B. T. Scheer), Ch. 3, Academic Press.

Wilbur, K. and Saleuddin, A., 1983. Shell formation. *The Mollusca*. K. Wilbur. New York, London Academic Press. 4 Physiology Part 1, 235 ff.

Wilbur, K. M. and Bernhardt, A. M., 1984. Effects of Amino-Acids, Magnesium, and Molluscan Extrapallial Fluid on Crystallization of Calcium-Carbonate – Invitro Experiments. *Biol. Bull.* 166(1), 251-259.

Yamada Y and Ikeda T., 1999. Acute toxicity of lowered pH to some oceanic zooplankton. *Plankton Biol. Ecol.* 46, 62–67.

Zeebe, R. E. and Wolf-Gladrow, D., 2001. *CO<sub>2</sub> in Seawater: Equilibrium, Kinetics, Isotopes*. Elsevier Oceanography Series, 65, pp. 346, Amsterdam.

## Chapter 1

# **Disentangling the Biological and Environmental Control of *M. edulis* Shell Chemistry\***

\*Published in *Geochemistry Geophysics Geosystems* (in press) as: Agnes Heinemann, Claas Hiebenthal, Jan Fietzke, Anton Eisenhauer, Martin Wahl; Disentangling the Biological and Environmental Control of *M. edulis* Shell Chemistry.

## 1.1 Abstract

Blue mussel individuals (*Mytilus edulis*) were cultured at 4 different salinities (17, 20, 29, and 34). During the course of the experiment temperature was gradually increased from 6 °C to 14 °C. Mg/Ca and Sr/Ca ratios of the shell calcite portions produced during the 9 weeks of experimental treatment as well parts that were precipitated before the treatment phase were measured by LA-MC-ICP-MS (Laser Ablation-Multicollector-Inductively Coupled Plasma-Mass Spectrometry). Mg/Ca ratios show a positive correlation with temperature for individuals cultured at salinity 29 and 34 ( $\text{Mg/Ca [mmol/mol]} \sim (0.2-0.3) * T [^{\circ}\text{C}]$ ), while for individuals cultured at low salinities (17, 20) no trend was observed. Sr/Ca ratios were not affected by temperature but strongly by salinity. The data show very strong biological influence (“individual differences” and “physiological variability”) on elemental ratios (79 % on Mg/Ca and 41 % on Sr/Ca) in *M. edulis* calcite. The results challenge the use of blue mussel shell data as environmental proxies.

## 1.2 Introduction

Understanding climate history helps interpreting fluctuations or directional shifts of parameters like temperature or CO<sub>2</sub> in the context of global change. Biological climate archives are valuable records of environmental conditions during the lifetime of the organism. Mussels have the potential to provide high resolution records of a large variety of environmental regimes due to their high growth rate, global distribution (Gosling 1992) and tolerance to a broad range of environmental conditions (Seed and Suchanek 1992) and some bivalves are extremely long-lived (e.g. Schöne et al. 2005). Trace metal distributions (e.g. Mg and Sr) in bivalve shells are a field of current interest because as a proxy archive (e.g. Klein et al. 1996a/b, Lazareth et al., 2003, Immenhauser et al. 2005, Freitas et al. 2008, Wanamaker et al. 2008), they may help reconstructing (paleo-)environmental conditions and thus deliver the data necessary to construct and improve models of past climate.

However, several recent studies (e.g. Klein et al. 1996b, Vander Putten et al. 2000, Gillikin et al. 2005, Carré et al. 2006, Freitas et al. 2006, Heinemann et al. 2008) on elemental ratios in bivalve shells failed to show unambiguous relationships between elemental ratios and environmental factors (e.g. temperature and salinity). The reasons are often referred to as “biological control” or “vital effects” meaning elemental ratios in the mussel shell (e.g. Mg/Ca, Sr/Ca) are not exclusively controlled by inorganic thermodynamic principles but also by individual physiological processes. For example Klein et al. (1996b) suggested that skeletal chemistry of *Mytilus trossulus* from the field is primarily controlled by rate of mantle metabolic activity (metabolic pumping of Ca<sup>2+</sup> to the extrapallial fluid (EPF)) and only secondarily modified by variation of seawater salinity. Also, in their study on the distribution of Mg, Sr and Pb in the calcite shell layer of *Mytilus edulis* Vander Putten et al. (2000) showed that patterns of these elements cannot be explained by seasonal variations in seawater composition alone. According to the latter study the direct use of Mg as a proxy in *M. edulis* shells is hampered by the absence of a consistent Mg-temperature relationship over the year. Crystal growth rate in two aragonitic marine bivalve species (*Mesodesma donacium* and *Chione subrugosa*) was found to be the main factor influencing trace elements concentrations, especially for Sr (explaining up to 74 % of the variance) (Carré et al. 2006). As a consequence, the environmental control on minor and trace elements in mollusks is often too weak to develop suitable proxies (Carré et al. 2006). The findings from recent bivalve studies corroborate the results of previous studies reporting a strong biological influence and the interaction among different environmental factors affecting elemental ratios in bivalve shells (e.g. Heinemann et al. 2008).

The ambiguity of results in recent studies raises the question as to whether the influence of a single environmental factor on bivalve shell composition can be strong enough to provide a reliable signal superimposing the “noise” produced by other environmental variables and/or by biological effects. Hence, it is important to quantify the influence of single environmental variables such as temperature or salinity as well as the combined effect of such factors on elemental ratios (i.e. Sr/Ca and Mg/Ca)



relative to the biological background “noise” such as genetics, physiology, growth and reproductive cycles and infections, respectively.

In the present study we investigated the influence of temperature, salinity, individual differences and physiological variability on element to calcium ratios in the calcite layer of juvenile blue mussels (*M. edulis*) to critically assess its suitability as a proxy archive.

### 1.3. Materials and Methods

#### 1.3.1 Culturing

Young (6-9 mm) blue mussels, *Mytilus edulis*, collected in August 2003 from settlement panels deployed in the Kiel Fjord in spring of the same year, were first kept under identical and controlled conditions in a flow through system of filtered sea water (salinity around 17) in the laboratory at 12 °C for five months. During this time, the bivalves were fed daily with natural plankton caught from Kiel Fjord (20-100 µm) at concentrations typical for the Baltic Sea ( $3 \times 10^3$  cells/ml (Clausen and Riisgard 1996)).

After this laboratory acclimatization phase, the juvenile *M. edulis* were partitioned into 4 treatment groups in 2 l aquaria. Subsequently, the bivalves were gradually adapted (salinity change by 5 units per week), to 4 different salinities (17, 20, 29, 34). Salinities higher than 17 (initial salinity) were obtained by adding artificial marine salt (Tropic Marin, Dr. Biener, Wartenberg) to natural Baltic Sea water. In this experimental setup, each experimental unit consisted of the 2-l-aquarium (replicate) containing 20 mussel individuals of similar size (pseudo replicates) and 2 reservoirs. A pump placed in a lower reservoir filled an upper reservoir, allowing the water to flow through the culture tanks (2 l aquaria) back into the lower reservoir. The setup resulted in a total water volume of ca. 75 l for each experimental unit. The water was exchanged once per week.

As in the Baltic Sea blue mussels' growth rates are normally highest in early spring and summer (Kautsky 1982a), the experiment was conducted from 4<sup>th</sup> of February to 13<sup>th</sup> of May 2004. In the course of the experiment temperature was continuously adjusted to the seasonal Kiel Fjord water temperature (20-year-average of the experimental period February till May, (Lehmann et al. 2002)) and ranged from 6 °C to 14 °C. In this treatment phase, food consisted of cultured algae (*Dunaliella* sp. and *Rhodomonas* sp.) at a concentration of  $6 \times 10^3$  cells/ml. Prior to the daily feeding, the algal suspension was adjusted to experimental salinity and constantly dripped (20 ml/min) into the aquaria over a period of 2 h ( $72 \times 10^4$  cells/mussel). Light exposure was 10 hours a day (~150 µE/m<sup>2</sup>/sec). For more details on culturing technique used see the study of Kossak (2006). Growth for each individual mussel was monitored by measuring shell length (from umbo to shell margin, longest distance) at five dates (4<sup>th</sup> of Feb., 9<sup>th</sup> and 25<sup>th</sup> of March, 22<sup>nd</sup> of April and 13<sup>th</sup> of May). At the end of the experiment the size range was 11-14 mm.

### 1.3.2 Sample preparation

At the end of the treatment phase, mussels were sacrificed by freezing (-18 °C) and their soft body removed. From each salinity treatment the shell of one individual (randomly selected among the survivors of the 20 pseudo replicates per experimental unit) was embedded in a two component epoxy resin (Buehler, EPO-THIN, Low Viscosity Epoxy Resin). When the resin had hardened, shells were repeatedly cut along the axis of maximum length using a microtome-saw (Leica SP 1600) producing 200 µm thick sections. These sections were mounted onto glass-slides with thermal wax (Crystalbond 509 Amber, Aremco Products Inc.).

### 1.3.3 Analytical methods

Ca<sup>2+</sup>, Sr<sup>2+</sup> and Mg<sup>2+</sup> profiles were measured in the calcite layer of the shell using LA-ICP-MS (Laser Ablation-Inductively Coupled Plasma-Mass Spectrometry) along the axis with spot size of 35 µm and a distance between spots of 100 µm (with Thermo Sci. AXIOM MC-ICP-MS (Multicollector- Coupled Plasma-Mass Spectrometry); New Wave Res. UP193solid state; parameters shown in Table 1.1) (Fietzke et al. 2008).

Table 1.1: Instrument parameters.

<b>AXIOM MC-ICP-MS</b>	
Cool gas	14 l/min
Auxiliary gas	1.5 l/min
Nebulizer gas	0.6 l/min
RF power	1000 W
Reflected power	2 W
Ion energy	4968 V
Cones	R.A. Chilton RAC19/RAC705
Resolution	500res
Integration time per scan	2 s
Measured isotopes	<sup>24</sup> Mg (L3), <sup>25</sup> Mg (Ax), <sup>26</sup> Mg (H3), <sup>44</sup> Ca (L4), <sup>46</sup> Ca (Ax), <sup>48</sup> Ca (H4), <sup>84</sup> Sr (L2), <sup>85</sup> Rb (L1), <sup>86</sup> Sr (Ax), <sup>87</sup> Sr (H1), <sup>88</sup> Sr (H2)
<b>UP193solid state</b>	
Ablation gas	0.6 l/min (He)
Spot size/distance between spots	35 µm/100µm
Fluence	3 J/cm <sup>2</sup>
Repetition rate	10 Hz
Ablation time	50 s
Wash out time	120 s

Subsequently, Mg/Ca and Sr/Ca ratios were calculated. Knowing the growth rates in the different experimental phases, the position of the laser spots allowed relating measured elemental ratios to the temperature at any given point in time (Figure 1.1).

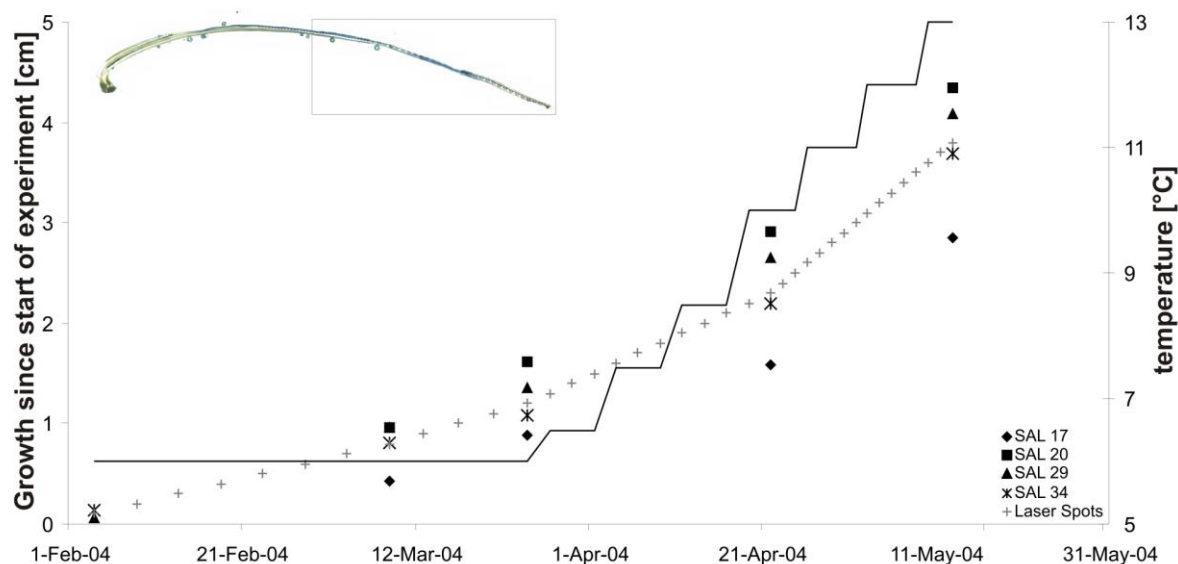


Figure 1.1: Growth of mussels since start of experiment. Length was measured at 5 dates. Distance between laser spots was 100  $\mu\text{m}$  and their location was calculated by the known points of growth. Line shows temperatures during experimental phase (Kossak 2006). The image shows a cross section of *M. edulis* shell with laser spots. The rectangle indicates the investigated part of the shell.

Since the entire length of the shell was sampled, we obtained elemental ratios from the three subsequent phases Kiel Fjord (means and variances are shown in Table 1.2), culture room with constant 6  $^{\circ}\text{C}$  and salinity treatment and, finally, with increasing temperature and salinity treatment.

Table 1.2: Means and variances of shell parts grown in nature.

	salinity 17	salinity 20	salinity 29	salinity 34
<b>Mg/Ca [mmol/mol]</b>				
mean	6.2	8.0	7.70	7.80
variance	1.6	3.0	2.5	0.50
<b>Sr/Ca [mmol/mol]</b>				
mean	1.379	1.55	1.54	1.47
variance	0.001	0.01	0.02	0.01

The relative contributions of biotic factors to the elemental ratios (Mg/Ca and Sr/Ca) were quantified (Figure 1.2) by (i) the mean variance among mean elemental ratios in parts of the shells of all 4

individuals grown *in situ* where we assumed environmental conditions to be identical for all individuals:

$$S^2_{\text{ind}} = \sum_{i=1}^n (\bar{x}_i - \bar{X})^2 / (n - 1) \quad (1)$$

(„individual differences“, where  $n$  is the number of individuals: 4,  $\bar{x}_i$  is the average elemental ratio of the individual  $i$  and  $\bar{X}$  is the average elemental ratio of all 4 individuals), (ii) the mean variance of elemental ratios of the 4 single individuals over different points in time during the phase of constant abiotic conditions:

$$S^2_{\text{phys}} = \sum_{i=1}^n (\sum_{i=1}^n (x_i - \bar{x}_i)^2 / (n - 1)) / n \quad (2)$$

(6 °C-phase, „physiological variability“, where  $n$  is the number of measures within one individual  $i$  and  $x_i$  is the elemental ratio of the measure  $i$ ). The influence of abiotic factors was calculated (i) by subtracting the value of the individual differences from the mean variance among the individuals cultured at different salinities during 6 °C-phase (“salinity”):

$$S^2_{\text{sal}} = S^2_{\text{ind}(6\text{ °C-phase})} - S^2_{\text{ind}} \quad (3)$$

and (ii) by subtracting the physiological variability from the average variance over the time while temperature increased (t↑-phase, “temperature”):

$$S^2_{\text{t}} = S^2_{\text{phys}(t\uparrow\text{-phase})} - S^2_{\text{phys}} \quad (4)$$

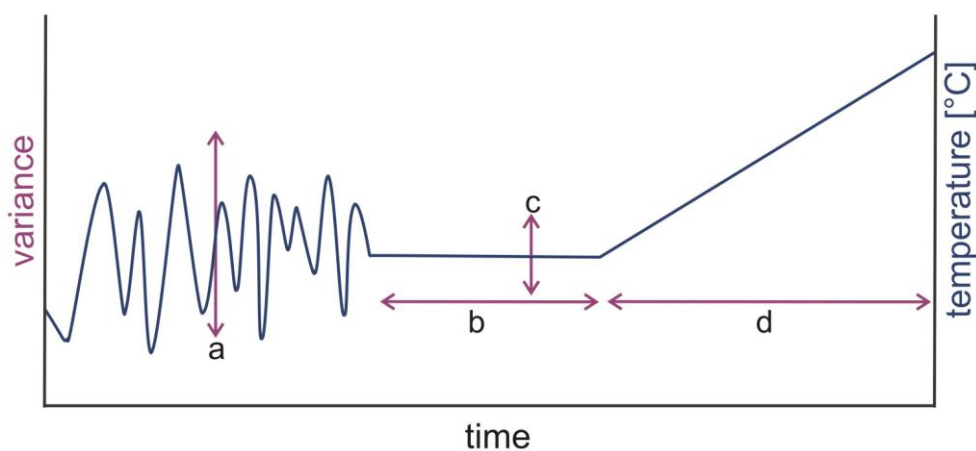


Figure 1.2: Scheme of values used for calculations of the relative contribution of individual differences (a), physiological variability (b), salinity (c-a) and temperature (d-b) to the overall variance of elemental ratios. Horizontal arrows display variances within one shell, vertical arrows between the four shells.

To reveal possible significant differences between contributions of different factors (physiological variability, individual differences, temperature, salinity) to the overall variance we performed multiple F-tests. To reduce the probability of type-1 errors the significance level (alpha) was Bonferroni-corrected.

## 1.4 Results and Discussion

Klein et al. (1996a) reported that skeletal Mg/Ca ratios of *Mytilus trossulus* grown in the field provide an accurate measure of temperature and that weekly sea-surface temperature may be estimated with an apparent accuracy of approximately  $\pm 1.5$  °C. In the shells of *M. edulis* individuals cultured at high salinities (29, 34) we observed Mg/Ca ratios in the calcite layer to be positively related to temperature, too (Figure 1.3a, 1.4).

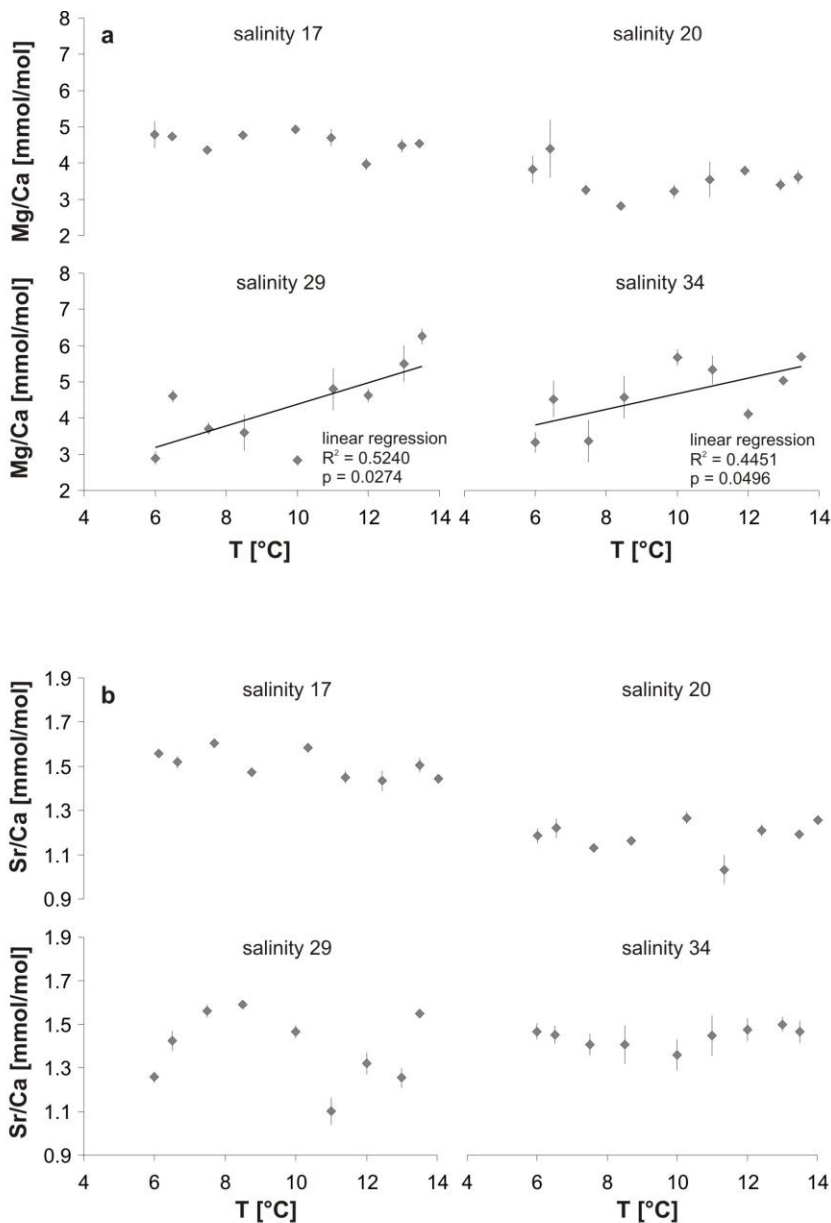


Figure 1.3: a) Mg/Ca and b) Sr/Ca ratios of the different salinity treatments in comparison to temperature. Each data point represents the median of all laser spots in the considered part of shell grown of a given temperature period. Errors are given as SE.

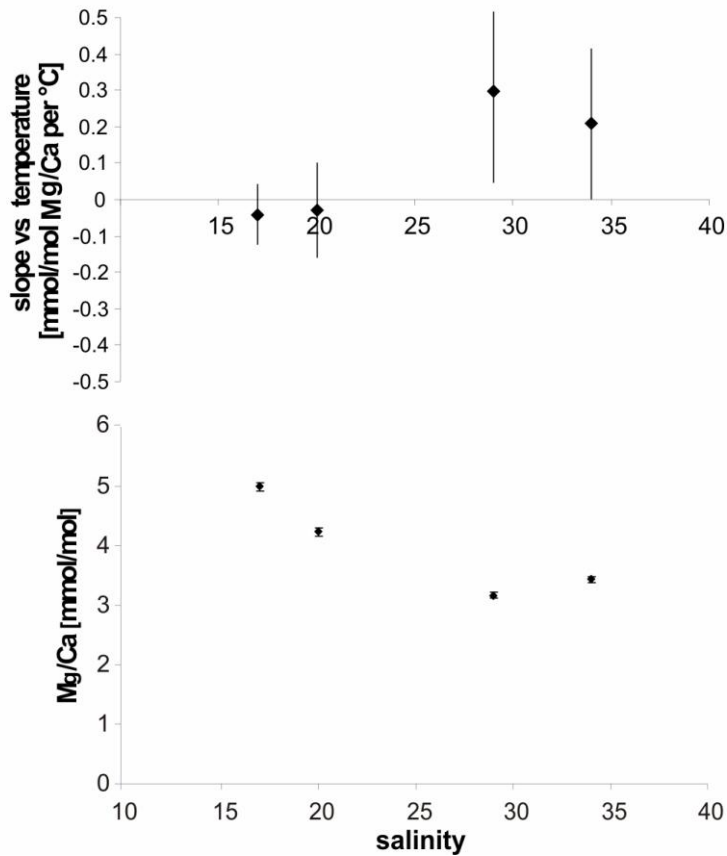


Figure 1.4: Temperature effects on Mg/Ca ratios (upper graph) and influence of salinity during constant temperature treatment (6 °C; lower graph). Errors in the upper graph are given as confidence interval. A non-overlap between CI-bars among each other or with the zero line indicates significant differences. In the lower graph means of one individual per treatment is shown with a typical measurement error (2SD, lower graph).

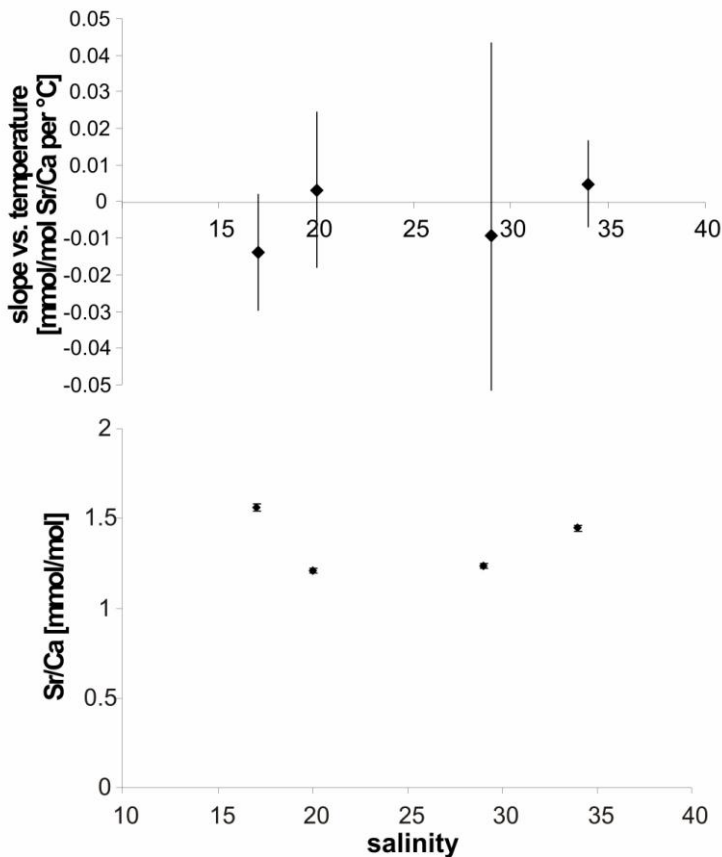


Figure 1.5: Temperature effects on Sr/Ca ratios (upper graph) and influence of salinity during constant temperature treatment (6 °C; lower graph). Errors in the upper graph are given as confidence interval. A non-overlap between CI-bars among each other or with the zero line indicates significant differences. In the lower graph means of one individual per treatment is shown with a typical measurement error (2SD, lower graph).

However, this pattern was not found in shells of individuals cultured at lower salinities (17, 20). Wanamaker et al. (2008) found a more robust Mg/Ca temperature relationship at salinity 23 and 28 than at higher salinity (32) in their study on Mg/Ca and Sr/Ca ratios in the calcite of juvenile *Mytilus edulis*. They concluded that Mg/Ca and Sr/Ca ratios in juvenile *M. edulis* calcite may possibly be used for reconstruction of water temperatures from an upper estuarine setting. For mean values of the investigated salinity range (23-32) Wanamaker et al. (2008) observed an increase of 6 %/°C for Mg/Ca and 1 %/°C for Sr/Ca, respectively. The results of Mg/Ca are nearly similar to the results of the overlapping salinity range of this study (29, 34) where a temperature relation of 6.5 %/°C was found. The different findings for Sr/Ca may be a result of adaptation and/or physiology as our animals originated from a low salinity habitat (~18) the ones cultured by Wanamaker et al. (2008) came from a salinity of ~31. Furthermore we investigated a smaller temperature range of 6-14 °C in contrast to 7-19.3 °C. Our results partly correspond with previous findings where Mg/Ca ratios of different taxa are also reported to be influenced by salinity. Dodd (1965) showed that the Mg concentration in the outer prismatic layer of *M. edulis* increases markedly with decreasing salinity and that it shows a weak positive correlation with temperature. Further, studies on foraminifera demonstrate that variations in temperature and salinity are reflected in the magnesium content of foraminifers' calcite (e.g. Nürnberg et al. 1996). Their experiments reveal that pronounced salinity changes (>10) at constant temperature significantly affect the Mg concentrations. Nürnberg et al. (1996) therefore suggested that Mg may serve as a paleo-proxy for past surface water temperatures, as long as salinity variations and post depositional alterations like carbonate dissolution can be shown to be small or absent. Our results likewise show that temperature interacts with other factors influencing Mg/Ca ratios in the shell of *M. edulis*. Strikingly, individual differences amongst mussels (34.0 %) living under similar environmental conditions and temporal variability within individuals in constant environmental conditions (45.2 %) contribute a substantially higher proportion to the overall variance of the Mg/Ca ratio than temperature does (20.8 %) (Figure 1.6a). As the influence of the physiological state of the bivalves on Mg/Ca incorporation into bivalve shells is likely to vary with environmental fluctuations as well as growth and reproductive cycles, food availability, fouling or infection rates, our findings may explain the absence of a consistent Mg/Ca-temperature relationship over the year in *M. edulis* calcite observed by Vander Putten et al. (2000). Additionally, as variances of Mg/Ca ratios among individuals decreased after placing the mussels into different salinity treatments relative to variability of Mg/Ca in shell parts grown in nature indicates that a putative salinity effect on Mg/Ca is smaller than inter-individual differences in a fluctuating natural environment. Consequently, no influence of salinity on the Mg/Ca ratio which was strong enough to emerge from the biological background “noise” could be detected. While Mg/Ca tended to be highest in the two low salinity treatments individuals' shells (SAL 17 and 20, Figure 1.4), partly corroborating Dodd's (1965) results

a reliable Mg/Ca-salinity effect was not apparent. Sr/Ca ratios in *M. edulis* shells were not significantly affected by temperature (Figure 1.3b, 1.5 and 1.6b).

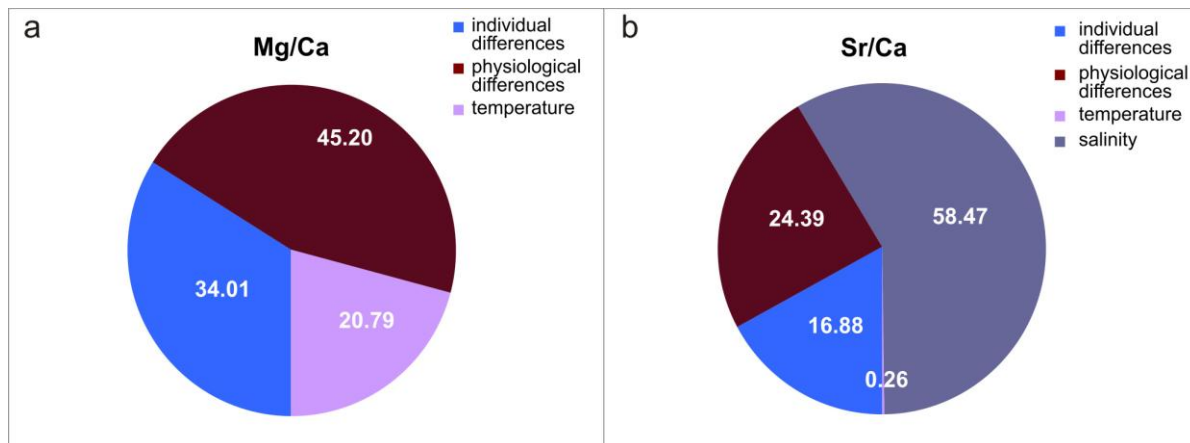


Figure 1.6: Influence of individual differences, physiological state, salinity and temperature on Mg/Ca (a) and Sr/Ca ratios (b) in the prismatic layer of *M. edulis* shells. Salinity contribution on Mg/Ca was not detectable.

The temperature contribution to the overall variance (0.3 %) was significantly smaller than the contribution of physiological state (24.4 %), individual differences (16.9 %) and salinity (58.5 %) (F-test,  $p < 0.0001$ ). Therefore, we cannot corroborate findings of Dodd (1965) who found that the strontium concentration in *M. edulis* calcite correlates positively with temperature. Instead, we found the salinity treatment to have the highest impact on Sr/Ca (58.5 %, Fig. 6b). We observed the highest Sr/Ca value in the shell grown at the lowest salinity (SAL 17). However, no significant Sr/Ca-salinity relationship was detected (Figure 1.5).

## 1.5 Conclusions

We observed relations between Mg/Ca ratios and temperature in two of the measured *Mytilus edulis* shells. Still, biological control (physiological state and individual differences) has a dominant influence (~79 % contribution to overall variance on Mg/Ca and ~41 % contribution on Sr/Ca) on the elemental ratios in *M. edulis* shells. This can be taken as a likely reason for the large discrepancies in the discussions whether carbonates of bivalve shells can be used as proxy archives. It appears that mussel carbonate can only be used as a proxy archive if the combination of environmental conditions and the major contribution of biology are considered. Therefore, the data stress the importance of replicating at the biological level, i.e. measure several animals from the same location and time, even though this drastically increases the measuring effort



## Acknowledgments

We gratefully acknowledge Ute Kossak for providing mussel shells. Finally, we thank Marghaleray Amini and Florian Böhm for their interest in this study and fruitful discussions.

## References

- Carré, M., I. Bentaleb, O. Bruguier, E. Ordinola, N. T. Barrett, and M. Fontugne (2006), Calcification rate influence on trace elements concentrations in aragonitic bivalve shells: Evidences and mechanisms, *Geochim. Cosmochim. Acta*, 70(19), 4906–4920.
- Clausen, I. and H. Riisgard (1996), Growth, filtration and respiration in the mussel *Mytilus edulis*: no evidence for physiological regulation of the filter-pump to nutritional needs. *Marine Ecology Progress Series*, 141, 37–45.
- Dodd, J.R. (1965), Environmental control of strontium and magnesium in *Mytilus edulis*, *Geochim. Cosmochim. Acta*, 29 (5), 385–398.
- Fietzke, J., V. Liebetrau, D. Günther, K. Gürs, K. Hametner, K. Zumholz, T. Hansteen, A. Eisenhauer (2008), An alternative data acquisition and evaluation strategy for improved isotope ratio precising using LA-MC-ICP-MS applied for stable and radiogenic strontium isotopes in carbonates, *JAAS*, 23, 955–961, doi: 10.1039/b717706b.
- Freitas, P. S., L. J. Clarke, H. A. Kennedy and C. A. Richardson (2008), Inter and intra-specimen variability masks reliable temperature control on shell Mg/Ca ratios in laboratory- and field-cultured *Mytilus edulis* and *Pecten maximus* (bivalvia), *Biogeosciences*, 5(5), 1245–1258.
- Gosling, E. M. (1992), Systematics and geographic distribution of *Mytilus*, in *The Mussel Mytilus: Ecology, Physiology, Genetics and Culture*, *Dev. Aquacult. Fish. Sci.*, vol. 25, edited by E. M. Gosling, chap. 1, pp. 1–20, Elsevier, New York.
- Heinemann, A., J. Fietzke, A. Eisenhauer, K. Zumholz (2008), Modification of Ca isotope and trace metal composition of the major matrices involved in shell formation of *Mytilus edulis*, *Geochem. Geophys. Geosyst.* 9 (1), Q01006, doi:10.1029/2007GC001777.
- Immenhauser, A., T. F. Nägler, T. Steuber and D. Hippler (2005), A critical assessment of mollusk  $O^{18}/O^{16}$ , Mg/Ca, and  $Ca^{44}/Ca^{40}$  ratios as proxies for Cretaceous seawater temperature seasonality, *Palaeogeography Palaeoclimatology Palaeoecology*, 215(3–4), 221–237.
- Kautsky, N (1982a), Growth and Size Structure in a Baltic *Mytilus edulis* Population, *Mar. Biol.*, 68, 117–133.
- Klein, R. T., K. C. Lohmann, C. W. Thayer (1996a), Bivalve skeletons record sea-surface temperature and  $\delta^{18}O$  via Mg/Ca and  $^{18}O/^{16}O$  ratios. *Geology*, 24 (5), 415–418.
- Klein, R. T., K. C. Lohmann, C. W. Thayer (1996b), Sr/Ca and  $^{13}C/^{12}C$  ratios in skeletal calcite of *Mytilus trossolus*: covariation with metabolic rate, salinity and carbon isotopic composition of sea water, *Geochim. Cosmochim. Acta*, 60, 4207–4221.
- Kossak, U. (2006), How climate change translates into ecological change: Impacts of warming and desalination on prey properties and predator-prey interactions in the Baltic Sea, Ph.D. thesis, Christian-Albrechts-Univ., Kiel, Germany.  
(Available at [http://eldiss.uni-kiel.de/macau/receive/dissertation\\_diss\\_00001910](http://eldiss.uni-kiel.de/macau/receive/dissertation_diss_00001910))

Lazareth, C. E., E. Vander Putten, L. Andre and F. Dehairs (2003), High resolution trace element profiles in shells of the mangrove bivalve *Isognomon ehippium*: a record of environmental spatio-temporal variations?, *Estuarine Coastal and Shelf Science*, 57(5-6), 1103-1114.

Lehmann, A., W. Krauss and H. H. Hinrichsen (2002), Effects of remote and local atmospheric forcing on circulation and upwelling in the Baltic Sea, *Tellus*, 54, 299- 316.

Nürnberg, D., J. Bijma, and C. Hemleben (1996), Assessing the reliability of magnesium in foraminiferal calcite as a proxy for water mass temperatures, *Geochim. Cosmochim. Acta*, 60(5), 803-814.

Seed, R., and T. H. Suchanek (1992), Population and community ecology of *Mytilus*, in *The Mussel Mytilus: Ecology, Physiology, Genetics and Culture*, *Dev. Aquacult. Fish. Sci.*, vol. 25, edited by E. M. Gosling, pp. 87– 170, Elsevier, New York.

Vander Putten, E., F. Dehairs, E. Keppens, and W. Baeyens (2000), High distribution of trace elements in the calcite shell layer of modern *Mytilus edulis*: Environmental and biological controls, *Geochim. Cosmochim. Acta*, 64(6), 997–1011.

## Chapter 2

# **The impacts of seawater carbonate chemistry on biomineralization and elemental concentrations of *Mytilus edulis* body fluids and its potential as a proxy archive\***

\*to be submitted as: Agnes Heinemann, Jörn Thomsen, Jan Fietzke, Magdalena A. Gutowska, Florian Böhm, Anton Eisenhauer, Dieter Garbe-Schönberg, Frank Melzner; The impacts of seawater carbonate chemistry on biomineralization and elemental concentrations of *Mytilus edulis* body fluids and its potential as a proxy archive.

## 2.1 Abstract

The use of bivalve shells as proxy archives is challenging since the mechanisms of biomineralization are still poorly understood. In experiments with variable seawater carbonate chemistry and food supply we investigated the impact on shell formation and element concentrations of extracellular body fluids. Specimens of the blue mussel *Mytilus edulis* from Kiel Fjord (Western Baltic Sea, Germany) were held in experimental culture for three months under different  $p\text{CO}_2$  conditions (380-4000  $\mu\text{atm}$ ). Calcification, shell length growth and inner surface structure were determined with different techniques (alkalinity anomaly technique, shell length increment measurements and  $\text{MnCl}_2$ -staining, optical observations and SEM). Calcification rate measurements indicated net dissolution in the highest  $p\text{CO}_2$  treatment (3352  $\mu\text{atm}$ ) while length growth did not differ between treatments. With decreasing calcification rates the intensity of the  $\text{MnCl}_2$ -marking lines was clearly higher at the beginning of the experiment rather than after six weeks which is interpreted to reflect reduced calcification with rising  $p\text{CO}_2$ . In our low food experiment inner shell surfaces became increasingly corroded with rising  $p\text{CO}_2$  and nacre structure was clearly disordered. As the results of the different techniques complement each other, future studies on bivalve shell growth should also consider a multi-technique approach for more detailed data interpretation. Trace metal concentrations ( $\text{Ca}^{2+}$ ,  $\text{Mg}^{2+}$  and  $\text{Sr}^{2+}$ ) of hemolymph (HL) and extrapallial fluid (EPF) samples from this and a second long-term growth experiment were measured via ICP-OES (Inductively Coupled Plasma-Optical Emission Spectrometry).  $\text{Mg}^{2+}$  and  $\text{Sr}^{2+}$  are generally enriched in the extracellular body fluids. This is interpreted as to reflect that mainly  $\text{Ca}^{2+}$  is extracted from the solution for shell formation. The inorganic composition of the fluids is highly variable between individuals ( $\pm 0.7$  mol/l for  $\text{Ca}^{2+}$ ,  $\pm 3.6$  mol/l for  $\text{Mg}^{2+}$ ,  $\pm 5.5$  mmol/l for  $\text{Sr}^{2+}$ ). It is likely that this is also reflected in the elemental shell signature, therefore complicating the use of *M. edulis* shell as a proxy archive.

## 2.2 Introduction

During the calcification process and depending on environmental conditions, calcium ( $\text{Ca}^{2+}$ ) can be displaced by other cations such as magnesium ( $\text{Mg}^{2+}$ ) and strontium ( $\text{Sr}^{2+}$ ). These varying elemental compositions are used as proxies to reconstruct (paleo-)environmental conditions. Bivalves are potentially good proxy archives as they are widely distributed (Gosling 1992), long living (Schöne et al. 2005) and geologically old (Seed 1976). However, several studies on different bivalve species show contradictory results regarding the use of bivalve shells as a proxy-archive (e.g. Klein et al. 1996b, Vander Putten et al. 2000, Gillikin et al. 2005, Carré et al. 2006, Heinemann et al. 2008).

Different factors influencing cation incorporation into bivalve shells, like mantle metabolic activity (Klein et al. 1996b) or crystal growth rate (Carré et al. 2006), were reported. Direct relationship of skeletal Mg/Ca in *Mytilus trossulus* and temperature were shown by Klein et al. 1996a. Freitas et al. (2005) observed Mg/Ca in *Pinna nobilis* shells being sensitive to specimen age. Salinity was also shown to have an effect on Mg/Ca ratios in *M. edulis* calcite (Dodd 1965). Sr/Ca seems likewise to be influenced by abiotic factors (Dodd 1965, Wanamaker et al. 2008). However, biotic factors like growth rate have also been reported to impact on Mg/Ca and Sr/Ca ratios in bivalve shells (Lorrain et al. 2005, Freitas et al. 2006, Ford et al. 2010).

In general, strong biological control appears to influence the calcification process (e.g. Vander Putten et al. 2000, Gillikin et al. 2005, Carré et al. 2006, Heinemann et al. 2008). Heinemann et al. (in press, Chapter 1 of this thesis) calculated physiological and individual differences having a very large impact on the Mg/Ca distribution in *M. edulis* calcite (~45 and ~34 % respectively). Sr/Ca seemed to be less affected (~24 and ~17 %). To overcome these problems in using bivalve shells as proxy archives, it is necessary to better understand the mechanisms of biomineralization and the change of elemental concentrations in body fluids and the shell with respect to water composition. In particular, the dependency of the EPF composition on different factors needs to be investigated as it is predicted to be the site of calcification. The biomineralization of marine organism's shells and skeletons is hypothesized to be reduced by rising surface seawater  $p\text{CO}_2$  and a resulting decline in pH.

Since preindustrial time atmospheric carbon dioxide ( $\text{CO}_2$ ) concentrations have increased from 280 to 390  $\mu\text{atm}$  (<http://www.esrl.noaa.gov/gmd/ccgg/trends/>). As the oceans have taken up ~50 % of the  $\text{CO}_2$  emitted (Sabine et al. 2004) oceanic pH has already decreased by 0.1 units (Orr et al. 2005). This results in ongoing surface ocean acidification. Caldeira and Wickett (2003) estimated an atmospheric  $p\text{CO}_2$  of 1900  $\mu\text{atm}$  which results in a similar increase of seawater  $p\text{CO}_2$  and a maximum drop in surface pH of 0.77 at around the year 2300 based on the IPCC business as usual scenario IS92a of  $\text{CO}_2$  emissions. Therefore, the carbonate system will be shifted towards lower calcium carbonate ( $\text{CaCO}_3$ ) concentrations (e.g. Feely et al. 2004). As a result of this, higher-latitude oceans are predicted to become under saturated ( $\Omega < 1$ ) with respect primarily to aragonite by the year 2050 (Orr et al. 2009, Cao and Caldeira 2008) which may have considerable consequences for marine calcifying organisms

(Orr et al. 2005). Several studies have reported declining calcification and/or dissolution in marine bivalve species, including *Mytilus edulis*, *Mytilus galloprovincialis*, *Crassostrea virginica* and *Crassostrea gigas* (e.g. Berge et al. 2006, Kurihara et al. 2007 and 2008, Gazeau et al. 2007 and 2010, Thomsen and Melzner 2010, Waldbusser et al. 2010). An abundant and widely distributed bivalve species in shallow marine ecosystems is the blue mussel *Mytilus edulis*. Their shells consist of an outer low magnesium-calcite and an inner aragonite (nacre) layer whereby low magnesium calcite (< 8.5 mole %  $\text{MgCO}_3$ ) is more stable than aragonite (Berner 1975). Blue mussel beds are also common in Kiel Fjord (Western Baltic Sea, Germany) (Enderlein and Wahl 2004) a habitat with challenging abiotic conditions (e.g. high  $p\text{CO}_2$  with max. values of >2300  $\mu\text{atm}$ ) resulting in low  $\text{CaCO}_3$  saturation state (min. values:  $\Omega_{\text{arag}} = 0.34$  and  $\Omega_{\text{calc}} = 0.58$ ) during summer (Thomsen et al. 2010). Despite these conditions, larval settlement and maximum growth rates occur in *M. edulis* and other calcifying organisms during this period (Kossak 2006, Thomsen et al. 2010). Nevertheless, Gazeau et al. (2007) showed negative calcification rates of *M. edulis* with a threshold of 1800  $\mu\text{atm}$  in a short-term experiment. After long-term acclimation, mussel calcification response was less sensitive to elevated  $p\text{CO}_2$  when food supply was sufficient. Thomsen and Melzner (2010) observed a linear decreased growth of shell length and shell mass with increasing  $p\text{CO}_2$  by 6-20 and 10-34 % in individuals from Kiel Fjord but net growth and calcification was still very high even under 4000  $\mu\text{atm}$  (6.3 mm; ~130 mg). In a summer experiment, Thomsen et al. (2010) found calcification rates similar to control rates under 1400  $\mu\text{atm}$   $p\text{CO}_2$  ( $\Omega_{\text{arag}} < 0.5$ ) and still high growth under 4000  $\mu\text{atm}$  ( $\Omega_{\text{arag}} < 0.2$ ). Like in all marine ectothermic animals (see Melzner et al. 2009 for a review) the body fluids of *M. edulis* are characterized by high  $p\text{CO}_2$  and therefore low pH and  $[\text{CO}_3^{2-}]$  (Thomsen et al. 2010, Heinemann et al. submitted, Chapter 4 of this thesis) values due to respiration. Especially in the EPF an additional shift towards higher  $p\text{CO}_2$  and resulting lower pH and  $[\text{CO}_3^{2-}]$  caused by higher external  $p\text{CO}_2$  may negatively influence calcification as it stands in direct contact to the shell.

To contribute to the understanding of the mechanisms of biomineralization and their sensitivity to ocean acidification, *M. edulis* from Kiel Fjord were cultured in two experiments under different  $\text{CO}_2$  levels (380-4000  $\mu\text{atm}$ ) and food conditions. Calcification rates and shell length growth were determined with different methods. To advance the knowledge about the suitability of *M. edulis* shells elemental compositions ( $\text{Ca}^{2+}$ ,  $\text{Mg}^{2+}$  and  $\text{Sr}^{2+}$ ) of bivalve extracellular fluids (hemolymph and extrapallial fluid) were investigated.

## 2.3 Material and Methods

### 2.3.1 General Setup

Two different experiments were arranged to investigate the influence of increased water CO<sub>2</sub> concentrations on calcification of *Mytilus edulis*. As today's atmospheric CO<sub>2</sub> is 380 µatm and concentrations are predicted to >1500 µatm between 2100 and 2200 (Wigley et al. 1996) levels for experiments were 380-1400 µatm. An additional 4000 µatm treatment was chosen as special habitats like the Kiel Fjord already reach seasonal values above 2000 µatm (Thomsen et al. 2010). Specimens for both experiments were collected from subtidal populations in Kiel Fjord (Western Baltic Sea; 54° 19.8' N; 10° 9.0' E), Germany, and cultured at the Leibniz Institute of Marine Science (IFM-GEOMAR) in Kiel, Germany. A more detailed description of the experimental setup and water condition data can be found in Heinemann et al. (submitted, Chapter 4 of this thesis) for experiment 1 and in Thomsen et al. (2010) for experiment 2.

Gas mixtures containing different partial pressures of CO<sub>2</sub> were provided by a central air-CO<sub>2</sub>-mixing device at the IFM-GEOMAR (Bleich et al. 2008). This CO<sub>2</sub> manipulation facility (Linde Gas & HTK Hamburg, Germany) measures ambient *p*CO<sub>2</sub> and adds the required amount of CO<sub>2</sub> to reach the pre-adjusted value into the air which is piped to the culturing rooms. The CO<sub>2</sub>-air mixtures were continuously pertubated into the aquaria. Ambient water was used as control (380 µatm). *A<sub>T</sub>* values were measured by potentiometric open cell titration with hydrochloric acid (Mintrop et al. 2000, Dickson et al. 2007) with a VINDTA (Versatile Instrument for the Determination of Titration Alkalinity, MARIANDA, Kiel, Germany) autoanalyzer. *C<sub>T</sub>* values of treatment water were coulometrically measured after Dickson et al. (2007) with a SOMMA (Single-Operator Multi-Metabolic Analyzer, University of Rhode Island, Kingston, RI) autoanalyzer. Certified Reference Material provided by Andrew Dickson (Scripps Institution of Oceanography) was used for *A<sub>T</sub>* and *C<sub>T</sub>* measurements. Water *p*CO<sub>2</sub> was calculated via CO2sys program (Dickson et al. 2003, Lewis and Wallace 1998) using the following parameters: Dissociation constants *K*<sub>1</sub> and *K*<sub>2</sub> (Mehrbach et al. 1973, Dickson and Millero 1987), KHSO<sub>4</sub> dissociation constant (Dickson 1990) and *pH*<sub>NBS</sub> scale.

Body fluids were directly taken after removing the bivalves from the aquaria. HL was taken with a syringe (needle: Ø 0.6 x 80 mm) from the posterior adductor muscle after valves were opened and fixed with a pipette tip. To draw the EPF from the extrapallial space the syringe needle was inserted between shell and pallial line. For experiment 2 only EPF was sampled as it was not possible to draw enough HL. After fluid samples were centrifuged to get rid of cells they were frozen (300-500 µl, -20 °C) until further measurements. Acid-base parameters were determined in body fluid subsamples of experiment 1 and are presented in Heinemann et al. (submitted, Chapter 4 of this thesis). Water samples from all aquaria were frozen and also stored for element determination. After unfreezing the samples were diluted 50fold with ultrapure 2 % HNO<sub>3</sub> and measured by ICP-OES (Inductively Coupled Plasma - Optical Emission Spectrometry, SPECTRO *Ciros*<sup>CCD</sup> SOP) at the Institute of

Geosciences, University Kiel, Germany. An intensity-ratio calibration procedure for the high-precision determination of Mg/Ca and Sr/Ca elemental ratios was applied using matrix-matched calibration standards. From this data elemental concentrations of Ca, Mg and Sr have been extracted. IAPSO seawater was used as a consistency standard. External precision of the elemental ratios was ~0.1 % and for elemental concentrations better than 0.5 % relative.

### 2.3.2 Experiment 1

The first experiment was conducted from 3<sup>rd</sup> of September to 18<sup>th</sup> of December 2008. *Mytilus edulis* with different size ranging from 1.24 cm to 4.67 cm were cultured at 6 different  $p\text{CO}_2$  levels (mean values: 577, 722, 839, 1041, 1195 and 3352  $\mu\text{atm}$ ). Size and number of mussels was chosen based on preliminary tests that illustrated the necessity of small mussels (< 3 cm) to quantify shell growth and large individuals (> 4 cm) for body fluid sampling. Body fluids were taken from the five largest bivalves ( $45.6 \pm 0.6$  mm). Shell length was measured at longest axis (from umbo to edge at opposite site) with a caliper. The experiment was conducted as a flow through system (200 ml/min) with water from Kiel Fjord. Aquaria had a 15 l volume and light exposure of 14 hours a day. 340 g of mussels (around 140 individuals) were placed into six containers one of which was aerated with ambient air (mean value 577  $\mu\text{atm}$   $\text{CO}_2$ ) the remaining five with  $\text{CO}_2$ -enriched air (Table 2.1). Temperature was  $12.2 \pm 0.6$  °C and salinity  $18.8 \pm 1.59$ . Food (DT's Live Marine Phytoplankton-Premium Reef Blend; DT's Plankton Farm, Sycamore, IL, USA) was provided 3 days a week (~75 mg algal dry weight biomass per day and aquarium) by closing the flow through for 4 hours and adding food directly into the aquaria. In the second half of the experiment *Artemia salina* (~45 mg dry weight biomass) was additionally fed as Wong and Levinton (2004) reported best growth by providing a food mixture (zoo- and phytoplankton).

Calcification rates were determined via the  $\Delta A_T$  (total alkalinity) technique described by Smith and Key (1975) which is based on the fact that the precipitation of 1 mole of  $\text{CaCO}_3$  consumes 1 mole of  $\text{Ca}^{2+}$  and 2 moles of  $\text{HCO}_3^-$ . Thus,  $A_T$  decreases by 2 equivalents per mole  $\text{CaCO}_3$ . Net calcification rate  $G$  (in this study given in nmol  $\text{CaCO}_3/\text{g FW/h}$ ) can be estimated by:

$$G = \Delta A_T / 2 \quad (1)$$

Once a week the flow through system was closed and a water sample from each aquarium was taken directly and after 5 hours. Water samples (500 ml) were immediately poisoned with 100  $\mu\text{l}$  saturated  $\text{HgCl}_2$  solution and total alkalinity was measured by potentiometric open cell titration with hydrochloric acid (Mintrop et al. 2000, Dickson et al. 2007) with a VINDTA (Versatile Instrument for the Determination of Titration Alkalinity, MARIANDA, Kiel, Germany) autoanalyzer. To ensure no other organisms were influencing the change in alkalinity incoming water was continuously filtered via 50-5  $\mu\text{m}$  filters and UV sterilization. The last feeding occurred 24 hours before alkalinity samples



were taken. All bivalve's lengths were measured before, in the middle and at the end of the experiment. Ten specimens ( $19.4 \pm 0.6$  mm) in each treatment were labeled individually with nitrocellulose lacquer and their lengths measured on 5 dates (28. Aug.; 18. Sep.; 14. Oct; 28. Oct. and 16. Dec. 2008) using a caliper. In order to label all bivalve shells 6 ml 10 %  $\text{MnCl}_2$  solution were added to the water at 4 dates (26. Aug.; 27. Aug.; 27. Oct. and 28. Oct. 2008) for 6 h each. The tank flow through was closed for 6 hours and bivalves incorporated manganese into their shells (Barbin et al. 2008). Two of the single marked shells were prepared for electron microprobe (EMP) analyses (carried out at IFM-GEOMAR Kiel, Germany, using a JEOL JXA 8200 "Superprobe" applying Wavelength Dispersive Spectrometry (WDS), using a focused beam, a resolution of  $20 \mu\text{m} \times 20 \mu\text{m}$  and an integration time per point of 500 ms). Two shells from a 577 and 3352  $\mu\text{atm}$  treatment was cut along the axis of maximum growth using a cut-off wheel and shell sections were embedded in a two component epoxy resin (Buehler, EPO-THIN, Low Viscosity Epoxy Resin) on a brass-slide. After hardening at  $50^\circ\text{C}$ , the sections were grounded with sand paper (grading (p): 240-600) and polished with diamond paste (grading 0.5-0.01  $\mu\text{m}$ ). The inner shell surface (nacre) of 25 individuals (ten of them individually marked with nitrocellulose lacquer) per treatment were investigated macroscopically via bright field stereo microscopic. One shell from the lowest and highest treatments was examined by SEM (scanning electron microscope) at the Institute of Geosciences, University Kiel, Germany.

### 2.3.3 Experiment 2

A second long-term growth experiment was carried out from 14<sup>th</sup> of May to 13<sup>th</sup> of July 2009 using three  $p\text{CO}_2$  levels (380, 1400 and 4000  $\mu\text{atm}$ ) with four replicates per treatment. The experiment was conducted under a mean temperature of  $13.8 \pm 0.6^\circ\text{C}$ , a salinity of  $15 \pm 0.6$  and a light/dark cycle of 14:10 hours. Food (*Rhodomonas sp.* suspension,  $2900 \pm 1200$  cells/ml) was provided continuously by adding it into the aquaria at a rate of 100 ml/min. Mean algae concentrations in the experimental aquaria were  $820 \pm 315$  cell/ml. Each aquarium (15 l) contained eight small (mean 5.5 mm) and eight medium sized (mean 13 mm) for growth and calcification measurements and two big (mean 40 mm) mussels for EPF element determination. At the beginning of the experiment shell length (caliper  $\pm 0.1$  mm) and fresh mass (precision balance  $\pm 1$  mg, Sartorius, Germany) were measured. At the end of the experiment somatic dry, shell mass and shell length were determined. For more details of experimental setup, *Rhodomonas sp.* culture and results of shell length and mass see Thomsen et al. (2010).

### 2.3.4 Statistics

Data were analyzed by regression analyses using SigmaPlot 10 and by ANOVA and ANCOVA using STATISTICA 8. Regressions slopes were compared by visual inspection of confidence intervals and ANCOVA (for element analyses). ANOVA results were tested for homogeneity of variances and significant results were tested using Tukeys post hoc test for unequal n (for calcification rate results).

## 2.4 Results and Discussions

Water  $p\text{CO}_2$  values (experiment 1) were calculated (via CO2Sys; Lewis and Wallace 1998) by weekly determination of total alkalinity ( $A_T$ ) and dissolved inorganic carbon ( $C_T$ ). Following parameters were used for the calculations: Dissociation constants  $K_1$  and  $K_2$  (Mehrbach et al. 1973, Dickson and Millero 1987),  $\text{KHSO}_4$  dissociation constant (Dickson 1990) and  $\text{pH}_{\text{NBS}}$  scale. The control values are higher than the suggested treatment level (380  $\mu\text{atm}$ ) since incoming water from Kiel Fjord has higher  $p\text{CO}_2$  levels most time of the year (Thomsen et al. 2010). Despite of preconditioning the water the high  $p\text{CO}_2$  values could not be entirely removed which leads to a mean value of  $577 \pm 95$   $\mu\text{atm}$  in the control. Mean values for the other treatments also differed from the assigned treatment levels. All water conditions are given in Table 2.1.

Table 2.1: Water conditions during experimental trials. Data for experiment 2 are from Thomsen et al. (2010). Errors are given as SD. Values represent mean over whole experiment.

Exp. 1:	temperature in °C	12.1 ± 0.6		salinity	18.8 ± 1.59	
Treatment $p\text{CO}_2$ theoretical value	$\text{pH}_{\text{NBS}}$	$A_T$ [ $\mu\text{mol/kg}$ ]	$C_T$ [ $\mu\text{mol/kg}$ ]	$p\text{CO}_2$ [ $\mu\text{atm}$ ]	$\Omega_{\text{calc}}$	$\Omega_{\text{arag}}$
387 $\mu\text{atm}$	8.02 ± 0.08	2030 ± 70	1970 ± 60	577 ± 95	1.8 ± 0.3	1.1 ± 0.2
560 $\mu\text{atm}$	7.93 ± 0.07	2030 ± 70	1990 ± 60	722 ± 97	1.5 ± 0.2	0.9 ± 0.1
840 $\mu\text{atm}$	7.86 ± 0.05	2030 ± 70	2000 ± 70	839 ± 80	1.3 ± 0.2	0.8 ± 0.1
1120 $\mu\text{atm}$	7.77 ± 0.05	2030 ± 70	2030 ± 66	1041 ± 93	1.1 ± 0.1	0.5 ± 0.1
1400 $\mu\text{atm}$	7.71 ± 0.05	2030 ± 70	2040 ± 70	1195 ± 98	0.9 ± 0.1	0.6 ± 0.1
4000 $\mu\text{atm}$	7.28 ± 0.08	2040 ± 70	2170 ± 70	3352 ± 566	0.4 ± 0.1	0.2 ± 0.04
Exp.: 2	temperature in °C	13.8 ± 0.6		salinity	15.0 ± 0.6	
Treatment	$\text{pH}_{\text{NBS}}$	$A_T$ [ $\mu\text{mol/kg}$ ]	$C_T$ [ $\mu\text{mol/kg}$ ]	$p\text{CO}_2$ [ $\mu\text{atm}$ ]	$\Omega_{\text{calc}}$	$\Omega_{\text{arag}}$
387 $\mu\text{atm}$	8.13 ± 0.02	1970 ± 3	1890 ± 5	500 ± 30	1.94 ± 0.04	1.14 ± 0.04
1400 $\mu\text{atm}$	7.72 ± 0.06	1970 ± 5	1980 ± 10	1350 ± 200	0.81 ± 0.09	0.48 ± 0.06
4000 $\mu\text{atm}$	7.26 ± 0.04	1970 ± 4	2130 ± 10	3950 ± 220	0.28 ± 0.02	0.17 ± 0.01

## 2.4.1 Calcification

### 2.4.1.1 Calcification rates

Calcification rates were determined once a week via the  $\Delta A_T$  (total alkalinity) method described by Smith and Key (1975) in all treatments of experiment 1. A trend towards less calcification with rising  $p\text{CO}_2$  (declining pH) could be observed when considering mean values per treatment (15 weekly measurements each, Figure 2.1). Values of calcification rates were negative at the 3352  $\mu\text{atm}$  treatment and therefore net  $\text{CaCO}_3$  dissolution took place (Figure 2.1, Table 2.2). In all other treatments animals showed positive calcification. This indicates a threshold for dissolution of shells between 2000 and 3000  $\mu\text{atm}$ .

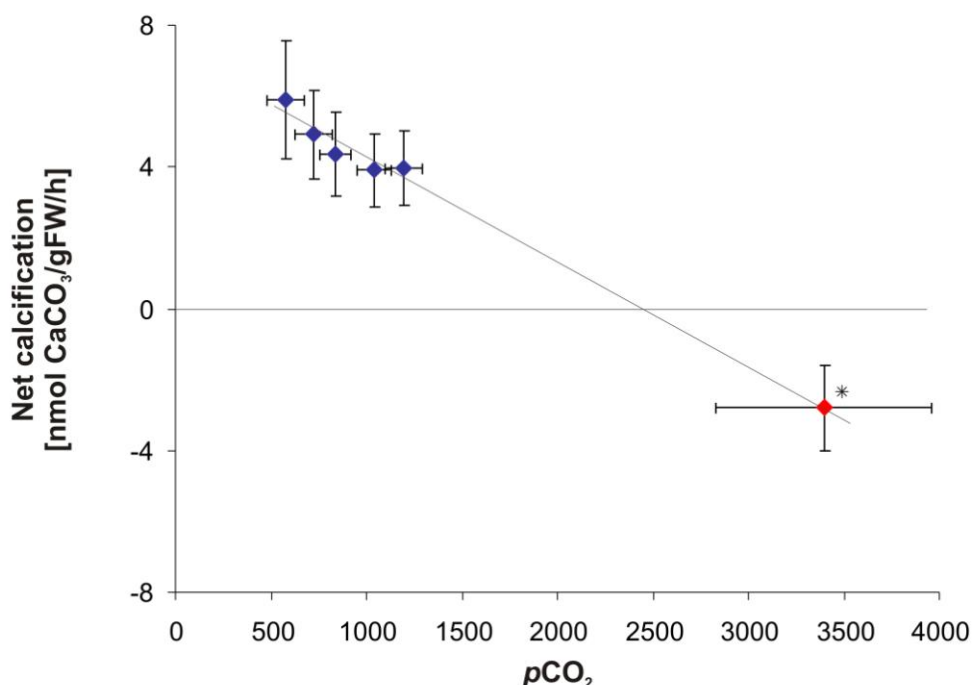


Figure 2.1: Mean calcification rates in the different treatments. Each point represents measurements of 15 different dates during experimental time. Errors are given as 2SE. Values from 577-1995  $\mu\text{atm}$  displayed in blue (given as a mean in Figure 2.2) and red (as single values in Figure 2.2). Diagonal line is not for statistical purposes rather support the estimation of a threshold value.

Control calcification rates were nearly the same in all aquaria before treatment started ( $9.2 \text{ nmol CaCO}_3/\text{gFW}/\text{h} \pm 1.5$ ). Calcification rates of the 577 to 1195  $\mu\text{atm}$  treatments clearly decreased during the first two weeks of treatment (Figure 2.2, Table 2.2). This effect may be due to the low food concentrations they experienced during the experimental period. Afterwards the calcification rates fluctuated within the range of 2 to 6  $\text{nmol CaCO}_3/\text{gFW}/\text{h}$ . The bivalves were rapidly exposed to elevated treatment  $p\text{CO}_2$ . In consequence, a drastic drop to  $-10.1 \text{ nmol CaCO}_3/\text{gFW}/\text{h}$  could be observed in the highest  $p\text{CO}_2$  treatment within the first day and partial recovery after one week.

However, calcification rates in this treatment were negative for the entire experimental duration, ranging from 0.4 to -4.8 indicating net dissolution took place. Only the highest treatment level had a significant negative effect on net biomineralization (ANOVA,  $F(5, 84) = 24.656$ ,  $p < 0.001$ , Tukeys test).

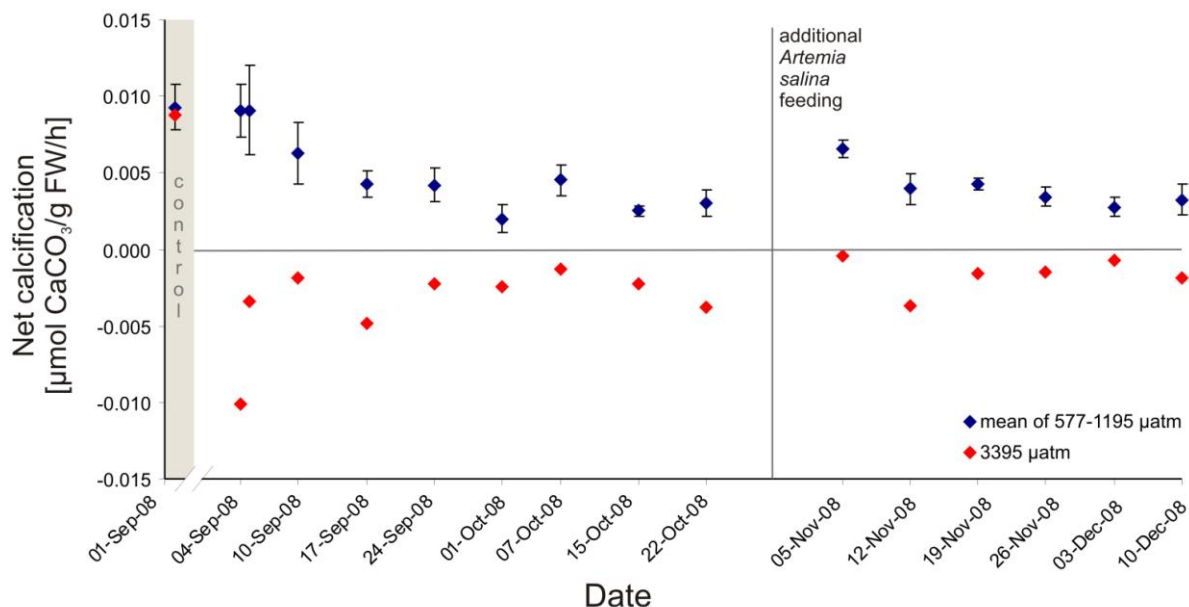


Figure 2.2: Calcification rates over time. First points are measured before  $\text{CO}_2$  was bubbled to the water. Values from 577-1195  $\mu\text{atm}$  are given as a mean and 3395  $\mu\text{atm}$  separately. Errors are given as 2SE.

	mean 577-1195 $\mu\text{atm}$ (2SE)	3352 $\mu\text{atm}$
<b>2-Sep-08</b>	0.0093 (0.0015)	0.0088
<b>04-Sep-08</b>	9.1 (0.0017)	-10.1
<b>05-Sep-08</b>	9.1 (0.0029)	-3.4
<b>10-Sep-08</b>	6.2 (0.0020)	-1.8
<b>17-Sep-08</b>	4.2 (0.0008)	-4.8
<b>24-Sep-08</b>	4.2 (0.0011)	-2.3
<b>01-Oct-08</b>	2.0 (0.0009)	-2.5
<b>07-Oct-08</b>	4.5 (0.0010)	-1.3
<b>15-Oct-08</b>	2.5 (0.0003)	-2.3
<b>22-Oct-08</b>	3.0 (0.0008)	-3.8
<b>05-Nov-08</b>	6.6 (0.0006)	-0.4
<b>12-Nov-08</b>	4.0 (0.0010)	-3.7
<b>19-Nov-08</b>	4.2 (0.0004)	-1.6
<b>26-Nov-08</b>	3.4 (0.0007)	-1.5
<b>03-Dec-08</b>	2.8 (0.0006)	-0.7
<b>10-Dec-08</b>	3.3 (0.0010)	-1.8

Table 2.2: Weekly measurements of calcification rates in  $\text{nmol CaCO}_3/\text{g FW/h}$ . Values from 577-1195  $\mu\text{atm}$  are given as a mean and from 3352  $\mu\text{atm}$  separately. Single values for all treatments can be found in the supplement.

Gazeau et al. (2007) observed a linear decline in calcification rates with increasing  $p\text{CO}_2$  in *Mytilus edulis* and *Crassostrea gigas*. In their study, *M. edulis* shells started to dissolve at  $p\text{CO}_2$  values higher than 1800  $\mu\text{atm}$  (corresponding to a pH of  $\sim 7.55$ ) which is lower than the threshold that could be expected for our study ( $\sim 2400$   $\mu\text{atm}$ ). In contrast to our long-term incubation of three months, they conducted short-term incubations (2h) which did not allow animals to acclimate. Waldbusser et al. (2010) found a significant decline of biocalcification in *Crassostrea virginica* with a reduction of  $\sim 0.5$  pH units. They observed high salinity mitigating this decline. The results of Waldbusser et al. (2010) should be viewed with caution as pH values were highly variable between different setups. But their results indicate bivalves from estuarine habitats may be more endangered by rising  $p\text{CO}_2$  values due to the low salinity. However, they used oysters originally reared at a salinity of 32 and therefore it can be assumed that the lower salinity treatment (SAL 16) caused additional stress to the animals. Nevertheless, due to the low buffer capacity low salinity waters are more susceptible to acidification. In Kiel Fjord, salinity is highly variable (10-20), but *M. edulis* from this area are most probably adapted to such conditions and therefore are not affected by these fluctuations (Thomsen et al. 2010, Thomsen and Melzner 2010). In the Baltic, mussels are able to survive in natural habitats with salinity down to 4.5 (Westerbom et al. 2002).

#### 2.4.1.2 Shell length growth

Several studies investigating the effects of elevated  $p\text{CO}_2$  focused on shell length or mass growth. Thomsen et al. (2010) observed increment length and also mass growth of *M. edulis* shells from Kiel Fjord at 1400  $\mu\text{atm}$   $p\text{CO}_2$  ( $\Omega_{\text{arag}} < 0.5$ ) to be similar to control rates. Even at 4000  $\mu\text{atm}$  ( $\Omega_{\text{arag}} < 0.2$ ) positive growth took place, although significantly less with respect to control and 1400  $\mu\text{atm}$ . In contrast to this study the experiment was conducted with continuous supply of *Rhodomonas* sp. suspension. Therefore, it is likely that the drop in calcification rates in our experiment was a result of food supply at only 3 days a week. It should be mentioned that shell length growth in our study was very low (0.46-0.72 mm) and highly variable. Interestingly, increment growth did not show a clear  $p\text{CO}_2$  dependency ( $F_{(5, 52)} = 0.484$ ,  $p = 0.786$ ) although calcification rates did (Figure 2.3, Table 2.3). This is in contrast to several studies that showed a decline in growth rates with increasing  $p\text{CO}_2$  in adult (Michaelidis et al. 2005, Berge et al. 2006, Thomsen et al. 2010, Thomsen and Melzner 2010) as well as larval bivalves (Kurihara et al. 2007 and 2008, Gazeau et al. 2010). Most of these studies observed higher length growth than in this experiment. Berge et al. (2006) also found only very little increment growth (0-2 mm; bivalves length was 11-21 mm) in *M. edulis* during an experimental time of 44 days. Within the pH range of 7.4 to 8.1 they also did not find a significant difference in length growth rate between the treatments, but there was a strong decrease in growth at pH = 7.1 and no growth at pH = 6.7. They attributed this observation to metabolic depression. The overall low growth

could be related to insufficient food supply (Berge et al 2006). As our lowest mean pH value was 7.28 no conclusion can be given about possible reduction in length growth for very low pH values.

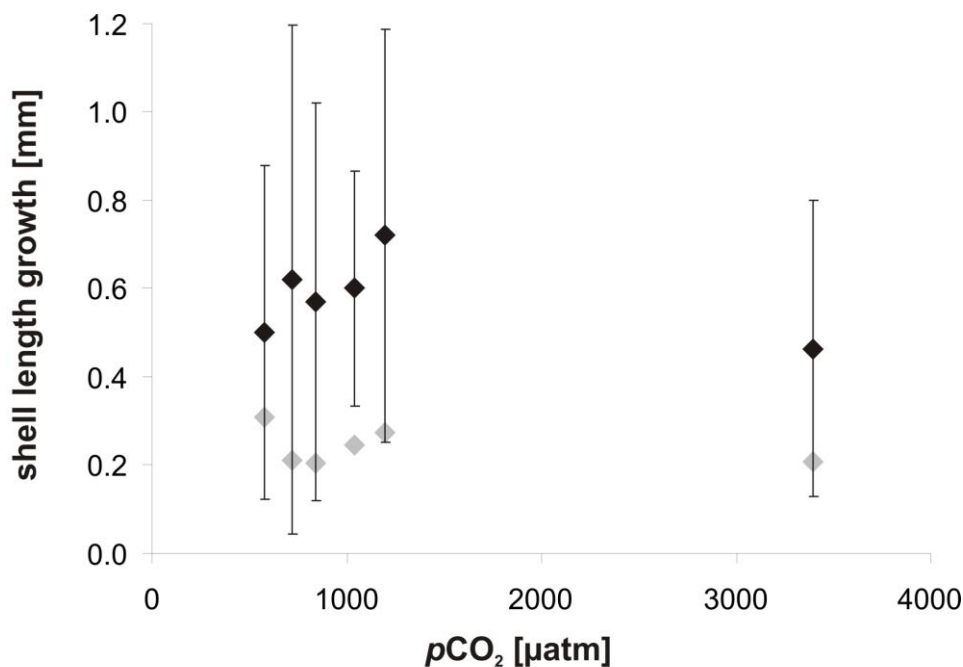


Figure 2.3: Mean shell length growth during the experimental interval (3 months) of all individuals (~140 specimens, light grey diamonds) and of eight to ten individually marked specimens per treatment (~ 20 mm; black diamonds). Errors are given as 1SD.

As measurements with a caliper are rather imprecise for a range < 0.2 mm (plus individual uncertainty of positioning the caliper) we investigated the MnCl<sub>2</sub>-labelled shells via EMP. The observation of this marking showed similar length growth for bivalves from 577 and 3352 µatm (Figure 2.4). This is in accordance with the measurements via caliper (Table 2.3).

The first lines (August, before treatment starts) are displayed much clearer (~0.5-0.8 % of Mn<sup>2+</sup>) than the ones in the middle of the experiment (October, ~0.2-0.25 %) which indicates more efficient calcification in the beginning. Still, the lines are also visible in the shell from the highest pCO<sub>2</sub> treatment even though net shell dissolution took place. This is in accordance with the observed shell length growth, the calcification process was not inhibited, but shell dissolution of older sections proceeds at a higher rate than biomineralization. MnCl<sub>2</sub> marking coupled with cathodoluminescence was successfully used by Langlet et al. (2006) in *Crassostrea gigas*. Barbin et al. (2007) showed the uptake of Mn<sup>2+</sup> into the shell of *C. gigas* being solely dependent on the manganese concentration in the water. The MnCl<sub>2</sub> concentration and incubation time in this study was the same (0.04 mg/l MnCl<sub>2</sub> compared to 0.017 mg/l Mn<sup>2+</sup>) for all dates of marking. The different intensity of the manganese lines

confirm the results of the calcification rates (Figure 2.2) which were clearly higher at the time of the first labeling (before treatment starts) compared to the remainder of the experiment. Shell  $\text{MnCl}_2$  incorporation consequently could serve as a good marker for calcification rates in *M. edulis*.

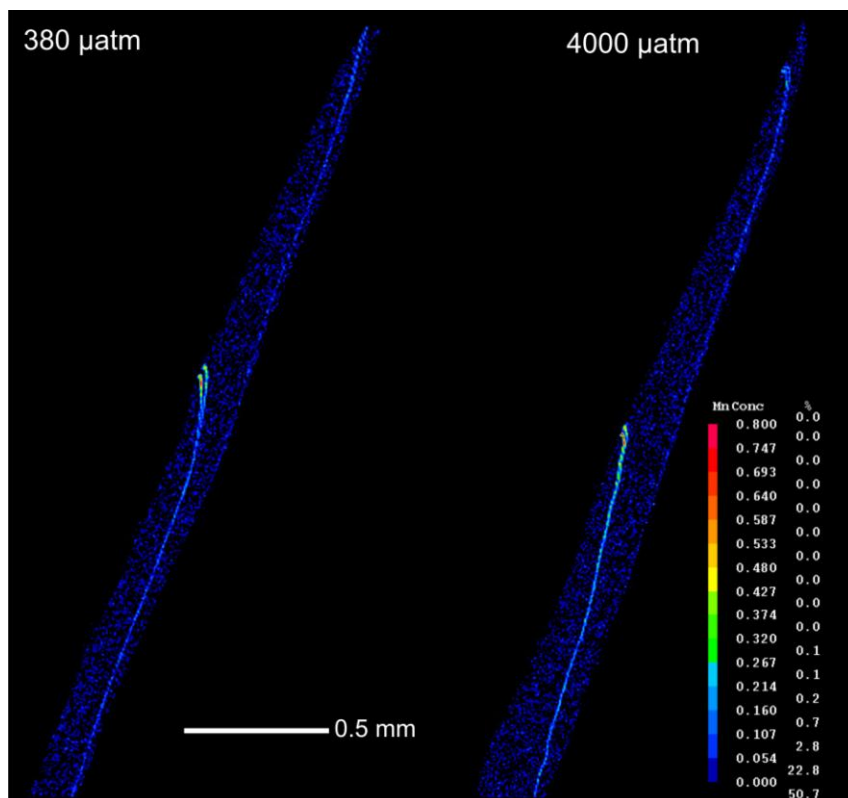


Figure 2.4: Microprobe images of newly grown calcite layer from a high and low  $p\text{CO}_2$  treatment with Mn-markings. Mn-content is given in %.

It offers the possibility to label bivalve shells very well-directed to e.g. investigate the cycle of calcification in more detail at different times of the year and even of the day. The advantage of this method compared to e.g. calcein is the quantitative determination that allows clear differentiation between the intensity of single lines and that the  $\text{Mn}^{2+}$  is permanently included in the shell without fading. Lartaud et al. (2010) showed a 30 min to 4 h exposure period with  $\text{Mn}^{2+}$  (90-120 mg/l) being sufficient to create a detectable mark in the shells of *C. gigas*. In consequence, they conclude that the  $\text{Mn}^{2+}$  marking is the fastest mollusk shell marking technique to date. A picture of wild *M. edulis* shell from Kiel Fjord with manganese marks illustrating weekly shell length growth can also be found in Thomsen et al. (2010).

Table 2.3: Mean values of shell length growth of ten individually marked mussels per treatment at the start of the experiment and four different time points until the end of the experiment.

$p\text{CO}_2$ -treatment [ $\mu\text{atm}$ ]	380	560	840	1120	1400	4000	
<b>Mean shell length [mm]</b>							
28.Aug.2008	20.06 (1.94)	19.24 (1.08)	19.82 (1.81)	19.60 (1.64)	19.29 (2.29)	18.38 (1.57)	
18.Sep.2008	20.17 (1.90)	19.40 (1.06)	19.83 (1.76)	19.63 (1.66)	19.31 (2.25)	18.39 (1.63)	
14.Oct.2008	20.23 (1.88)	19.45 (1.16)	19.97 (1.84)	19.72 (1.64)	19.53 (2.28)	18.40 (1.79)	
28.Oct.2008	20.36 (1.87)	19.67 (1.17)	20.04 (1.85)	19.85 (1.66)	19.52 (2.38)	18.44 (1.87)	
16.Dec.2008	20.56 (1.92)	19.86 (1.34)	20.39 (1.76)	20.20 (1.55)	20.00 (2.52)	18.84 (1.81)	
<b>Shell length growth increment [mm]</b>	0.50 (0.34)	0.62 (0.47)	0.57 (0.27)	0.60 (0.45)	0.72 (0.58)	0.46 (0.38)	
<b>Shell length [mm] of EMP analyzed individuals</b>							
28.Aug.2008						17.6	20.7
28.Oct.2008						18.6	21.6
16.Dec.2008						18.7	21.6

#### 2.4.1.3 Internal shell dissolution

However, despite net shell dissolution at 3352  $\mu\text{atm}$ , net shell length growth took place in this treatment. Consequently, the negative calcification rates must result from another factor, which is most likely inner shell dissolution. The shell structure of the ten individually marked animals and 15 other individuals showed increasing macroscopically visible corroded areas of the inner surfaces (nacre) at higher  $p\text{CO}_2$  treatments (Figure 2.5, Table 2.4).

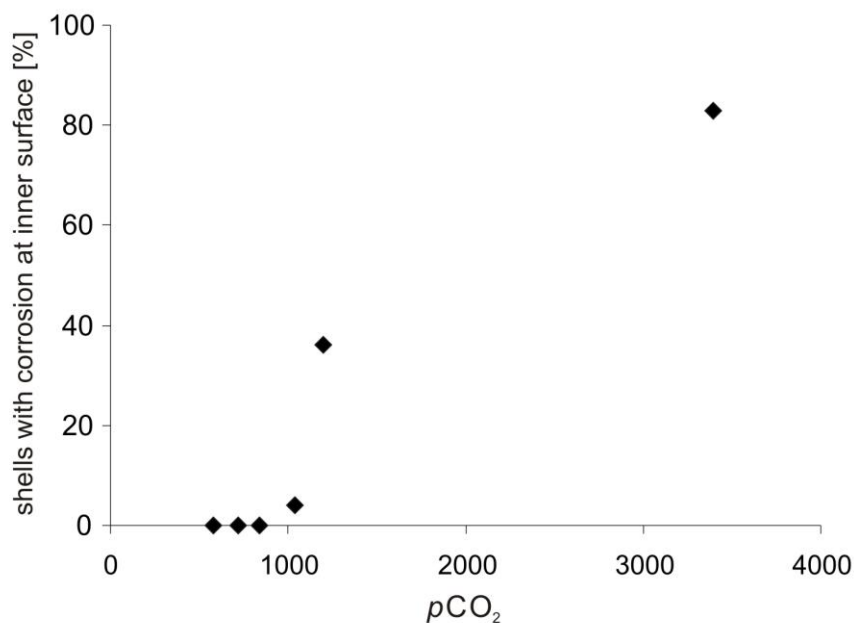


Figure 2.5: Amount of shells with etched areas at inner shell surface. 25 individuals per treatment.



Additional SEM images of the inner shell surface clearly showed the typical hexagonal shaped nacre crystals in non-corroded shells from 577  $\mu\text{atm}$  while no clear crystal shape could be observed in corroded areas (shell from 3352  $\mu\text{atm}$ ) (Figure 2.6). None of the shells from the 577  $\mu\text{atm}$  treatment showed signs of etching while the majority of shells (83 %) from the 3352  $\mu\text{atm}$  treatment had distinct etched areas at the inner surface. Inner shell dissolution has been discussed by several authors to result from different factors. Recently, Thomsen et al. (2010) observed thinner nacre layers under 4000  $\mu\text{atm}$  but no etched inner shell surfaces from well fed specimens. Melzner et al. (submitted) observed corroded inner shell surfaces also at control  $p\text{CO}_2$  under low food conditions, whereas under high food conditions elevated corrosion was limited to shells from 2400 and 4000  $\mu\text{atm}$  treatments. Already in 1939, Dugal showed carbonate dissolution in *Mercenaria mercenaria* as a response to elevated organic acid (probably lactic acid) after clams were kept out of the water for a period of days. Crenshaw and Neff (1969) investigated the impact of shell closure in *M. mercenaria* via measurements of  $\text{Ca}^{2+}$ ,  $\text{CO}_2$  and  $\text{H}^+$  concentrations in the EPF. The results and measurements of  $\text{Ca}^{2+}$  concentrations and succinic acid in the tissues led them to conclude that succinic acid produced by anaerobic metabolism was probably neutralized by shell dissolution. Lindinger et al. (1984) and Michaelidis et al. (2005) suggested shell dissolution in *M. edulis/M. galloprovincialis* raises extracellular  $\text{HCO}_3^-$  concentration for pH buffering. Also Dwyer et al. (1996) observed increased  $\text{Ca}^{2+}$  concentrations in the HL of *Crassostrea virginica* when the HL became more acidic. These results could not be confirmed by Thomsen et al. (2010) and Heinemann et al. (submitted, Chapter 4 of this thesis) and may be due to the closed/recirculating experimental setup of the two studies. Bibby et al. (2008) investigated the immune response of *M. edulis* to ocean acidification and demonstrated a significant impact of the latter. They suggest that elevated  $\text{Ca}^{2+}$  concentrations in the HL resulting from shell dissolution (indicated by previous studies, Lindinger et al. 1984, Gazeau et al. 2007) affect cellular metabolism, function and signaling pathways. However, our results, and that of Thomsen et al. 2010 do not indicate any  $\text{Ca}^{2+}$  accumulation in the HL or the EPF. Akberali et al. (1983) found a shell mass decrease of 15 % after three weeks in *Scrobicularia plana* as a result of acidic product of anaerobic respiration due to valve closing under stress. They observed changes in the structure of the inner shell surface over the course of a normal intertidal emersion (six hours). Therefore, this effect seems to be common in intertidal bivalves. Tunnicliffe et al. (2009) investigated the vent mussel *Bathymodiolus brevior* living at a submarine volcano where naturally acidic pH values of 5.36 to 7.29 dominate. Mussels showed clearly thinner shells at this location compared to a location with higher pH values. Furthermore, they describe a dead mussel with only small remaining disc of shell  $\text{CaCO}_3$  embedded in a husk of periostracum. Consequently, the periostracum might be the most important protection against hypercapnia. This is in accordance with our observation of increasing external calcite dissolution at the umbo region with rising  $p\text{CO}_2$  by trend. Dissolution in this area seems to occur when the periostracum is damaged (Thomsen et al. 2010). Nevertheless, although permanent net

dissolution took place in the highest  $p\text{CO}_2$  treatment, no significant impact on the shell mass could be observed after 3 months of experimental exposure. Summing up the expected loss of  $\text{CaCO}_3$  from shell dissolution calculated from the delta TA incubations only account for around 250 mg for all individuals of each aquarium. Therefore, absolute shell corrosion is only marginal and thus, a possible explanation of the results of Ries et al. (2009) who did not observe a significant effect of high seawater  $p\text{CO}_2$  on the calcification of *Mytilus edulis* by measuring shell weights. In this study overall mass increment was low which may indicate insufficient food supply and thereby masked significant effects.

However, the observed negative calcification rates (net dissolution) of this study seem to result from inner shell corrosion. As no long-time valve closing and no accumulation of bicarbonate could be observed (Heinemann et al. submitted, Chapter 4 of this thesis) it can be assumed that corrosion resulted from the combination of low food supply and elevated  $p\text{CO}_2$ . Palmer (1992) investigated the cost of calcification in two gastropods and found the synthesis of the organic matrix accounts for nearly 50 % of the cost when shell material contains 5 % organic matrix. Therefore, shell material production is a process with high energy demand. Additionally, the organic periostracum consists mainly of proteins and its production requires a similar amount of energy. Thomsen and Melzner (2010) observed increasing respiration and  $\text{NH}_4^+$  excretion in Baltic *Mytilus edulis* under elevated  $p\text{CO}_2$ . Living in an environment with additional stressors like elevated  $p\text{CO}_2$  appears to demand extra energy. Therefore, it can be assumed that limited energy under low food conditions leads to negligence of maintaining the shell structure (see also Melzner et al. submitted). Also under high food, calcification or production of required proteins is down regulated first at elevated  $p\text{CO}_2$  compared to animal soft tissue growth (Thomsen and Melzner 2010). Consequently, a strong biological control dictates the shell structure and its maintenance.

Table 2.4: Calcification rates before  $\text{CO}_2$  gassing (2<sup>nd</sup> of Sep. 2008; control) and mean calcification rates during the whole experiment, increment of growth from beginning of the experiment to the end and amount of shells with etched areas of the inner surface.

mean $p\text{CO}_2$ from days of alkalinity sampling [ $\mu\text{atm}$ ]	calcification rate CONTROL [nmol $\text{CaCO}_3/\text{g FW/h}$ ]	calcification rate during whole experiment (2SE) [nmol $\text{CaCO}_3/\text{g FW/h}$ ]	increment of growth of marked individuals (SD; n) [mm]	shells with inner surface etched [%]
577	8.0	5.9 (1.7)	0.5 (0.34; 10)	0
722	7.4	4.9 (1.2)	0.62 (0.47; 10)	0
839	11.6	4.4 (1.2)	0.57 (0.27; 10)	0
1041	10.2	3.9 (1.0)	0.6 (0.45; 10)	4
1195	9.2	4.0 (1.1)	0.72 (0.58 ;9)	36
3352	8.8	-2.8 (1.2)	0.52 (0.31; 8)	83

In summary, it is likely that the inner shell surface of *Mytilus edulis* is more sensitive to elevated  $p\text{CO}_2$  values than the outer for several reasons: 1) The nacre is made from aragonite which is 50 % more soluble than calcite (Mucci 1983) 2) the outer calcite layer is protected by the periostracum 3) due to respiratory  $p\text{CO}_2$  the EPF has higher  $p\text{CO}_2$  values than the external water and is more depleted with respect to  $[\text{CO}_3^{2-}]$ .

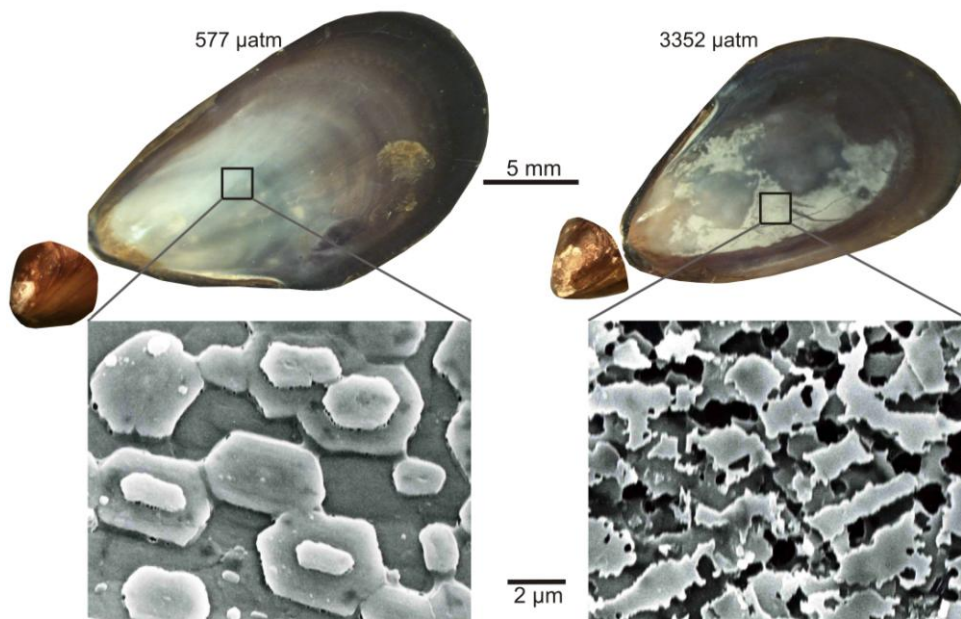


Figure 2.6: Pictures and SEM images of the inner surface (nacre) and the umbo region of shells from high and low  $p\text{CO}_2$  treatment.

#### 2.4.2 Elemental composition of body fluids

Numerous studies investigated elemental ratios in bivalve shells to use them as proxies for paleo-climate reconstruction (e.g. Klein et al. 1996a/b, Vander Putten et al. 2000, Lazareth et al. 2003, Gillikin et al. 2005, Immenhauser et al. 2005, Carré et al. 2006, Freitas et al. 2008, Wanamaker et al. 2008). To our knowledge only very few studies investigated the inorganic composition of HL and EPF, although the latter fills the space where shell formation occurs (Wilbur 1972). The precise mechanisms of biomineralization in bivalves are still unknown but shell formation occurs in the extrapallial space. It is evident that shell formation must be controlled as high  $\text{Mg}^{2+}$  concentrations, as observed in the EPF, would inhibit calcite formation (Berner 1975). Several studies indicate that organic components, such as a hydrophobic silk gel, acidic proteins, chitin and amorphous calcium carbonate (ACC) as a precursor phase, are involved in the formation of bivalve shells (e.g. Levi-Kalisman et al. 2001, Weiss et al. 2009, Suzuki et al. 2009, Weiss 2010). These studies suggested that crystal formation is taking place in a microenvironment separated from the EPF. In a recent study

(Jacob et al. 2010) ACC was found as a precursor phase in shells of adult Unionoida. The authors observed ACC in a narrow zone at the interface between periostracum and the prism layer. Most studies on element concentrations in bivalve's body fluids focused only on  $\text{Ca}^{2+}$  and did not investigate the geochemical context. In several studies increased  $\text{Ca}^{2+}$  concentration in bivalve's extracellular body fluids with respect to ambient water were observed. This was attributed to decreased extracellular pH as a result of air exposure (Crenshaw 1972, Jokumsen and Fyhn 1982), inner shell dissolution during valve closure (Crenshaw and Neff 1969, Wada and Fujinuki 1976) or as a consequence of elevated water  $p\text{CO}_2$  (Booth et al. 1984, Lindinger et al. 1984, Michaelidis et al. 2005). As the two latter studies were conducted in closed/recirculating systems, it can be assumed that  $[\text{Ca}^{2+}]$  also increased in the ambient water due to external shell dissolution at the umbo region (Thomsen et al. 2010). This is due to the inability of mussels to maintain elevated ion concentrations in body fluids with respect to surrounding seawater when the shell halves remain open. Additionally, flow through systems prevent an increase of  $\text{Ca}^{2+}$  and  $\text{Mg}^{2+}$  concentrations by shell dissolution in ambient water. Misogianes and Chasteen (1979) and Nair and Robinson (1998) reported that most of the  $\text{Ca}^{2+}$  (~85 %) in EPF of *M. edulis*/blood of *M. mercenaria* is bound to macromolecules. Misogianes and Chasteen (1979) suggested that  $\text{CaCO}_3$  deposition may be controlled by this complexation.

#### 2.4.3 $\text{Ca}^{2+}$ , $\text{Mg}^{2+}$ and $\text{Sr}^{2+}$ concentrations

No relationship between  $\text{Ca}^{2+}$ ,  $\text{Mg}^{2+}$  or  $\text{Sr}^{2+}$  concentrations or elemental ratios and elevated water  $p\text{CO}_2$  could be observed in this study (Table 2.S3). Therefore, element data from different  $p\text{CO}_2$  treatments are considered similar. Thomsen et al. (2010) also did not find significant changes of HL  $\text{Ca}^{2+}$  and  $\text{Mg}^{2+}$  concentrations with respect to the  $p\text{CO}_2$ . In contrast to most of the above mentioned studies we measured the inorganic composition of all fluids, the ambient water, HL and EPF (Figure 2.7). All fluids showed a positive linear relationship between  $\text{Ca}^{2+}$  and  $\text{Mg}^{2+}$  as well as  $\text{Sr}^{2+}$ .  $\text{Mg}^{2+}$  decreases in between 4.0-5.4 mmol/l and  $\text{Sr}^{2+}$  in between 8.2-8.6  $\mu\text{mol/l}$  per mmol/l  $\text{Ca}^{2+}$ . For  $\text{Sr}^{2+}$  no significant difference between water and the body-fluids could be observed for given  $\text{Ca}^{2+}$  concentrations while the  $\text{Mg}^{2+}$  concentration is significantly lower in the water compared to the body-fluids. This could be a result of the fact that the ion radius of  $\text{Sr}^{2+}$  (1.13 Å) is more similar to that of  $\text{Ca}^{2+}$  (0.99 Å) and is therefore incorporated into the shell in a higher relative amount than  $\text{Mg}^{2+}$  (0.65 Å). In consequence,  $\text{Sr}^{2+}$  becomes more depleted in the body-fluids than  $\text{Mg}^{2+}$ . When only those data were considered of individuals where HL and EPF was available both  $\text{Mg}^{2+}$  and  $\text{Sr}^{2+}$  depletions are strictly correlated to those of  $\text{Ca}^{2+}$ . Nevertheless, depletion is most pronounced for  $\text{Ca}^{2+}$ . As a consequence  $\text{Mg}^{2+}$  concentrations are offset relative to  $\text{Ca}^{2+}$  by  $2.5 \pm 0.8 \%$  (HL) and  $3.9 \pm 0.9 \%$  (EPF) while  $\text{Sr}^{2+}$  displays offsets of  $0.4 \pm 0.3 \%$  (HL) and  $1.3 \pm 0.4 \%$  (EPF), respectively. In general, most of the fluid concentrations are lower than those of the water. This indicates that they are depleted

in all elements during calcification. The amount of depletion in element concentrations depends on the rate of calcification, possible shell dissolution and the activity of the organism and therefore probably on the rate of exchange/circulation of the body fluids.

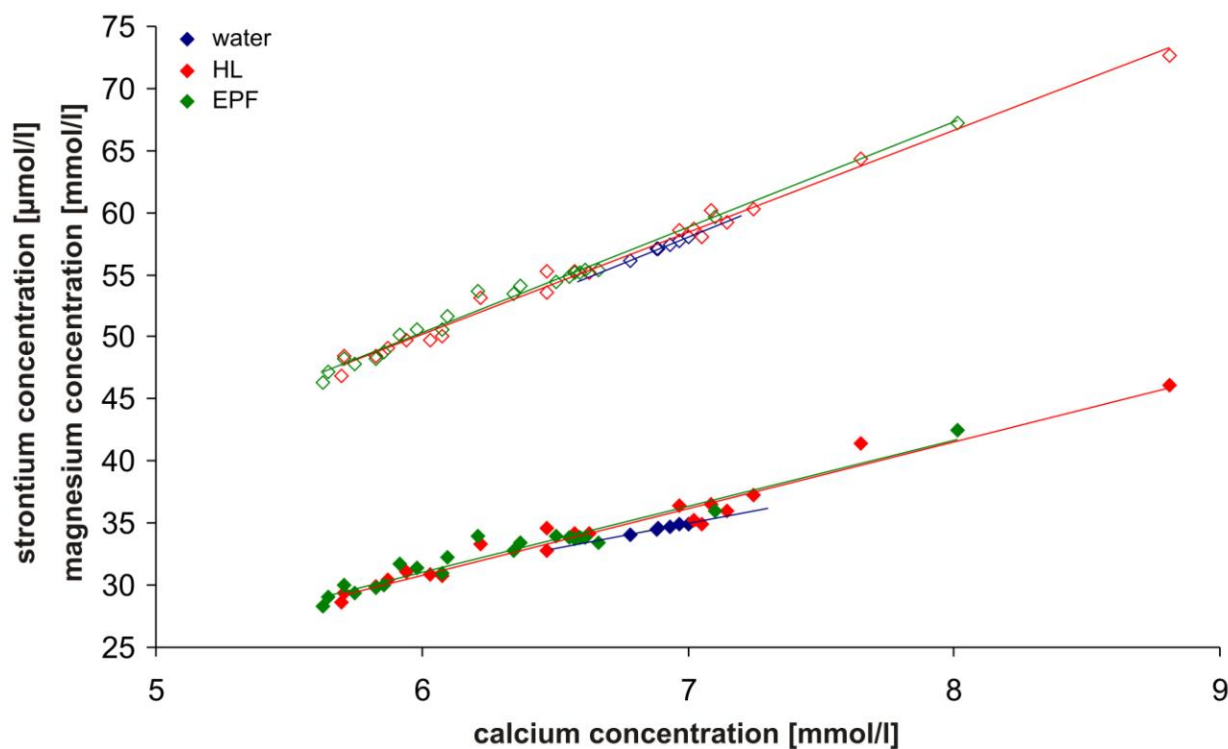
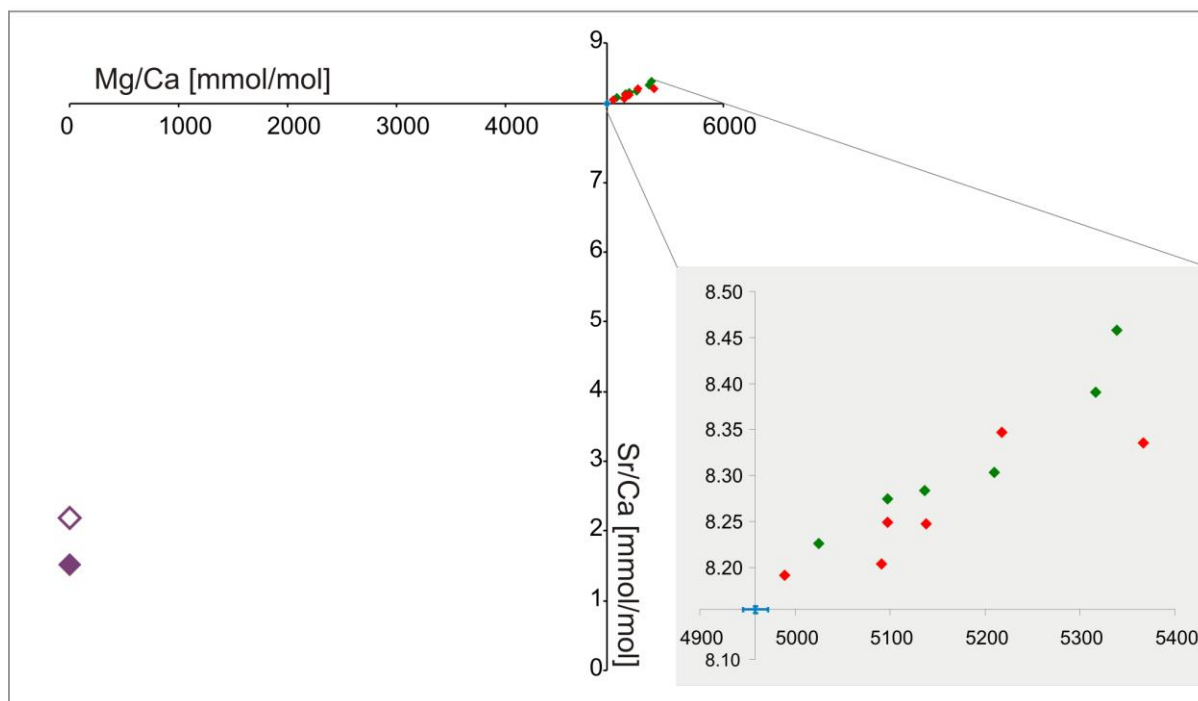


Figure 2.7: Changes of  $Mg^{2+}$  and  $Sr^{2+}$  concentrations in the body fluids of *Mytilus edulis* and the ambient water relative to changes in  $Ca^{2+}$ .  $Mg^{2+}$  is indicated by the closed diamonds and  $Sr^{2+}$  by the open diamonds. Each data point for HL and EPF displays one individual and each data point for water one aquarium.

In experiment 2 only EPF could be sampled as there was not enough HL volume. Due to higher salinity during the experimental period, element concentrations of the EPF are higher than that of experiment 1 (Table 2.S4). In general, one could expect lower  $Ca^{2+}$  concentrations in the EPF of experiment 2 as much higher calcification occurred. Mean values show EPF concentrations only being slightly (not significantly) lower than in the ambient water (Table 2.5). This again indicates the strong dependency on food supply and therefore the organisms' energy budget. When enough food is available the animal can invest more energy into shell growth. The whole organism is more active and therefore the circulation/replacement of the body fluids may occur faster. Additionally, a higher ion gradient exists when ions are rapidly removed from the fluid. Wada and Fujinuki (1976) reported the activity in the metabolism of shell formation to differ among bivalve species. The different activities are accompanied by formation and dissolution of shell and exhibit seasonal variations and physiological differences in EPF  $Ca^{2+}$  and  $CO_3^{2-}$  concentrations in the EPF. The dependency of the

inorganic fluid composition on so many different factors may be responsible for the differing and contradictory results on element concentrations and ratios in bivalve shells.

The elemental ratios examined in this study complement an earlier investigation (Heinemann et al. 2008) (Figure 2.8) however in this study we investigated more individuals and additionally sampled HL. In both studies we observed elemental ratios of the body fluids being higher than that of the ambient water. No consistent difference in the inorganic composition between the HL and the EPF could be found. But the body fluid elemental ratios follow a linear trend which emphasizes the relationship between the different elements. Studies using elemental ratios in bivalve shells as proxies contain contradictory results and several failed to show clear relationships between elemental ratios and environmental factors (e.g. Klein et al. 1996b, Vander Putten et al. 2000, Gillikin et al. 2005, Carré et al. 2006, Freitas et al. 2006, Heinemann et al. 2008, Heinemann et al. in press, Chapter 1 of this thesis). The so often called “vital effect” is reported as a reason for this and in consequence it is responsible for the high individual and physiological variability (Heinemann et al. in press, Chapter 1 of this thesis). Carré et al. (2006) proposed a calcification model where the ion transport through epithelial Ca-channels is dependent on the calcification rate as the channels become less-specific with rising growth rate. The results of Takesue et al. (2008) are consistent with this model. Additionally, they found high amounts of non-lattice-bound  $Mg^{2+}$  and  $Mn^{2+}$  in *Corbula amurensis* and therefore organic parts of the shell are rich in these elements. This is consistent with earlier findings of Misogianes and Chasteen (1979) who found the majority of manganese in the EPF of *M. edulis* being bound to small molecules. Takesue et al. (2008) conclude that these facts are the reason for the high dissimilarity of element to calcium (Me/Ca) ratios among five same-sized shells and in consequence the variations in the shells can only be attributed to internal biological processes. This can be confirmed by our findings as elemental ratios in the body fluids between individuals are highly variable ( $\pm 1$  % for Sr/Ca and  $\pm 2.4$  % for Mg/Ca;  $n = 15$ ) although the specimens originated from water with similar inorganic composition (Table 2.5). There is less variability in Sr/Ca than in Mg/Ca which is in accordance with the findings of Heinemann et al. (2008; in press, Chapter 1 of this thesis) in the calcite shell layer of *M. edulis*. Therefore, it is likely that the high variability of the extracellular fluids is also displayed in the shell and leads to the contradictory results as most studies only investigated a limited number of individuals. In consequence, it is essential to investigate all matrices involved in shell formation and compare them to each other and not solely use the shell as proxy archive. The elemental ratios of the shell (taken from Heinemann et al. 2008) show values lower than water and the extracellular fluids.



*Figure 2.8:* Sr/Ca ratios of body fluids and water from this study and from shell of Heinemann et al. 2008 relative to Mg/Ca. Each EPF/HL data point represents the mean value of all individuals of one aquaria and the water point is the mean value of the six aquaria. Purple diamond: aragonite, filled purple: calcite, blue: water, red: HL, green: EPF. Error bars of the water are given as SD. Due to the high individual variability errors of body fluids are high and are not displayed here to keep the figure well-arranged. They are shown in Table 2.5.

The examination of the elemental ratios contains the assumption that  $\text{Ca}^{2+}$  for shell formation is taken from the EPF as it becomes depleted in higher amounts in  $\text{Ca}^{2+}$  than in  $\text{Mg}^{2+}$  and  $\text{Sr}^{2+}$ . The shell (data from Heinemann et al. 2008) is clearly enriched in  $\text{Ca}^{2+}$  as it consists of  $\text{CaCO}_3$  and other elements substitute  $\text{Ca}^{2+}$  only in minor amounts. Takesue et al. (2008) found a linear relationship between growth rate and elemental ratios in bivalve shells, which is in accordance with other studies (e.g. Klein et al. 1996b, Carré et al. 2006, Ford et al. 2010). In the fluids of experiment 1 we could not find such a correlation which probably is a result of the very low calcification rates. Mg/Ca, Sr/Ca and additionally B/Ca of the fluids from experiment 2 show a trend (even if not significant) towards decreasing Me/Ca in the EPF relative to the water with decreasing growth rates (Heinemann et al. submitted, Chapter 4 of this thesis). However, the elemental shell signature seems to be strongly related to the inorganic composition of the extracellular body fluids.

Table 2.5: Mean elemental ratios of all matrices per aquarium. Shell data are taken from Heinemann et al. 2008.

		<b>Mg/Ca [mmol/mol]</b> <b>(SD, n)</b>	<b>Sr/Ca [mmol/mol]</b> <b>(SD, n)</b>
<b>water</b>	452	4980	8.151
	574	4962	8.154
	731	4959	8.159
	906	4955	8.151
	1123	4938	8.159
	2724	4957	8.150
<b>HL</b>	452	5097 (96; 2)	8.25 (0.091; 2)
	574	5217 (123; 2)	8.35 (0.093; 2)
	731	5091 (120; 3)	8.20 (0.039; 3)
	906	5366	8.34
	1123	5138 (37; 3)	8.25 (0.030; 3)
	2724	4989 (44; 4)	8.19 (0.035; 4)
<b>EPF</b>	452	5097 (22; 2)	8.27 (0.032; 2)
	574	5338 (124; 2)	8.46 (0.078; 2)
	731	5136 (55; 3)	8.28 (0.048; 3)
	906	5316	8.39
	1123	5209 (70; 3)	8.30 (0.063; 3)
	2724	5024 (31; 4)	8.23 (0.027; 4)
<b>aragonite</b>		7.53 (3.1; 3)	2.29 (1.2; 3)
<b>calcite</b>		9.80 (2.3; 3)	1.58 (0.05; 3)



## 2.5 Conclusions

Our results challenge the use of bivalve shells as proxy archives and underline that future studies should not only focus on examination of the shell but also on the body fluids. Element determinations lead to the conclusion that the inorganic composition of HL and EPF are modified during shell formation and are highly variable between individuals. This is also displayed in the shell and therefore body fluids and elemental shell signature are strongly correlated.

This study tends to confirm the finding of other studies that found reduced calcification under high  $p\text{CO}_2$  (e.g. Gazeau et al. 2007, Thomsen et al. 2010, Melzner et al. submitted) and again underline that food appears to be the main limiting factor for calcification. Without sufficient nutrient supply *Mytilus edulis* is not able to maintain nacre structure during exposure to elevated  $p\text{CO}_2$ . As zoo- as well as phytoplankton are negatively affected by changes in water pH (Yamada and Ikeda 2000, Hinga 2002) ocean acidification may impact *M. edulis* indirectly already at lower degrees of hypercapnia. The majority (up to 83 %) of *Mytilus* shell is made up of the more soluble  $\text{CaCO}_3$  form, aragonite (e.g. Hubbard et al. 1981). Therefore, acidified seawater will be a considerable problem for *M. edulis* especially at the inner shell surface. As length growth in *M. edulis* is mainly dominated by the calcite layer and thickening by the nacre layer (Wheeler et al. 1975), shells will become thinner. Our results revealed that the use of different techniques to quantify calcification rates provides information for different aspects of shell formation. Calcite precipitation is less sensitive to acidified conditions as indicated by ongoing shell length growth and  $\text{Mn}^{2+}$  marking results. In contrast, aragonite dissolution is observed by SEM and bright field stereo microscopic images and increased alkalinity during  $\Delta A_T$  incubations. The lowering of calcification rates during long-term experiments with low food supply are also confirmed by measurements using  $\Delta A_T$  and less pronounced  $\text{Mn}^{2+}$  marking. Therefore, future investigations should not only focus on one way to determine shell growth but combine different methods in order to consider the different responses of mussel calcification towards abiotic stressors such as ocean acidification.

In summary, a better understanding of the general biomineralization mechanisms and the impacts of different environmental factors is necessary to use bivalve shells as proxy archives. Since the results of this study indicate that shell elements originate from the EPF the connection between this fluid and the shell should be considered in future studies.

## References

- Akberali, H. B., Brear, K., Currey, J. D., 1983. Mechanical and morphological properties of the shell of *Scrobicularia plana* (da Costa) under normal and stress conditions. *J. Mollus. Stud.* 43, 93-97.
- Barbin, V., Ramseyer, K., Elfman, M., 2007. Biological record of added manganese in seawater: a new efficient tool to mark in vivo growth lines in the oyster species *Crassostrea gigas*. *Int. J. Earth. Sci.* 97, 193-199.
- Berge, J., Bjerkeng, B., Pettersen, O., Schaanning, M., Øxnevad, S., 2006. Effects of increased sea water concentrations of CO<sub>2</sub> on growth of the bivalve *Mytilus edulis* L.. *Chemosphere* 62(4):681-687.
- Berner, R. A., 1975. The role of magnesium in the crystal growth of calcite and aragonite from sea water, *Geochim. Cosmochim. Acta* 39, 489–504.
- Bibby, R., Widdicombe, S., Parry, H., Spicer, J., Pipe, R., 2008. Effects of ocean acidification on the immune response of the blue mussel *Mytilus edulis*. *Aquat. Biol.* 2: 67–74. doi: 10.3354/ab00037.
- Bijma, J., Spero, H. J., and Lea, D. W.: Reassessing Foraminiferal Stable Isotope Geochemistry: Impact of the Oceanic Carbonate System (Experimental Results), in: Use of Proxies in Palaeoceanography: Examples from the South Atlantic., edited by: Fischer, G. and Wefer, G., 489–512, Springer-Verlag, Heidelberg, 1999.
- Bleich, M., F. Melzner, C. Hiebenthal, H. Mempel, K. Schulz, U. Riebesell, M. Wahl, F. Sommer, U. Sommer, A. Form, U. Piatkowski, R. Hanel, D. Piepenburg, M. Spindler, A. Eisenhauer, A. Franke, V. Möller, G. Baumert and C. Clemmesen-Bockelmann (2008). Poster: Kiel CO<sub>2</sub> manipulation experimental facility (KICO2). Second Symposium on The Ocean in a High-CO<sub>2</sub> World. Monaco.
- Caldeira, K. and Wickett, M.E., 2003. Anthropogenic carbon and ocean pH. *Nature.* 25(6956), 365-365.
- Cao, L. and Caldeira, K., 2008. Atmospheric CO<sub>2</sub> stabilization and ocean acidification. *Geophys. Res. Lett.* 35(19).
- Carré, M., Bentaleb, I., Bruguier, O., Ordinola, E., Barrett, N.T., Fontugne, M., 2006. Calcification rate influence on trace elements concentrations in aragonitic bivalve shells: Evidences and mechanisms. *Geochim. Cosmochim. Ac.* 70 (19), 4906-4920.
- Crenshaw, M. A. and Neff, J. M., 1969. Decalcification at the mantle-shell interface in molluscs. *Am. Zool.* 9, 881-889.
- Crenshaw, M. A., 1972. Inorganic composition of molluscan extrapallial fluid. *Biol. Bull.* 143, 506-512.
- Dickson, A. G., and Millero, F. J., 1987. A comparison of the equilibrium-constants for the dissociation of carbonic-acid in seawater media, *Deep-Sea.* 34, 1733-1743.
- Dickson, A. G., 1990. Standard potential of the reaction - AgCl<sub>S</sub>+1/2 H<sub>2</sub> = Ag<sub>S</sub>+HCl<sub>Aq</sub> and the standard acidity constant of the ion HSO<sub>4</sub><sup>-</sup> in synthetic sea-water from 273.15-K to 318.15-K. *J. Chem. Thermodyn.* 22, 113-127.
- Dickson, A. G., Afghan J. D., Anderson, G. C., 2003. Reference materials for oceanic CO<sub>2</sub> analysis: a method for the certification of total alkalinity. *Mar. Chem.* 80(2-3), 185-197.

- Dickson, A. G., Sabine, C. L., Christian, J. R., 2007. Guide to best practices for ocean CO<sub>2</sub> measurements. PICES Special Publication 3, IOCCP Report No. 8. 191 pp.
- Dodd, J. R., 1965. Environmental control of strontium and magnesium in *Mytilus edulis*. *Geochim. Cosmochim. Ac.* 29 (5), 385-398.
- Dugal, L.P., 1939. The use of calcereous shell to buffer the product of glycolysis in *Venus Mercenaria*. *J. Cell Comp. Physiol.* 13, 235-250.
- Dwyer, J. J. and Burnett, J. L., 1996. Acid-Base Status of the Oyster *Crassostrea virginica* in Response to Air Exposure and to Infections by *Perkinsus marinus*. *Biol. Bull.* 190, 139-147.
- Enderlein, P. and M. Wahl, 2004. Dominance of blue mussels versus consumer-mediated enhancement of benthic diversity. *J. Sea Res.* 51(2), 145-155.
- Feely, R.A., Sabine, C.L., Lee, K., Berelson, W., Kleypas, J.A., Fabry, V.J., Millero, F.J., 2004. Impact of anthropogenic CO<sub>2</sub> on the CaCO<sub>3</sub> system in the oceans. *Science* 305(5682), 362-366.
- Ford, H., Schellenberg, S. A., Becker, B. J., Deutschman, D. L., Dyck, K. A., Koch P. L., 2010. Evaluating the skeletal chemistry of *Mytilus californianus* as a temperature proxy: Effects of microenvironment and ontogeny *Paleoceanography* 25, PA1203, doi:10.1029/2008PA001677
- Freitas, P., Clarke L. J., Kennedy, H., Richardson, C., Abrantes, F., 2005. Mg/Ca, Sr/Ca, and stable-isotope (delta O-18 and delta C-13) ratio profiles from the fan mussel *Pinna nobilis*: Seasonal records and temperature relationships. *Geochem. Geophys. Geosys.* 6, Q04D14, doi:10.1029/2004GC000872, 2005.
- Freitas, P., Clarke L. J., Kennedy, H., Richardson, C., Abrantes, F., 2006. Environmental and biological controls on elemental (Mg/Ca, Sr/Ca and Mn/Ca) ratios in shells of the king scallop *Pecten maximus*, *Geochim. Cosmochim. Ac.*, 70, 5119–5133.
- Freitas, P. S., Clarke, L. J., Kennedy, H. A., Richardson, C. A., 2008. Inter and intra-specimen variability masks reliable temperature control on shell Mg/Ca ratios in laboratory- and field-cultured *Mytilus edulis* and *Pecten maximus* (bivalvia). *Biogeosciences* 5(5), 1245-1258.
- Gazeau, F., Quiblier, C., Jansen, J. M., Gattuso, J.-P., Middelburg, J. J., Heip, C. H. R., 2007. Impact of elevated CO<sub>2</sub> on shellfish calcification, *Geophys. Res. Lett.* 34, 5.
- Gazeau, F., Gattuso, J.-P., Dawber, C., Pronker, A. E., Peene, F., Peene, J., Heip, C. H. R., Middelburg, J. J. 2010. Effect of ocean acidification on the early life stages of the blue mussel (*Mytilus edulis*). *Biogeosciences Discuss.* 7, 2927-2947. doi:10.5194/bgd-7-2927-2010.
- Gillikin D. P., Lorrain A., Navez J., Taylor J. W., Keppens E., Baeyens W., Dehairs F., 2005. Strong biological controls on Sr/Ca ratios in aragonitic marine bivalve shells. *Geochem. Geophys. Geosyst.* 6, Q05009 doi:10.1029/2004GC000874.
- Gosling, E. 1992. Systematics and Geographic Distribution of *Mytilus*, in Gosling, E. (Ed.) *The Mussel Mytilus: Ecology, Physiology, Genetics and Culture*. Amsterdam, Elsevier Science Publishers B.V. pp. 1-19.
- Heinemann, A., Fietzke, J., Eisenhauer, A., Zumholz, K., 2008. Modification of Ca isotope and trace metal composition of the major matrices involved in shell formation of *Mytilus edulis*. *Geochem. Geophys. Geosyst.* 9 (1), Q01006, doi:10.1029/2007GC001777.

Heinemann, A., Hiebenthal, C., Fietzke, J., Eisenhauer, A., Wahl, M. Disentangling the Biological and Environmental Control of *M. edulis* Shell Chemistry. *Geochem. Geophys. Geosyst.* doi:10.1029/2010GC003340, in press.

Heinemann, A., Fietzke, J., Melzner, F., Böhm, F., Thomsen, J., Garbe-Schönberg, D., Eisenhauer, A., Responses of *Mytilus edulis* extracellular body fluids and shell composition to decreased pH: acid-base status, trace elements and  $\delta^{11}\text{B}$ . Submitted to *Chemical Geology*.

Hinga, K. R., 2002. Effects of pH on coastal marine phytoplankton. *Mar. Ecol. Prog. Ser.* 238, 281–300

Hoegh-Guldberg, O., Mumby, P. J., Hooten, A. J., Steneck, R. S., Greenfield, P., Gomez, E., Harvell, C. D., Sale, P. F., Edwards, A. J., Caldeira, K., Knowlton, N., Eakin, C. M., Iglesias-Prieto, R., Muthiga, N., Bradbury, R. H., Dubi, A., Hatziolos, M. A., 2007. Coral Reefs Under Rapid Climate Change and Ocean Acidification. *Science* 318, 1737. DOI: 10.1126/science.1152509

Houghton, J., Ding, Y., Griggs, D., Noguer, M., van der Linden, P., Xiaosu, D., 2001. *Climate Change 2001: The Scientific Basis* (Contribution of Working Group I to the Third Assessment Report of the IPCC). *Cambridge University Press*, Cambridge.

Hubbard F., McManus J., Al-Dabbas M., 1981. Environmental influences on the shell mineralogy of *Mytilus edulis*. *Geo.-Mar. Lett.* 1, 267–269.

Immenhauser, A., Nägler, T.F., Steuber, T., Hippler, D., 2005. A critical assessment of mollusk  $^{18}\text{O}/^{16}\text{O}$ , Mg/Ca, and  $^{44}\text{Ca}/^{40}\text{Ca}$  ratios as proxies for Cretaceous seawater temperature seasonality. *Palaeogeogr. Palaeoclimatol.* 215(3-4), 221-237.

Jacob, D.E., Wirth, R., Soldati, A. L., Wehrmeister, U., Schreiber, A., 2010. Amorphous calcium carbonate in the shells of adult Unionoida. *J. Struc. Biol.* 10.1016/j.jsb.2010.09.011.

Jokumsen, A. and Fyhn, J., 1982. The influence of aerial exposure upon respiratory and osmotic properties of haemolymph from two intertidal mussels, *Mytilus edulis* L. and *Modiolus modiolus*. *J. Exp. Mar. Biol. Ecol.* 61, 189-203.

Klein, R. T., Lohmann, K. C., Thayer, C. W., 1996a. Bivalve skeletons record sea-surface temperature and  $\delta^{18}\text{O}$  via Mg/Ca and  $^{18}\text{O}/^{16}\text{O}$  ratios. *Geology* 24 (5), 415-418.

Klein, R. T., Lohmann, K. C., Thayer, C. W., 1996b. Sr/Ca and  $^{13}\text{C}/^{12}\text{C}$  ratios in skeletal calcite of *Mytilus trossolus*: covariation with metabolic rate, salinity and carbon isotopic composition of sea water. *Geochim. Cosmochim. Ac.*, 60, 4207-4221.

Kossak, U., 2006. How climate change translates into ecological change: Impacts of 308 warming and desalination on prey properties and predator-prey interactions in the Baltic 309 Sea, Ph.D. thesis, Christian-Albrechts-Univ., Kiel, Germany. 310  
(Available at [http://eldiss.uni-kiel.de/macau/receive/dissertation\\_diss\\_00001910](http://eldiss.uni-kiel.de/macau/receive/dissertation_diss_00001910))

Kurihara, H., Ishimatsu, A., 2008. Effects of high  $\text{CO}_2$  seawater on the copepod (*Acartia tsuensis*) through all life stages and subsequent generations. *Mar. Pollut. Bull.*, 56(6):1086-1090.

Kurihara, H., Kato, S., Ishimatsu, A., 2007. Effects of increased seawater  $p\text{CO}_2$  on early development of the oyster *Crassostrea gigas*. *Aquatic Biology* 1, 91-98

- Langlet, D., Alunno-Bruscia, M., Rafélis, M., Renard, M., Roux, M., Schein, E., Buestel, D., 2006. Experimental and natural cathodoluminescence in the shell of *Crassostrea gigas* from Thau lagoon (France): ecological and environmental implications. *Mar. Ecol. Prog. Ser.* 317, 143–156.
- Lartaud, F., de Rafelisa, M., Roperc, M., Emmanuela, L., Geairond, P., Renarda, M., 2010. Mn labeling of living oysters: Artificial and natural cathodoluminescence analyses as a tool for age and growth rate determination of *C. gigas* (Thunberg, 1793) shells. *Aquaculture* 300(1-4), 206-217.
- Lazareth, C.E., Vander Putten, E., Andre, L., Dehairs F., 2003. High resolution trace element profiles in shells of the mangrove bivalve *Isognomon ephippium*: a record of environmental spatio-temporal variations?, *Estuar. Coastal Shelf S.*, 57(5-6), 1103-1114.
- Levi-Kalisman, Y., Falini G., Addadi, L., Weiner, S., 2001. Structure of the Nacreous Organic Matrix of a Bivalve Mollusk Shell Examined in the Hydrated State Using Cryo-TEM. *J. Struct. Biol.* 135, 8–17. doi:10.1006/jsbi.2001.4372
- Lewis, E. and Wallace, D., 1998. Program Developed for CO<sub>2</sub> System Calculations. ORNL/CDIAC-105. Carbon Dioxide Information Analysis Center, Oak Ridge National Laboratory, U.S. Department of Energy. Oak Ridge, Tennessee.
- Lindinger, M.I., Lauren, D.J., McDonald, D.G., 1984. Acid-base-balance in the sea mussel, *Mytilus edulis*. 3. Effects of environmental hypercapnia on intracellular and extracellular acid-base-balance, *Mar. Biol. Lett.* 5, 371-381.
- Lorrain, A., Gillikin, D., Paulet, Y.M., Chavaud, L., Lemercier, A., Navez, J., Andre, L., 2005. Strong kinetic effects on Sr/Ca ratios in the calcitic bivalve *Pecten maximus*. *Geology* 33, 965–968.
- Mehrbach, C., Culberso, C. H., Hawley, J. E., Pytkowic, R. M., 1973. Measurement of apparent dissociation-constants of carbonic-acid in seawater at atmospheric-pressure. *Limnol. Oceanogr.* 18, 897-907.
- Melzner, F., Gutowska, M. A., Langenbuch, M., Dupont, S., Lucassen, M., Thorndyke, M. C., Bleich, M., Pörtner, H.-O., 2009. Physiological basis for high CO<sub>2</sub> tolerance in marine ectothermic animals: pre-adaptation through lifestyle and ontogeny?. *Biogeosciences* 6, 2313–2331. doi:10.5194/bg-6-2313-2009.
- Melzner, F., Stange, P., Trübenbach, K., Thomsen, J., Casties, I., Panknin, U., Gutowska, M. A., 2010. Interactive effects of food supply and seawater pCO<sub>2</sub> on calcification and internal shell dissolution in the blue mussel *Mytilus edulis*. submitted to PLoS ONE.
- Michaelidis, B., Ouzounis, C., Palaras, A., Pörtner, H.-O., 2005. Effects of long-term moderate hypercapnia on acid-base balance and growth rate in marine mussels *Mytilus galloprovincialis*. *Mar. Ecol.-Prog. Ser.* 293, 109-118.
- Mintrop, L., Perez, F. F., Gonzalez-Davila, M., Santana-Casiano, M. J., Körtzinger, A., 2000. Alkalinity determination by potentiometry: Intercalibration using three different methods. *Cienc. Mar.* 26, 23-37.
- Misogianes, M. J., and Chasteen, N. D., 1979. Extrapallial fluid: a chemical and spectral characterization of the extrapallial fluid of *Mytilus edulis*. *Anal. Biochem.* 100, 324-334.
- Mucci, A., 1983. The solubility of calcite and aragonite in seawater at various salinities, temperatures, and 1 atmosphere total pressure. *Am. J. Sci.* 238, 780–799.

- Nair, P. S., and Robinson, W. E., 1998. Calcium Speciation and Exchange Between Blood and Extrapallial Fluid of the Quahog *Mercenaria mercenaria* (L.). Biol.Bull. 195, 43-51.
- Orr, J. C., Fabry, V. J., Aumont, O., Bopp, L., Doney, S. C., Feely, R. A., Gnanadesikan, A., Gruber, N., Ishida, A., Joos, F., Key, R. M., Lindsay, K., Maier-Reimer, E., Matear, R., Monfray, P., Mouchet, A., Najjar, R. G., Plattner, G. K., Rodgers, K. B., Sabine, C. L., Sarmiento, J. L., Schlitzer, R., Slater, Riebesell, U., Zondervan, I., Rost, B., Tortell, P. D., Zeebe, R. E., Morel, F. M. M., 2000. Reduced calcification of marine plankton in response to increased atmospheric CO<sub>2</sub>. Nature 407, 364–367.
- Orr, J. C., Fabry, V. J., Aumont, O., Bopp, L., Doney, S. C., Feely, R. A., Gnanadesikan, A., Gruber, N., Ishida, A., Joos, J., Key, R. M., Lindsay, K., Maier-Reimer, E., Matear, R., Monfray, P., Mouchet, A., Najjar, R. G., Plattner, G. K., Rodgers, K. B., Sabine, C. L., Sarmiento, J. L., Schlitzer, R., Slater, R. D., Totterdell, I. J., Weirig, M. F., Yamanaka, Y., Yool, A., 2005. Anthropogenic ocean acidification over the twenty-first century and its impact on calcifying organisms. Nature 437(7059), 681- 686.
- Orr, J. C., Caldeira, K., Fabry, V., Gattuso, J.-P., Haugan, P., Lehodey, P., Pantoja, S., Pörtner, H.-O., Riebesell, U., Trull, T., Urban, E., Hood, M., Broadgate, W., 2009. Research priorities for understanding ocean acidification: Summary from the Second Symposium on the Ocean in a High-CO<sub>2</sub> World. Oceanography 22(4),182–189.
- Palmer, A. R., 1992. Calcification in marine molluscs: How costly is it? Ecology 89, 1379-1382.
- Riebesell, U., Zondervan, I., Rost, B., Tortell, P. D., Zeebe, R. E., Morel, F. M. M.: Reduced calcification of marine plankton in response to increased atmospheric CO<sub>2</sub>. Nature 407, 364–367.
- Ries, J.B., Cohen, A.L., McCorkle, D.C., 2009. Marine calcifiers exhibit mixed responses to CO<sub>2</sub>-induced ocean acidification. Geology 37, 1131-1134.
- Sabine, C. L., Feely, R. A., Gruber, N., Key, R. M., Lee, K., Bullister, J. L., Wanninkhof, R., Wong, C. S., Wallace, D. W. R., Tilbrook, B., Millero, F. J., Peng, T. H., Kozyr, A., Ono, T., Rios, A. F., 2004. The oceanic sink for anthropogenic CO<sub>2</sub>. Science 305(5682), 367-371.
- Schöne, B. R., Fiebig, J., Pfeiffer, M., Gless, R., Hickson, J., Johnson, A. L. A., Dreyer, W., Oschmann, W., 2005. Climate records from a bivalved Methuselah (*Arctica islandica*, Mollusca; Iceland). Palaeogeogr. Palaeocl. 228(1-2), 130-148.
- Seed, R. 1976. Ecology. In: Bayne, B. L. (Ed.), Marine Mussels. Cambridge Univ. Press, Cambridge, 13-66.
- Smith, S. V. and Key, G. S. 1975. Carbon-Dioxide and Metabolism in Marine Environments. Limnol. Oceanogr. 20(3): 493-495.
- Suzuki, M., Saruwatari, K., Kogure, T., Yamamoto, Y., Nishimura, T., Kato, T., Nagasawa, H., 2009. An Acidic Matrix Protein, Pif, Is a Key Macromolecule for Nacre Formation. Science 325, 1388. DOI: 10.1126/science.1173793.
- Takesue, R. K., Bacon, C. R., Thompson, J. K., 2008. Influences of organic matter and calcification rate on trace elements in aragonitic estuarine bivalve shells. Geochim. Cosmochim. Ac. 72, 22, 5431-5445. doi:10.1016/j.gca.2008.09.003

Thomsen, J., Gutowska, M. A., Saphörster, J., Heinemann, A., Trübenbach, K., Fietzke, J., Hiebenthal, C., Eisenhauer, A., Körtzinger, A., Wahl, M., Melzner, F., 2010. Calcifying invertebrates succeed in a naturally CO<sub>2</sub> enriched coastal habitat but are threatened by high levels of future acidification. *Biogeosciences*, 7, 3879–3891. doi:10.5194/bg-7-3879-2010

Thomsen, J. and Melzner, F., 2010. Moderate seawater acidification does not elicit long-term metabolic depression in the blue mussel *Mytilus edulis*. *Mar. Biol.* 157(12), 2667-2676. DOI: 10.1007/s00227-010-1527-0.

Tunncliffe V., Davies, K. T. A., Butterfield, D. A., Embley, R. W., Rose, J. M., Chadwick Jr., W. W., 2009. Survival of mussels in extremely acidic waters on a submarine volcano. *Nature Geoscience*. DOI: 10.1038/NGEO500 .

Vander Putten, E., Dehairs, F., Keppens, E., Baeyens, W., 2000. High distribution of trace elements in the calcite shell layer of modern *Mytilus edulis*: Environmental and biological controls. *Geochim. Cosmochim. Ac.* 64(6), 997–1011.

Wada, K. and Fujinuki, T., 1976. Biomineralization in bivalve molluscs with emphasis on the chemical composition of the extrapallial fluid, in *Mechanisms of Mineralization in the Invertebrates and Plants*, edited by N. Watabe and K. M. Wilbur, pp. 175–190, Univ. of S. C. Press, Columbia.

Waldbusser, G. G., Voigt, E. B., Bergschneider, H., Green, M. A., Newell, R. I. E., 2010. Biocalcification in the Eastern Oyster (*Crassostrea virginica*) in Relation to Long-term Trends in Chesapeake Bay pH. *Estuaries and Coasts*. DOI 10.1007/s12237-010-9307-0.

Wanamaker, A. D., Kreutz, K. J., Wilson, T., Borns, H. W., Introne, D. S., Feindel S., 2008. Experimentally determined Mg/Ca and Sr/Ca ratios in juvenile bivalve calcite for *Mytilus edulis*: implications for paleotemperature reconstructions. *Geo-Mar. Lett.* 28(5-6), 359-368.

Wheeler, A. P., Blackwelder, P. L., Wilbur, K. M., 1975. Shell growth in the scallop *Argopecten irradians*. I: Isotope incorporation with reference to diurnal growth. *Biol. Bull.* 148: 472-482.

Wigley, T. M. L., R. Richels and J. A. Edmonds (1996). "Economic and environmental choices in the stabilization of atmospheric CO<sub>2</sub> concentrations." *Nature* 379(6562): 240-243.

Weiss, I.M., Kaufmann, S., Heiland, B., Tanaka M., 2009. Covalent modification of chitin with silk-derivatives acts as an amphiphilic self-organizing template in nacre biomineralization. *J. Struct. Biol.* 167, 68–75. doi:10.1016/j.jsb.2009.04.005

Weiss, I.M., 2010. Jewels in the Pearl. *Chem. Bio. Chem.* 11, 297-300. DOI: 10.1002/cbic.200900677

Westerbom, M., Kilpi, M., Mustonen, O., 2002. Blue mussels, *Mytilus edulis*, at the edge of the range: population structure, growth and biomass along a salinity gradient in the north-eastern Baltic Sea. *Mar. Biol.* 140: 991–999.

Wilbur K. M., 1972. Shell formation in molluscs. In: *Chemical Zoology Vol. 7* (eds M. Florkin and B. T. Scheer), Ch. 3, Academic Press.

Wong W. H. and Levinton, J. S., 2004. Culture of the blue mussel *Mytilus edulis* (Linnaeus, 1758) fed both phytoplankton and zooplankton: a microcosm experiment. *Aquaculture Res.* 35, 965-969. doi:10.1111/j.1365-2109.2004.01107.x.

Yamada Y and Ikeda T., 1999. Acute toxicity of lowered pH to some oceanic zooplankton. *Plankton Biol. Ecol.* 46, 62–67.

## Supplement

2.S1: Alkalinity measurements of the different treatments with date and incubation time.

	<b>577</b>	<b>722</b>	<b>839</b>	<b>1041</b>	<b>1195</b>	<b>3395</b>
<b>02. Sep.2008</b>	1924.68	1919.22	1922.52	1921.15	1924.15	1920.96
<b>3h</b>	1908.61	1904.07	1899.14	1900.52	1905.74	1903.06
<b>04. Sep.2008</b>	1989.84	1989.92	1992.13	1996.09	1994.12	2004.43
<b>3h</b>	1967.64	1971.17	1971.43	1984.22	1975.98	2024.94
<b>05. Sep.2008</b>	2019.76	2020.85	2020.79	2018.80	2023.93	2049.38
<b>3h</b>	1990.74	2000.97	2007.74	2001.60	2011.21	2056.19
<b>10. Sep.2008</b>	2026.99	2025.84	2024.68	2026.22	2026.24	2044.08
<b>3h</b>	2007.86	2010.53	2015.81	2017.70	2015.15	2047.83
<b>17. Sep.2008</b>	1965.14	1968.41	1966.69	1968.92	1967.89	1974.42
<b>5h</b>	1947.32	1953.21	1953.68	1953.20	1958.47	1990.67
<b>24. Sep.2008</b>	1933.59	1927.87	1938.04	1932.31	1939.99	1945.04
<b>5h</b>	1916.00	1911.85	1920.35	1923.61	1929.54	1952.67
<b>01. Oct.2008</b>	1893.61	1894.33	1894.80	1895.97	1894.88	1900.60
<b>5h</b>	1883.25	1884.30	1892.22	1890.44	1889.69	1908.93
<b>07. Oct.2008</b>	2038.23	2040.58	2039.27	2041.36	2040.19	2043.24
<b>5h</b>	2016.82	2015.88	2023.73	2027.54	2024.18	2048.51
<b>15. Oct.2008</b>	1991.50	1991.27	1989.63	1995.96	1993.88	2001.31
<b>5h</b>	1981.42	1982.11	1981.12	1988.79	1986.74	2008.99
<b>22. Oct.2008</b>	1979.74	1979.64	1985.54	1982.82	1982.64	1985.39
<b>5h</b>	1969.53	1971.42	1969.92	1974.31	1974.15	1998.14
<b>05. Nov.2008</b>	2045.04	2046.02	2043.32	2045.20	2044.71	2045.56
<b>5h</b>	2024.28	2019.59	2016.71	2020.96	2021.24	2047.13
<b>12. Nov.2008</b>	2047.39	2049.74	2041.42	2051.73	2049.62	2050.16
<b>5h</b>	2030.31	2039.50	2032.89	2035.28	2035.42	2062.80
<b>19. Nov.2008</b>	2158.62	2156.70	2157.80	2158.78	2159.39	2160.29
<b>5h</b>	2143.77	2143.42	2142.04	2143.35	2147.25	2165.68
<b>26. Nov.2008</b>	2141.48	2139.08	2137.90	2140.08	2141.36	2144.52
<b>5h</b>	2125.64	2127.54	2126.56	2130.29	2131.81	2149.54
<b>03. Dec.2008</b>	2126.24	2127.61	2127.11	2129.43	2129.57	2138.19
<b>5h</b>	2113.64	2117.74	2116.93	2123.08	2122.03	2140.55
<b>10. Dec.2008</b>	2090.97	2092.76	2092.39	2091.88	2092.25	2095.31
<b>5h</b>	2074.08	2079.82	2083.81	2084.57	2083.13	2101.53



## 2.S2: Length growth of individually marked specimens at five dates during experiment.

	28. Aug. 2008	18. Sep. 2008	14. Oct. 2008	28. Oct. 2008	16. Dec. 2008
<b>380 <math>\mu\text{atm}</math></b>					
1	2.13	2.14	2.13	2.11	2.15
2	1.76	1.81	1.83	1.86	1.87
3	2.03	2.06	2.06	2.08	2.12
4	1.91	1.92	1.93	1.93	1.95
5	2.30	2.32	2.33	2.36	2.38
6	1.70	1.69	1.69	1.71	1.72
7	1.96	1.97	1.96	1.98	2.00
8	2.27	2.25	2.25	2.26	2.28
9	1.99	2.00	2.03	2.03	2.05
10	2.01	2.01	2.02	2.04	2.04
<b>560 <math>\mu\text{atm}</math></b>					
1	1.92	1.92	1.89	1.91	1.93
2	1.82	1.87	1.86	1.89	1.89
3	1.99	2.01	2.00	2.04	2.05
4	2.11	2.11	2.12	2.14	2.18
5	2.03	2.07	2.12	2.14	2.21
6	1.97	1.98	1.99	2.01	2.02
7	1.82	1.83	1.85	1.87	1.88
8	1.96	1.97	1.98	2.00	2.02
9	1.77	1.79	1.79	1.81	1.82
10	1.85	1.85	1.85	1.86	1.86
<b>840 <math>\mu\text{atm}</math></b>					
1	2.41	2.40	2.44	2.45	2.46
2	1.87	1.86	1.87	1.89	1.92
3	1.97	1.97	1.99	1.99	2.02
4	2.00	1.97	2.00	1.98	2.03
5	1.90	1.93	1.91	1.92	1.95
6	2.17	2.17	2.17	2.19	2.22
7	1.87	1.87	1.90	1.90	1.96
8	1.79	1.80	1.80	1.81	1.86
9	1.93	1.92	1.92	1.94	1.95
10	1.91	1.94	1.97	1.97	2.02
<b>1120 <math>\mu\text{atm}</math></b>					
1	2.03	2.03	2.02	2.01	2.04
2	1.90	1.91	1.93	1.96	1.99
3	2.05	2.05	2.05	2.08	2.08
4	2.01	2.01	2.03	2.04	2.05
5	2.24	2.25	2.25	2.27	2.30
6	1.81	1.81	1.81	1.81	1.82
7	2.10	2.10	2.11	2.13	2.16
8	1.69	1.69	1.70	1.73	1.84
9	1.98	1.99	2.02	2.02	2.09
10	1.79	1.79	1.80	1.80	1.83
<b>1400 <math>\mu\text{atm}</math></b>					
1	1.99	1.99	1.99	2.00	2.01
2	2.35	2.34	2.40	2.42	2.55
3	1.68	1.67	1.77	1.68	1.75
4	1.97	1.97	1.98	1.98	2.01
5	1.91	1.90	1.92	1.92	1.94
6	2.18	2.19	2.20	2.20	2.22
7	1.76	1.79	1.78	1.80	1.88
8	1.65	1.66	1.67	1.70	1.74
9	1.87	1.87	1.87	1.87	1.91
<b>4000 <math>\mu\text{atm}</math></b>					
1	2.07	2.12	2.12	2.16	2.16
2	1.93	1.92	1.93	1.93	1.99
3	1.96	1.95	1.95	1.95	2.00
4	1.85	1.85	1.85	1.85	1.90
5	2.01	2.00	2.01	2.00	2.03
6	1.80	1.79	1.78	1.79	1.81
7	1.62	1.63	1.62	1.63	1.67
8	1.70	1.70	1.70	1.71	1.80

2.S3: Element concentrations of water, HL and EPF (experiment 1).

Fluid	Treatment [µatm]	Number of animal	Ca <sup>2+</sup> [mol/l]	Mg <sup>2+</sup> [mol/l]	Sr <sup>2+</sup> [mmol/l]
water	380		6.79	34.09	56.15
water	560		6.89	34.55	57.10
water	840		6.89	34.44	57.10
water	1120		6.94	34.73	57.45
water	1400		7.00	34.92	58.05
water	4000		6.97	34.88	57.70
HL	380	1	5.87	30.45	49.10
HL	380	2	6.47	32.80	53.60
HL	380	16	5.94	31.05	49.75
HL	380	17	7.09	36.48	60.15
HL	560	3	5.83	29.94	48.45
HL	560	4	6.47	34.55	55.25
HL	840	5	8.81	46.09	72.70
HL	840	6	6.03	30.84	49.75
HL	840	7	7.15	35.97	59.25
HL	840	18	5.71	29.42	48.45
HL	1120	8	7.65	41.38	64.35
HL	1120	19	6.22	33.29	53.10
HL	1120	20	6.58	34.12	55.33
HL	1400	9	6.63	34.14	55.15
HL	1400	10	7.25	37.30	60.33
HL	1400	11	6.97	36.44	58.55
HL	4000	12	5.70	28.58	46.90
HL	4000	13	6.08	30.76	50.05
HL	4000	14	7.05	34.94	58.10
HL	4000	15	7.02	35.27	58.65
EPF	380	1	5.86	29.96	48.80
EPF	380	2	6.62	33.89	55.40
EPF	380	21	6.35	32.78	53.50
EPF	560	3	5.71	30.04	48.20
EPF	560	4	6.21	33.91	53.70
EPF	560	22	5.98	31.42	50.60
EPF	840	5	5.65	29.05	47.15
EPF	840	6	6.51	33.97	54.45
EPF	840	7	6.60	33.83	55.15
EPF	840	23	6.37	33.37	54.10
EPF	1120	8	5.92	31.71	50.15
EPF	1120	24	5.75	29.39	47.78
EPF	1400	9	8.02	42.53	67.25
EPF	1400	10	6.58	33.70	55.20
EPF	1400	11	6.10	32.22	51.65
EPF	1400	25	6.08	30.93	50.60
EPF	1400	26	6.56	33.85	54.80
EPF	4000	12	5.63	28.29	46.35
EPF	4000	13	5.83	29.75	48.25
EPF	4000	14	6.67	33.44	55.40
EPF	4000	15	7.10	35.95	59.60

## 2.S4: Element concentrations of water and EPF (experiment 2).

Fluid	Treatment [ $\mu\text{atm}$ ]	Aquarium	Ca <sup>2+</sup> [mol]	Mg <sup>2+</sup> [mol]	Sr <sup>2+</sup> [mmol]
water	380	1	5.26	25.54	42.17
water	380	4	4.45	21.78	35.88
water	380	10	5.19	25.21	41.41
water	1400	2	4.84	25.07	39.27
water	1400	5	5.22	25.55	41.96
water	1400	8	5.11	25.47	41.18
water	1400	11	5.21	25.61	41.80
water	4000	3	5.05	24.62	40.49
water	4000	6	5.22	25.36	41.77
water	4000	9	5.05	24.43	40.14
water	4000	12	5.02	25.65	41.46
EPF	380	1	4.90	24.78	39.74
EPF	380	1	4.89	24.05	39.09
EPF	380	4	4.67	23.35	37.42
EPF	380	7	5.17	25.69	42.25
EPF	380	7	5.06	25.32	41.78
EPF	380	10	4.48	24.80	40.22
EPF	380	10	5.03	25.15	40.87
EPF	1400	2	4.72	23.55	37.90
EPF	1400	2	4.70	23.28	37.58
EPF	1400	5	5.37	25.17	41.89
EPF	1400	8	4.86	25.81	41.82
EPF	1400	11	5.16	25.56	41.92
EPF	4000	3	4.78	23.11	37.85
EPF	4000	6	5.12	25.20	41.42
EPF	4000	6	5.27	24.96	41.78
EPF	4000	9	4.76	24.82	41.02
EPF	4000	12	5.12	25.01	41.42
EPF	4000	12	5.15	24.93	41.04

## Chapter 3

### **Boron isotope ratio determination in carbonates via LA-MC-ICP-MS using soda-lime glass standards as reference material\***

\*published in *Journal of Analytical Atomic Spectrometry* as: Jan Fietzke, Agnes Heinemann, Isabelle Taubner, Florian Böhm, Jonathan Erez and Anton Eisenhauer; Boron isotope ratio determination in carbonates via LA-MC-ICP-MS using soda-lime glass standards as reference material.

### 3.1 Abstract

A new in-situ method using LA-MC-ICP-MS (193nm excimer laser) for the determination of stable boron isotope ratios ( $\delta^{11}\text{B}$ ) in carbonates was developed. Data were acquired via a standard sample standard bracketing procedure typically providing a reproducibility of 0.5 ‰ (SD) for samples containing 35 ppm of boron. A single ablation interval consumed about 5  $\mu\text{g}$  of sample corresponding to about 0.2 ng of boron. The major finding was the similar instrumental fractionation behavior of carbonates, soda-lime glass and sea salt with respect to boron isotopes. As no matrix induced offset was detectable between these distinct materials we propose the use of NIST glasses as internal standards for boron isotope ratio measurements via LA-MC-ICP-MS. This finding overcomes the problem of a missing matrix matched carbonate standard for in-situ boron isotope studies. As a first application a set of coral samples from a culturing experiment was analyzed.  $\delta^{11}\text{B}$  values range from 19.5-25 ‰ depending on the pH of the water used in the particular treatment. This is in good agreement with the results of earlier studies.

### 3.2 Introduction

The element boron has two stable isotopes,  $^{10}\text{B}$  (~19.9 %) and  $^{11}\text{B}$  (~80.1 %), respectively. Boron isotope ratio data are usually reported relative to NIST-SRM951 using the  $\delta$ -notation:

$$\delta^{11}\text{B}[\text{‰}] = 1000 \cdot \left( \frac{(^{11}\text{B}/^{10}\text{B})_{\text{sample}}}{(^{11}\text{B}/^{10}\text{B})_{\text{NIST951}}} - 1 \right) \quad (1)$$

All  $\delta^{11}\text{B}$  data reported in this paper are expressed relative to the NIST-SRM951, too. Uncertainties are given as SD in rounded brackets for the last significant digits (e.g. 20.41(33) means  $20.41 \pm 0.33$  (SD)).

Boron is a volatile element with a high relative mass difference between its isotopes of about 10 %. As a consequence it is strongly fractionated in different major reservoirs of the earth. Of particular interest in marine geochemistry is the fractionation of boron isotopes during the precipitation of carbonates from sea water ( $\delta^{11}\text{B}$  seawater = 39.5 ‰). Boron is present in sea water in two different species:  $\text{B}(\text{OH})_3$  dominating at low pH and  $\text{B}(\text{OH})_4^-$  at high pH, respectively (Dickson 1990). Between the two species a strong equilibrium fractionation of about 20-30 ‰ exists (Kakihana 1977, Palmer et al. 1987, Zeebe, 2005, Klochko et al. 2006). Carbonates (calcite, aragonite) precipitated from seawater are believed to incorporate primarily the borate ion  $\text{B}(\text{OH})_4^-$  into their lattice (Vengosch et al. 1991, Hemming and Hanson 1992, Hemming et al. 1995, Pagani et al. 2005, Klochko et al. 2009). Thus, the boron isotopic signature of  $\text{B}(\text{OH})_4^-$  as a consequence of its pH dependent abundance and equilibrium fractionation relative to  $\text{B}(\text{OH})_3$  is recorded in the precipitate.

In recent years several studies focused on the application of this systematic to reconstruct sea water pH from  $\delta^{11}\text{B}$  data (Hemming and Hönisch 2007). To a certain degree many biogenic marine carbonates deviate from the  $\delta^{11}\text{B} \sim \text{pH}$  relation determined for inorganically precipitated carbonates (Sanyal et al. 2000). The latter is a result of the influence of biological control on the process of calcification referred to as “vital effects”. On the one hand this leads to a need for species-specific calibrations, on the other hand it provides the fascinating option to study the process of biomineralization itself. Several analytical techniques for the determination of boron isotopes were used so far:

- 1) Thermal ionization mass spectrometry (N-TIMS (Duchateau and de Bièvre 1983, Heumann and Zeininger 1985, Vengosch et al. 1989, Hemming and Hanson 1992), P-TIMS (Spivack and Edmond 1986)).
- 2) Inductively coupled plasma mass spectrometry (MC-ICP-MS (Lécuyer 2002, Foster 2008), LA-MC-ICP-MS (Le Roux et al. 2004)).
- 3) Secondary ion mass spectrometry (SIMS (Rollion-Bard et al. 2003, Kasemann et al. 2009, Rollion-Bard and Erez 2010)).

The TIMS method is perhaps the most commonly used approach to date. TIMS and MC-ICP-MS provide the highest precision and accuracy (Aggarwal et al. 2009). The strength of the third technique is the high spatial resolution of several  $\mu\text{m}$  measuring directly at the solid sample surface.

A recent inter-laboratory calibration study revealed certain limitations of the different analytical methods reporting a significant spread in the results reported by the participating labs (Aggarwal et al. 2009). There are several analytical challenges inherent in boron isotope measurements. Unlike other elements (e.g. Ca, Pb, U...) boron just has two stable/long-lived isotopes which prevent the application of double- or triple spike methods. This fact is a serious burden for all methods where a separation of boron from the sample matrix is required as no control is possible for any fractionation induced by the sample separation procedure. It is also a limitation for methods where a strong variable fractionation during the measurement occurs. Contamination is another issue for boron analyses. In particular for the in-situ  $\delta^{11}\text{B}$  measurements in carbonates the major limitation so far was the absence of any solid state matrix standard. The stated obstacles and limitations justify the need for improved analytical methods to further develop and strengthen applications of boron isotopes in geochemistry.

### 3.3 Experimental

#### 3.3.1 Standard and sample preparation

Three types of standards were used in this study:

- 1) soda-lime glass SRM (NIST610/611/612)
- 2) carbonate pressed powder pellets (TIMS calibrated sponge aragonite Ce95-1, 125 ky old coral aragonite FCA)
- 3) seawater evaporites (NIST-SRM951 boric acid mixed with IAPSO sea water standard, NASS-5 sea water standard)

All carbonate samples were bleached to remove organic compounds using 10 % NaClO (1 % active chlorine). The bleaching was done over a period of 3 days, renewing the NaClO each day including ultrasonication for about 10 min. To finally remove NaClO the samples were washed several times using MilliQ water (18.2 MOhm/cm). This water was adjusted to a pH of  $\sim 9$  by adding small amounts of  $\text{NH}_4\text{OH}$  to prevent dissolution of the carbonates.

Carbonate powder standards Ce95-1 and FCA were pressed as pellets. For easier handling and stabilization these pellets were set into epoxy resin. A blank pellet of the epoxy resin was prepared, too. Ablation of this pellet yielded no detectable boron signal. After removing the surface contamination with the first  $\sim 10$  shots the signals of both boron isotopes decayed rapidly to the background level. The rest of the 900 shots just showed typical background signals.

The TIMS calibration measurement was done on a split from a larger Ce95-1 bulk sample which was bleached according to the described procedure. From another split of this already bleached bulk powder the pellet for this study was prepared. Thus, the material used for both techniques was completely equal.

A set of *Pocillopora sp.* coral aragonite samples from a culturing experiment carried out at the Hebrew University Jerusalem was prepared as a first test application. The corals grew in aquaria at different pH levels (pH = 7.8-8.3). Details of the culturing experiment will be presented elsewhere. Despite from bleaching no further treatment was done with these samples.

Two sea salt evaporite standards were prepared from sea water (IAPSO sea water standard). 2 ml of sea water were evaporated in a vacuum cabinet at 20 °C. One of the two solutions was enriched in boron by a factor of 20 using boric acid (NIST-SRM951).

### 3.3.2 Instrumentation, data acquisition and evaluation

All measurements were performed on a Thermo Fisher MC-ICP-MS AXIOM (originally designed and manufactured by VG) connected to an ESI New Wave Research UP193FX excimer laser ablation system equipped with a ESI New Wave Research LFC (large format cell). Typical operation parameters can be found in Table 3.1.

<b>AXIOM MC-ICP-MS</b>	
Cool gas	14 l/min
Auxiliary gas	1.8 l/min
Nebulizer gas	0.9 l/min (Ar)
RF power	1250 W
Reflected power	3 W
Accelerating voltage	4972 V
Cones	R.A. Chilton RAC19/RAC705
Resolution	500res
<b>UP193FX</b>	
Ablation cell gas	0.6 l/min (He)
Spot size	100-150 µm
Fluence	2.5 J/cm <sup>2</sup>
Repetition rate	30 Hz
Scan mode	Spot analysis (500-900 shots)

Table 3.1: Instrumental parameters.

Data for amu10 (atomic mass unit) and amu11 were simultaneously collected using the outermost Faraday Cups (L4 and H4). For the data reduction no separate baseline measurement was carried out, because the breaks between ablation periods were sufficient to collect the respective gas blank data.



Our method differs from the published laser-based analytical method (Le Roux et al. 2004) for boron isotope ratio determination using an AXIOM MC-ICP-MS, too, threefold:

- 1) use of an 193nm excimer in contrast to a 213nm solid state LA system
- 2) data collection using Faraday Cups instead of multi-ion counting
- 3) different data reduction

Despite the fact that some earlier studies (Le Roux et al. 2004, Foster 2008) already made clear statements on the absence of disturbing interferences on both masses this is still disputed in the community. Thus, we did collect for both spectral areas the signals in low (500 res) and high resolution (5500 res) with and without ablation. The results are summarized in Figure 3.1.

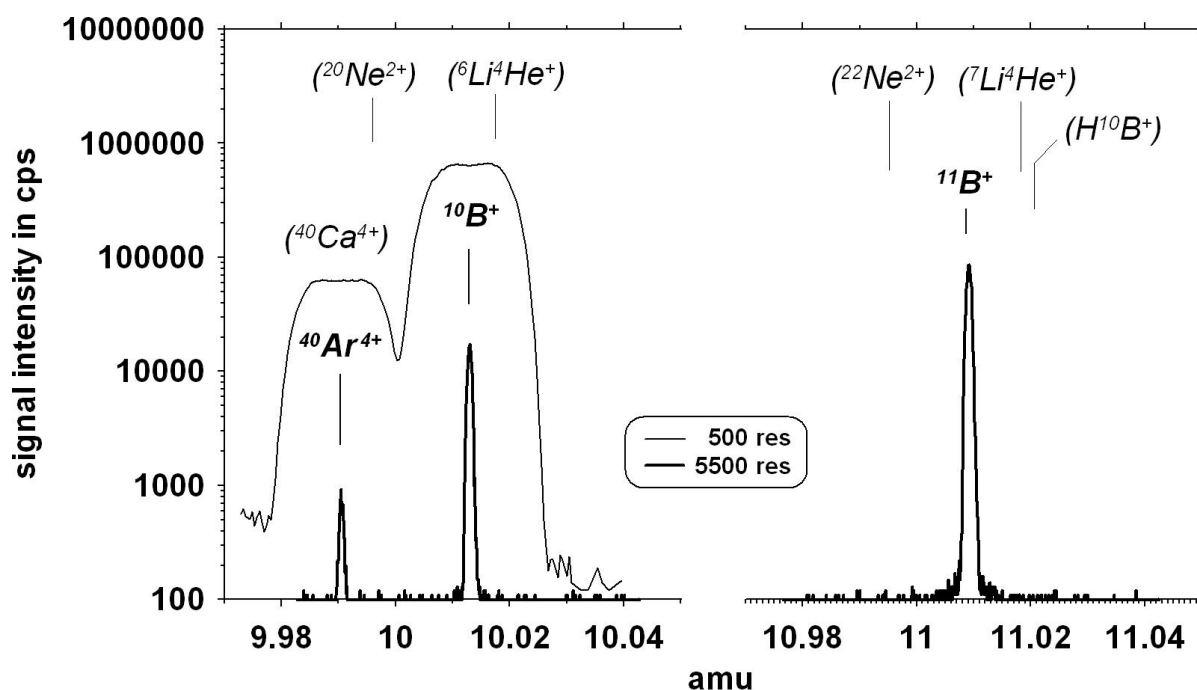


Figure 3.1: Spectra around  $^{10}\text{B}$  and  $^{11}\text{B}$  in low and high resolution mode. Besides the boron peaks only the  $^{40}\text{Ar}^{4+}$  could be clearly identified via its exact mass in the high-res spectra. The latter peak did not change regardless of the ablation running or not indicating no additional occurrence of  $^{40}\text{Ca}^{4+}$  from ablated material (NIST 612). Other possible interferences (italic in brackets) indicated by their expected position in the spectra were not observed.

Prior to analysis all areas intended to be analyzed were preablated (3 s @ 10 Hz; 30 shots ~ 3  $\mu\text{m}$  depth) to remove contaminations from the sample surface. Running the laser at a repetition rate of 30 Hz using a spot diameter of 150  $\mu\text{m}$  provided a total B signal of about 70 mV for a sample containing 35 ppm of boron. During one ablation interval of 30 s the laser excavated to a depth of

about 100  $\mu\text{m}$  corresponding to a sample amount of 5  $\mu\text{g}$  ( $\sim 0.2$  ng total B). After each ablation period the laser was paused for 60 s. Due to the superior washout characteristic of the LFC ablation cell the signal dropped to the baseline level within less than 3 s. We did not observe any deviations from this performance depending on the position within the LFC but excluded the area closer than 1 cm from the outer boundaries.

Test measurements comparing spot and raster analysis revealed no measurable differences (while keeping the aspect ratio during the spot ablation below 1). As this method is supposed to be used for high spatial resolution work we continued with spot ablation. Measurements were performed using the sample standard sample bracketing procedure. Typically, one analysis included 7 ablation periods of the sample bracketed by 8 ablation periods of the standard (see example in Figure 3.2). Thus, the whole analysis of one sample took less than 30 min. Data were collected using integration times of 6 s. Initially all measurements were done using the Ce95-1 as bracketing standard as this carbonate was independently determined via TIMS for its boron isotopic composition. The only exception was the first test of IAPSO vs. IAPSO-NIST SRM951 mixture.

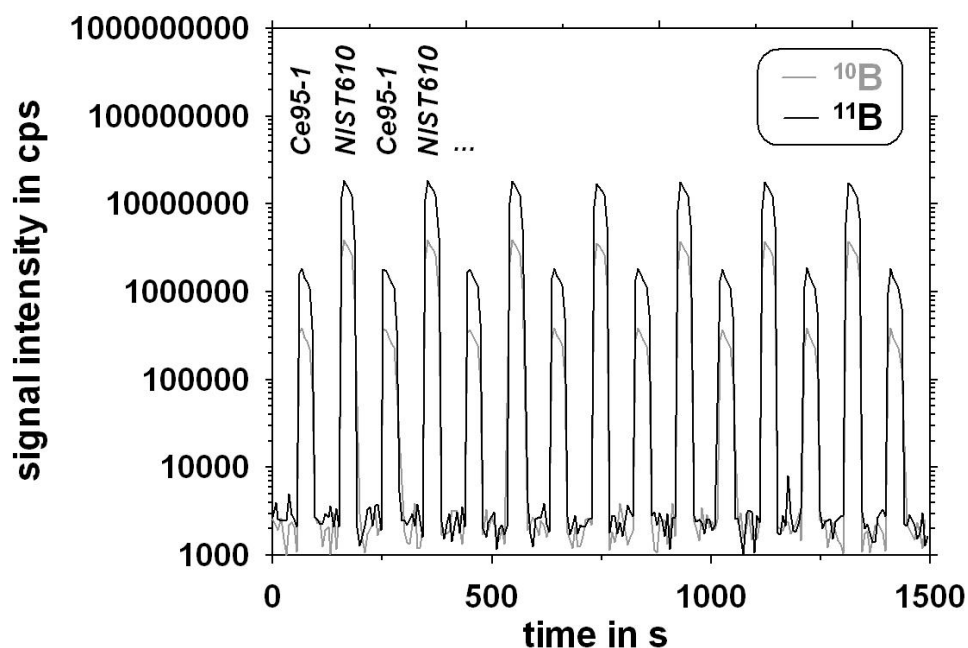


Figure 3.2: One analytical run of 7 ablation periods on NIST610 (as unknown sample) bracketed by 8 ablation periods on Ce95-1 as bracketing standard. Applying the TIMS value for the Ce95-1 ( $\delta^{11}\text{B} = 20.4$  ‰) this analysis yielded a  $\delta^{11}\text{B}$  of  $-0.41(39)$  ‰ for NIST SRM610.

After establishing the constant isotopic difference between Ce95-1 and the NIST glass standards we did switch to the NIST SRM610 glass as bracketing standard due to its higher boron concentration (improved internal precision).

Data collected during one ablation period and the backgrounds prior and after ablation were evaluated as single data sets using the procedure initially developed for laser ablation Cl and Sr isotope ratio

determination (Fietzke et al. 2008a/b). In the case of boron isotopes the slope of the linear fit of  $^{11}\text{B}$  plotted against  $^{10}\text{B}$  intensities is used, covering the whole simultaneous signal development for both isotopes from baseline to maximum intensities. The merits of this method when compared to a conventional baseline reduction were already explained in detail in the papers mentioned above (Fietzke et al. 2008a/b).

For samples with low boron concentration (or if high spatial resolution limitates the sample amount) a slightly modified instrumental setup was tested. Instead of using two Faraday Cups a combination of one Faraday Cup (H5:  $^{11}\text{B}$ ) and one electron multiplier (MH:  $^{10}\text{B}$ ) was used. When running the laser at 30 Hz with 150  $\mu\text{m}$  spots both methods show a comparable precision for samples containing about 10-15 ppm of boron. For lower concentrations the multiplier/cup combination is preferable as the amplifier noise limits the precision of the cup/cup combination (e.g. 5-10  $\mu\text{V}$  noise;  $^{10}\text{B}$  signal of 3 mV at 10 ppm B). On the other hand the multiplier/cup combination is limited by the fact that the multiplier is tripping frequently at signal intensities of higher than 100.000 cps restricting its use to low concentration/high spatial resolution applications. This is not due to the normal trip level ( $\sim 2.000.000$  cps) but a consequence of the much to steep signal increase when the laser starts ablating. The latter activates the multiplier self-protection.

## 3.4 Results and discussion

### 3.4.1 Standards

A summary of all standard  $\delta^{11}\text{B}$  results are given in Table 3.2. First test measurements were carried out using the two sea water evaporite standards (IAPSO; IAPSO mixed with NIST-SRM951 boric acid). For the combined standard we had to consider the contribution of both materials to the isotopic composition of the mixture. The NIST-SRM951 ( $\delta^{11}\text{B} = 0 \text{ ‰}$ ) contributed 95 % of the total B. The IAPSO boron isotopic composition was calculated from the results of the pure and mixed evaporite standards to  $\delta^{11}\text{B}$  IAPSO = 39.2(5)  $\text{‰}$  (SD), being in good agreement to the published seawater value of 39.5  $\text{‰}$  (Spivack et al. 1987, Foster et al. 2006).

The two in-house carbonate standards Ce95-1 (recent sclerosponge aragonite) and FCA (prepared from 125 ky old fossil coral aragonite) were measured against each other. The Ce95-1 was previously measured by TIMS at IFM-GEOMAR Kiel, Germany for boron isotopes yielding a  $\delta^{11}\text{B}$  of 20.4(6)  $\text{‰}$  and 19.4(9)  $\text{‰}$  at Bristol University (Foster et al. 2006). Using the first value as a reference we calibrated the FCA to  $\delta^{11}\text{B} = 24.0(4) \text{ ‰}$  ( $n = 9$ ) being a reasonable result for a coral (Hönisch et al. 2004). Prior to this analysis the homogeneity of both standards was tested by ablating randomly distributed regions of the respective standard.  $\delta^{11}\text{B}$  variations were below 0.5  $\text{‰}$  in both standards, being insignificant with respect to the reproducibility of the measurements.

<b>Sea water evaporites</b>	<b><math>\delta^{11}\text{B}</math> in ‰ ; n repeats</b>
IAPSO	39.2(5) ; 4
NASS-5	39.4(3) ; 7
<b>Carbonates</b>	
Ce95-1	20.4(6) *
FCA	24.0(4) ; 9
FCA (rep. rate 5 Hz)	23.5(5) ; 10
FCA (rep. rate 10 Hz)	24.5(3) ; 10
FCA (rep. rate 20 Hz)	23.9(4) ; 10
FCA (rep. rate 40 Hz)	23.8(3) ; 10
<b>Silicate glasses</b>	
NIST610	-0.55(53) ; 16
NIST611	-0.48(31) ; 5
NIST612	-0.56(49) ; 20

Table 3.2:  $\delta^{11}\text{B}$  results of standards analyzed. \*TIMS result used for calibration. Uncertainties as SD in brackets.

The influence of the amount of material introduced into the plasma by ablation was tested by firing the laser at different repetition rates (from 5 to 40 Hz) ablating the FCA standard. The FCA used as bracketing standard was ablated at 20 Hz. No significant influence of the repetition rate on the  $\delta^{11}\text{B}$  result could be found (see Table 3.2) indicating the robustness of the method with respect to variable matrix loads introduced into the plasma.

Typically, during a single ablation period (900 shots, 30 Hz, 150  $\mu\text{m}$  spot) the laser penetrated about 100  $\mu\text{m}$  deep into the sample surface. This corresponds to a sample amount of approximately 5  $\mu\text{g}$  or 0.15-0.25 ng of boron (for B concentrations of 30-50 ppm). For this sample amount the  $^{11}\text{B}/^{10}\text{B}$  ratio was determined with a reproducibility of 0.5 ‰ (SD) determined in long-term reproducibility test measurements using NIST612 as unknown and NIST610 as bracketing standard.

To evaluate matrix induced systematic offsets, soda-lime glass standards (NIST610, 611, 612) were analyzed using the two carbonate in-house standards for the bracketing. Despite the fact that the B concentration differs by one order of magnitude within this set of silicate standards (35-360 ppm B) the  $\delta^{11}\text{B}$  values are indistinguishable for all three NIST glasses analyzed. This appears to be reasonable, pointing at the same B source used for the preparation of these standards by NIST.

NIST610 and NIST611 should yield the same result anyway as both standards were prepared from the same bulk material just cut differently with respect to thickness of the glass discs (Eggins and Shelley

2002). Nevertheless, we wanted to provide data for both standards as some databases also report values for this standards separately.

The results agree with published results obtained by solution MC-ICP-MS and TIMS, reporting  $\delta^{11}\text{B}$  values ranging from -0.2 to -1.2 ‰ (Le Roux et al. 2004, Kasemann et al. 2009, Kasemann et al. 2001, Schmitt et al. 2002). Surprisingly, this indicates that no matrix related offset seems to exist between soda-lime glass and carbonates when applying the described method. Both matrices show an identical behavior during ablation as well as evaporation and ionization within the plasma. Boron isotopes undergo the same degree of instrumental mass fractionation regardless of ablation from a carbonate or silicate glass matrix.

This is a major difference to the behavior boron isotopes show during SIMS measurements. Typically, SIMS boron isotopic ratio results from NIST glass show an offset of about +50 ‰ when compared to carbonates (Kasemann et al. 2009). Obviously, the mass fractionation of boron isotopes during ion sputtering is to a large degree dependent on the local composition of the sample, but fairly insensitive to the latter during ablation using 193nm deep-UV laser radiation.

This result has an important consequence. So far in-situ B isotope studies in carbonates were difficult due to the absence of any carbonate standard being homogeneous and certified for boron isotopic ratios. In this study we showed that soda-lime glass standards like the NIST glasses may serve as an adequate reference material for this particular field of application.

With the observed matrix insensitivity for carbonates and silicate glasses we carried out further test measurements. NIST glasses were used as internal standards for boron isotope ratio determination of a freshly prepared seawater evaporite sample (produced from NASS-5 sea water standard). We measured a  $\delta^{11}\text{B}$  value of 39.4(3) ‰ ( $n = 7$ ) being in accord with the published seawater value of 39.5 ‰. Again we found no measurable matrix induced offset.

For the three investigated matrices ( $\text{CaCO}_3$ , Si-Na-Ca-Al glass, NaCl) boron isotopes behave matrix-insensitive within the limits of measurement uncertainty.

### 3.4.2 Coral samples

A set of coral samples (*Pocillopora sp.*) from a lab-culturing experiment carried out at the Hebrew University Jerusalem (Israel) was used to test the application of the described method.

The corals were grown in aquaria at constant temperature of 25 °C and five different pH levels (7.8-8.3). Branch tips (~ 5 mm in size) of the corals were bleached (see above). The aragonite precipitated during the culturing was analyzed using either FCA carbonate or NIST612 glass standard for bracketing during different analytical sessions. Within the limits of uncertainty the results were identical regardless which standard was used. The mean results are given in Table 3.3.

Culturing water pH	$\delta^{11}\text{B}$ in ‰ ; n repeats
7.77	19.75(36) ; 18
7.92	19.81(60) ; 12
8.06	21.51(47) ; 17
8.19	22.90(23) ; 18
8.32	24.98(10) ; 6

Table 3.3:  $\delta^{11}\text{B}$  results of cultured corals (pH-treatment, NBS scale). Uncertainties as SD in brackets.

In Figure 3.3 our coral  $\delta^{11}\text{B}$  data are compared with widely used theoretical and measured boron isotope fractionation curves for  $\text{B}(\text{OH})_4^-$  and the results from earlier coral culturing experiments are shown (Kakahana et al. 1977, Hönisch et al. 2004, Reynaud et al. 2004, Klochko et al. 2006). In general the LA-MC-ICP-MS results from this study plot in a comparable range as published coral data showing a clear dependence on the ambient water pH. Nevertheless, deviations from both, the theoretical curve and results of earlier studies were found. The latter can be due to several reasons:

- 1) species-specific offsets (“vital effects”): different coral species were used in the experiments
- 2) culturing setup: water conditions and method used for pH adjustment differ in the studies
- 3) analytical offsets: as shown in a recent cross-calibration study  $\delta^{11}\text{B}$  results from different labs show a significant variability (Aggarwal et al. 2009).

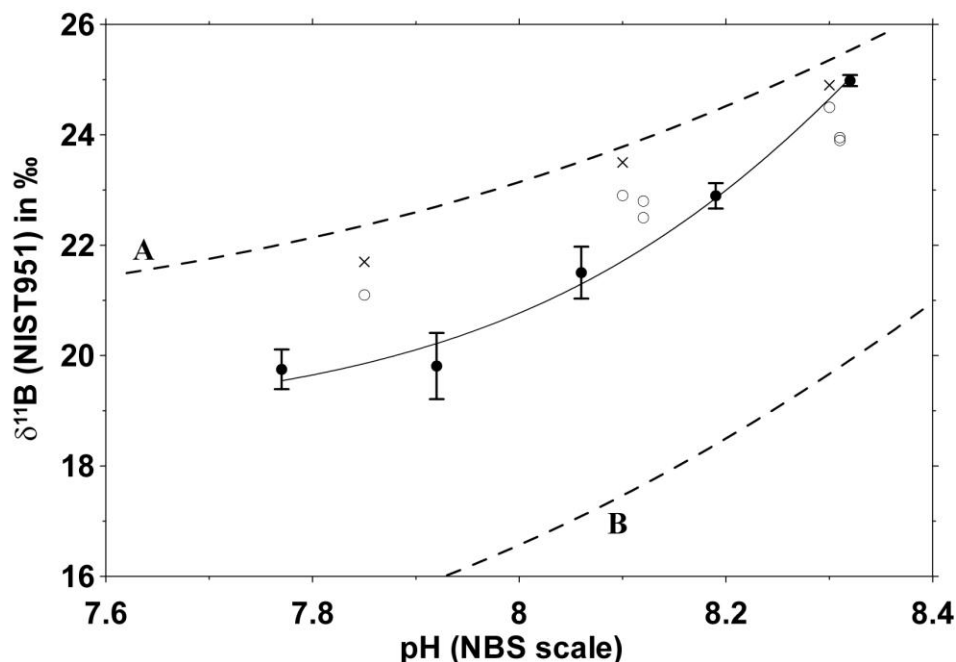


Figure 3.3:  $\delta^{11}\text{B}$  in corals cultured under different pH conditions. *Pocillopora sp.* samples (filled circles) from this study measured by LA-MC-ICP-MS; *Acropora* (open circles) and *Porites* (crosses) data from the previous studies measured via N-TIMS (Hönisch et al. 2004, Reynaud et al. 2004). For comparison published data for the theoretical and measured  $\delta^{11}\text{B}$  fractionation curves of  $\text{B}(\text{OH})_4^-$  are provided (A:  $^{11-10}K_B = 1.0194$  and B:  $^{11-10}K_B = 1.0272$ ) (Kakahana et al. 1977, Klochko et al. 2006).

The comparison of theoretical  $\delta^{11}\text{B}$  fractionation curves with the coral results provides an interesting observation. The best fit for the coral data is:

$$\delta^{11}\text{B} = \frac{39.5 + 18.93 \cdot 10^{\left(\frac{8.53 - \text{pH}}{0.553}\right)}}{1 + 10^{\left(\frac{8.53 - \text{pH}}{0.553}\right)}} \quad (2)$$

This corresponds to a  $^{11-10}\text{K}_\text{B} = 1.0202$  (close to the 1.0194 of Kakihana) and an apparent boric acid dissociation constant of  $\text{pK}^* = 8.53$  (close to the  $\text{pK}_\text{B}$  of 8.60 for seawater at 25°C and open ocean salinity (Dickson 1990)). The major difference to the theoretical curves is the value of 0.553 in the denominator of the exponents. This parameter can be interpreted as the activity factor  $\alpha_{\text{B(OH)}_4^-}$  for the  $\text{B(OH)}_4^-$  ion in the respective solution. While the theoretical curve was calculated with the total concentration we consider the activity of  $\text{B(OH)}_4^-$  being the appropriate representative as the conditions are far from an ideal (infinitely diluted) solution.

For future studies we propose the three parameters:

- 1) fractionation factor  $^{11-10}\text{K}_\text{B}$
- 2) apparent dissociation constant  $\text{pK}^*$
- 3) activity factor  $\alpha_{\text{B(OH)}_4^-}$

as a base to evaluate and compare the results for the pH dependent  $\delta^{11}\text{B}$  fractionation in carbonates.

### 3.5 Conclusions

A new in-situ method for the determination of  $\delta^{11}\text{B}$  using LA-MC-ICP-MS was presented. Using the standard-sample-standard bracketing approach single periods of sample ablation typically provided  $\delta^{11}\text{B}$  reproducibilities of 0.5 ‰ (SD) consuming about 0.2 ng of total boron.

We could overcome the long-standing issue of standardization for boron isotope solid state analytics. No matrix-related offsets could be found within the limits of uncertainty for three distinct matrices: soda-lime glass, carbonate and sea salt (evaporated sea water). Thus, we propose the use of soda-lime glass standards (e.g. NIST glasses) as internal standard for boron isotope studies in carbonates.

A first application of the new method shows a strong dependence of  $\delta^{11}\text{B}$  in coral aragonite on the ambient water pH. The deviation of the observed boron isotope systematic from theoretical curves points to the importance of considering the activity of  $\text{B(OH)}_4^-$  for the boric acid dissociation instead of the total concentration.

## Acknowledgements

This study is a contribution to the BIOACID joint project, funded by the German Ministry of Research and Technology. Additional funding was provided by German Research Council DFG within the Cluster of Excellence “The Future Ocean”. The authors wish to thank Nikolaus Gussone for TIMS measurement of sponge sample Ce95-1. Finally, we are grateful to two anonymous referees who provided detailed valuable reports. The latter efforts helped to significantly improve the manuscript.

## References

- Aggarwal, J. K., Mezger, K., Pernicka, E., Meixner, A., 2004. The effect of instrumental mass bias on  $\delta^{11}\text{B}$  measurements: a comparison between thermal ionisation mass spectrometry and multiple-collector ICP-MS. *Int. J. Mass Spectrom.* 232, 259–263.
- Aggarwal, J. K., Böhm, F., Foster, G., Halas, S., Hönlisch, B., Jiang, S.-Y., Kosler, J., Liba, A., Rodushkin, I., Sheehan, T., Jiun-San Shen, J., Tonarini, S., Xie, Q., Chen-Feng You, Zhi-Qi Zhao and Zuleger, E., 2009. How well do non-traditional stable isotope results compare between different laboratories: Results from the interlaboratory comparison of boron isotope measurements, *J. Anal. At. Spectrom.*, 24, 825-831, doi:10.1039/b815240c.
- Duchateau, N. L. and Bièvre P. De, 1983. Boron isotopic measurements by thermal ionization mass spectrometry using the negative  $\text{BO}_2^-$  ion. *Int. J. Mass Spectrom. Ion Proc.* 54, 289–297.
- Dickson A. G. (1990) Thermodynamics of the dissociation of boric acid in synthetic seawater from 273.15 to 318.15 K. *Deep-Sea Res.* 37, 755-766.
- Eggins, S. M., and Shelley, J. M. G., 2002. Compositional heterogeneity in NIST SRM 610-617 glasses. *Geostandards Newsletter*, 26, 269-286.
- Fietzke, J., Frische, M., Hansteen, T., Eisenhauer, A., 2008. A simplified procedure for the determination of stable chlorine isotope ratios ( $\delta^{37}\text{Cl}$ ) using LA-MC-ICP-MS. *JAAS* 23, 769-772 doi>10.1039/b718597a.
- Fietzke, J., Liebetrau, V., Günther, D., Gürs, K., Hametner, K., Zumholz, K., Hansteen, T., Eisenhauer, A., 2008. An alternative data acquisition and evaluation strategy for improved isotope ratio precising using LA-MC-ICP-MS applied for stable and radiogenic strontium isotopes in carbonates. *JAAS* 23, 955-961, doi>10.1039/b717706b.
- Foster, G. L., Ni, Y., Haley, B., Elliott, T., 2006. Accurate and precise isotopic measurement of sub-nanogram sized samples of foraminiferal hosted boron by total evaporation NTIMS. *Chem. Geol.*, 230, 161–174, doi:10.1016/j.chemgeo.2005.12.006.
- Foster, G. L., 2008. Seawater pH,  $p\text{CO}_2$  and  $[\text{CO}_3^{2-}]$  variations in the Caribbean Sea over the last 130 kyr: A boron isotope and B/Ca study of planktic foraminifera. *Earth Planet. Sci. Lett.* 271, 254–266, doi:10.1016/j.epsl.2008.04.015.J.



- Gaillardet, J., Allègre, C. J., 1995. Boron isotopic compositions of corals: Seawater or diagenesis record? *EPSL* 136, 665-676.
- Hemming, N. G., Hanson, G. N., 1992. Boron isotopic composition and concentration in modern marine carbonates. *Geochim. Cosmochim. Ac.* 56, 537-543.
- Hemming, N. G., Reeder, R., J., Hart S. R., 1995. Mineral-fluid partitioning and isotopic fractionation of boron in synthetic calcium carbonate. *Geochim. Cosmochim. Ac.* 59, 371-379.
- Hemming, N. G., Hönlisch, B., 2007. Boron Isotopes in Marine Carbonate Sediments and the pH of the Ocean. *Development in Mar. Geol.* 1, 717-734.
- Heumann, K. G., Zeininger, H., 1985. Boron trace determination in metals and alloys by isotope dilution mass spectrometry with negative thermal ionization. *International Journal of Mass Spectrometry and Ion Processes.* 67, 237-252.
- Hönlisch, B., Hemming, N. G., Grottoli, A. G., Amat, A., Hanson, G. N., Bijma, J., 2004. Assessing scleractinian corals as recorders for paleo-pH: empirical calibration and vital effects. *Geochim. Cosmochim. Ac.* 68, 3675-3685.
- Kakihana, H., Kotaka, M., Satoh, S., Nomura, M., Okamoto, M., 1977. Fundamental studies on the ion-exchange separation of boron isotopes. *Chem. Soc. Jpn., B* 50, 158-163.
- Kasemann, S. A., Schmidt, D. N., Bijma, J., Foster, G. L., 2009. In situ boron isotope analysis in marine carbonates and its application for foraminifera and palaeo-pH. *Chem. Geol.* 260, 138-147.
- Kasemann, S. A.; Meixner, A.; Rocholl, A.; Vennemann, T.; Rosner, M.; Schmitt, A. K.; Wiedenbeck, M., 2001. Boron and oxygen isotopic composition of certified reference materials NIST SRM610/612 and reference materials JB-2 and JR-2. *Geostandard Newsletters - The Journal for Geostandards and Geoanalysis*, 25, 2, 405-416.
- Klochko K., Cody G. D., Tossell J. A., Dera P. and Kaufman A. J., 2009. Re-evaluating boron speciation in biogenic calcite and aragonite using  $^{11}\text{B}$  MAS NMR. *Geochim. Cosmochim. Ac.* 73, 1890-1900.
- Lécuyer, C., Grandjean, P., Reynard, B., Albarède, F., Telouk, P., 2002.  $^{11}\text{B}/^{10}\text{B}$  analysis of geological materials by ICP-MS Plasma 54: Application to the boron fractionation between brachiopod calcite and seawater. *Chem. Geol.*, 186, 45-55, doi:10.1016/S0009-2541(01)00425-9.
- Pagani, M., Lemarchand, D., Spivack, A., Gaillardet, J., 2005. A critical evaluation of the boron isotope-pH proxy: the accuracy of ancient pH estimates. *Geochim. Cosmochim. Ac.* 69, 953-961.
- Palmer, M. R., Spivack, A. J., Edmond, J. M., 1987. Temperature and pH controls over isotopic fractionation during adsorption of boron on marine clay. *Geochim. Cosmochim. Ac.* 51, 2319-2323.
- Reynaud, S., Hemming, N. G., Leclerc, A. J., Gattuso, J.-P., 2004. Effect of  $p\text{CO}_2$  and temperature on the boron isotopic composition of the zooxanthellate coral *Acropora sp.*. *Coral Reefs* 23, 539-546. DOI 10.1007/s00338-004-0399-5
- Rollion-Bard, C., Chaussidon, M., France-Lanord, C., 2003. pH control on oxygen isotopic composition of symbiotic corals. *Earth Planet. Sci. Lett.* 215, 275-288.

- Rollion-Bard, C. and Erez, J., 2010. Intra-shell boron isotope ratios in the symbiont-bearing benthic foraminiferan *Amphistegina lobifera*: Implications for  $\delta^{11}\text{B}$  vital effects and paleo-pH reconstructions. *Geochim. Cosmochim. Ac.* 74, 1530-1536.
- Roux, P. J. le, Shirey, S.B., Benton, L., Hauri, E. H., Mock, T. D., 2004. In situ, multiple-multiplier, laser ablation ICP-MS measurement of boron isotopic composition ( $\delta^{11}\text{B}$ ) at the nanogram level. *Chemical Geology* 203 (2004) 123-138.
- Sanyal, A., Nugent, M., Reeder, R. J., Bijma, J., 2000. Seawater pH control on the boron isotopic composition of calcite: evidence from inorganic calcite precipitation experiments. *Geochim. Cosmochim. Ac.* 64, 1551-1555.
- Schmitt A. K., Kasemann S., Meixner A., Rhede D., 2002. Boron isotopic composition of Central Andean ignimbrites: implications for crustal boron cycles in active continental margin. *Chem. Geol.* 183, 333-347.
- Spivack, A. J. and Edmond, J. M., 1986. Determination of boron isotope ratios by thermal ionization mass spectrometry of the dicesium metaborate cation. *Anal. Chem.* 58, 31-35.
- Vengosch, A., Chivas, A. R., McCulloch, M. T., 1989. Direct determination of boron and chlorine isotopic compositions in geological materials by negative thermal-ionization mass spectrometry, *Chem. Geol.*, 79, 333-343.
- Vengosh, A., Kolodny Y., Starinsky A., Chivas A. R., McCulloch, M. T., 1991. Coprecipitation and isotopic fractionation of boron in modern biogenic carbonates. *Geochim. Cosmochim. Ac.* 55, 2901–2910. doi:10.1016/0016-7037(91)90455-E.
- Zeebe, R., 2005. Stable boron isotope fractionation between dissolved  $\text{B}(\text{OH})_3$  and  $\text{B}(\text{OH})_4^-$ . *Geochim. Cosmochim. Acta* 69, 2753-2766.

## Chapter 4

### **Responses of *Mytilus edulis* extracellular body fluids and shell composition to decreased pH: acid-base status, trace elements and $\delta^{11}\text{B}$ \***

\*under review at *Chemical Geology* as: Agnes Heinemann, Jan Fietzke, Frank Melzner, Florian Böhm, Jörn Thomsen, Dieter Garbe-Schönberg, Anton Eisenhauer; Responses of *Mytilus edulis* extracellular body fluids and shell composition to decreased pH: acid-base status, trace elements and  $\delta^{11}\text{B}$ .

## 4.1 Abstract

*Mytilus edulis* were cultured for 3 months under six different seawater  $p\text{CO}_2$  levels ranging from 380 to 4000  $\mu\text{atm}$ . Specimens were taken from Kiel Fjord (Western Baltic Sea, Germany) which is a habitat with high and variable seawater  $p\text{CO}_2$  and related shifts in carbonate system speciation (e.g. low pH and low  $\text{CaCO}_3$  saturation state). Hemolymph (HL) and extrapallial fluid (EPF) samples were analyzed for pH and total dissolved inorganic carbon ( $C_T$ ) to calculate  $p\text{CO}_2$  and  $[\text{HCO}_3^-]$ . A second experiment was conducted for 2 months with three different  $p\text{CO}_2$  levels (380, 1400 and 4000  $\mu\text{atm}$ ). Boron isotopes ( $\delta^{11}\text{B}$ ) were investigated by LA-MC-ICP-MS (Laser Ablation-Multicollector-Inductively Coupled Plasma-Mass Spectrometry) in shell portions precipitated during experimental treatment time. Additionally, elemental ratios (B/Ca, Mg/Ca and Sr/Ca) in the EPF of specimens from the second experiment were measured via ICP-OES (Inductively Coupled Plasma-Optical Emission Spectrometry). Extracellular pH was not significantly different in HL and EPF but systematically lower than ambient water pH. This is due to high extracellular  $p\text{CO}_2$  values, a prerequisite for metabolic  $\text{CO}_2$  excretion. No accumulation of extracellular  $[\text{HCO}_3^-]$  was measured. Elemental ratios (B/Ca, Mg/Ca and Sr/Ca) in EPF increased slightly with pH which is in accordance with increasing growth and calcification rates at higher seawater pH values. Boron isotope ratios were highly variable between different individuals but also within single shells. This corresponded to a high individual variability in fluid elemental B/Ca ratios and may be due to high B concentrations in the organic parts of the shell. The mean  $\delta^{11}\text{B}$  value showed no trend with pH but appeared to represent internal pH (EPF) rather than ambient water pH.

## 4.2 Introduction

About half of anthropogenic carbon dioxide (CO<sub>2</sub>) released to the atmosphere is absorbed by the global oceans. It is predicted that the oceans approach a pH of ~7.3 within the next 300 years (e.g. Caldeira and Wickett 2003, Sabine et al. 2004). This leads to a shift in the inorganic carbon equilibrium towards higher CO<sub>2</sub> and lower CO<sub>3</sub><sup>2-</sup> concentrations. Therefore, the calcium carbonate (CaCO<sub>3</sub>) saturation state ( $\Omega$ ) will decrease (e.g. Feely et al. 2004) and higher-latitude oceans are predicted to become undersaturated with respect to aragonite by the year 2050 (Orr et al. 2009, Cao and Caldeira 2008) which may have considerable consequences for marine calcifying organisms (Orr et al. 2005). Many (mostly short-term studies, days to week duration) ocean acidification experiments have been conducted and different responses to high  $p\text{CO}_2$  were found. The majority of the investigated species showed declining rates of calcification and reproduction (see Doney et al. 2009 and Ries et al. 2009 for review) with rising  $p\text{CO}_2$ . Most ocean acidification perturbation experiments are not able to properly account for the genetic adaptation potential of marine species, as time limitations usually prevent multi generation experiments. Thus, calcifying marine organisms from habitats with naturally high CO<sub>2</sub> concentrations can serve as analogues for future ocean conditions (e.g. Hall-Spencer et al. 2008).

Kiel Fjord (Western Baltic Sea, Germany) provides ideal conditions for ocean acidification studies due to summer hypoxia in bottom waters and upwelling of CO<sub>2</sub> enriched waters (Hansen et al. 1999, Lehmann et al. 2002). Kiel Fjord is already today frequently exposed to seawater  $p\text{CO}_2$  values that are predicted for the future global ocean of the next 100-300 years (Thomsen et al. 2010, Caldeira and Wickett 2003). The habitat is characterized by low salinity (10-20), low alkalinity (1900-2150  $\mu\text{mol/kg}$ ), low pH (minimum value <7.5) during summer and autumn, and high  $p\text{CO}_2$  (maximum value of 2340  $\mu\text{atm}$ ; 1  $\mu\text{atm}$  = 0.101 Pa) events. The CaCO<sub>3</sub> saturation state in the Kiel Fjord therefore can reach minimum values of  $\Omega_{\text{arag}} = 0.34$  and  $\Omega_{\text{calc}} = 0.58$  (Thomsen et al. 2010). It can be assumed that calcifying communities in this habitat have already been adapted to a fluctuating carbonate system speciation with frequent high  $p\text{CO}_2$  events for multiple generations.

Predictions of future ocean pH scenarios can be improved by studies of climate shifts in the past. In this regard the elemental and isotopic composition of biogenic carbonates (e.g. bivalve shells, coral skeletons, foraminifera) serve as proxies for the reconstruction of past ocean chemistry. In particular, boron to calcium ratios (B/Ca) have been shown to decrease with declining pH in some biological and inorganic carbonates (Hemming and Hanson 1992, Sanyal et al. 2000). This results from the fact that in aqueous solutions, boric acid dissociates to borate (B(OH)<sub>4</sub><sup>-</sup>) and H<sup>+</sup> (equation 1). Consequently, the proportion of boric acid to borate is pH dependent.



The borate ion is suggested to be preferentially incorporated into carbonates precipitated from seawater (Vengosch et al. 1991, Hemming and Hanson 1992, Hemming et al. 1995, Pagani et al. 2005). For this reason, the isotopic signature of  $\text{B}(\text{OH})_4^-$  will be recorded in the carbonate. Klochko et al. (2009) proposed that both species can be incorporated. In contrast, Foster et al. (2008) investigated B/Ca ratio in foraminifera and reported that the partition coefficient of borate between water and shell carbonate is primarily influenced by seawater  $[\text{CO}_3^{2-}]$  and not directly by seawater pH. The results of Yu et al. (2007) showed the opposite trend of those shown by Foster et al. (2008). Foster et al. (2008) suggested this is indicating a species specific control on boron incorporation.

Boron isotopes ( $\delta^{11}\text{B}$ ) have been measured in skeletons of different organisms like corals (Reynaud et al. 2004, Hönisch et al. 2004) and foraminifera (Hönisch et al. 2003, Foster et al. 2008, Rollion-Bard and Erez 2010) as a pH proxy. Therefore, the combination of these two proxies (B/Ca for  $[\text{CO}_3^{2-}]$  and  $\delta^{11}\text{B}$  for pH reconstruction) might offer the opportunity to reconstruct the marine paleo-carbonate system as it is necessary to know two of the six parameters (pH,  $[\text{CO}_2]$ ,  $[\text{HCO}_3^-]$ ,  $[\text{CO}_3^{2-}]$ , total alkalinity ( $A_T$ ) and dissolved inorganic carbon ( $C_T$ )) to constrain the system and to establish how  $\text{CaCO}_3$  saturation state of the oceans changed in the past (Foster et al. 2008).

Several studies showed marine calcifying organisms being sensitive to elevated  $p\text{CO}_2$  and lower pH (e.g. see Doney et al. 2009). However, blue mussels from Kiel Fjord showed the ability to settle, survive and even calcify under similar low pH conditions, when food concentrations are high (Thomsen et al. 2010). Therefore mussels may be good candidate species to provide high resolution records of environmental conditions (like temperature, salinity, pH) and thus contribute to the reconstruction of past climate. Additionally, the wide distribution and adaptation to a broad range of environments (Gosling 1992) suggests *M. edulis* as a model organism for such studies.

Since different studies using bivalve shells as proxy archives yielded contradictory results (Klein et al. 1996a/b, Vander Putten et al. 2000, Lazareth et al. 2003, Immenhauser et al. 2005, Freitas et al. 2008, Wanamaker et al. 2008) it is necessary to understand fundamental processes of bivalve biomineralization in order to understand differences between studies (e.g. Carré et al. 2006, Heinemann et al. 2008). Extracellular body fluids (hemolymph and extrapallial fluid) are the connection between tissues and shell. Especially the extrapallial fluid (EPF) may influence calcification processes as it fills the extrapallial cavity enclosed by the shell, the periostracum and the outer mantle margin (Wilbur and Saleuddin 1983).

Thus, to contribute to the understanding of the ability of calcifying organisms to live under acidified conditions and of biomineralization mechanisms of *M. edulis* we sampled hemolymph (HL) and extrapallial fluid (EPF) of mussels at the end of two  $\text{CO}_2$  perturbation experiments. Fluids were analyzed for pH,  $C_T$  and elemental ratios. To consider the suitability of *M. edulis* shell as a proxy archive for ocean pH, boron isotopes ( $\delta^{11}\text{B}$ ) were investigated by LA-MC-ICP-MS (Fietzke et al.

2010) in shell portions precipitated during the experimental incubation (shells from the long-term growth study described by Thomsen et al. 2010).

## 4.3 Material and methods

### 4.3.1 Culture and samples

#### 4.3.1.1 General setup

Two experiments were conducted to investigate how increased water  $p\text{CO}_2$  influences different parameters ( $p\text{CO}_2$ , pH,  $[\text{HCO}_3^-]$ ,  $[\text{CO}_3^{2-}]$  and B/Ca, Mg/Ca and Sr/Ca ratios) of *Mytilus edulis* extracellular fluids and to test whether shell boron isotopes can be used as a pH proxy.

Atmospheric  $p\text{CO}_2$  averaged 386  $\mu\text{atm}$  (<http://www.esrl.noaa.gov/gmd/ccgg/trends/>) in 2009 and concentrations are predicted to reach values between 700-1000  $\mu\text{atm}$  by the year 2100 (IPCC 2007). Particular marine habitats like Kiel Fjord (Western Baltic Sea, Germany) are already exposed to values above 2000  $\mu\text{atm}$  and might occasionally encounter  $p\text{CO}_2$  values of  $>4000$   $\mu\text{atm}$  if water surface  $p\text{CO}_2$  doubles (see Thomsen et al. 2010). Thus,  $p\text{CO}_2$  levels of 380-4000  $\mu\text{atm}$  were chosen for the experimental incubations. All specimens used in the experiments were collected from subtidal populations in Kiel Fjord (54° 19.8' N; 10° 9.0' E) and cultured at the culturing facilities of the Leibniz Institute of Marine Sciences (IFM-GEOMAR) in Kiel. Animals were acclimated under control conditions for 2 weeks prior to experimentation.

The experiments were conducted in a flow through system (200 ml/min per experimental unit) using water from Kiel Fjord which was filtered (50-5  $\mu\text{m}$  filters, UV-sterilized) and pumped into a storage tank, where it was aerated. The air saturated water was pumped to a header tank and then supplied to the aquaria via gravity feed. Different  $\text{CO}_2$ -air-mixtures were used to equilibrate the experimental seawater (for a more detailed description see supplement).

Water pH was measured daily between Mondays and Fridays with a WTW pH meter (pH 340i, electrode: Sen Tix 81 (calibrated with Radiometric IUPAC precision pH buffer 7 and 10), WTW GmbH, Weilheim, Germany). All pH values measured with the pH meter were corrected with respect to the pH values calculated from weekly  $A_T$  and  $C_T$  measurements ( $n = 223$ ,  $R^2 = 0.949$ ) as they provide more accurate results:

$$\text{pH}_{\text{corrected}} = 0.9781 * \text{pH}_{\text{measured}} + 0.2123 \quad (2)$$

For all pH values reported in this paper, the NBS scale was used. Hemolymph (HL) and extrapallial fluid (EPF) samples were taken directly after removing the bivalves from the aquaria. Valves were opened carefully to not injure the mantle and held open with a 1000  $\mu\text{l}$  pipette tip. Hemolymph was

drawn anaerobically with a syringe from the posterior adductor muscle and EPF was taken from the extrapallial space by inserting a flexible syringe needle ( $\varnothing$  0.6 x 80 mm) between shell and the pallial line.

From all aquaria water temperature, salinity (with WTW cond 315i salinometer and WTW TETRACON 325 probe) and pH were measured daily.  $A_T$  and  $C_T$  samples were taken for carbonate system calculations (Table 4.1; for more details of exp. 2 see Thomsen et al. 2010).

Table 4.1: Water conditions during experimental trials. Data for experiment 2 are from Thomsen et al. (2010). Errors are given as SD. Values represent mean over whole experiment.

Exp. 1:	temperature in °C $12.1 \pm 0.6$			salinity	$18.8 \pm 1.59$	
Treatment	pH <sub>NBS</sub>	$A_T$	$C_T$	$pCO_2$	$\Omega_{calc}$	$\Omega_{arag}$
theoretical value		[ $\mu$ mol/kg]	[ $\mu$ mol/kg]	[ $\mu$ atm]		
387 $\mu$ atm	8.02 $\pm 0.08$	2031 $\pm 74$	1965 $\pm 63$	577 $\pm 95$	1.8 $\pm 0.3$	1.1 $\pm 0.2$
560 $\mu$ atm	7.93 $\pm 0.07$	2031 $\pm 74$	1988 $\pm 62$	722 $\pm 97$	1.5 $\pm 0.2$	0.9 $\pm 0.1$
840 $\mu$ atm	7.86 $\pm 0.05$	2032 $\pm 72$	2004 $\pm 65$	839 $\pm 80$	1.3 $\pm 0.2$	0.8 $\pm 0.1$
1120 $\mu$ atm	7.77 $\pm 0.05$	2033 $\pm 73$	2026 $\pm 66$	1041 $\pm 93$	1.1 $\pm 0.1$	0.5 $\pm 0.1$
1400 $\mu$ atm	7.71 $\pm 0.05$	2033 $\pm 73$	2040 $\pm 66$	1195 $\pm 98$	0.9 $\pm 0.1$	0.6 $\pm 0.1$
4000 $\mu$ atm	7.28 $\pm 0.08$	2040 $\pm 72$	2172 $\pm 66$	3352 $\pm 566$	0.4 $\pm 0.1$	0.2 $\pm 0.04$
Exp.: 2	temperature in °C $13.8 \pm 0.6$			salinity	$15.0 \pm 0.6$	
Treatment	pH <sub>NBS</sub>	$A_T$	$C_T$	$pCO_2$	$\Omega_{calc}$	$\Omega_{arag}$
		[ $\mu$ mol/kg]	[ $\mu$ mol/kg]	[ $\mu$ atm]		
387 $\mu$ atm	8.13 $\pm 0.02$	1966 $\pm 3$	1891 $\pm 5$	500 $\pm 30$	1.94 $\pm 0.04$	1.14 $\pm 0.04$
1400 $\mu$ atm	7.72 $\pm 0.06$	1968 $\pm 5$	1984 $\pm 12$	1350 $\pm 200$	0.81 $\pm 0.09$	0.48 $\pm 0.06$
4000 $\mu$ atm	7.26 $\pm 0.04$	1970 $\pm 4$	2126 $\pm 13$	3950 $\pm 220$	0.28 $\pm 0.02$	0.17 $\pm 0.01$

#### 4.3.1.2 Experiment 1

The first experiment was conducted from September, 3<sup>rd</sup> to December, 18<sup>th</sup> 2008. We cultured *Mytilus edulis* (~140 individuals per tank) ranging in size from 12.4 mm to 46.7 mm at six different  $pCO_2$  levels (380, 560, 840, 1120, 1400 and 4000  $\mu$ atm). Shell length was measured at the longest axis (from umbo to edge at opposite site of the shell) using calipers with an accuracy of 0.1 mm. Fluids were sampled from the five largest bivalves ( $45.6 \pm 0.6$  mm) in each treatment. The experimental



aquaria had a volume of 15 l and were exposed to a 14:10 hour light:dark cycle. Water pH ranged from  $8.02 \pm 0.08$  to  $7.28 \pm 0.08$  in the different treatments. Temperature was  $12.2 \pm 0.6$  °C and salinity  $18.8 \pm 1.6$ .

During the first 6 weeks mussels were fed with „DTs Live Marine Phytoplankton-Premium Reef Blend“ (DT's Plankton Farm, Sycamore, IL, USA), a live phytoplankton mixture of three marine algae species (*Phaeodactylum tricornutum* (40 %), *Nannochloropsis oculata* (40 %) and *Chlorella sp.* (20%)). Since mussel growth was unsatisfactory during that period the animals were additionally fed with *Artemia salina* after that period as Wong and Levinton (2004) reported best growth of *M. edulis* with a mixture of phyto- and zooplankton. Food was provided on 3 days a week (~75 mg algal biomass and ~45 mg *Artemia salina* (both dry weight)/day/aquarium) by closing the flow through for 4 hours and adding food directly into the aquaria.

Fluid samples were centrifuged (30 s) and pH was measured with a microelectrode (WTW Mic-D). Then total dissolved inorganic carbon ( $C_T$ ) was determined immediately after sampling via a Corning 965 CO<sub>2</sub> analyzer, (Olympic Analytical Service Essex, UK; accuracy 0.1 mM) in two 100 µl subsamples. Carbonate parameters ( $p\text{CO}_2$ ,  $[\text{HCO}_3^-]$ , and  $[\text{CO}_3^{2-}]$ ) of the fluids were calculated from measured pH and  $C_T$  with using the Henderson-Hasselbalch equation:

$$p\text{CO}_2 = C_T \left( 10^{\text{pH} - \text{pK}'_1} \cdot \alpha_{\text{CO}_2} + \alpha_{\text{CO}_2} \right)^{-1} \quad (3)$$

$$[\text{HCO}_3^-] = 10^{\text{pH} - \text{pK}'_1} \cdot \alpha_{\text{CO}_2} \cdot p\text{CO}_2 \quad (4)$$

$$[\text{CO}_3^{2-}] = 10^{\text{pH} - \text{pK}'_2} \cdot [\text{HCO}_3^-] \quad (5)$$

$$\text{pK}'_1 = \text{pH} - \log \left( \frac{C_T}{p\text{CO}_2 \alpha_{\text{CO}_2}} - 1 \right) \quad (6)$$

Where  $\alpha$  is the CO<sub>2</sub> solubility coefficient.  $\text{pK}'_1$  and  $\text{pK}'_2$  are the first and second apparent dissociation constants of carbonic acid.  $\alpha_{\text{CO}_2}$  was calculated (0.045 mol/l\*µatm; Weiss, 1974) and  $\text{pK}'_2$  (9.321; Roy et al., 1993) was chosen according to experimental temperature and salinity.  $\text{pK}'_1$  was calculated from  $\text{pH}_{\text{NBS}}$ ,  $C_T$  and  $p\text{CO}_2$  (measured in *Mytilus edulis* body fluids by Thomsen et al. (2010)) using equation 6 (Albers and Pleschka, 1967). A linear relationship was found for  $\text{pK}'_1$  in relation to  $\text{pH}_{\text{NBS}}$ . After adjusting temperature and salinity according to this experiment the regression for  $\text{pK}'_1$  for *M. edulis* internal fluids was  $\text{pK}'_1 = -0.1323\text{pH} + 7.2371$  ( $R^2 = 0.3027$ ).

### 4.3.1.3 Experiment 2

From 14<sup>th</sup> of May to 13<sup>th</sup> of July a second (long-term growth) experiment was conducted using three  $p\text{CO}_2$  levels (380, 1400 and 4000  $\mu\text{atm}$ ). The level of replication was four. Each 15 l aquarium contained eight small (mean 5.5 mm), eight medium sized (mean 13 mm) and two big (mean 40 mm) mussels. Shells from the medium specimens ( $13.3 \pm 1.4$  mm) and fluids from the big specimens were investigated in this study. The experiment was conducted under a mean temperature of  $13.8 \pm 0.6$  °C and a salinity of  $15 \pm 0.6$ . The light/dark cycle was 14:10 hours. Food (*Rhodomonas sp.* suspension,  $2900 \pm 1200$  cells/ml) was provided continuously by adding it into the aquaria at a rate of 100 ml/min. Body fluids of the big specimens were frozen at  $-20^\circ\text{C}$  directly after sampling and used for elemental analyses by ICP-OES (SPECTRO *Ciros<sup>CCD</sup> SOP*) at the Institute of Geosciences, University Kiel, Germany. The tissue of the medium sized mussels was removed and shells were dried at 20 °C for 5 days.

EPF pH could not be measured directly in experiment 2 specimens as there was not enough material for sub sampling and therefore no possibility to measure pH directly without contaminating the fluid samples with boron (due to the high boron content of the glass pH electrode). Therefore boron isotopes and elemental ratios (experiment 2) were compared to EPF pH values estimated from experiment 1 fluid values ( $n = 12$ ) and HL pH values measured in large *M. edulis* of an additional experiment presented by Thomsen et al. (2010). The regression for the fluids and the corresponding water was  $\text{pH}_{\text{EPF}} = 0.3826 \text{ pH}_{\text{water}} + 4.4928$  ( $R^2 = 0.914$ ). Additionally the mean offset between EPF and HL (experiment 1 this study;  $n = 6$  each) was considered. Regression results for each treatment and the mean offset between HL and EPF pH have been subtracted from water pH of experiment 2.

### 4.3.2 Analytical methods

The fluids from the second experiment (5-7 samples per treatment) were thawed and diluted 50fold with ultrapure 2 %  $\text{HNO}_3$ . They were analyzed for Mg/Ca, Sr/Ca and B/Ca elemental ratios by ICP-OES (Inductively Coupled Plasma - Optical Emission Spectrometry; SPECTRO *Ciros<sup>CCD</sup> SOP*) at

the Institute of Geosciences, University Kiel, Germany. An intensity-ratio calibration procedure was applied using matrix-matched calibration standards and IAPSO seawater as a consistency standard. External precision of the elemental ratios was  $\sim 0.1$  % RSD for Mg/Ca and Sr/Ca, and 1-4 % RSD for B/Ca.

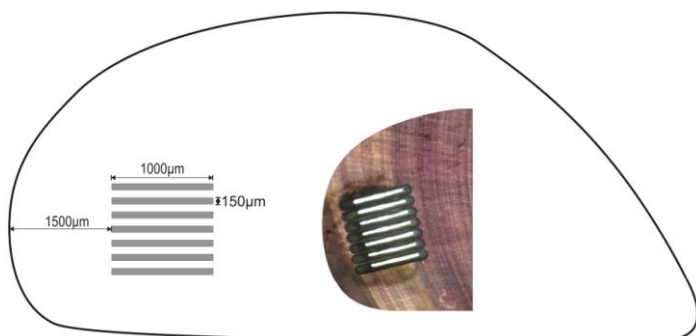


Figure 4.1: Position of laser ablation lines on *M. edulis* shell (scheme of whole shell and picture of sampled laser area).

Ten shells from each treatment of the second experiment were broken to obtain fragments that were grown under treatment conditions (defined by length growth). Subsequently, the fragments were bleached in 10 % NaOCl (1 % active chlorine) for two days to remove organic components (periostracum and other shell organics). After 24 hours samples were placed into an ultra sonic bath for 10 min and the bleaching solution was replaced.

Afterwards shells were rinsed three times with ultrapure water (18.2 MOhm) and then dried at 20 °C. To prevent dissolution of the carbonates the water was adjusted to a pH of ~9 by adding NH<sub>4</sub>OH. Boron isotopes were measured by LA-MC-ICP-MS (Laser Ablation-Multicollector-Inductively Coupled Plasma-Mass Spectrometry; Thermo Fisher MC-ICP-MS *AXIOM*, originally designed and manufactured by VG) connected to an ESI New Wave Research *UP193FX* excimer laser ablation system equipped with an ESI New Wave Research *LFC* (large format cell) via a standard sample standard bracketing procedure described by Fietzke et al. (2010). Soda lime glass SRM (NIST610) was used as external standard. First, three lines (1000 µm x 150 µm) were measured on the NIST. Then, seven lines of sample and seven lines of standard were measured in alternation. Prior to each of these measuring procedures, a preablation was conducted to remove surface contamination. All instrumental parameters are given in Table 4.2. The location of the sample lines on *M. edulis* shells is shown in Figure 4.1.

<b>AXIOM MC-ICP-MS</b>	
Cool gas	14 l/min
Auxiliary gas	1.8 l/min
Nebulizer gas	0.9 l/min (Ar)
RF power	1250 W
Reflected power	3 W
Accelerating voltage	4972 V
Cones	R.A. Chilton RAC19/RAC705
Resolution	500res
<b>UP193FX</b>	
Ablation cell gas	0.6 l/min (He)
Spot size	150 µm
Fluence	2.3 J/cm <sup>2</sup>
Fluence Preablation	0.6 J/cm <sup>2</sup>
Repetition rate	30 Hz
Scan mode	Line scan (1000 µm @ 12 µm/s)
Scan mode Preablation	Line scan (1000 µm @ 50 µm/s)
Pause between lines	90 s

Table 4.2: Instrumental parameters for Laser Ablation.

## 4.4 Results and Discussion

### 4.4.1 Water parameters

Since the experimental incubation systems used in this study were flow through designs with continuous supply of water from Kiel Fjord, all treatments were influenced by changes in Kiel Fjord water chemistry. Although the water was vigorously aerated prior to introduction into the experimental aquaria, mean seawater  $p\text{CO}_2$  deviated from the nominal values. Mean seawater conditions during the two experiments are given in Table 4.1. Carbonate system speciation measured in the extracellular fluids are not compared to these mean values but to values from dates of sampling (Table 4.3).

### 4.4.2 Acid-base parameters of fluid samples (experiment 1)

Overviews of all mean extracellular acid-base parameters of the internal fluids (HL and EPF) are given in Table 4.3 and Figure 4.2 (for detailed data and regressions see supplement). High extracellular  $p\text{CO}_2$  values between 1000-4000  $\mu\text{atm}$  are found in all aquatic ectothermic metazoans, as diffusive excretion of metabolic  $\text{CO}_2$  depends on a relatively steep gradient of  $\text{CO}_2$  from the body fluids to the seawater (see Melzner et al. 2009 for a review). Additional increases in extracellular  $p\text{CO}_2$  under hypercapnia (Pörtner et al. 2004, Michaelidis et al. 2005, Spicer et al. 2007, Thomsen et al. 2010) are necessary in order to maintain metabolic  $\text{CO}_2$  flux. In this study a linear increase of fluid  $p\text{CO}_2$  with increasing water  $p\text{CO}_2$  was measured, with slightly lower values in the HL (1648-3122  $\mu\text{atm}$ ) than in the EPF (1938-3430  $\mu\text{atm}$ ). However,  $p\text{CO}_2$  values in HL and EPF were not significantly different from each other. At the highest  $p\text{CO}_2$  treatment a reduced  $p\text{CO}_2$  diffusion gradient could be observed (only low offset between water and extracellular body fluid  $p\text{CO}_2$ ), indicating reductions in metabolism in experiment 1. Similar reductions in metabolic rate have been observed in *M. galloprovincialis* under increased water  $p\text{CO}_2$  by Michaelidis et al. (2005). This was indicated by a significant decrease in oxygen consumption. However, no reductions in metabolism were witnessed in another experiment using Baltic Sea *M. edulis* at 4000  $\mu\text{atm}$  under higher food concentrations, suggesting that the observed reduction in the  $\text{CO}_2$  diffusion gradient in experiment 1 of this study might be due to food limitation (Thomsen and Melzner 2010). Further studies are needed to clarify the role of food supply on metabolic rates and acid-base status under acidified conditions.

Table 4.3: Acid-base status of hemolymph and extrapallial fluid and of the water at date of sampling (exp. 1).

	treatment $p\text{CO}_2$ [ $\mu\text{atm}$ ] at day of sampling	EPF (SD, n)	HL (SD, n)	water at day of sampling
<b>pH</b>	452	7.52 (0.04; 3)	7.54 (0.05; 3)	8.10
	574	7.50 (0.09; 4)	7.53 (0.05; 3)	8.01
	731	7.46 (0.05; 3)	7.52 (0.04; 3)	7.91
	906	7.45 (0.02; 3)	7.47 (0.05; 4)	7.82
	1123	7.41 (0.04; 4)	7.47 (0.07; 4)	7.73
	2724	7.34 (0.09; 4)	7.37 (0.02; 4)	7.39
<b><math>C_T</math> [mM]</b>	452	1.79 (0.18; 3)	1.63 (0.31; 3)	1.96
	574	1.41 (0.03; 4)	1.62 (0.24; 3)	1.98
	731	1.71 (0.18; 3)	1.79 (0.21; 3)	2.01
	906	1.55 (0.07; 3)	1.77 (0.14; 4)	2.03
	1123	1.85 (0.05; 3)	1.61 (0.34; 4)	2.05
	2724	1.91 (0.07; 4)	1.89 (0.31; 4)	2.15
<b><math>\text{CO}_2</math> [mM]</b>	452	0.087 (0.004; 3)	0.074 (0.008; 3)	0.02
	574	0.077 (0.019; 4)	0.073 (0.009; 3)	0.03
	731	0.104 (0.013; 3)	0.090 (0.017; 3)	0.03
	906	0.092 (0.008; 3)	0.100 (0.016; 4)	0.04
	1123	0.118 (0.008; 3)	0.099 (0.099; 4)	0.05
	2724	0.155 (0.031; 4)	0.141 (0.026; 4)	0.12
<b><math>p\text{CO}_2</math> [<math>\mu\text{atm}</math>]</b>	452	1938 (93; 3)	1648 (183; 3)	452
	574	1717 (427; 4)	1623 (190; 3)	574
	731	2297 (284; 3)	1987 (383; 3)	731
	906	2033 (169; 3)	2226 (348; 4)	906
	1123	2611 (181; 4)	2199 (744; 4)	1123
	2724	3430 (696; 4)	3122 (578; 4)	2724
<b><math>\text{HCO}_3^-</math> [mM]</b>	452	1.70 (0.18; 3)	1.55 (0.30; 3)	1.85
	574	1.33 (0.04; 4)	1.54 (0.23; 3)	1.89
	731	1.61 (0.17; 3)	1.70 (0.19; 3)	1.92
	906	1.46 (0.07; 3)	1.67 (0.13; 4)	1.94
	1123	1.73 (0.06; 4)	1.52 (0.31; 4)	1.96
	2724	1.77 (0.08; 4)	1.75 (0.28; 4)	2.02
<b><math>\text{CO}_3^{2-}</math> [mM]</b>	452	0.028 (0.005; 3)	0.027 (0.009; 3)	0.085
	574	0.020 (0.005; 4)	0.027 (0.005; 3)	0.070
	731	0.022 (0.004; 3)	0.027 (0.003; 3)	0.056
	906	0.020 (0.001; 3)	0.024 (0.003; 4)	0.047
	1123	0.023 (0.003; 4)	0.021 (0.003; 4)	0.038
	2724	0.019 (0.004; 4)	0.019 (0.003; 4)	0.017

High HL and EPF  $p\text{CO}_2$  values are the primary driving force for comparatively low HL and EPF pH values: values range from 7.37 to 7.54 (HL) and 7.34 to 7.52 (EPF) respectively, which is significantly lower in all treatments than seawater pH with values of 7.39 to 8.10.

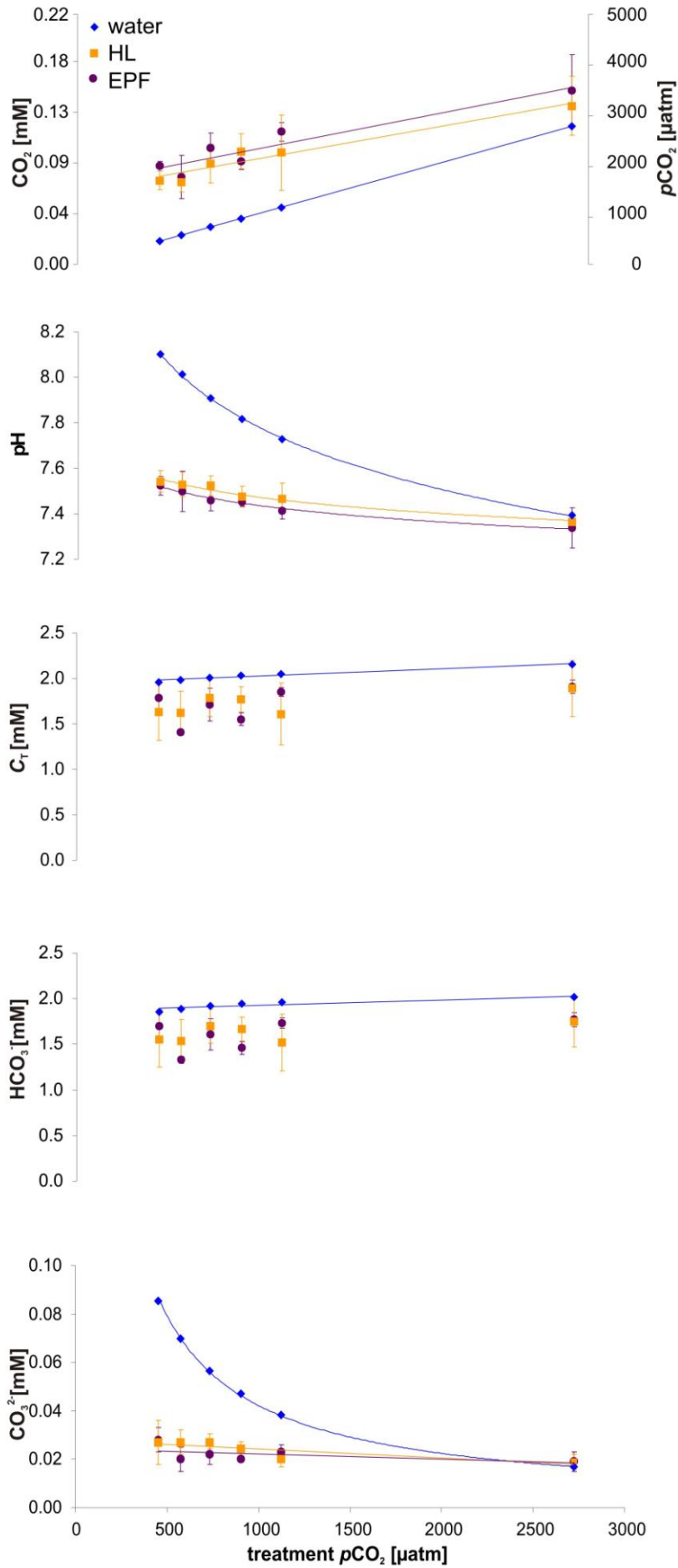


Figure 4.2: Acid-base status of hemolymph and extrapallial fluid and of the seawater at sampling day compared to treatment  $p\text{CO}_2$  at day of sampling (exp. 1).

Due to the progressive reductions in the  $p\text{CO}_2$  gradient between extracellular fluids and seawater, the pH offset between fluids and water decreased as well. At the highest seawater  $p\text{CO}_2$  level (2724  $\mu\text{atm}$ ) pH values of EPF/HL and water became nearly identical. For each treatment, pH values of HL were slightly lower than EPF pH with a mean offset of 0.04 units. However, these differences were not significantly different. Fluid pH values decreased by 0.17 units in the HL and by 0.18 units in the EPF compared to a drop of 0.71 units in the water. The change of hemolymph pH relative to the change in seawater ( $\Delta\text{pH}_{\text{HL}}/\Delta\text{pH}_{\text{SW}}$ ) in this study was consistent with that found by Michaelidis et al. (2005) (Table 4.4). The pH in *M. galloprovincialis* HL decreased from 7.55 to 7.36 (SW: 8.05 to 7.3). Although the control water  $p\text{CO}_2$  in their study was more than double compared to the study of Thomsen et al. (2010) and this study (1079  $\mu\text{atm}$  and 470/452  $\mu\text{atm}$ , respectively) the water pH was nearly the same. This may be due to the difference in alkalinity but also to the observed accumulation of bicarbonate in that study. In general the Mediterranean Sea is characterized by a higher alkalinity (2500  $\mu\text{mol/kg}$ ) in comparison to the Baltic Sea (~1900  $\mu\text{mol/kg}$ ). The resulting higher buffer capacity leads to a smaller drop in pH in the Mediterranean Sea at comparable seawater  $p\text{CO}_2$  values. This explains the different results with respect to hemolymph pH between the studies of Thomsen et al. (2010) and of Michaelidis et al. (2005) although the  $p\text{CO}_2$  was nearly similar. Thomsen et al. (2010) measured a drop in *M. edulis* HL pH relative to ambient water pH twice as high (8.05 to 7.08 (SW) related to 7.59 to 7.16 (HL)) as measured by Michaelidis et al (2005) and in this study. Thomsen et al. (2010) conducted experiments at  $p\text{CO}_2$  values ranging from 470 to 4250  $\mu\text{atm}$ . However, total alkalinity in the present study was 130 to 150  $\mu\text{mol/kg}$  higher than in that of Thomsen et al. (2010), which is related to the lower salinity in the latter (11.8 compared to 18.8 in this study). This disparity in salinity/alkalinity was due to the high seasonal variability in Kiel Fjord and is likely to be responsible for the different drop in body fluid pH. These results show the high variability in extracellular pH that can be caused by the strong influence of alkalinity and of the reduced metabolism (after three months of experiment with low food conditions) on the pH decrease in response to increased  $p\text{CO}_2$ .

Table 4.4: Comparison between the hemolymph acid-base of this study and the studies of Michaelidis et al. (2005) and Thomsen et al. (2010).

		$p\text{CO}_2_{\text{SW}}$ [ $\mu\text{atm}$ ]	$p\text{CO}_2_{\text{HL}}$ [ $\mu\text{atm}$ ]	$\Delta p\text{CO}_2$ (HL-SW)	$\text{pH}_{\text{SW}}$	$\text{pH}_{\text{HL}}$	$\Delta\text{pH}_{\text{HL}}/\Delta\text{pH}_{\text{SW}}$	salinity	$A_T$
<i>M. edulis</i> this study	control	452	1648	1196	8.10	7.54	0.239	18.8	2031
	treatment	2724	3122	398	7.39	7.37		18.8	2040
<i>M. edulis</i> Thomsen et al. 2010	control	470	1697	1227	8.05	7.55	0.402	15.0	1901
	treatment	4310	4960	650	7.08	7.16		15.0	1891
<i>M. galloprovincialis</i> Michaelidis et al. 2005	control	1079	1513	434	8.05	7.59	0.267	32.0	
	treatment	5026	5724	697	7.30	7.36		32.0	

However, no extracellular accumulation of bicarbonate ( $\text{HCO}_3^-$ ) could be measured in HL or EPF, indicating that *M. edulis* does not actively buffer HL or EPF to avoid decreasing pH values. For both fluids,  $[\text{HCO}_3^-]$  was below that of the seawater and no significant differences (non-linear regressions) were found between HL and EPF. Accumulation of  $[\text{HCO}_3^-]$  (nearly equivalent to a net excretion of protons) is an efficient mechanism of extracellular pH stabilization that is primarily employed by active marine ectothermic organisms that are characterized by pH sensitive respiratory pigments (see Melzner et al. 2009 for a review). The magnitude of this  $[\text{HCO}_3^-]$  accumulation response varies between taxa, but highest degrees of  $[\text{HCO}_3^-]$  related pH compensation are found in teleost fish, decapod crustaceans and cephalopod molluscs (Larsen et al. 1997, Pane and Barry 2007, Gutowska et al. 2010). Two studies also reported  $[\text{HCO}_3^-]$  accumulation in mussels to buffer extracellular pH (Lindinger et al. 1984, Michaelidis et al. 2005). However, both of these were conducted in closed/recirculating systems and it is evident (Lindinger et al. 1984) or very possible (Michaelidis et al. 2005) that this increase in extracellular  $[\text{HCO}_3^-]$  was due to increases in ambient water  $[\text{HCO}_3^-]$  due to external/internal shell dissolution (see Thomsen et al. 2010). Consequently, carbonate concentrations are lower in HL and EPF than in seawater, decreasing with decreasing pH (increasing  $p\text{CO}_2$ ). In the highest  $p\text{CO}_2$  treatment (2724  $\mu\text{atm}$ ), HL and EPF  $[\text{CO}_3^{2-}]$  were almost equal to seawater  $[\text{CO}_3^{2-}]$  within error bars.

Table 4.5: pH and Me/Ca ratios of treatment water and EPF. Water pH values represent the day of sampling. SD represents the error of different individuals (EPF) and different aquaria, respectively. The precision based on repeated standard (IAPSO) measurements was 0.20-0.25 % for Mg, Ca and Sr and 0.88 % for boron. EPF pH was calculated from experiment 1 and Thomsen et al. (2010) (see methods).

Treatment in $\mu\text{atm}$	Culture pH (SD; n)		EPF pH calculated	shell mass growth		
	exp. 2			[%]		
380	8.08 (0.01; 3)		7.55	242		
1400	7.68 (0.01; 4)		7.40	236		
4000	7.23 (0.03; 4)		7.22	158		

Treatment in $\mu\text{atm}$	EPF B/Ca (SD; n) in mmol/mol	water B/Ca (SD; n) in mmol/mol	EPF Sr/Ca (SD; n) in mmol/mol	water Sr/Ca (SD; n) in mmol/mol	EPF Mg/Ca (SD; n) in mmol/mol	water Mg/Ca (SD; n) in mmol/mol
380	56.2 (1.08; 5)	54.3 (1.54; 3)	8.10 (0.09; 6)	8.09 (0.05; 3)	4947 (54; 6)	4859 (22; 3)
1400	55.0 (3.56; 5)	53.9 (3.72; 4)	8.05 (0.12; 5)	8.13 (0.04; 4)	4878 (125; 5)	4974 (124; 4)
4000	52.7 (2.71; 6)	53.1 (2.09; 4)	8.06 (0.08; 6)	8.13 (0.12; 4)	4817 (62; 6)	4898 (116; 4)

Generally, it is important to note that the acid-base conditions in the body fluids, especially in the EPF, which is in direct contact with the inner shell surface, may impact calcification and existing shell structures. Reduced shell growth under high  $p\text{CO}_2$  (4000  $\mu\text{atm}$ ) was reported by Thomsen et al. (2010)



and Thomsen and Melzner (2010). Yet experiment 2 specimens increased their shell mass by >150 % during the 8 week experiment, indicating great biological control and an ability to precipitate a shell in fluids that are highly undersaturated with regard to calcium carbonate. However, results from Thomsen et al. (2010) demonstrate that external shell dissolution at the umbo region and thinner aragonite layers may be consequences of high seawater and EPF  $p\text{CO}_2$  values.

#### 4.4.3 Elemental ratios of extrapallial fluid and water (experiment 2)

Elemental ratios (B/Ca, Mg/Ca and Sr/Ca) were measured in the EPF of *M. edulis* cultured under three different  $p\text{CO}_2$  levels (experiment 2, Table 4.5). Figure 4.3 shows the elemental ratios compared to EPF pH. The pH values were extrapolated using a regression of HL data on water pH (see methods). An increase of all elements ( $\text{B}^{3+}$ ,  $\text{Mg}^{2+}$  and  $\text{Sr}^{2+}$ ) relative to Ca could be observed with rising pH. Although a high variability of the element concentrations was found in the fluid, especially B/Ca and Mg/Ca showed a linear trend. This variability between different individuals may be due to a strong individual physiological influence on element partitioning. The magnitude of increase with pH was variable for the different elements. For B/Ca ratios (19.8 %) it was slightly more than twice as high as for Mg/Ca ratios (7.9 %) and lowest for Sr/Ca ratios (1.2 %). Only minor amounts of  $\text{Mg}^{2+}$  and  $\text{Sr}^{2+}$  substitute for  $\text{Ca}^{2+}$  during calcification. Boron is believed to be incorporated into carbonates as  $\text{B}(\text{OH})_4^-$  replacing the carbonate ion in the lattice (Vengosch et al. 1991, Hemming and Hanson 1992, Hemming et al. 1995, Pagani et al. 2005, Klochko et al. 2009).

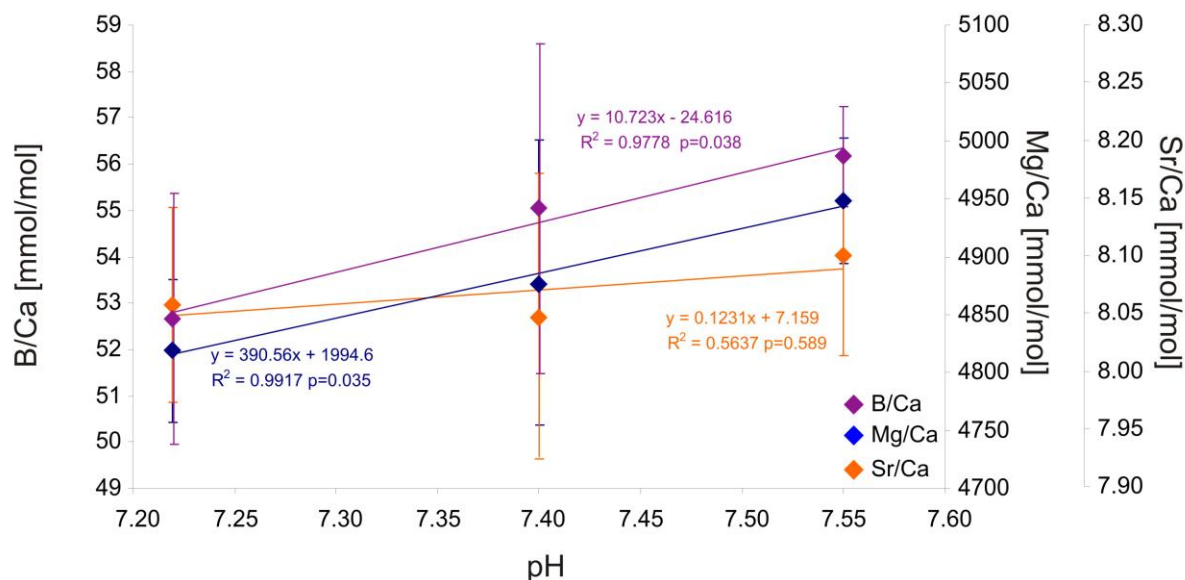


Figure 4.3: Elemental ratios vs. calculated internal pH values. Error bars show 1SD. Linear regressions show an increase of 19.8 % for B/Ca, 7.9 % for Mg/Ca and 1.2 % for Sr/Ca.

Several studies reported different abiotic factors influencing the composition of bivalve shells. The B/Ca ratio has been shown to be related to pH in different carbonates (Hemming and Hanson 1992,

Hobbs and Reardon 1999, Sanyal et al. 2000, Foster et al. 2008). Ni et al. (2007) found a systematic increase of B/Ca in *G. ruber* and *G. sacculifer* with increasing test size and suggested growth rate variations influencing the incorporation of boron. The results of McCoy et al. (2009) in *Mytilus californianus* shell did not reflect a distinct year-to-year correlation of boron concentrations with pH. However, the annual boron concentration probably reflects seasonal pH changes. The authors concluded that biological control of pH and/or boron concentrations in the EPF are the reasons for these observations. Our results show low EPF pH to be a result of high extracellular  $p\text{CO}_2$  (Figure 4.2). As discussed above, high EPF  $p\text{CO}_2$  values are necessary to excrete metabolic  $\text{CO}_2$ . Mg/Ca ratios in carbonates have been shown to be temperature related in inorganically precipitated calcite (e.g. Oomori et al. 1987, Lopez et al. 2009) as well as in biogenic carbonates precipitated by different species like foraminifera (Nürnberg et al. 1990, Elderfield and Ganssen 2000, Kısakürek et al., 2008) or bivalves (Klein et al. 1996a, Wanamaker et al. 2008). Hiebenthal (2009) also reported a positive Mg/Ca-temperature relation in *M. edulis* shells from Kiel Fjord. Salinity was shown to likewise have an effect on Mg/Ca ratios in *M. edulis* calcite (Dodd 1965).

Other studies suggested different biological influences being responsible for the variations of Me/Ca ratios between individuals of one species but also within single shells. In addition to their results mentioned above, McCoy et al. (2009) found organic-rich winter growth bands containing elevated B/Ca ratios. A comparable effect was reported by Schöne et al. (2010) for trace elements in *Arctica islandica* shells. They found a strong influence of organic matrix on the determination of Mg, Sr and Ca. This confirms our results from qualitative laser ablation qualitative measurements that show boron concentrations in the periostracum being about one magnitude higher than in the carbonate. Carré et al. (2006) observed increasing Me/Ca ratios (for  $\text{Mg}^{2+}$ ,  $\text{Ba}^{2+}$ ,  $\text{Mn}^{2+}$  and especially  $\text{Sr}^{2+}$ ) in aragonitic bivalve shells (*Mesodesma donacium*, *Chione subrugosa*) when crystal growth rates increase. Their model predicts decreasing  $\text{Ca}^{2+}$ -channel selectivity when rates increase. Klein et al. (1996b) found significantly higher Sr/Ca ratios in a young, rapidly grown *Mytilus trossulus* than in a slowly grown adult individual. They concluded that shell precipitation along lateral margins is dominantly controlled by mantle metabolic activity at the site of carbonate formation. This suggests that also the elemental composition is dependent on the mantle activity as it seems to be influenced by growth rates. Carré et al. (2006) suggested the Sr/Ca measurements from different sections of *M. trossulus* shells (measured by Klein et al. 1996b) can also be explained by differences in crystal growth. The results from Ford et al. (2010) support that of this study and show Mg/Ca ratios in shells of *Mytilus californianus* to be a function of growth rate rather than temperature related. Takesue et al. (2008) also found growth rate dependent alterations in Sr/Ca, B/Ca and Ba/Ca ratios in valves from *Corbula amurensis*. Sr/Ca seems to be influenced by both temperature and salinity (Dodd 1965, Wanamaker et al. 2008) but also by precipitation rates (Lorens 1981, Lorrain et al. 2005, Freitas et al. 2006).

Experiment 2 consisted of four replicate aquaria (two big individuals per aquarium) for each treatment, and variability in the elemental ratios of the water between different aquaria was observed (single values see supplement). To eliminate this problem Figure 4.4 shows the distribution coefficients between EPF and water. When plotted against growth rates (shell mass growth during experiment in % from Thomsen et al. 2010) elemental ratios are slightly lower in the EPF than in the ambient water at lower growth rates at 4000  $\mu\text{atm}$ . For this treatment external shell dissolution at the umbo region as well as thinner aragonite layers were observed (Thomsen et al. 2010). At high growth rates (385 and 1400  $\mu\text{atm}$ ), elemental ratios are higher in the EPF than in the ambient water. Thus, with increasing growth rates elements like  $\text{B}^{3+}$ ,  $\text{Mg}^{2+}$  and  $\text{Sr}^{2+}$  become enriched in the EPF with respect to  $\text{Ca}^{2+}$ . This effect may be due to higher growth and calcification rates. Therefore the EPF is more depleted with respect to calcium when compared to other elements and the elemental ratios of the EPF are shifted. As elemental ratios in the EPF increased with growth rate it is likely that also the elemental ratios in the shells rose when precipitated from altered fluids. Therefore our results support findings from different studies showing increased Me/Ca ratios in shells grown at high rates (e.g. Klein et al. 1996b, Carré et al. 2006, Ford et al. 2010).

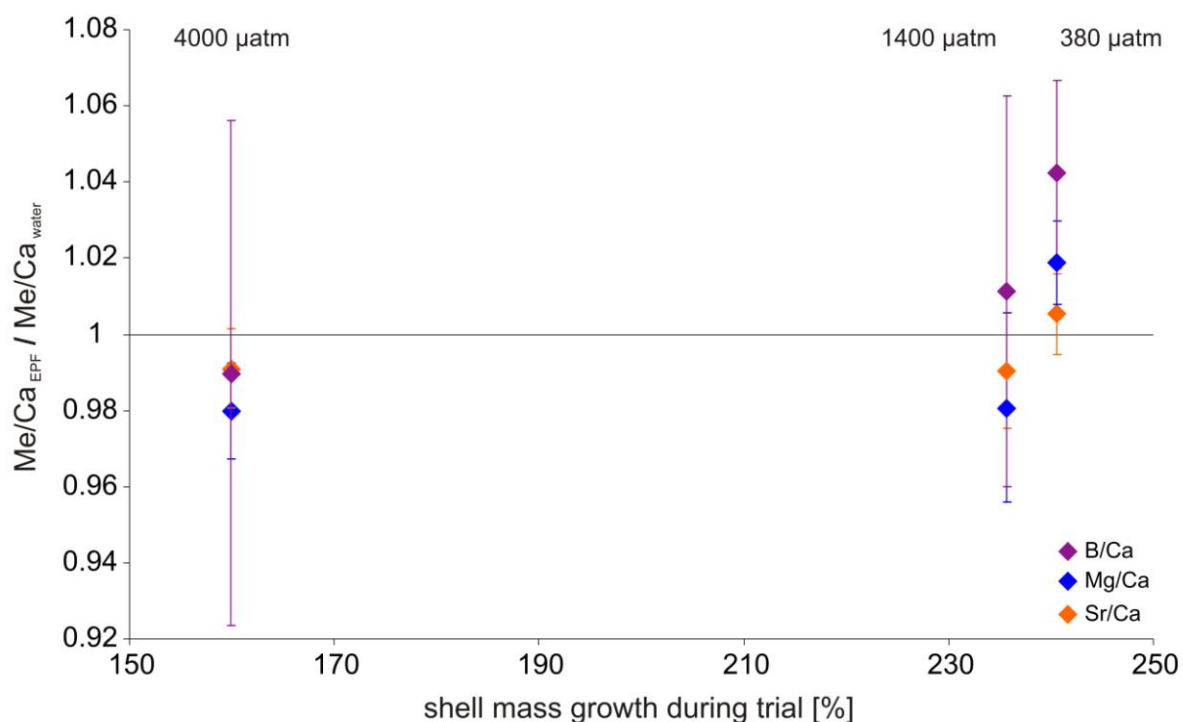


Figure 4.4: Distribution coefficient of EPF and water elemental ratios compared to shell mass growth of bivalves during experimental time (exp. 2). Errors are given as 1SD.

Food availability, temperature, salinity and elevated  $p\text{CO}_2$  (decreased pH) are influencing growth rates (and accordingly amount of organic matter in the shell) of *M. edulis* (e.g. Malone and Dodd 1967, Kautsky 1982, Kossak 2006, Thomsen et al. 2010). While the biological performance depends on these biotic and abiotic factors, seawater  $p\text{CO}_2$  or pH does not seem to be directly reflected in Me/Ca ratios of bivalve carbonates, rather, they might influence them indirectly via decreased rates of growth and calcification due to a repartitioning of the energy budget of the mussel (Thomsen & Melzner 2010). Our results show that the dependence between growth and Me/Ca ratios incorporation is represented in the extrapallial fluid. Thus, elemental ratios (B/Ca, Mg/Ca, and Sr/Ca) in the EPF of *M. edulis* may primarily serve as an indicator for growth rates/shell dissolution as they become enriched with increasing length growth and depleted by dissolution. This indicates that *M. edulis* shells can not be directly used as archive for experienced environmental conditions. Extensive calibrations are necessary to see how parameters such as temperature or salinity influence growth rate. With such calibrations and one for the influence of growth rate on Me/Ca ratios in the shell it may be possible to reconstruct environmental conditions. However, the encountered variability is high due to individual physiology and a high amount of replicates must be measured.

#### 4.4.4 Boron isotope ( $\delta^{11}\text{B}$ ) data of *M. edulis* shells (experiment 2)

Shell portions precipitated during the experimental duration (additional length growth) were investigated for their  $\delta^{11}\text{B}$  composition (Table 4.6).

Table 4.6: pH and  $\delta^{11}\text{B}$  of treatment water and EPF. Water pH values represent mean values over treatment time. 1SD represents the error between different individuals. Shell lengths reflect mean size at the end of the experiment. Initial mean length was  $13.3 \pm 1.4$  mm over all treatments.

Culturing water pH (2SE; n)	EPF pH calculated	Shell $\delta^{11}\text{B}$ (SD; n)	Shell length (SD; n)
exp. 2		in ‰ exp. 2	in mm exp. 2
8.11 (0.008; 53)	7.546	17.4 (3.1; 10)	22.9 (2.4; 10)
7.73 (0.020; 53)	7.396	18.3 (4.8; 11)	24.0 (1.4; 11)
7.28 (0.035; 53)	7.221	17.9 (5.5; 11)	20.7 (1.9; 11)

While the analytical precision of the boron isotope ratio determination was in the order of 0.9 ‰ the variability between individuals from the same treatment was much higher (3.1-5.5 ‰). The results showed a high variability not only between different individuals but also within single shells. The high individual variability was already observed for the fluid elemental ratios. Additionally the considerable amount of boron in the periostracum (see 3.3) suggests the organic matrix surrounding every single carbonate crystal being a reason for this variability. Bivalve shells typically contain up to 5 % of organic matter (e.g. Wilbur 1984). The variability may be caused by individual and

physiological influences as well as (crystal) growth rate. It is obvious that one factor inducing the variability in shell  $\delta^{11}\text{B}$  is the variability in body fluid pH (EPF), not only between individuals but also over time. Extracellular pH for example was shown to decrease when bivalves close their shell valves (e.g. Crenshaw and Neff 1969, Crenshaw 1972). Crenshaw (1972) observed a drop in EPF pH of *Mercenaria mercenaria* from 7.41 to 7.25 while valves were closed for 15 min or longer and a maximum drop in *M. edulis* to 7.2. The pattern how often and how long they close their valves for instance can be different between individuals. Average values of  $\delta^{11}\text{B}$  ranged from 17.4 in the lowest  $p\text{CO}_2$  (highest pH) to 17.9 ‰ in the highest  $p\text{CO}_2$  (lowest pH) treatment, respectively. However, the highest value (18.3 ‰) was found at 1400  $\mu\text{atm}$  but within the high variability no significant difference could be observed. Moreover no clear trend could be observed with pH but values differed from those of other biominerals when plotted against ambient water pH (Figure 4.5).

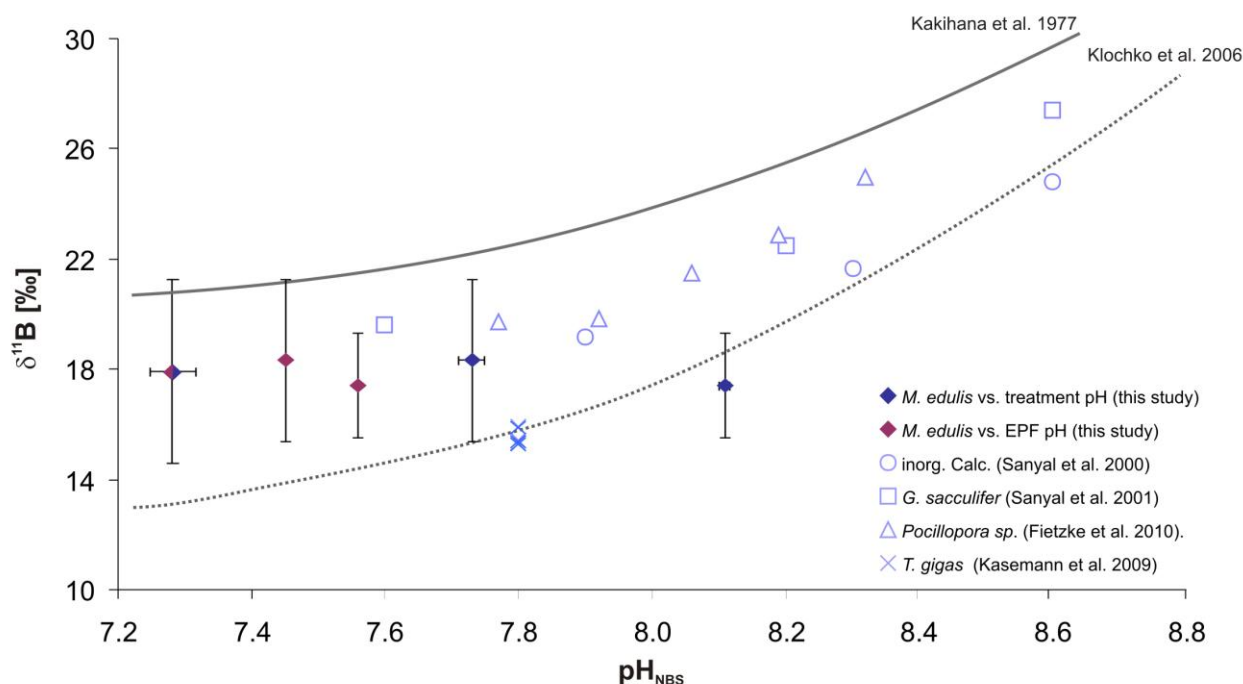


Figure 4.5:  $\delta^{11}\text{B}$  measured in *M. edulis* shells and precipitated under different  $p\text{CO}_2$  conditions in relation to data of other carbonates. Blue diamonds are displayed versus mean water pH during time of experiment 2, pink diamonds display the same  $\delta^{11}\text{B}$  data plotted against EPF pH from experiment 1. *Tridacna gigas* data from Kasemann et al. (2009) are shown as a function of the approximated EPF pH value of *Tridacna squamosa* (at 28 °C, SAL 31) observed by Ip et al. (2006) as no other data could be found. Errors are given as 1SD.

Inorganically precipitated calcite (Sanyal et al. 2000), foraminifera (Sanyal et al. 2001) and corals (Hönisch et al. 2004, Reynaud et al. 2004) are characterized by  $\delta^{11}\text{B}$  values that fit above the measured  $\delta^{11}\text{B}$  curve of  $\text{B}(\text{OH})_4^-$  presented by Klochko et al. (2006; Figure 4.4) which correlates well with ambient water pH. Our data, when plotted against ambient water pH differ from this pattern. When depicted against EPF pH, the pH at the calcification site, they also fit into this range between

theoretical and measured curve. As HL and EPF pH are relatively low (calculated 7.22-7.55 for this experiment),  $\delta^{11}\text{B}$  plots in a section of the curve where pH dependent changes in  $\delta^{11}\text{B}$  are less pronounced. It seems likely that  $\delta^{11}\text{B}$  in *M. edulis* shell reflects the internal fluid pH (EPF) and not that of ambient water. Because pH changes of internal fluids are minor in comparison to ambient water pH changes, only small changes in boron isotope fractionation of the shell can be expected. This fact and the high individual variability render boron isotopes in *M. edulis* shells a less sensitive pH-proxy for seawater pH variations.

However, boron isotopes may be beneficial in providing more information on the processes of biomineralization in bivalves. The extrapallial space is described as the area where calcification takes place. Recent studies show how complex the underlying biological mechanisms probably are. Various organic components, such as a hydrophobic silk gel, acidic proteins, chitin and amorphous calcium carbonate as precursor phases are probably involved in the formation of bivalve shells (e.g. Levi-Kalisman et al. 2001, Weiss et al. 2009, Suzuki et al. 2009, Weiss 2010). Suzuki et al. (2009) recently identified acidic matrix proteins (Pif97, Pif80) that bind to aragonite crystals and to chitin and might be important regulators of nacre formation. Suzuki et al. (2009) and Weiss (2010) proposed that crystals are formed in a microenvironment separated from the extrapallial fluid via a chitinous membrane. Nevertheless  $\delta^{11}\text{B}$  in the shell indicate that shell formation proceeds at pH values typical of the EPF which indicates that calcification is influenced by EPF conditions independent whether calcification occurs separated in a microenvironment close to the shell.

## 4.5 Conclusions

Body fluids of *Mytilus edulis* from Kiel Fjord kept under different seawater  $p\text{CO}_2$  levels are characterized by low HL and EPF pH values. This is due to the requirements of metabolic  $\text{CO}_2$  excretion. HL and EPF pH decreases with 0.024 units per 0.1 units in seawater pH. No significant bicarbonate accumulation to buffer internal pH could be observed. Elemental ratios (Me/Ca) in the extrapallial fluid correlate with growth rates due to the higher consumption of  $\text{Ca}^{2+}$  during calcification compared to other elements. More data on the mechanisms of biomineralization and the general composition of shells not only related to ambient water but also to the body fluids are needed. Also the impact of the EPF on calcification independent of the exact precipitation area (directly the EPF or a microenvironment) and the involvement of components like hydrophobic silk gel, acidic proteins, chitin and also maybe amorphous calcium carbonate should be subject of future studies. Its necessary to better understand the underlying mechanisms of trace element partitioning and isotope fractionation in order to demonstrate a robust use of proxies in bivalve shells. Trace metal composition of the extrapallial fluid and hence of the shell seems to reflect abiotic conditions only indirectly via the impact on metabolism and growth rate. Boron isotopes in *M. edulis* shell do not reflect seawater pH, they seem to correlate with internal pH (EPF). In addition, boron isotopes show a high variability between individuals and also within single shells. This may reflect variable contributions of boron rich organic matrices present between single crystals. In the future, more attention should be paid to these organic shell parts also with respect to geochemistry as they often are not completely removed before measuring carbonates.

## Acknowledgments

The authors wish to kindly acknowledge Magdalena Gutowska for constantly supporting this study. We thank Ulrike Panknin for help with bivalve sampling and culturing algae, Karin Kißling for supporting ICP-OES measurements and Susann Grobe for carbonate chemistry analysis. AH is grateful for statistical help provided by Claas Hiebenthal and Martin Wahl. This study was funded by DFG Excellence Cluster “Future ocean” grants to FM. This work is a contribution to the German Ministry of Education and Research (BMBF)-funded project “Biological Impacts of Ocean ACIDification” (BIOACID).

## References

- Albers, C. and Pleschka, K., 1967. Effect of temperature on CO<sub>2</sub> transport in elasmobranch blood. *Resp. Phys.* 2, 261–273.
- Caldeira, K. and Wickett, M. E., 2003. Anthropogenic carbon and ocean pH. *Nature*. 25(6956): 365-365.
- Cao, L. and Caldeira, K., 2008. Atmospheric CO<sub>2</sub> stabilization and ocean acidification. *Geophys. Res. Lett.* 35(19).
- Carré, M., Bentaleb, I., Bruguier, O., Ordinola, E., Barrett, N. T., Fontugne, M., 2006. Calcification rate influence on trace elements concentrations in aragonitic bivalve shells: Evidences and mechanisms. *Geochim. Cosmochim. Ac.* 70 (19), 4906-4920.
- Crenshaw, M. A. and Neff, J. M., 1969. Decalcification at the mantle-shell interface in molluscs. *Am. Zool.* 9, 881-889.
- Crenshaw, M. A., 1972. Inorganic composition of molluscan extrapallial fluid. *Biol. Bull.* 143, 506-512.
- Dickson, A. G., and Millero, F. J., 1987. A comparison of the equilibrium-constants for the dissociation of carbonic-acid in seawater media, *Deep-Sea.* 34, 1733-1743.
- Dickson, A. G., 1990. Standard potential of the reaction - AgCl<sub>S</sub>+1/2 H<sub>2</sub> = Ag<sub>S</sub>+HCl<sub>Aq</sub> and the standard acidity constant of the ion HSO<sub>4</sub><sup>-</sup> in synthetic sea-water from 273.15-K to 318.15-K. *J. Chem. Thermodyn.* 22, 113-127.
- Dickson, A. G., Afghan J. D., Anderson, G. C., 2003. Reference materials for oceanic CO<sub>2</sub> analysis: a method for the certification of total alkalinity. *Mar. Chem.*, 80(2-3), 185-197.
- Dickson, A., Sabine, C. L., Christian, J., 2007. Guide to best practices for ocean CO<sub>2</sub> measurements. PICES Special Publication 3, IOCCP Report 8, 191.
- Dodd, J. R., 1965. Environmental control of strontium and magnesium in *Mytilus edulis*. *Geochim. Cosmochim. Ac.* 29 (5), 385-398.



Doney, S. C., Fabry, V. J., R., Feely, R. A., Kleypas, J. A., 2009. Ocean Acidification: The Other CO<sub>2</sub> Problem. *Annu. Rev. Mar. Sci.* 1, 169–92.

Elderfield, H. and Ganssen, G., 2000. Past temperature and delta O-18 of surface ocean waters inferred from foraminiferal Mg/Ca ratios. *Nature* 405(6785), 442-445.

Feely, R. A., Sabine, C. L., Lee, K., Berelson, W., Kleypas, J. A., Fabry, V. J., Millero, F. J., 2004. Impact of anthropogenic CO<sub>2</sub> on the CaCO<sub>3</sub> system in the oceans. *Science* 305(5682), 362-366.

Fietzke, J., Heinemann, A., Taubner, I., Böhm, F., Erez, J., Eisenhauer, A., 2010. Boron isotope ratio determination in carbonates via LA-MC-ICP-MS using soda-lime glass standards as reference material. *J. Anal. At. Spectrom.* 25, 1953-1957. DOI: 10.1039/C0JA00036A

Ford, H., Schellenberg, S. A., Becker, B. J., Deutschman, D. L., Dyck, K. A., Koch P. L., 2010. Evaluating the skeletal chemistry of *Mytilus californianus* as a temperature proxy: Effects of microenvironment and ontogeny. *Paleoceanography*, 25, PA1203, doi:10.1029/2008PA001677.

Foster, G. L., 2008. Seawater pH, pCO<sub>2</sub> and [CO<sub>3</sub><sup>2-</sup>] variations in the Caribbean Sea over the last 130 kyr: A boron isotope and B/Ca study of planktic foraminifera. *Earth Planet. Sci. Lett.* 271, 254–266, doi:10.1016/j.epsl.2008.04.015.

Freitas, P., Clarke, L., Kennedy, H., Richardson, C. A., Abrantes, F., 2006. Environmental and biological controls on elemental (Mg/Ca, Sr/Ca and Mn/Ca) ratios in shells of the king scallop *Pecten maximus*. *Geochim. Cosmochim. Ac.* 70, 5119–5133.

Freitas, P.S., Clarke, L.J., Kennedy, H.A., Richardson, C.A., 2008. Inter and intra-specimen variability masks reliable temperature control on shell Mg/Ca ratios in laboratory- and field-cultured *Mytilus edulis* and *Pecten maximus* (bivalvia). *Biogeosciences* 5(5), 1245-1258.

Gosling, E. 1992. Systematics and Geographic Distribution of *Mytilus*, in Gosling, E. (Ed.) *The Mussel Mytilus: Ecology, Physiology, Genetics and Culture*. Amsterdam, Elsevier Science Publishers B.V. pp. 1-19.

Gutowska, M.A., Melzner, F., Langenbuch, M., Bock, C., Claireaux, G., Pörtner, H. O., 2010. Acid-base regulatory ability of the cephalopod (*Sepia officinalis*) in response to environmental hypercapnia. *J. Comp. Physiol. B.* 180, 323-335.

Hall-Spencer, J.M., Rodolfo-Metalpa, R., Martin, S., Ransome, E., Fine, M., Turner, S.M., Rowley, S.J., Tedesco, D., Buia, M.C., 2008. Volcanic carbon dioxide vents show ecosystem effects of ocean acidification. *Nature*, 454, 96–99.

Hansen, H., Giesenhausen, H., Behrends, G., 1999. Seasonal and long-term control of bottom-water oxygen deficiency in a stratified shallow-water coastal system. *ICES J. Mar. Sci.* 56, 65-71.

Heinemann, A., Fietzke, J., Eisenhauer, A., Zumholz, K., 2008. Modification of Ca isotope and trace metal composition of the major matrices involved in shell formation of *Mytilus edulis*. *Geochem. Geophys. Geosyst.* 9 (1), Q01006, doi:10.1029/2007GC001777.

Hemming, N. G., Hanson, G. N., 1992. Boron isotopic composition and concentration in modern marine carbonates. *Geochim. Cosmochim. Ac.* 56, 537–543.

Hemming N. G., Reeder, R., J., Hart S. R., 1995. Mineral-fluid partitioning and isotopic fractionation of boron in synthetic calcium carbonate. *Geochim. Cosmochim. Ac.* 59, 371–379.

- Hiebenthal, C., 2009. Sensitivity of *A. islandica* and *M. edulis* towards Environmental Changes: A Threat to the Bivalves - an Opportunity for Palaeo-Climatology? Ph.D. thesis, Christian-Albrechts-Univ., Kiel, Germany.  
(Available at [http://eldiss.uni-kiel.de/macau/receive/dissertation\\_diss\\_00003647](http://eldiss.uni-kiel.de/macau/receive/dissertation_diss_00003647))
- Hobbs, M. Y., Reardon, E. J., 1999. Effect of pH on boron coprecipitation by calcite: Further evidence for nonequilibrium partitioning of trace elements. *Geochim. Cosmochim. Ac.* 63, 1013-1021.
- Hönisch B., Bijma J., Russell A. D., Spero H. J., Palmer M. R., Zeebe R. E., Eisenhauer, A., 2003. The influence of photosynthesis on the boron isotopic composition of foraminifera shells. *Mar. Micropaleontol.* 49, 87–96.
- Hönisch, B., Hemming, N.G., Grottoli, A.G., Amat, A., Hanson, G.N., Bijma, J., 2004. Assessing scleractinian corals as recorders for paleo-pH: empirical calibration and vital effects. *Geochim. Cosmochim. Ac.* 68, 3675–3685.
- Immenhauser, A., Nägler, T. F., Steuber, T., Hippler, D., 2005. A critical assessment of mollusk  $^{18}\text{O}/^{16}\text{O}$ , Mg/Ca, and  $^{44}\text{Ca}/^{40}\text{Ca}$  ratios as proxies for Cretaceous seawater temperature seasonality. *Palaeogeogr. Palaeoclimatol.* 215(3-4), 221-237.
- Ip, Y. K., Loong, A. M., Hiong, K. C., Wong, W. P., Chew, S. F., Reddy, K., Sivaloganathan, B., Ballantyne, J. S., 2006. Light induces an increase in the pH of and a decrease in the ammonia concentration in the extrapallial fluid of the giant clam *Tridacna squamosa*. *Physiol Biochem Zool.* 79(3), 656-64.
- IPCC: Climate Change 2007: The Physical Science Basis. Contribution of Working Group I to the Fourth Assessment Report of the Intergovernmental Panel on Climate Change, Cambridge University Press, Cambridge, United Kingdom and New York, NY, USA, 2007.
- Kakihana, H., Kotaka, M., Satoh, S., Nomura, M., Okamoto, M., 1977. Fundamental studies on the ion-exchange separation of boron isotopes. *Chem. Soc. Jpn.*, B 50, 158–163.
- Kasemann, S.A., Schmidt, D.N., Bijma, J., Foster, G.L., 2009. In situ boron isotope analysis in marine carbonates and its application for foraminifera and palaeo-pH. *Chem. Geol.* 260, 138–147.
- Kautsky, N., 1982. Growth and Size Structure in a Baltic *Mytilus edulis* Population. *Mar. Biol.* 68: 117-133.
- Kısakürek, B., Eisenhauer, A., Böhm, F., Garbe-Schönberg, D., Erez, J., 2008. Controls on shell Mg/Ca and Sr/Ca in cultured planktonic foraminiferan, *Globigerinoides ruber* (white). *Earth Planet. Sc. Lett.* 273 (3-4), 260-269. ISSN 0012-821X
- Klein, R. T., Lohmann, K. C., Thayer, C. W., 1996a. Bivalve skeletons record sea-surface temperature and  $\delta^{18}\text{O}$  via Mg/Ca and  $^{18}\text{O}/^{16}\text{O}$  ratios. *Geology* 24 (5), 415-418.
- Klein, R. T., Lohmann, K. C., Thayer, C. W., 1996b. Sr/Ca and  $^{13}\text{C}/^{12}\text{C}$  ratios in skeletal calcite of *Mytilus trossolus*: covariation with metabolic rate, salinity and carbon isotopic composition of sea water. *Geochim. Cosmochim. Ac.*, 60, 4207-4221.
- Klochko, K., Kaufman, A. J., Yoa, W., Byrne, R. H., Tossell, J. A., 2006. Experimental measurement of boron isotope fractionation in seawater. *Earth Planet. Sci. Lett.* 248, 261–270.
- Klochko K., Cody G. D., Tossell J. A., Dera P., Kaufman A. J., 2009. Re-evaluating boron speciation in biogenic calcite and aragonite using  $^{11}\text{B}$  MAS NMR. *Geochim. Cosmochim. Ac.* 73, 1890–1900.

- Kossak, U. 2006. How climate change translates into ecological change: Impacts of warming and desalination on prey properties and predator-prey interactions in the Baltic Sea, Ph.D. thesis, Christian-Albrechts-Univ., Kiel, Germany.  
(Available at [http://eldiss.uni-kiel.de/macau/receive/dissertation\\_diss\\_00001910](http://eldiss.uni-kiel.de/macau/receive/dissertation_diss_00001910))
- Larsen, B., Pörtner, H., Jensen, F., 1997. Extra- and intracellular acid-base balance and ionic regulation in cod (*Gadus morhua*) during combined and isolated exposures to hypercapnia and copper. *Mar. Biol.*, 128(2), 337-346.
- Lazareth, C. E., Vander Putten, E., Andre, L., Dehairs F., 2003. High resolution trace element profiles in shells of the mangrove bivalve *Isognomon ehippium*: a record of environmental spatio-temporal variations?, *Estuar. Coastal Shelf S.*, 57(5-6), 1103-1114.
- Lehmann, A., Krauss, W., Hinrichsen H. H., 2002. Effects of remote and local atmospheric forcing on circulation and upwelling in the Baltic Sea. *Tellus A* 54(3), 299-316.
- Levi-Kalisman, Y., Falini, G., Addadi, L., Weiner, S., 2001. Structure of the Nacreous Organic Matrix of a Bivalve Mollusk Shell Examined in the Hydrated State Using Cryo-TEM. *J. Struct. Biol.* 135, 8–17. doi:10.1006/jsbi.2001.4372
- Lewis, E., Wallace D. W. R., 1998. Program Developed for CO<sub>2</sub> System Calculations. ORNL/CDIAC-105. Carbon Dioxide Information Analysis Center, Oak Ridge National Laboratory, U.S. Department of Energy. Oak Ridge, Tennessee.
- Lindinger, M.I., Lauren, D.J., McDonald, D.G., 1984. Acid-base-balance in the sea mussel, *Mytilus edulis*. 3. Effects of environmental hypercapnia on intracellular and extracellular acid-base-balance, *Mar. Biol. Lett.* 5, 371-381.
- Lopez, O., Zuddas, P., Faivre, D., 2009. The influence of temperature and seawater composition on calcite crystal growth mechanisms and kinetics: Implications for Mg incorporation in calcite lattice. *Geochim. Cosmochim. Ac.* 73(2), 337-347.
- Lorens, R., 1981. Sr, Cd, Mn and Co distribution coefficients in calcite as a function of calcite precipitation rate, *Geochim. Cosmochim. Ac.* 45, 553-561.
- Lorrain, A., Gillikin, D., Paulet, Y. M., Chavaud, L., Lemercier, A., Navez, J., Andre, L., 2005. Strong kinetic effects on Sr/Ca ratios in the calcitic bivalve *Pecten maximus*. *Geology*, 33, 965–968.
- Malone, P., Dodd, J., 1967. Temperature and salinity effects on calcification rate in *Mytilus edulis* and its paleoecological implicatons. *Limnol. Oceanogr.* 12(3), 432-436.
- Marin F. and Luquet, G., 2004. Molluscan shell proteins. *Comptes Rendus Palevol* 3, 469-492.
- McCoy, S. J., Robinson, L. F., Pfister, C. A., Wootton, J., Shimizu, N., Glover, D. M., 2009. High-resolution B concentration analyses by SIMS in *M. californianus* as a potential record of ocean acidification American Geophysical Union, Fall Meeting 2009, abstract #V51E-1787
- Mehrbach, C., Culberso, C. H., Hawley, J. E., Pytkowic, R. M., 1973. Measurement of apparent dissociation-constants of carbonic-acid in seawater at atmospheric-pressure. *Limnol. Oceanogr.* 18, 897-907.

- Melzner, F., Gutowska, M. A., Langenbuch, M., Dupont, S., Lucassen, M., Thorndyke, M.C., Bleich, M., Pörtner, H.-O., 2009. Physiological basis for high CO<sub>2</sub> tolerance in marine ectothermic animals: pre-adaptation through lifestyle and ontogeny?. *Biogeosciences* 6, 2313–2331. doi:10.5194/bg-6-2313-2009.
- Michaelidis, B., Ouzounis, C., Palaras, A., Pörtner, H.-O., 2005. Effects of long-term moderate hypercapnia on acid-base balance and growth rate in marine mussels *Mytilus galloprovincialis*. *Mar. Ecol.-Prog. Ser.* 293, 109-118.
- Mintrop, L., Perez, F. F., Gonzalez-Davila, M., Santana-Casiano, M. J., Körtzinger, A., 2000. Alkalinity determination by potentiometry: Intercalibration using three different methods. *Cienc. Mar.* 26, 23-37.
- Ni, Y., Foster, G. L., Bailey, B., Elliott, T., Schmidt, D. N., Pearson, P., Haley, B., Coath, C., 2007. A core top assessment of proxies for the ocean carbonate system in surface-dwelling foraminifers. *Paleoceanography* 22, PA3212. doi:10.1029/2006PA001337.
- Nürnberg, D., Bijma, J., Hemleben, C., 1996. Assessing the reliability of magnesium in foraminiferal calcite as a proxy for water mass temperatures. *Geochim. Cosmochim. Ac.* 60(5), 803–814.
- Oomori, T., Kaneshima, H., Maezato, Y., Kitano, Y., 1987. Distribution Coefficient of Mg<sup>2+</sup> Ions between Calcite and Solution at 10-50-Degrees-C. *Mar. Chem.* 20(4), 327-336.
- Orr, J. C., Fabry, V. J., Aumont, O., Bopp, L., Doney, S. C., Feely, R. A., Gnanadesikan, A., Gruber, N., Ishida, A., Joos, J., Key, R. M., Lindsay, K., Maier-Reimer, E., Matear, R., Monfray, P., Mouchet, A., Najjar, R. G., Plattner, G. K., Rodgers, K. B., Sabine, C. L., Sarmiento, J. L., Schlitzer, R., Slater, R. D., Totterdell, I. J., Weirig, M. F., Yamanaka, Y., Yool, A., 2005. Anthropogenic ocean acidification over the twenty-first century and its impact on calcifying organisms. *Nature* 437(7059), 681-686.
- Orr, J. C., Caldeira, K., Fabry, V., Gattuso, J.-P., Haugan, P., Lehodey, P., Pantoja, S., Pörtner, H.-O., Riebesell, U., Trull, T., Urban, E., Hood, M., Broadgate, W., 2009. Research priorities for understanding ocean acidification: Summary from the Second Symposium on the Ocean in a High-CO<sub>2</sub> World. *Oceanography* 22(4),182–189.
- Pagani, M., Lemarchand, D., Spivack, A., Gaillardet, J., 2005. A critical evaluation of the boron isotope-pH proxy: the accuracy of ancient pH estimates. *Geochim. Cosmochim. Ac.* 69, 953–961.
- Pane, E.F., Barry, J.P., 2007. Extracellular acid–base regulation during short-term hypercapnia is effective in a shallow-water crab but ineffective in a deep-sea crab. *Marine Ecology Progress Series* Vol. 334: 1–9, 2007
- Pörtner H.-O., Langenbuch, M., Reipschläger, A., 2004. Biological Impact of Elevated Ocean CO<sub>2</sub> Concentrations: Lessons from Animal Physiology and Earth History. *J Oceanogr.* 60, 705-718.
- Reynaud, S., Hemming, N. G., Leclerc, A. J., Gattuso, J.-P., 2004. Effect of pCO<sub>2</sub> and temperature on the boron isotopic composition of the zooxanthellate coral *Acropora sp.*. *Coral Reefs* 23, 539–546. DOI 10.1007/s00338-004-0399-5
- Ries, J. B., Cohen, A. L., McCorkle, D. C., 2009. Marine calcifiers exhibit mixed responses to CO<sub>2</sub>-induced ocean acidification. *Geology* 37, 1131-1134.

- Rollion-Bard, C. and Erez, J., 2010. Intra-shell boron isotope ratios in the symbiont-bearing benthic foraminiferan *Amphistegina lobifera*: Implications for  $\delta^{11}\text{B}$  vital effects and paleo-pH reconstructions. *Geochim. Cosmochim. Ac.* 74, 1530–1536.
- Roy, R. N., Roy, L. N., Vogel, K. M., Porter-Moore, C., Pearson, T., Good, C. E., Millero, F. J., Campbell, D. M., 1993. The dissociation constants of carbonic acid in seawater at salinities 5 to 45 and temperatures 0 to 45 °C. *Mar. Chem.* 44, 249–267.
- Sabine, C. L., Feely, R. A., Gruber, N., Key, R. M., Lee, K., Bullister, J. L., Wanninkhof, R., Wong, C. S., Wallace, D. W. R., Tilbrook, B., Millero, F. J., Peng, T. H., Kozyr, A., Ono, T., Rios, A. F., 2004. The oceanic sink for anthropogenic  $\text{CO}_2$ . *Science* 305(5682), 367–371.
- Sanyal, A., Nugent, M., Reeder, R. J., Bijma, J., 2000. Seawater pH control on the boron isotopic composition of calcite: evidence from inorganic calcite precipitation experiments. *Geochim. Cosmochim. Ac.* 64, 1551–1555.
- Sanyal, A., Bijma, J., Spero, H., Lea, D. W., 2001. Empirical relationship between pH and the boron isotopic composition of Globigerinoides sacculifer: implications for the boron isotope paleo-pH proxy. *Paleoceanography* 16, 515–519.
- Schöne, B. R., Zhang, Z., Jacob, J., Gillikin, D. G., Tütken, T., Garbe-Schönberg, D., MacConnaughey, T., Soldati, A., 2010. Effect of organic matrices on the determination of the trace element chemistry (Mg, Sr, Mg/Ca, Sr/Ca) of aragonitic bivalve shells (*Arctica islandica*)-Comparison of ICP-OES and LA-ICP-MS data. *Geochem. J.* 44, 23–37.
- Spicer, J. I., Raffo, A., Widdicombe, S., 2007. Influence of  $\text{CO}_2$ -related seawater acidification on extracellular acid–base balance in the velvet swimming crab *Necora puber*. *Mar. Biol.* 151, 1117–1125.
- Suzuki, M., Saruwatari, K., Kogure, T., Yamamoto, Y., Nishimura, T., Kato, T., Nagasawa, H., 2009. An Acidic Matrix Protein, Pif, Is a Key Macromolecule for Nacre Formation. *Science* 325, 1388. DOI: 10.1126/science.1173793
- Takesue, R. K., Bacon, C. R., Thompson, J. K., 2008. Influences of organic matter and calcification rate on trace elements in aragonitic estuarine bivalve shells. *Geochim. Cosmochim. Ac.* 72, 22, 5431–5445. doi:10.1016/j.gca.2008.09.003
- Thomsen, J., Gutowska, M. A., Saphörster, J., Heinemann, A., Trübenbach, K., Fietzke, J., Hiebenthal, C., Eisenhauer, A., Körtzinger, A., Wahl, M., Melzner, F., 2010. Calcifying invertebrates succeed in a naturally  $\text{CO}_2$  enriched coastal habitat but are threatened by high levels of future acidification. *Biogeosciences*, 7, 3879–3891. doi:10.5194/bg-7-3879-2010
- Thomsen, J. and Melzner, F., 2010. Moderate seawater acidification does not elicit long-term metabolic depression in the blue mussel *Mytilus edulis*. *Mar. Biol.* 157(12), 2667–2676. DOI: 10.1007/s00227-010-1527-0
- Vander Putten, E., Dehairs, F., Keppens, E., Baeyens, W., 2000. High distribution of trace elements in the calcite shell layer of modern *Mytilus edulis*: Environmental and biological controls. *Geochim. Cosmochim. Ac.* 64(6), 997–1011.
- Vengosh, A., Kolodny Y., Starinsky A., Chivas A. R., McCulloch, M.T., 1991. Coprecipitation and isotopic fractionation of boron in modern biogenic carbonates. *Geochim. Cosmochim. Ac.* 55, 2901–2910. doi:10.1016/0016-7037(91)90455-E.

Wanamaker, A. D., Kreutz, K. J., Wilson, T., Borns, H. W., Introne, D. S., Feindel S., 2008. Experimentally determined Mg/Ca and Sr/Ca ratios in juvenile bivalve calcite for *Mytilus edulis*: implications for paleotemperature reconstructions. *Geo-Mar. Lett.* 28(5-6), 359-368.

Weiss, I. M., Kaufmann, S., Heiland, B., Tanaka M., 2009. Covalent modification of chitin with silk-derivatives acts as an amphiphilic self-organizing template in nacre biomineralization. *J. Struct. Biol.* 167, 68–75. doi:10.1016/j.jsb.2009.04.005

Weiss, I. M., 2010. Jewels in the Pearl. *Chem. Bio. Chem.* 11, 297-300. DOI: 10.1002/cbic.200900677

Weiss R. F., 1974. Carbon dioxide in water and seawater: The solubility of a non-ideal gas. *Mar. Chem.* 2, 203-215.

Wilbur, K. and Saleuddin, A., 1983. Shell formation, in: Wilbur, K., (Ed.), *The Mollusca.* New York, London Academic Press. 4 Physiology Part 1, pp. 235 ff.

Wilbur, K. M. and Bernhardt, A. M., 1984. Effects of Amino Acids, Magnesium and Molluscan Extrapallial Fluid on Crystallization of Calcium Carbonate: In Vitro Experiments. *Biol. Bull.* 166, 251-259.

Wong, W. H. and Levinton, J. S., 2004. Culture of the blue mussel *Mytilus edulis* (Linnaeus, 1758) fed both phytoplankton and zooplankton: a microcosm experiment. *Aquac. Res.* 35(10), 965-969.

Yu, J., Elderfield, H., Hoenisch, B., 2007. B/Ca in planktonic foraminifera as a proxy for surface seawater pH. *Paleoceanography* 22, PA2202. doi:10.1029/2006PA001347.

## Supplement

### 4.S1: Detailed description of gas mixture facilities.

Gas mixtures containing different partial pressures of CO<sub>2</sub> were provided by a central air-CO<sub>2</sub>-mixing device at the IFM-GEOMAR (Bleich et al. 2008). This CO<sub>2</sub> manipulation facility (Linde Gas & HTK Hamburg, Germany) measures ambient *p*CO<sub>2</sub> and adds the required amount of CO<sub>2</sub> to reach the pre-adjusted value into the air which is piped to the culturing rooms. The CO<sub>2</sub>-air mixtures were directly added to the aquaria. *A*<sub>T</sub> values were measured by potentiometric open cell titration with hydrochloric acid (Mintrop et al. 2000, Dickson et al. 2007) with a VINDTA (Versatile Instrument for the Determination of Titration Alkalinity, MARIANDA, Kiel, Germany) autoanalyzer. *C*<sub>T</sub> values of treatment water were coulometrically measured after Dickson et al. (2007) with a SOMMA (Single-Operator Multi-Metabolic Analyzer, University of Rhode Island, Kingston, RI) autoanalyzer. Certified Reference Material provided by Andrew Dickson (Scripps Institution of Oceanography) was used for *A*<sub>T</sub> and *C*<sub>T</sub> measurements. Water *p*CO<sub>2</sub> was calculated via CO2sys program (Dickson et al. 2003, Lewis and Wallace 1998) using the following parameters: Dissociation constants *K*<sub>1</sub> and *K*<sub>2</sub> (Mehrbach et al. 1973, Dickson and Millero 1987), KHSO<sub>4</sub> dissociation constant (Dickson 1990) and *pH*<sub>NBS</sub> scale.

### 4.S2: Single values of acid-base status of the body fluids.

EPF	452	574	731	906	1123	2724
<b>pH</b>						
1	7.55	7.51	7.52	7.44	7.38	7.39
2	7.54	7.54	7.50	7.44	7.42	7.43
3	7.47	7.45	7.41	7.45	7.47	7.24
4	7.57	7.38	7.44	7.49	7.40	
5	7.50	7.61	7.44	7.45	7.39	7.28
<b><i>C</i><sub>T</sub> [mM]</b>						
1					2.53	1.96
2	1.89	1.38	1.86	1.51	1.86	1.96
3		1.45	1.77		1.89	1.96
4	1.89	1.38	1.51	1.51		
5	1.57	1.42		1.64	1.80	1.83
<b><i>p</i>CO<sub>2</sub> [μatm]</b>						
1					4004	3004
2	2047	1472	22067	2070	2673	2757
3		1918	2616		2406	4308
4	1884	2213	2070	1849		
5	1885	1269		2180	2754	3655
<b>CO<sub>2</sub> [mM]</b>						
	0.9	0.7	1.0	0.9	1.8	1.4
		0.9	1.2		1.2	1.2
	0.8	1.0	0.9	0.8	1.1	1.9
	0.9	0.6		1.0	1.2	1.6

<b>HCO<sub>3</sub><sup>-</sup> [mM]</b>						
1					2.35	1.82
2	1.80	1.32	1.76	1.42	1.74	1.83
3		1.36	1.65		1.79	1.76
4	1.81	1.29	1.42	1.43		
5	1.49	1.36		1.54	1.67	1.67
<b>CO<sub>3</sub><sup>2-</sup> [mM]</b>						
1					0.027	0.022
2	0.030	0.022	0.027	0.019	0.022	0.024
3		0.019	0.020		0.025	0.015
4	0.032	0.015	0.019	0.021		
5	0.022	0.027		0.021	0.020	0.015
<b>HL</b>	<b>452</b>	<b>574</b>	<b>731</b>	<b>906</b>	<b>1123</b>	<b>2724</b>
<b>pH</b>						
1	7.50	7.58	7.48	7.43	7.37	7.35
2	7.54	7.58	7.54	7.44	7.43	7.36
3	7.53	7.49	7.48	7.46	7.52	7.35
4	7.63	7.46	7.57	7.54	7.47	
5	7.51	7.54	7.55	7.50	7.54	7.40
<b>C<sub>T</sub> [mM]</b>						
1		1.89	1.80	1.89	1.77	2.27
2	1.70	1.51	1.99	1.64	2.02	1.99
3						1.57
4	1.89		1.57	1.67	1.32	
5	1.29	1.45		1.89	1.35	1.73
<b>pCO<sub>2</sub> [µatm]</b>						
1		1834	2258	2630	2857	3866
2	1836	1468.3	2154.7	2260	2820	3293
3						2684
4	1639		1549	1780	1667	
5	1470	1566		2233	1452	2644
<b>CO<sub>2</sub> [mM]</b>						
	0.8	0.7	1.0	1.2	1.3	1.7
			1.0	1.0	1.3	1.5
						1.2
	0.7		0.7	0.8	0.8	
	0.7	0.7		1.0	0.7	1.2
<b>HCO<sub>3</sub><sup>-</sup> [mM]</b>						
1		1.81	1.70	1.78	1.64	2.10
2	1.62	1.45	1.89	1.54	1.89	1.84
3						1.46
4	1.82		1.51	1.59	1.25	
5	1.22	1.38		1.79	1.29	1.62
<b>CO<sub>3</sub><sup>2-</sup> [mM]</b>						
1		0.033	0.024	0.023	0.018	0.023
2	0.027	0.026	0.031	0.020	0.024	0.020
3						0.016
4	0.037		0.027	0.026		
5	0.019	0.023		0.027	0.021	0.019
<b>water</b>	<b>452</b>	<b>574</b>	<b>731</b>	<b>906</b>	<b>1123</b>	<b>2724</b>
<b>pH</b>	<b>8.10</b>	<b>8.01</b>	<b>7.91</b>	<b>7.82</b>	<b>7.73</b>	<b>7.39</b>
<b>C<sub>T</sub> [µmol/l]</b>	<b>1960</b>	<b>1985</b>	<b>2010</b>	<b>2031</b>	<b>2053</b>	<b>2153</b>
<b>pCO<sub>2</sub> [µatm]</b>	<b>452</b>	<b>574</b>	<b>731</b>	<b>906</b>	<b>1123</b>	<b>2724</b>
<b>CO<sub>2</sub> [mM]</b>	<b>0.02</b>	<b>0.03</b>	<b>0.03</b>	<b>0.04</b>	<b>0.05</b>	<b>0.12</b>
<b>HCO<sub>3</sub><sup>-</sup> [mM]</b>	<b>1.85</b>	<b>1.89</b>	<b>1.92</b>	<b>1.94</b>	<b>1.96</b>	<b>2.02</b>
<b>CO<sub>3</sub><sup>2-</sup> [mM]</b>	<b>0.085</b>	<b>0.070</b>	<b>0.056</b>	<b>0.047</b>	<b>0.038</b>	<b>0.017</b>



## 4.S3: Results of regressions of body fluid acid-base parameters.

factor	fluid	R <sup>2</sup>	a	b	p	CI	regression model
pH	EPF	0.99	8.16	0.104	0.00	8.04 - 8.28	$y=a+b \cdot \ln x$
	HL	0.98	8.18	0.102	0.00	8.01 - 8.35	$y=a+b \cdot \ln x$
	water	1	10.53	0.397	0.00	10.45 - 10.06	$y=a+b \cdot \ln x$
C <sub>T</sub>	EPF	0.58	1.56	0.58	0.23	1.22 - 1.9	$y=a+b \cdot x$
	HL	0.72	1.61	0.72	0.11	1.44 - 1.79	$y=a+b \cdot x$
	water	0.97	1.95	0.97	0.00	1.91 - 1.98	$y=a+b \cdot x$
pCO <sub>2</sub>	EPF	0.88	1637.11	0.70	0.02	954 - 2320	$y=a+b \cdot x$
	HL	0.96	1445.44	0.63	0.00	1142 - 1748	$y=a+b \cdot x$
	water	1	0.000004	1	0.00	0.000004-0.000004	$y=a+b \cdot x$
HCO <sub>3</sub> <sup>-</sup>	EPF	0.44	1.51	0.00011	0.37	1.11 - 1.91	$y=a+b \cdot x$
	HL	0.63	1.54	0.00007	0.18	1.38 - 1.71	$y=a+b \cdot x$
	water	0.90	1.86	0.00006	0.01	1.81 - 1.92	$y=a+b \cdot x$
CO <sub>3</sub> <sup>2-</sup>	EPF	0.57	0.025	-0.000002	0.00	0.02 - 0.03	$y=a+b \cdot x$
	HL	0.78	0.028	-0.000004	0.00	0.02 - 0.03	$y=a+b \cdot x$
	water	0.88	0.080	-0.000025	0.00	14.3 - 23.2	$y=ax^{-b}$

## 4.S4: Single results of elemental ratios.

treatment in µatm	EPF B/Ca in mmol/mol	water B/Ca in mmol/mol	EPF Sr/Ca in mmol/mol	water Sr/Ca in mmol/mol	EPF Mg/Ca in mmol/mol	Water Mg/Ca in mmol/mol
380	8.13	8.09	5026	4839	56.94	53.66
380	8.03	8.09	4861	4839	54.48	53.66
380	8.04	8.14	4947	4884	56.98	56.01
					56.77	53.10
380	8.18	8.05	4957	4856	55.70	53.10
1400	8.06	8.18	4969	5154	58.48	56.98
1400	8.04	8.18	4909	5154	59.26	56.98
1400	7.85	8.11	4659	4880	52.56	49.05
1400	8.13	8.12	4939	4958	51.55	52.82
1400	8.18	8.09	4915	4906	53.36	56.62
4000	7.96	8.09	4777	4861	51.76	52.94
4000	8.10	8.07	4905	4843	54.14	51.70
4000	7.96	8.07	4724	4843	48.03	51.70
4000	8.13	8.04	4849	4821	55.31	51.63
4000	8.14	8.30	4831	5070	51.93	56.09
4000	8.05	8.30	4820	5070	54.81	56.09

4.S5: Single results of  $\delta^{11}\text{B}$  and final shell length of the investigated individuals.

treatment $p\text{CO}_2$ [ $\mu\text{atm}$ ]	$\delta^{11}\text{B}$ (2SE) in ‰	shell length [mm]
380		
	19.59 (1.2)	19.38
	16.61 (0.6)	19.54
	18.59 (1.3)	23.82
	17.83 (0.7)	23.53
	16.10 (0.8)	27.31
	14.93 (0.7)	24.60
	18.53 (0.2)	22.19
	23.83 (0.7)	23.65
	12.44 (1.0)	21.09
	15.57 (0.2)	24.18
1400		
	14.24 (0.9)	24.22
	13.27 (0.6)	24.25
	14.75 (0.8)	22.37
	18.98 (0.7)	22.25
	21.30 (0.4)	22.84
	15.94 (0.4)	27.20
	22.77 (0.9)	23.90
	29.59 (0.5)	24.18
	18.15 (0.9)	23.22
	16.65 (0.8)	25.53
	15.13 (1.2)	23.68
4000		
	19.39 (1.5)	19.20
	15.25 (1.9)	15.73
	22.51 (0.7)	21.32
	14.64 (0.9)	20.93
	17.21 (1.4)	21.07
	12.67 (1.0)	21.09
	17.29 (0.8)	21.11
	21.27 (0.9)	22.40
	30.90 (1.7)	21.17
	12.68 (1.3)	22.60
	12.56 (0.7)	21.52

## Summary and Conclusions

One consequence of the anthropogenic release of carbon dioxide (CO<sub>2</sub>) is the ocean acidification as the atmospheric CO<sub>2</sub> is absorbed by surface waters (Caldeira and Wickett 2003). These changes in water chemistry have an impact on marine ecosystems and communities. *Mytilus edulis* is highly abundant in different marine ecosystems and an important ecosystem engineer, filter feeder and CaCO<sub>3</sub> producer. Its shell growth and acid-base status but also elemental and isotopic composition of the extracellular body fluids and the shell can be influenced by abiotic factors such as pCO<sub>2</sub>, temperature and salinity. Hence, studies on *M. edulis* may help to better understand ecosystem metabolism and individual biomineralization. Secondly, the improvement of present numerical and computational models for future climate requires the reconstruction of past climate change. Recent studies show that the chemical shell composition of different bivalve species are partly dependent on seawater temperature and salinity and may have the potential to serve as proxy archives. However, the results of these studies showed contradictory results.

The main aim of this study was to better understand the impact of elevated pCO<sub>2</sub> on *Mytilus edulis* acid-base status, calcification and inorganic body fluid and shell composition. A second goal was to test its suitability as a proxy archive in general and for pH reconstruction in particular. In an interdisciplinary approach of biology and marine geochemistry the potential of Mg/Ca, Sr/Ca and δ<sup>11</sup>B in *M. edulis* shell to reconstruct temperature, salinity and pH was investigated. Furthermore, elemental ratios/concentrations (Mg/Ca, Sr/Ca, B/Ca, Ca<sup>2+</sup>, Mg<sup>2+</sup>, Sr<sup>2+</sup>) and the acid-base status of the hemolymph (HL) and the extrapallial fluid (EPF) have been determined. Calcification, shell length growth and inner surface structure were determined with different techniques (alkalinity anomaly technique, length increment measurements, MnCl<sub>2</sub>-stainings, optical observations and SEM). The results of this thesis considerably contribute to the knowledge about the response of *M. edulis* to an environment of changing pCO<sub>2</sub>, its biomineralization and potential as a proxy archive.

Elemental ratios (Mg/Ca and Sr/Ca) and boron isotopes (δ<sup>11</sup>B) in the shell of *M. edulis* investigated in this study showed high variability between shells and also within single shells (± 8 % for Sr/Ca, ± 24 % for Mg/Ca, ± 4.5 ‰ for δ<sup>11</sup>B). This was consistent with the high variability of the inorganic body fluid composition and can be explained hereby (± 1 % for Sr/Ca and ± 2.4 % for Mg/Ca). The results of modeling environmental (temperature and salinity) and biological influences on the elemental ratios (Mg/Ca and Sr/Ca) in the calcite layer showed physiological and individual differences having a significant impact on the Mg/Ca (~45 and ~34 % respectively) and the Sr/Ca (~24 and ~17 %) distribution in *M. edulis* calcite.

The δ<sup>11</sup>B results of the shell again showed high variability (± 4.5 ‰) and no correlation with the seawater pH. The latter can be explained when considering the extracellular pH. Due to the requirements of metabolic CO<sub>2</sub> excretion the pH values of EPF and HL were significantly lower than

seawater pH. The high variability within shells is likely owed to boron rich organic matrices in the shell.

At high growth rates elemental ratios (B/Ca, Mg/Ca and Sr/Ca) in the EPF increased slightly with pH which was in accordance with increasing growth and calcification rates at higher seawater pH values. However, this increase was not significant and just indicates a correlation between elemental ratios in the EPF and growth rate. No dependency between different  $p\text{CO}_2$  treatments and elemental concentrations/ratios could be observed in an experiment with extremely low length growth however, the elemental concentrations in the HL and the EPF from this experiment indicated the modification of the fluid composition during calcification. The  $\text{Mg}^{2+}$  and  $\text{Sr}^{2+}$  concentrations were generally depleted in the extracellular body fluids relative to ambient water accompanied by an even stronger depletion in  $\text{Ca}^{2+}$ . This was interpreted to reflect that mainly  $\text{Ca}^{2+}$  is extracted from the solution for shell formation. Again the variability between individuals was very high ( $\pm 10.3\%$  for  $\text{Ca}^{2+}$ ,  $\pm 10.9\%$  for  $\text{Mg}^{2+}$ ,  $\pm 10.3\%$  for  $\text{Sr}^{2+}$ ).

In this study no  $\text{CO}_2$  dependent reduction in shell length growth rate could be observed under low food conditions. But net dissolution and corroded areas at the inner shell surface was found in the highest  $p\text{CO}_2$  treatment (3352  $\mu\text{atm}$ ). In an experiment under optimal food conditions Thomsen et al. (2010) found no corroded areas at the inner shell surface. This implies that shell dissolution could be diminished by higher food levels. In general, shells become thinner when inner shell dissolution takes place and make them more vulnerable for predators like crabs and infestation by e.g. *Polydora ciliata*. An increasing reduction of *Mytilus edulis* abundance would have broad consequences. With the loss of mussel beds other animals would lose attachment possibilities and humans would lose a major organism in aquaculture. The detailed understanding of the biomineralization processes in different taxa is important to predict their calcification response to ocean acidification and also their use as paleoceanographic proxies.

Several different calcification models for bivalves have been proposed and steadily advanced. The EPF is suggested as the site of calcification regulating aragonite-calcite polymorphism via its composition (especially magnesium) (Kitano et al. 1979, Lorens and Bender 1980, Wilbur and Bernhardt 1984, Niedermayr et al. 2010).

On the other hand different organic molecules (in the EPF), interlamellar sheets and enzymes (e.g. carbonic anhydrase) were found to influence crystal formation (e.g. Mutvei 1969, Kitano et al. 1969, Crenshaw 1972, Misogianes and Chasteen 1979, Wilbur and Saleuddin 1983, Wheeler and Sikes 1984, Wheeler 1992, Falini et al. 1996, Miyamoto et al. 2005). A very recent model was proposed by Weiss (2010) who combined the results from Falini et al. (1996), Levi-Kalisman et al. (2001) and Suzuki et al. (2009). In this model nacre formation occurs by means of Pif complex in a microenvironment separated by two chitin layers. In contrast, McConnaughey and Gillikin (2008) proposed a calcification model with respect to carbon isotopes ( $\delta^{13}\text{C}$ ) in mollusc shell carbonates.

Their model assumes that EPF pH is raised under calcifying conditions (by ca 0.5 units), based on studies of pH regulation in the EPF of bivalves (Crenshaw and Neff 1969, Ip et al. 2006). The modification of the carbonate system during calcification causes a diffusion  $\text{CO}_2$  influx,  $\text{CO}_3^{2-}$  accumulation and therefore a  $\text{CaCO}_3$  super saturation (Cohen and McConnaughey 2003).

In this study no accumulation of bicarbonate, carbonate or  $\text{Ca}^{2+}$  could be found in the HL or EPF of *M. edulis*. This indicates that there is no directional oversaturation of the EPF which leads to an inorganic precipitation of  $\text{CaCO}_3$ . The pH measurements of HL and EPF showed low values (~ 7.3-7.5) in all individuals and treatments (380-4000  $\mu\text{atm}$ ). Therefore, suggestions that the EPF pH is raised under calcifying conditions could not be confirmed. This was emphasized by the results of  $\delta^{11}\text{B}$  measurements. The mean  $\delta^{11}\text{B}$  values in *M. edulis* shells were similar for all  $p\text{CO}_2$  treatments within the error and do not reflect seawater pH however they seem to represent internal EPF pH. While the measurements of the body fluids are only a snapshot shell measurements cover the whole time of growth. Thus, it is likely that in bivalves the pH of the EPF is not raised during calcification. This stands in contrast to e.g. foraminifera where seawater vacuolization plays a major role in the calcification process. The seawater vacuoles undergo a pH increase relative to seawater accumulating  $[\text{CO}_3^{2-}]$  (deNooijer et al. 2009, Bentov et al. 2009). Afterwards, they are exocytosed into the delineated calcification site. These differences in calcification strategies may cause different reactions to ocean acidification. As *Mytilus edulis* calcifies under low pH conditions they may be less affected by decreasing water pH. This is also indicated by the observations of corroded inner shell surfaces under high  $p\text{CO}_2$  which could be diminished by sufficient nutrient supply. Thus, it seems energy supply is more relevant for bivalve calcification than the ambient water  $p\text{CO}_2$  or the EPF pH.

No evidence was found in this study that the EPF ion composition regulates the polymorphism of the shell. The elemental concentrations and ratios lead to the conclusion that the EPF is depleted in higher amounts in  $\text{Ca}^{2+}$  than in  $\text{Mg}^{2+}$  and  $\text{Sr}^{2+}$  during calcification. Therefore, the EPF can be interpreted as an elemental reservoir.

In summary, these results disprove assumptions of increasing EPF pH or accumulation of elements and bicarbonate during the calcification process. It can be supposed that a calcification model such as that from Weiss (2010) is likely and the EPF is not the direct site of calcification. However, it may act as a precursor fluid which delivers the necessary components for calcification (e.g. calcium, bicarbonate, proteins and other organic molecules) for a possible distinct microenvironment within the extrapallial space.

In addition, these observations and the above mentioned high variability of elemental/isotopic composition between individuals in both, the shell and the extracellular body fluids challenge the use of *M. edulis* shells as proxy archives. The shell composition seems to reflect the influences on the biological level and not directly the abiotic factors. For example temperature has an impact on the availability of phytoplankton controlling the food/energy supply which then influences bivalves'

growth rate. The growth rate again influences the composition of the shell. In the end e.g. the Mg/Ca composition, often used as a temperature proxy, is however only indirectly influenced by temperature after some intermediate steps. Hence, it is questionable if a sufficient calibration, which considers the complexity of influences, for the proper use of *M. edulis* as proxy archive is feasible at all.

## Outlook

Future studies should subordinate the question whether *M. edulis* shells can serve as reliable proxy archives and focus on the mechanisms of biomineralization. Due to its shell, which is of two different CaCO<sub>3</sub> polymorphs, *M. edulis* remains an interesting object for further investigations on biomineralization. A lot of interdisciplinary work is needed in order to better understand the role of single components (ions, cells, organic matrices) and precursor phases such as amorphous calcium carbonate during calcification. The EPF is one important component and should be further investigated however it seems not to be the definite site of calcification. It is proposed that the EPF is separated into two spaces. Therefore, the calcification mechanisms for the two polymorphs may also be distinct from each other and different components may be involved. More investigation of calcification characteristics are possible by labeling bivalve shells with e.g. MnCl<sub>2</sub> very well-directed to e.g. investigate the cycle of calcification in more detail at different times of the year and even of the day. On the other hand the results of different methods investigating several aspects of calcification show how they complement each other and future studies on bivalve shell growth should combine them. This could provide more detailed results which are the dominant responses of the shell (e.g. thinning, reduced length, less rigidity, disturbed crystal structure) and thus support estimations what will happen to mussel beds under future hypercapnia.

## References

- Bentov, S., Brownlee, C., Erez, J., 2009. The role of seawater endocytosis in the biomineralization process in calcareous foraminifera. *PNAS* 106(51), 21500–21504. doi\_10.1073\_pnas.0906636106
- Caldeira, K. and Wickett, M.E., 2003. Anthropogenic carbon and ocean pH. *Nature*. 25(6956), 365-365.
- Cohen, A. L. and McConnaughey, T., 2003. Geochemical perspectives on coral mineralization. In: Dove, P. M., De Yoreo, J. J. and Weiner, S. (eds) *Biomineralization. Reviews in Mineralogy and Geochemistry* 54, 151–187.
- Crenshaw, M. A. and Neff, J. M., 1969. Decalcification at the mantle-shell interface in molluscs. *Am. Zool.* 9, 881-889.
- Crenshaw, M. A., 1972. Inorganic composition of molluscan extrapallial fluid. *Biol. Bull.* 143, 506-512.
- de Nooijer, L. J., Toyofuku, T., Kitazato, H., 2009. Foraminifera promote calcification by elevating their intracellular pH. *Proc Natl Acad Sci USA* 106:15374–15378.
- Falini, G., Albeck, S., Weiner, S., Addadi, L., 1996. Control of aragonite or calcite polymorphism by mollusk shell macromolecules. *Science* 271, 67–69.
- Ip, Y. K., Loong, A. M., Hiong, K. C., Wong, W. P., Chew, S. F., Reddy, K., Sivaloganathan, B., Ballantyne, J. S., 2006. Light induces an increase in the pH of and a decrease in the ammonia concentration in the extrapallial fluid of the giant clam *Tridacna squamosa*. *Physiol Biochem Zool.* 79(3), 656-64.
- Kitano, Y., Kanamori, N., Tokuyama, A., 1969. Effects of Organic Matter on Solubilities and Crystal Form of Carbonates. *Am. Zool.* 9, 681
- Kitano, Y., Akira, T., Arakaki, T., 1979. Magnesium calcite synthesis from calcium bicarbonate solution containing magnesium and barium ions. *Geochem. J.* 13, 181–185.
- Levi-Kalisman, Y., Falini, G., Addadi, L., Weiner, S., 2001. Structure of the Nacreous Organic Matrix of a Bivalve Mollusk Shell Examined in the Hydrated State Using Cryo-TEM. *J. Struct. Biol.* 135, 8–17. doi:10.1006/jsbi.2001.4372
- Lorens, R. B. and Bender, M. L., 1980. The impact of solution chemistry on *Mytilus edulis* calcite and aragonite. *Geochim. Cosmochim. Ac.* 44, 1265-1278.
- McConnaughey, T. A. and Gillikin D. P., 2008. Carbon isotopes in mollusk shell carbonates. *Geo-Mar. Lett.* 28(5-6), 287-299.
- Misogianes, M. J., and Chasteen, N. D., 1979. Extrapallial fluid: a chemical and spectral characterization of the extrapallial fluid of *Mytilus edulis*. *Anal. Biochem.* 100, 324-334.
- Miyamoto, H, Miyoshi F, Kohno J., 2005. The carbonic anhydrase domain protein nacrein is expressed in the epithelial cells of the mantle and acts as a negative regulator in calcification in the mollusc *Pinctada fucata*. *Zoolog Sci. Mar.* 22(3), 311-5.
- Mutvei, H., 1969. On the micro and ultrastructure of conchiolin in the nacreous layer of some recent and fossil molluscs. *Stockholm Contr. Geol.* 20, 1–17.

Niedermayr, A., Dietzel, M., Köhler, S.J., Petautschnig, S., 2010. Magnesium and Strontium Incorporation into Calcium Carbonate Polymorphs and ACC – Experimental Study. *Geophysical Research Abstracts* Vol. 12, EGU2010-12633.

Suzuki, M., Saruwatari, K., Kogure, T., Yamamoto, Y., Nishimura, T., Kato, T., Nagasawa, H., 2009. An Acidic Matrix Protein, Pif, Is a Key Macromolecule for Nacre Formation. *Science* 325, 1388. DOI: 10.1126/science.1173793

Thomsen, J., Gutowska, M. A., Saphörster, J., Heinemann, A., Trübenbach, K., Fietzke, J., Hiebenthal, C., Eisenhauer, A., Körtzinger, A., Wahl, M., Melzner, F., 2010. Calcifying invertebrates succeed in a naturally CO<sub>2</sub> enriched coastal habitat but are threatened by high levels of future acidification. *Biogeosciences*, 7, 3879–3891. doi:10.5194/bg-7-3879-20

Weiss, I. M., 2010. Jewels in the Pearl. *Chem. Bio. Chem.* 11, 297-300. DOI: 10.1002/cbic.200900677

Wheeler, A. P. and Sikes, C. S., 1984. Regulation of Carbonate Calcification by Organic Matrix *Amer. Zool.* 24, 933-944.

Wilbur, K. M. and Bernhardt, A. M., 1984. Effects of Amino-Acids, Magnesium, and Molluscan Extrapallial Fluid on Crystallization of Calcium-Carbonate – Invitro Experiments. *Biol. Bull.* 166(1), 251-259.

Wilbur, K. and Saleuddin, A., 1983. Shell formation. *The Mollusca*. K. Wilbur. New York, London Academic Press. 4 Physiology Part 1, 235 ff.



## Danksagung

Viele Menschen haben auf unterschiedliche Weise dazu beigetragen, dass diese Arbeit möglich war. Außerdem möchte ich das Ende dieses wichtigen Lebensabschnittes nutzen auch den Menschen zu danken, die bereits auf dem Weg davor mein Leben geteilt und bereichert haben. Allen, die ich möglicherweise vergessen habe, möchte ich hier schon mal danken. Mein Dank gilt:

Prof. Dr. **Anton Eisenhauer** und Prof. Dr. **Frank Melzner** für die Ermöglichung und Betreuung dieser Arbeit. Außerdem für die interessanten Diskussionen der Arbeit aus unterschiedlichen fachlichen Sichtweisen, welche diese sehr bereichert haben.

**Jan Fietzke** für seine hervorragende Unterstützung und Betreuung in meiner Zeit als Hiwi, Diplomandin und Doktorandin. **Claas Hiebenthal** dafür, dass ich an seinem Versuchsaufbau teilhaben durfte und für Diskussionen vieler Fragen, besonders statistischer Natur. **Jörn Thomsen** für die Unterstützung beim Versuchsaufbau und -unterhalt. Außerdem danke ich ihm und **Magdalena Gutowska** für das zur Verfügung stellen der Muschelschalen aus Kapitel 3 sowie diverse hilfreiche Diskussionen. **Florian Böhm** für viele geduldige Stunden und hilfreiche Diskussionen. **Martin Wahl** für die Unterstützung bei Kapitel 1, sowie Rat und Tat bei statistischen Fragen. **Ute Schuldt** und **Christian Samtleben** für den Beistand bei REM-Aufnahmen und einiges mehr. **Jutta Heinze** für ein stets offenes Ohr und die Lösung von Problemen aller Art. **Martin Frank**, dass er mir trotz hart umkämpfter Ressourcen einen Büroplatz zur Verfügung gestellt hat. Meinen **beiden Arbeitsgruppen** (MG und JRG A1) und den **Mädels vom Flur**, insbesondere **Karen Hißmann**, **Basak Kısakürek**, **Almuth Harbers**, **Marion Kohn**, **Federica Ragazzola** und **Isabelle Taubner**, für ein angenehmes Arbeitsklima und unterschiedlichste Unterstützung. **Frauke Rathjen** für vielfältigen Beistand und Unterstützung. **Ulrike Panknin** für die Hilfe beim Sammeln, Hältern und Schlachten von Muscheln sowie viele Gespräche. **Dieter Garbe-Schönberg** und **Karin Kibling** für die ICP-OES Messungen aus den Kapiteln 2/4 und Hilfe bei ihrer Auswertung. **Susann Grobe** für die Messung der DIC-/TA-Daten und **Ute Kossak** für die Muschelschalen aus Kapitel 1.

**Annika Potthast**, **Elisabeth Moek** und **Kim Raddatz** ein besonders großes Danke für ihre langjährige bedingungslose Freundschaft und ehrliche Worte, wie sie nur Freunde finden. *Freunde sind Engel, die Dir wieder auf die Beine helfen, wenn Deine Flügel vergessen haben wie man fliegt.* **Jana Kramer** und besonders **Annika Regulin** für Berlin, Dänemark, ihre Freundschaft und intensive Unterstützung. *Ihr werdet mir fehlen.* Familie **Kardel-Kramer-Sickliger** für die angenehme Nachbarschaft, vielseitige Unterstützung und das unermüdliche Entgegennehmen meiner Post.

**Jasmin Spieß** und **Volker Reese** dafür, dass sie Mitglieder unserer „krassen Herde“ sind und sie auf viele schöne Weisen sehr bereichern. Volker, danke für viel leckeres Essen und sonntägliche Anrufe.

Mein größter Dank gilt meinen Eltern **Brigitte** und **Curt Heinemann**. Ohne sie wären das Studium, die Dissertation und unendlich viele, andere schöne Erlebnisse so nicht möglich gewesen. Den beiden und meinem Bruder **Dag Heinemann** vielen Dank dafür, dass sie immer an mich geglaubt und mich auf meinem Weg begleitet, geprägt und unterstützt haben! *Ich habe Euch sehr lieb!*

## **Erklärung**

Hiermit erkläre ich, dass ich diese Arbeit, abgesehen der Beratung durch meine Betreuer, selbständig angefertigt und mich dabei an die Regeln der guten wissenschaftlichen Praxis gehalten habe. Es wurden keine weiteren als die angegebenen Hilfsmittel und Quellen verwendet. Diese Arbeit wurde weder ganz noch zum Teil einer anderen Stelle im Rahmen eines Prüfungsverfahrens vorgelegt. Ich habe bisher keinen anderen Promotionsversuch unternommen.

Kiel, den

(Agnes Heinemann)

# Curriculum Vitae

Agnes Heinemann  
geboren am 19.05.1981 in Steinheim  
Staatsangehörigkeit: deutsch

Gänsewiese 7  
24107 Kiel

## Ausbildung und wissenschaftlicher Werdegang

- 12/2007 - heute      **Promotion** am Leibniz-Institut für Meereswissenschaften (IFM-GEOMAR), Kiel (Marine Geosysteme und biologische Ozeanographie)
- 10/2007 - 11/2007    **Praktikum** am Institut für Zoophysiologie, Christian-Albrechts-Universität zu Kiel
- 06/2007 - 09/2007    **Wissenschaftliche Mitarbeiterin** am Leibniz-Institut für Meereswissenschaften (IFM-GEOMAR), Kiel (Marine Geosysteme)
- 03/2007                **Diplom** in Biologie (Gesamtnote 'sehr gut'), Fächer: Zoologie, Molekularbiologie, Rechtsmedizin, Toxikologie
- 03/2006 - 02/2007    **Diplomarbeit** am Leibniz-Institut für Meereswissenschaften (IFM-GEOMAR), Kiel (Marine Geosysteme und Benthosökologie)  
*„Untersuchungen zur Eignung von Mytilus edulis als Proxyarchiv“*
- 11/2005 - 02/2006    **Praktikum** am Institut für Rechtsmedizin, Universitätsklinikum Schleswig-Holstein, Kiel (forensische Toxikologie)
- 01/2006 - 02/2007    **Studentische Hilfskraft** am Leibniz-Institut für Meereswissenschaften (IFM-GEOMAR), Kiel (Marine Geosysteme)
- 08/2001 - 12/2005    **Studentische Hilfskraft** am Leibniz-Institut für Meereswissenschaften (IFM-GEOMAR), Kiel (Paläozeanographie)
- 2001 - 2007            **Studium** der Biologie, Christian-Albrechts-Universität zu Kiel  
Währenddessen **Forschungsarbeit** am Institut für Toxikologie und Pharmakologie, Universitätsklinikum Schleswig-Holstein, Kiel  
*„Nachweis von Organochlorverbindungen im Fett des Seehundes“*
- 2000 - 2001            Studium der Geologie, Christian-Albrechts-Universität zu Kiel
- 1991 - 2000            Städtisches Gymnasium Blomberg; **Abitur**; Leistungskurse Biologie und Chemie
- 1987 - 1991            Grundschule Blomberg

